Cdk1-dependent phosphorylation of the APC^{Cdc20} regulates its activation at anaphase onset in *S. cerevisiae*

Elizabeth C. Williams, B.Sc.

Thesis submitted to the
Faculty of Graduate and Postdoctoral Studies
in partial fulfillment of the requirements
for the Doctorate in Philosophy degree in Biochemistry

Ottawa Institute of Systems Biology
Department of Biochemistry, Microbiology and Immunology
Faculty of Medicine
University of Ottawa

Abstract

The metaphase to anaphase transition of the cell cycle is triggered by activation of the anaphase promoting complex (APC) bound to its mitotic activator, Cdc20. The APC is a multisubunit E3 ubiquitin ligase that targets mitotic substrates for proteasomal degradation, including securin (Pds1 in *S. cerevisiae*), which allows for the separation of sister chromatids at anaphase onset. Activation of the APC is thought to be regulated by both Cdk1-dependent phosphorylation and the binding of Cdc20. We show that inhibition of Cdk1-dependent phosphorylation of the APC, by overexpression of the tyrosine kinase Wee1 (Swe1 in *S. cerevisiae*), stabilizes mitotic substrates, impairs sister chromatid separation and arrests cells in metaphase. Inhibition of Cdk1-dependent phosphorylation of the APC also inhibits ubiquitination activity in vitro. We further show that although Cdk1 phosphorylation of the subunits Cdc16, Cdc23 and Cdc27 is important for ubiquitination activity, Cdk1 likely phosphorylates additional subunits of the APC that contribute to maximal activity at the metaphase-anaphase transition. In contrast to previous reports, however, we find that this phosphorylation does not influence binding of the mitotic activator, Cdc20. Mitotic APC activity is also regulated by the spindle assembly checkpoint (SAC), which inhibits Cdc20-dependent activity in response to spindle damage or unattached kinetochores. We find that preventing Cdk1-dependent phosphorylation of the TPR subunits delays recovery from activation of the SAC. We also show that preventing this phosphorylation in combination with loss of the APC subunits Cdc26 and Mnd2 causes sensitivity to activation of the spindle assembly checkpoint. Overall, we argue that Cdk1-dependent phosphorylation is important for APC^{Cdc20} activity at the metaphase-anaphase transition. In addition, our data suggests that

this phosphorylation may also be important for normal SAC function, defining a novel function for Cdk1 phosphorylation of the APC.

Acknowledgements

First and foremost, I'd like to thank Adam Rudner for being a great mentor throughout my graduate studies. I'm grateful for the support, guidance and wisdom you've provided over the course of my PhD. Your enthusiasm for science is unparalleled.

There have been many members of the Rudner lab during my time, and I'm thankful to have met each and every one of you. I've learned something from everyone who has passed through, whether for a short visit or for the long haul: you have all made the lab an incredible place to do research. I'm grateful for Noel Lianga for forging the way with me as the first students of the lab. I'll never forget Alex Weirich for her incredible enthusiasm and positivity, Erin Kennedy, for embracing her inner geekiness, and Carole Doré who will forever be remembered as the DJ of the lab. And last but not least, Kate Harding, for sharing my love of science, coffee, and running.

And finally, to my friends, both my families, and my husband, Brian: you have always kept me grounded, and that has been integral to my success and happiness. I couldn't have done this without your support.

Table of Contents

List of Abbreviations

A
APC - anaphase promoting complex
ATP - adenosine triphosphate

B
BSA - bovine serum albumin
BME - β-mercaptoethanol

C
CBP - calmodulin binding peptide
CDK - cyclin dependent kinase
CRL - cullin-RING ligase

D
D box - destruction box
DMF - dimethylformamide
DNA - deoxyribonucleic acid
DTT - dithiothreitol

E
EM - electromicroscopy
EDTA - ethylene diamine tetraacetic acid
EGTA - ethylene glycol tetraacetic acid

F
FACS - fluorescence activated cell sorting

G
GFP - green fluorescent protein
GST - glutathione S-transferase

H
HECT - homologous to E6-AP carboxyl terminus
HEPES - 4-(2-hydroxyethyl)-1-piperazineethanesulfonic acid
HRP - horseradish peroxidase

I
IgG - immunoglobulin G
IPTG - isopropyl β-D-1-thiogalactopyranoside
IR tail - isoleucine-arginine tail

L
latA- latrunculin A
LLnL - N-acetyl-Leu-Leu-Norleu-al

M
MBP - maltose binding protein
MCC - mitotic checkpoint complex
MEN - mitotic exit network
MAPK - mitogen-activated protein kinase
MPF - maturation promoting factor

P
PBS - phosphate buffered saline
PC - proteasome/cyclosome
PCR - polymerase chain reaction
PKA - protein kinase A
PMSF - phenylmethylsulfonyl fluoride
PP2A - protein phosphatase 2A

R
RING - really interesting new gene
RNAi- RNA interference

S
SAC - spindle assembly checkpoint
SCF - Skp1-Cullin-1-F box protein
SDS - sodium dodecyl sulfate
SEM - standard error of the mean

T
TAP - tandem affinity purification
TBS - tris buffered saline
TBS-T - tris buffered saline + 0.1% Tween-20
TPR - tetracopeptide repeat

Y
YEP - yeast extract peptone media
YEPD - yeast extract peptone media + 2% dextrose

List of Figures

Chapter 1: General introduction

Chapter 2: Materials and Methods

Chapter 3: Cdk1 phosphorylation of the APC regulates anaphase onset

Chapter 4: TPR subunit phosphorylation and co-activator binding

Chapter 1: General Introduction

1.1 The Cell Cycle: An Overview

A brief history of the cell cycle

The eukaryotic cell cycle is defined by distinct events: DNA is replicated in S phase, and chromosome segregation and nuclear division occur during M phase. These phases are separated by gap phases, which allow for the coordination of growth with cell division: G1 is the gap phase between M and S phases, while G2 is the phase between S and M phases (Fig. 1.1A). This co-ordination between cell growth and the steps of the cell cycle is critical for ensuring cell division occurs under the appropriate conditions. Cells will monitor cell size and nutrient availability in G1, and if conditions are favourable, they will pass through a point in G1 called Start, which commits the cell to S phase and the initiation of DNA replication. In addition to the passage through Start, entry into and exit from mitosis are also regulated. Early cell fusion experiments also suggested a functional hierarchy among the different phases of the cell cycle: the mitotic state of one cell could accelerate the onset of mitosis in a non-mitotic cell, and an S phase cell could induce cells in G1, but not cells in G2, to replicate their DNA (Rao and Johnson, 1970). These experiments suggested two important facts about cell cycle progression: (1) the existence of a freely diffusible factor that can induce cell cycle transitions, and that (2) these cell cycle transitions are unidirectional: once the cell has passed through G2 it cannot initiate DNA replication a second time until it has undergone cell division.

a

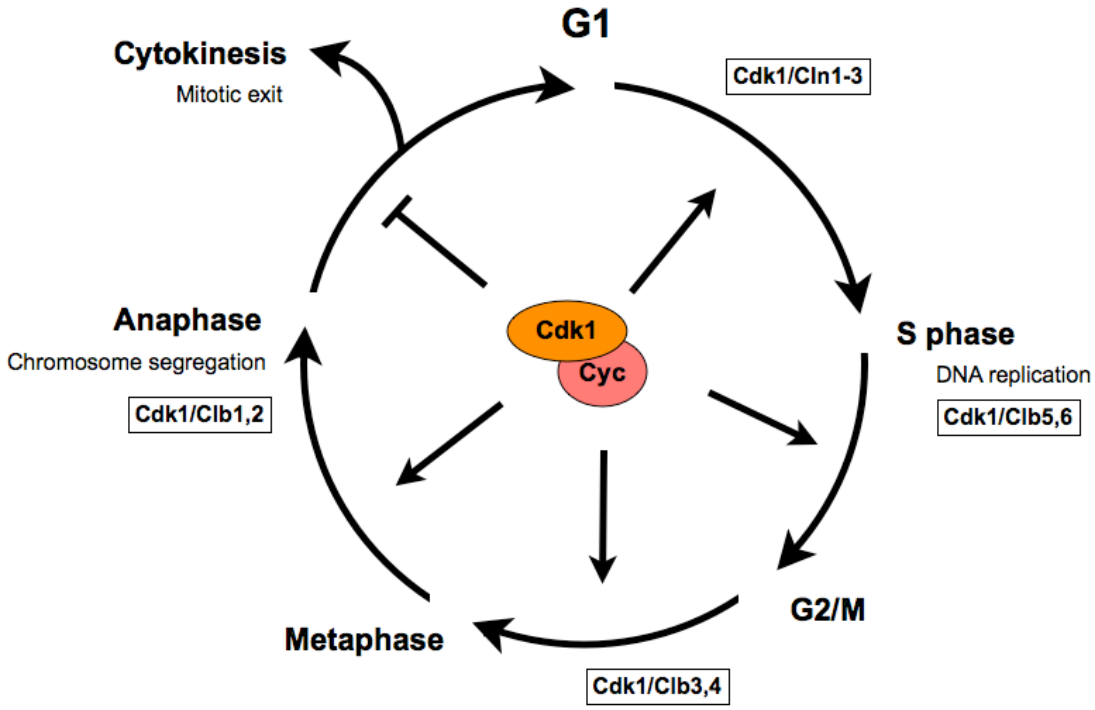
G1
Cdk1/Cln1-3
S phase
DNA replication
Cdk1/Clb5,6
G2/M
Cdk1/Clb3,4
Metaphase
Anaphase
Chromosome segregation
Cdk1/Clb1,2
Cytokinesis
Mitotic exit
Cdk1
Cyc

b

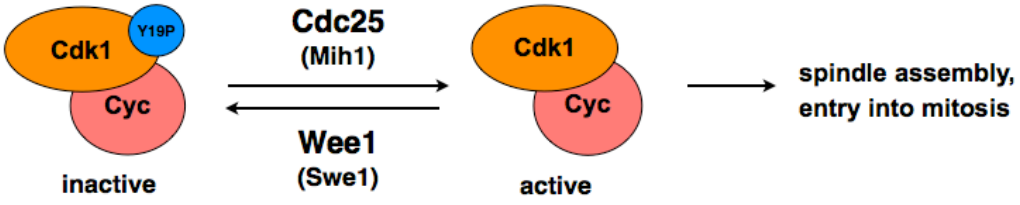
Cdk1
Y19P
Cyc
inactive
Cdc25
(Mih1)
Wee1
(Swe1)
Cdk1
Cyc
active
spindle assembly,
entry into mitosis

Figure 1.1 Cdk1 activity and the cell cycle

(A) Oscillations in Cdk1 activity drive the many stages of the cell cycle. When bound to mitotic cyclins, active Cdk1/cyclin complexes phosphorylate mitotic substrates that are important for triggering events such as DNA replication in S phase, and chromosome segregation at the metaphase-anaphase transition. In anaphase, the cyclin subunit is degraded, inactivating Cdk1/cyclin complexes, which is required for mitotic exit and subsequent entry into the following G1. (B) Wee1 (Swe1 in budding yeast) phosphorylates Cdk1 on a conserved tyrosine residue (Y19), inhibiting its activity. This inhibitory phosphorylation prevents mitotic entry until appropriate conditions are met. Phosphorylation is removed by the phosphatase Cdc25 (Mih1 in budding yeast), and active Cdk1 can trigger mitotic entry.

Much of our understanding of the eukaryotic cell cycle has come from studies in yeast. Several cdc (cell division cycle) genes were characterized from screens in budding and fission yeast that identified temperature sensitive mutants that arrested division at a specific stage of the cell cycle (Hartwell et al., 1970). Most notably, cyclin-dependent kinase (Cdk), the primary driver of cell cycle events, was first discovered in budding and fission yeast as temperature sensitive mutations of the CDC28 and $cdc2^{+}$ genes, respectively (Hartwell et al., 1974; Nurse and Thuriaux, 1980).

The discovery of the cytoplasmic factor MPF, termed maturation promoting factor (MPF) for its ability to "mature" oocytes into unfertilized eggs, was also integral to understanding cell cycle control (Masui and Markert, 1971). The presence of MPF could initiate cleavage divisions of the embryo, and its activity, which was dependent on protein synthesis, appeared periodically in dividing eggs during mitosis, being highest at mitosis and undetectable in S phase (Gerhart et al., 1984; Wasserman and Smith, 1978). Further studies discovered these oscillations in activity were achieved through cyclical degradation of the cyclin subunit, which were first identified as proteins degraded at the end of mitosis in the sea urchin embryo (Evans et al., 1983). In fact, in the absence of all other protein synthesis, cyclin synthesis alone could drive cell extracts into mitosis (Murray and Kirschner, 1989). It was discovered that human Cdc2 could complement the temperature sensitive cdc2 mutant in fission yeast (Lee and Nurse, 1987), and biochemical studies subsequently demonstrated that MPF, Cdc28 and Cdc2 all encode homologous kinases (Nurse, 1990). The evolutionarily conserved cyclins were later found to be cell cycle regulated activating targeting subunits for these kinases.

Cdk1 activity and the cell cycle

The cell cycle in the budding yeast *Saccharomyces cerevisiae*, as in all eukaryotes, is driven by oscillations in Cdk/cyclin activity. While invertebrates and vertebrates have multiple Cdks, there exists only a single cyclin-dependent kinase, Cdk1 (encoded by the *CDC28* gene) responsible for cell cycle control in budding yeast. As the name implies, Cdk activation requires the binding of a cyclin subunit. Cdk/cyclin complexes are serine/threonine kinases that phosphorylate the consensus sequence (S/T)PX(K/R), although there is increasing evidence that the minimal (S/T)P sequence is sufficient (Harvey et al., 2005; Holt et al., 2008; Rudner and Murray, 2000).

Cdk1 activity, in association with different cyclin subunits, drives many mitotic events, including spindle assembly during mitotic entry and chromosome segregation at anaphase onset (Fig. 1.1A), as well as nuclear envelope breakdown (NEBD) and chromosome condensation in larger eukaryotes. The ordering of mitotic events therefore requires the ordered and coordinated phosphorylation and dephosphorylation of many Cdk1 substrates. This ordering is achieved by two mechanisms: substrate specificity conferred by different cyclin subunits, and a stepwise increase in total Cdk1 activity that reaches a maximum at anaphase onset (Stern and Nurse, 1996; Uhlmann et al., 2011). Inactivation of Cdk1 is essential for mitotic exit and entry into the next G1. In budding yeast, the G1 cyclins, Cln1-3, drive progression through G1, and the six mitotic cyclins, Clb1-6, drive mitosis. In general, Clb5/6 are important for initiating DNA replication, whereas Clb1/2, the major mitotic cyclins, drive mitotic entry. These mitotic cyclins exhibit overlapping functions, however, and can often substitute for one another.

Mitotic onset is regulated in all eukaryotes by an increase in Cdk1 activity caused by the dephosphorylation of Cdk1 on a conserved inhibitory tyrosine (tyrosine 19 in budding yeast) (Dunphy and Kumagai, 1991; Gautier et al., 1991; Harvey et al., 2005; Nurse, 1990; Russell and Nurse, 1986). The kinase and phosphatase responsible for the modification of this residues are Wee1 (Swe1 in *S. cerevisiae*) and Cdc25, respectively (Mih1 in *S. cerevisiae*) (Gould et al., 1990; Gould and Nurse, 1989) (Fig. 1.1B). *wee1* mutants in fission yeast shorten G2 by causing premature activation of Cdk1, whereas *cdc25* mutants never accumulate sufficient Cdk1 activity to enter mitosis (Nurse, 1975; Russell and Nurse, 1986; 1987). Wee1 and Cdc25 are the targets of numerous cell cycle checkpoints, all of which delay mitotic entry by activating Wee1 or inhibiting Cdc25 (Harvey and Kellogg, 2003).

Cdk1 activity is also required for anaphase onset. Mutants in Cdk1 delay in metaphase, and mutation of two mitotic cyclins, *CLB1* and *CLB2*, causes a permanent arrest before anaphase initiation (Rahal and Amon, 2008; Rudner et al., 2000), suggesting that only a low level of Cdk1 activity is needed for cells to reach metaphase. Current models suggest that Cdk1 regulation of anaphase onset occurs by the phosphorylation and activation of the APC (discussed in section 1.5) (Félix et al., 1990; King et al., 1995; Kraft et al., 2003; Lahav-Baratz et al., 1995; Patra and Dunphy, 1998; Rudner and Murray, 2000; Shteinberg et al., 1999).

Phosphatases and the cell cycle

The dephosphorylation of Cdk1 substrates is also integral in normal cell cycle progression. Inactivation of phosphatases promotes mitosis, and their activation assists entry

into G1 (Mochida and Hunt, 2012; Stegmeier and Amon, 2004; Uhlmann et al., 2011). In budding yeast, the phosphatase Cdc14 is released from the nucleolus in early anaphase and dephosphorylates many Cdk1 substrates (Bouchoux and Uhlmann, 2011; Jaspersen et al., 1999; Visintin et al., 1998). Although the *CDC14* gene is highly conserved, the reversal of mitotic phosphorylation in other eukaryotes depends primarily on other phosphatases such as protein phosphatase 1 (PP1) and protein phosphatase 2A (PP2A) (Wurzenberger and Gerlich, 2011). PP2A is a heterotrimeric complex composed of a catalytic subunit, an A-regulatory or scaffolding subunit, and one of two B-regulatory subunits (*CDC55* or *RTS1*) (Healy et al., 1991; Lin and Arndt, 1995; Shu et al., 1997; Stark, 1996; Wurzenberger and Gerlich, 2011). The B-regulatory subunits provide specificity to the forms of the phosphatase, $PP2A^{Cdc55}$ and $PP2A^{Rts1}$. PP2A opposes Cdk1 phosphorylation of Wee1 and Cdc25, and is also believed to be the major phosphatase that antagonizes Cdk1 during mitosis (Castilho et al., 2009; Chen et al., 2007; Harvey et al., 2011; Kumagai and Dunphy, 1992; Labit et al., 2012; Mochida et al., 2009; Wicky et al., 2011). $PP2A^{Cdc55}$ has been shown to dephosphorylate the APC in vitro, and loss of Cdc55 results in increased APC phosphorylation in vivo (Lianga et al., 2013).

Discovery of the APC

Cyclin synthesis alone is sufficient to drive the early embryonic cell cycle (Murray and Kirschner, 1989), and a non-degradable cyclin mutant is sufficient to prevent inactivation of MPF and the subsequent exit from mitosis (Murray et al., 1989). More detailed analysis of this non-degradable cyclin mutant revealed the existence of a conserved destruction box (D

box) motif. This motif was found to be necessary and sufficient for the degradation of cyclin through the ubiquitin pathway (Glotzer et al., 1991), which led to the idea that cyclin must be recognized by some unidentified component of the ubiquitin-conjugating system.

The genes that encode the APC subunits Cdc16, Cdc23 and Cdc27 in *S. cerevisiae* were originally identified as temperature sensitive mutants required for the normal progression of mitosis (Hartwell et al., 1973). A screen for mutants impaired in Clb2 proteolysis also identified Cdc16 and Cdc23 (Irniger et al., 1995), and injection of antibodies to the human homologs of Cdc16 and Cdc27 induces a mitotic arrest (Tugendreich et al., 1995). Sequence analysis of Cdc16, Cdc23 and Cdc27 identified tandem TPR (tetratricopepide repeat) motifs (Hirano et al., 1990; Sikorski et al., 1990), which were found to mediate the assembly of these proteins into a complex required for the onset of anaphase (Irniger et al., 1995; Lamb et al., 1994).

The fractionation of mitotic *X. laevis* egg extracts also identified the components required for cyclin degradation: two distinct E2 ubiquitin conjugating enzymes, and a 20S complex that included homologs of Cdc27 and Cdc16 (King et al., 1995). This complex was found to act with E1 and E2 enzymes to ubiquitinate cyclin B1 in vitro, and was termed the Anaphase Promoting Complex (APC) (King et al., 1995). Experiments in clam oocyte extracts also identified a mitotic fraction containing E3 ubiquitination activity, and cyclin degradation by this fraction depended on the presence of the destruction box motif (Sudakin et al., 1995). Sudakin et al (1995) called this fraction the cyclosome, and as a result the complex is often referred to as the APC/C (Anaphase Promoting Complex/Cyclosome). For simplicity, APC will be used throughout this thesis. Immunopurification of this complex

from both *X. laevis* and *S. cerevisiae* identified Apc1 as an essential subunit, in addition to Cdc16, Cdc23 and Cdc27, as well as the non-essential subunit Cdc26 in *S. cerevisiae* (Peters et al., 1996; Zachariae et al., 1996). Subsequent studies identified additional subunits by mass spectrometric analysis, and many of the subunits were found to be conserved in all organisms studied (Hall et al., 2003; Hwang and Murray, 1997; Kurasawa and Todokoro, 1999; Yamada et al., 1997; Yu et al., 1998; Zachariae et al., 1998b).

APC-dependent degradation of securin triggers anaphase onset

The idea that Cdk1 inactivation triggered anaphase was an attractive model, and early experiments in both egg extracts and yeast suggested cyclin degradation was the trigger for anaphase onset (Ghiara et al., 1991; Murray et al., 1989). Subsequent experiments, however, proved otherwise: expression of a non-degradable cyclin B didn't block anaphase, but inhibition of ubiquitination did, suggesting the existence of an unidentified anaphase inhibitor, whose degradation by the ubiquitin pathway would be the trigger for anaphase onset (Holloway et al., 1993). Similar experiments in budding yeast indicated that non-degradable Clb2 prevented mitotic exit, but not entry into anaphase (Irniger et al., 1995; Surana et al., 1993), confirming cyclin degradation was not required for anaphase onset.

The metaphase to anaphase transition of the cell cycle is characterized by the segregation of replicated chromosomes to opposite spindle poles. Analysis of a temperature sensitive mutation of Cut2 demonstrated that the proteolysis of Cut2 was essential for chromosome segregation in fission yeast (Funabiki et al., 1996). An analogous protein in budding yeast, Pds1, was also identified in a screen for mutants that underwent precocious

dissociation of sister chromatids (Yamamoto et al., 1996). Shortly thereafter, Pds1 (securin in vertebrates) was found to be degraded in an APC-dependent manner and this degradation was required for the initiation of anaphase (Cohen-Fix et al., 1996; Funabiki et al., 1996). Pds1/Cut2/securin degradation triggers sister separation by releasing the protease separase (Esp1 in *S. cerevisiae,* Cut1 in *S. pombe*) (Ciosk et al., 1998; Uhlmann et al., 2000). Active Esp1 is then able to cleave the Scc1 (Mcd1 in *S. cerevisiae*) subunit of the cohesin complex which holds sister chromatids together (Uhlmann et al., 2000; 1999). The APC is also responsible for the degradation of mitotic cyclins, which inactivates Cdk1/cyclin complexes allowing for mitotic exit (Fig. 1.2). In fact, Pds1 and the mitotic cyclins are the only essential targets of the APC (Shirayama et al., 1999; Thornton and Toczyski, 2003).

1.2 APC ARCHITECTURE

The APC is an E3 ubiquitin ligase

Ubiquitin-mediated proteolysis is a multi-step process that targets proteins for degradation by the 26S proteasome (reviewed in (Hershko and Ciechanover, 1998)). The ubiquitination reaction is catalyzed by the sequential action of three enzymes. The ubiquitin activating enzyme (E1) initially forms a thiol ester with the terminal carboxyl group of the ubiquitin molecule in an ATP-dependent process. The ubiquitin molecule is then transferred to a sulfhydryl group on one of many ubiquitin conjugating enzymes (E2), which are characterized by a catalytic core of approximately 150 residues with a cysteine at the active site. Finally, the ubiquitin ligase (E3) transfers the activated ubiquitin molecule from the E2 to a lysine residue in the substrate, forming an isopeptide bond. Multiubiquitination refers to

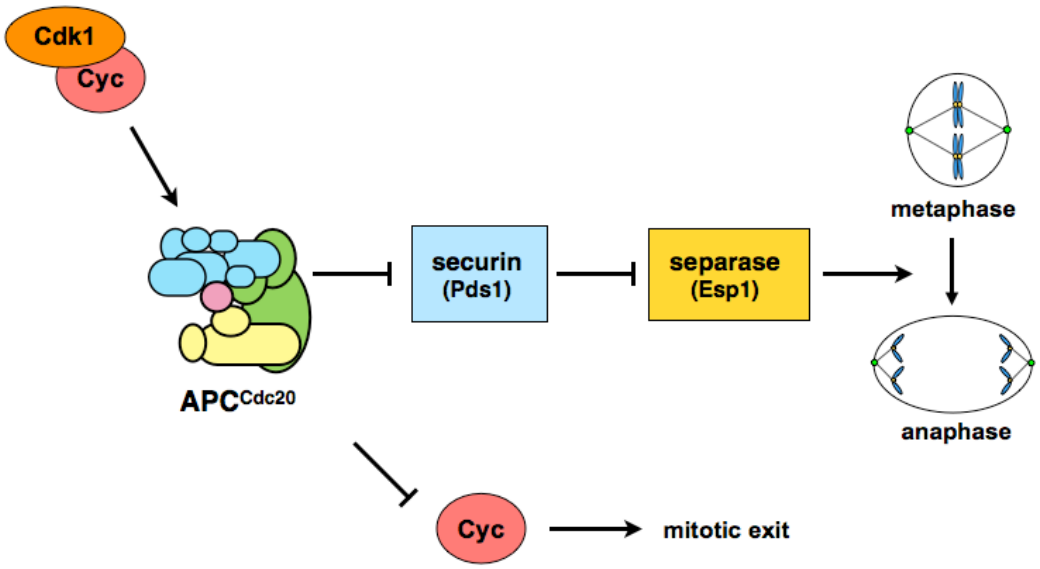
Cdk1
Cyc
APC^Cdc20
securin
(Pds1)
separase
(Esp1)
metaphase
anaphase
Cyc
mitotic exit

Figure 1.2 Activation of the APC^{Cdc20} triggers the metaphase-anaphase transition

Activation of the APC^{Cdc20} triggers the ubiquitination and subsequent degradation of securin (Pds1 in budding yeast). This relieves Pds1 inhibition of separase (Esp1 in budding yeast). Releasing active Esp1 allows for the cleavage of the cohesin complex that holds sister chromatids together, and progression into anaphase. The APC^{Cdc20} also triggers the initial degradation of the mitotic cyclins, which is required for inactivation of Cdk1/cyclin complexes, and mitotic exit.

the addition of ubiquitin molecules to more than one lysine residue within the target protein, while polyubiquitination is the transfer of additional ubiquitin molecules to a lysine residue within the ubiquitin molecule itself. Ubiquitin chains of at least four molecules must be generated on a substrate in order to recognized for degradation by the proteasome (Chau et al., 1989; Thrower et al., 2000).

The APC is an unusually large E3 ubiquitin ligase (1MDa) that consists of 13 core subunits in *Saccharomyces cerevisiae* (Fig. 1.3). Homologs for all but one of these subunits have been identified in larger organisms. This multisubunit complex is considered a member of the RING (Really Interesting New Gene) finger family of E3 ubiquitin ligases, which is one of two major classes of ubiquitin ligases in eukaryotes. The second family, characterized by the HECT (Homologous to the E6-AP Carboxyl Terminus) domain, generates covalent linkages with ubiquitin before transfer of the ubiquitin molecule to a substrate, while RING finger ligases do not: the ubiquitin molecule is transferred directly from the E2 enzyme to the substrate (Metzger et al., 2012). Beyond the RING finger domain, there is little homology among the family members of this class of ubiquitin ligases. Many of the RING finger ubiquitin ligases are part of a complex that contains a subunit with a cullin homology domain to mediate substrate recognition (Deshaies and Joazeiro, 2009). In fact, these form a separate family of RING-based E3s called the cullin-RING ligases (CRLs). Another notable multisubunit RING-finger based E3 ubiquitin ligase is the SCF. Briefly, the SCF (Skp1-Cullin-1-F box protein) consists of a scaffold protein, Cullin-1, which interacts with both an adaptor protein, Skp1, and a RING-finger protein RBX1 or RBX2. Skp1 interacts with one of many F-box proteins that mediate substrate specificity (reviewed in (Cardozo and Pagano,

a

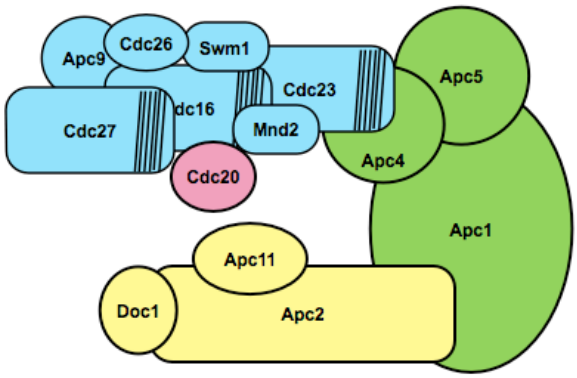

b

Budding yeast	Human	Fission yeast	Essential	Function/motifs
Apc1	Apc1	Cut4	Yes	Scaffolding complex; PC repeats
Apc4	Apc4	Lid1	Yes	Scaffolding complex; required for TPR complex binding to Apc1
Apc5	Apc5	Apc5	Yes	Scaffolding complex; required for TPR complex binding to Apc1
Apc2	Apc2	Apc2	Yes	Catalytic core, E2 binding, cullin homology
Apc11	Apc11	Apc11	Yes	Catalytic core, E2 binding, RING finger
Doc1	Apc10	Apc10	No*	Catalytic core, processivity factor, IR domain, substrate binding
Cdc16	Apc6	Cut9	Yes	TPR complex, activator binding
Cdc23	Apc8	Cut23	Yes	TPR complex, activator binding, bridge to scaffold
Cdc27	Apc3	Nuc2	Yes	TPR complex, activator binding
-	Apc7	-	ND	TPR complex
Cdc26	Cdc26	Hcn1	No*	TPR complex, binds to Cdc16 and completes TPR repeat
Apc9	-	-	No	TPR complex, promotes Cdc27 association
Swm1	Apc13	Apc13	No*	TPR complex, promotes TPR association
Mnd2	Apc15	Apc15	No	TPR complex, regulates Ama1 binding in meiosis, regulates MCC eviction
-	-	Apc14	No	?
Cdc20	Cdc20	Slp1	Yes	Substrate recognition, component of MCC, WD40 domain
Cdh1	Cdh1	Ste9	No	Substrate recognition, WD40 domain
Ama1	-	Mfr1	No	Substrate recognition in meiosis, WD40 domain

Figure 1.3 The Anaphase Promoting Complex (APC)

(A) Representation of the current view of APC architecture, complexed with Cdc20, with the different sub-complexes highlighted: the catalytic arm (yellow), the TPR sub-complex (blue), and the scaffolding subunits (green). The APC activator subunits are highlighted in pink, although only Cdc20 is depicted in (A). Adapted from (Thornton et al., 2006). (B) The APC subunits in budding yeast, and homologs in other organisms. Important functions and motifs are also indicated. *Doc1, Cdc26 and Swm1 are essential in fission yeast, but not in budding yeast. ND: not determined.

2004)). The SCF targets many substrates for ubiquitin-mediated degradation, including the Cdk1 inhibitor Sic1, which allows for the activation of S phase Cdk1/cyclin complexes (Patton et al., 1998). Degradation of the G1 cyclins in budding yeast is also dependent on the SCF (Willems et al., 1996).

The E1 enzyme exhibits the least specificity in the ubiquitination reaction: most organisms, including *S. cerevisiae*, encode only one ubiquitin activating enzyme (McGrath et al., 1991). Each E3 ubiquitin ligase is usually served by one or a few specific E2s. The specificity of this reaction is conferred by the E3: while only a small number of E1 and E2 enzymes exist, more than 600 human ubiquitin ligases have been identified to date. Two E2 enzymes are responsible for mitotic APC-dependent ubiquitin chain formation in *S. cerevisiae*. These enzymes work cooperatively to allow for the initiation, and the elongation of ubiquitin chains on a substrate. Ubc4 catalyzes the transfer of the first ubiquitin to the substrate, while Ubc1 promotes the elongation of K48-linked ubiquitin chains (Rodrigo-Brenni and Morgan, 2007). A similar mechanism of chain formation exists in higher eukaryotes: UbcH10 initiates chain formation, and chain elongation is accomplished by Ube2S, although exclusively through K11 of ubiquitin (Jin et al., 2008; Williamson et al., 2009). Ubiquitination by the APC is processive: multiple ubiquitin molecules are added in a single substrate binding event (Carroll and Morgan, 2002; Rape et al., 2006).

General APC architecture

Structural studies of the APC have revealed that the complex has an overall triangular shape, with a large inner cavity surrounded by a protein shell (Dube et al., 2005; Herzog et

al., 2009; Ohi et al., 2007; Passmore and Barford, 2005). This central cavity is argued to be large enough to hold both the E2-ubiquitin conjugate, and the substrate. The core of the APC can be subdivided into three distinct sub-complexes: the catalytic arm and the TPR sub-complexes, which are linked through a scaffolding complex (Thornton et al., 2006). Each of these sub-complexes are described in greater detail below. The core complex is activated by one of two homologous substoichiometric co-activators in mitosis: Cdc20 or Cdh1. In order to classify the APC into these sub-complexes, one particular study mapped out many of the subunit interdependencies using a budding yeast strain that made the APC non-essential (Thornton et al., 2006). A more recent study developed an overexpression system that allowed for the reconstitution of all 13 APC subunits to generate a functional E3 ligase. Structural analysis of this reconstituted APC allowed for even greater insight into the overall organization of this complex, as well as further detail into specific subunit interactions (Schreiber et al., 2011).

The catalytic arm: Apc2, Apc11 and Doc1

The catalytic core of the APC includes the cullin-like subunit Apc2, the RING-H2 finger subunit Apc11, and the processivity factor Doc1/Apc10 (Hwang and Murray, 1997). Apc2 independently tethers Apc11 and Doc1 to the complex (Thornton et al., 2006). The N terminus of Apc2 contains three cullin repeats of approximately 130 residues. The cullin family of proteins includes Cdc53, a component of the SCF^{Cdc4} (Kramer et al., 1998b; Yu et al., 1998; Zachariae et al., 1998b). This cullin domain mediates the interaction of Apc2 with Apc11 (Tang et al., 2001b). Apc11 is a highly conserved member of the diverse family of

RING finger proteins (Gmachl et al., 2000; Ohta et al., 1999; Zachariae et al., 1998b). The RING-H2 finger found in Apc11 consists of a cluster of cysteine and histidine residues that chelate two zinc atoms, and this motif is thought to be involved in protein-protein interactions (Borden and Freemont, 1996). This zinc binding ability of Apc11 is essential for its ubiquitin ligase activity, and has been shown to bind directly to the E2 enzyme, Ubc4 (Leverson et al., 2000; Tang et al., 2001b). Apc2 and Apc11 alone are sufficient for a modest level of ubiquitin ligase activity in vitro in the presence of E1 and Ubc4, although with no specificity (Gmachl et al., 2000; Leverson et al., 2000; Ohta et al., 1999; Tang et al., 2001b). In fact, Apc11 will ubiquitinate wild type and destruction box mutant cyclin equally well in the absence of the rest of the APC, arguing that at least some of remaining subunits are involved in substrate recognition (Gmachl et al., 2000).

The non-essential subunit Doc1 was originally identified in a screen isolating mutants defective in cyclin proteolysis (Hwang and Murray, 1997). It was found to directly interact with Apc2, and loss of Doc1 leads to a decrease in substrate binding, and enzyme processivity, but otherwise does not affect complex integrity (Carroll et al., 2005; Thornton et al., 2006).

The TPR subcomplex: Cdc16, Cdc23 and Cdc27

The TPR subcomplex includes the essential TPR containing proteins: Cdc16, Cdc23, and Cdc27 (Lamb et al., 1994; Sikorski et al., 1990). These subunits are conserved from yeast to humans, although vertebrate APC contains an additional subunit, Apc7, that is not conserved in budding yeast (Yu et al., 1998). The TPR repeats are protein-protein interaction

domains: one repeat is 34 residues folded into two antiparallel α helices (Lamb et al., 1994; Sikorski et al., 1990). Each TPR subunit has at least 9 repeats, and multiple repeats can pack together to form a protein binding groove (D'Andrea and Regan, 2003). While the exact stoichiometry is not known, it is believed there exists at least two copies of each of these subunits in the overall complex (Dube et al., 2005; Ohi et al., 2007; Passmore and Barford, 2005; Thornton and Toczyski, 2006). Consistent with this, EM structures have isolated both monomeric and dimeric forms of the APC (Passmore and Barford, 2005).

These subunits are tethered to the large scaffolding protein Apc1 through Apc4 and Apc5: both Apc4 and Apc5 are required for the interaction of Cdc16, Cdc23 and Cdc27 with Apc1 (Thornton et al., 2006). Both genetic and EM analysis support an ordered binding among these subunits: Cdc23 associates with Cdc16, which binds Cdc27, the outermost subunit (Ohi et al., 2007; Thornton et al., 2006). In fact, the TPR arm can form a complex independent of the rest of the APC (Thornton et al., 2006). Apc4 and Apc5 bind this TPR arm through Cdc23. The TPR subunits are primarily involved in activator binding, which is discussed in greater detail in section 1.3.

The TPR subcomplex: the non-essential subunits

In addition to the essential subunits described above, the TPR subcomplex of the APC also includes the proteins Cdc26, Apc9, Swm1/Apc13 and Mnd2/Apc15 (Thornton et al., 2006). Cdc26 is a small, acidic protein, with no obvious motifs to indicate structure or function. While it behaves as a *cdc* mutant (Hartwell et al., 1973), it is generally considered a non-essential subunit of the APC. Only at elevated temperatures does Cdc26 become

essential for cell viability, and arrests cells in metaphase (Zachariae et al., 1998b). Several reports have suggested that the loss of Cdc26 causes a decrease in the amounts of purified Cdc16, Cdc27 and Apc9 (Schwickart et al., 2004; Zachariae et al., 1998b), while another report argues the APC subunit stoichiometry and ubiquitination activity in *cdc26*Δ cells appears normal (Passmore et al., 2003). Structural studies on the human Cdc26 have shown that Cdc26 interacts directly with Cdc16 and forms a TPR repeat with Cdc16 (Wang et al., 2009).

Loss of Apc9, a subunit specific to the budding yeast APC, from the APC causes loss of Cdc27 (Zachariae et al., 1998a), but otherwise exhibits only modest defects (Hall et al., 2003; Page et al., 2005; Passmore et al., 2003; Zachariae et al., 1998b). Structural analysis of reconstituted APC confirms that the loss of Apc9 only disrupts the association of Cdc27, and that the remainder of the complex remains intact (Schreiber et al., 2011).

The *SWM1* gene was initially identified because of its role in the activation of sporulation genes, and for the assembly of functional spore walls (Ufano et al., 1999). Mass spectrometric analysis later identified Swm1 as a constitutive component of the APC (Zachariae et al., 1998b). Swm1/Apc13 is important for complex integrity, and has been shown in budding yeast to be required for efficient binding of Cdc16, Cdc27, and Apc9 (Schwickart et al., 2004). A direct interaction between Swm1 and Cdc23 has also been observed (Hall et al., 2003). Structural analysis of the APC suggests that Apc13, the vertebrate Swm1, interacts with the conserved TPR superhelices of Cdc16 and Cdc23, and EM analysis of a *swm1*Δ APC places Swm1 near Cdc16 and Cdc27 (Buschhorn et al., 2011; Schreiber et al., 2011).

Similar to Swm1, the *MND2* gene was initially identified because of its involvement in the recombination process during meiosis (Rabitsch et al., 2001). Not long after, however, it was found to be a constitutive component of the APC, and shown to interact with Apc1, Apc5 and Cdc23 (Hall et al., 2003; Passmore et al., 2003). Structural studies of the APC have not focused on Mnd2, although there exists an unexplained density in the reconstituted APC protruding from the C terminal TPR motifs of Cdc23 that has tentatively been assigned to Mnd2 (Schreiber et al., 2011). More recent work has argued Mnd2/Apc15 plays a role in recovery from activation of the spindle assembly checkpoint (SAC) (discussed in section 1.6).

The scaffolding subunits: Apc1, Apc4 and Apc5

The scaffolding complex consists of the conserved subunits Apc1, Apc4 and Apc5. This complex acts to bridge the catalytic core of the enzyme and the TPR arm (Thornton et al., 2006). Apc1, the largest subunit of the complex, contains at least eight tandem repeats of a 35-40 amino acid motif, the PC (proteasome/cyclosome) repeats, in its C terminus region (Lupas et al., 1997). As described earlier, Apc4 and Apc5, through Apc1, are thought to mediate interaction with the TPR arm through Cdc23, while structural analysis of reconstituted APC indicates that Apc1 connects Apc2 to Cdc23 (Schreiber et al., 2011; Thornton et al., 2006).

1.3 Regulation by Co-Activators: Cdc20 and Cdh1

Discovery of the co-activators, Cdc20 and Cdh1

The APC is a cell cycle regulated enzyme, initially activated at the metaphase-anaphase transition, which remains active through mitotic exit, and into G1. APC activity during this time frame, however, is temporally regulated by two distinct but homologous co-activator subunits. Cdc20 was the first to be identified: *cdc20-1* mutants, as well as mutation of fizzy, the *D. melanogaster* homolog of Cdc20, arrest in metaphase before activation of the APC (Dawson et al., 1993; Hartwell et al., 1973; Sethi et al., 1991; Sigrist et al., 1995), and Cdc20 was found to be essential for anaphase onset (Zachariae and Nasmyth, 1996). It was subsequently shown that Cdc20 is required for activation of the APC in mitosis (Fang et al., 1998; Schwab et al., 1997; Visintin et al., 1997; Yeong et al., 2000). It is now known that the APC^{Cdc20} targets a number of mitotic substrates for degradation, but its only essential function is the proteolysis of Pds1 and Clb5 in order to initiate anaphase and trigger sister chromatid separation (Shirayama et al., 1999; Thornton and Toczyski, 2003).

Cdc20 is a cell cycle regulated protein in both yeast and mammalian cells, and is only present during periods of high Cdk1 activity, and in fact, its degradation is APC-dependent (Kramer et al., 2000; Prinz et al., 1998; Shirayama et al., 1998; Weinstein, 1997). Although Cdc20 is essential for triggering anaphase, it is not well understood how the APC^{Cdc20} is initially activated to trigger anaphase onset. Cdc20 expression is limited to mitosis, yet the protein begins to accumulate in S phase before the APC is active (Fang et al., 1998; Prinz et al., 1998), and the ectopic overexpression of Cdc20 in both yeast and human cells is not sufficient to induce cyclin B proteolysis (Kramer et al., 2000; Prinz et al., 1998). The

expression pattern of Cdc20, therefore, is not be sufficient to explain the timing of APC activation at the metaphase-anaphase transition, arguing the existence of additional mechanisms to regulate activation of the APC^{Cdc20}.

Cdh1 was identified based on its homology to Cdc20, as well as its ability to suppress *cdc20* mutants when expressed in high copy number (Fang et al., 1998; Schwab et al., 1997; Visintin et al., 1997). Unlike Cdc20, Cdh1 is not an essential gene, although the overexpression of Cdh1 is lethal (Schwab et al., 1997; Visintin et al., 1997). Cdh1 is expressed throughout the cell cycle, but its association with the APC is inhibited by Cdk1 phosphorylation (Fang et al., 1998; Jaspersen et al., 1999; Kramer et al., 2000; Prinz et al., 1998; Zachariae et al., 1998a). This limits Cdh1 association with the APC to periods of low Cdk1 activity, and thus the APC^{Cdh1} functions after the APC^{Cdc20}, in late mitosis and early G1. The APC^{Cdc20} initiates cyclin proteolysis, inactivating Cdk1/cyclin complexes, but this task is completed by the APC^{Cdh1} as Cdc20 initiates its own APC-dependent proteolysis (Prinz et al., 1998).

Co-activators bind the APC core and bridge interactions with substrates

Both Cdh1 and Cdc20 activate the APC by direct binding (Fang et al., 1998), and bridge interactions with substrates. This interaction with substrates is mediated by WD40 repeats found within both co-activators that are ideal for mediating protein-protein interactions (Burton and Solomon, 2001; Hilioti et al., 2001; Kraft et al., 2005; Schwab et al., 2001). In addition, Cdc20 and Cdh1 contain two highly conserved sequences important for binding the APC core: an 8 residue N terminal motif (the C box), and an IR (isoleucine-

arginine) motif at the C terminus (Passmore et al., 2003; Schwab et al., 2001; Vodermaier et al., 2003).

Binding of both co-activators to the APC core is thought to occur primarily through the TPR subunits. Cdc27 is particularly important in binding: peptides with an IR motif will bind Cdc27 (Vodermaier et al., 2003), and activator can be cross-linked to Cdc27 (Kraft et al., 2005). Deletion of this IR motif, however, still allows for nearly maximal activation of the APC in vitro. In addition, the APC can still be stimulated in the absence of Cdc27, arguing the existence of additional binding sites important for interaction with the APC core (Thornton et al., 2006). A screen for mutations in the TPR subunits defective in co-activator binding confirmed the role of Cdc27, and also identified important sites on Cdc23 (Matyskiela and Morgan, 2009). The C terminal IR motif also interacts with Apc7, a vertebrate subunit with no homolog in *S. cerevisiae* (Vodermaier et al., 2003). Efficient binding of Cdh1 to the core APC also requires the catalytic subunit Apc2: loss of Apc2 reduces Cdh1 binding in vitro by approximately 10 fold (Thornton et al., 2006). Consistent with this, cryo-EM models of APC structure situate Apc2 near Cdh1, and suggest that Apc2 may interact with the C box of Cdh1 (Dube et al., 2005; Schreiber et al., 2011). Since co-activators are important for substrate recruitment, localizing Cdh1 near the catalytic core of the enzyme would be important for efficient ubiquitination.

The IR tail in Cdh1, which interacts with Cdc27, is essential for viability in budding yeast (Kraft et al., 2005). This motif, however, is not required for the APC-Cdc20 interaction: the *cdc20*Δ*IR* mutant shows normal turnover of APC^{Cdc20} substrates (Thornton et al., 2006), suggesting an important difference in the mechanisms whereby these activators bind and

activate the APC. Consistent with this, the loss of Cdc27 can be bypassed by the overexpression of the Cdk1 inhibitor, Sic1. This overexpression downregulates Cdk1 activity in the *cdc27*Δ background after sister chromatid separation has been completed, which is normally regulated by the APC^{Cdh1} (Thornton et al., 2006). The ability to bypass the essential function of Cdc27 suggests that Cdc27 is not required for Cdc20-dependent activation of the APC, and that Cdc20 may make additional contacts on the APC.

1.4 Substrate Recognition

APC recognition motifs

Although the direct binding of co-activators is essential for activation of the APC, these co-activators also serve another purpose by contributing to substrate specificity through the recognition of particular motifs found within substrates. The D box sequence, a nine residue motif (RxxLxxI/VxN), was the first sequence shown to be important in targeting APC substrates for proteolysis (Glotzer et al., 1991). The D box is common to most, although not all, APC substrates, and interacts directly with the conserved WD40 repeat domains of Cdh1, which is essential for its ubiquitination (Kraft et al., 2005). A second APC degron, the KEN box motif (KENxxxN/D), was later identified, and is usually present in addition to the D box (Pfleger and Kirschner, 2000). In most cases, efficient ubiquitination of a substrate containing a D box and a KEN box is dependent on the presence of both (Burton and Solomon, 2001; Passmore et al., 2003). The use of two distinct degrons allows for some distinction between the APC^{Cdc20} and the APC^{Cdh1}. In general, the APC^{Cdc20} is more dependent on the D box, and the APC^{Cdh1} is more dependent on the KEN box, although this

is not a strict rule (Passmore et al., 2005; Zur and Brandeis, 2002). In addition to the D box and KEN box, additional non-canonical APC recognition motifs have been proposed, which include the A box of the human Aurora A kinase (Castro et al., 2002; Littlepage and Ruderman, 2002), a C terminal element of Cin8 (Hildebrandt and Hoyt, 2001), a 43 residue segment at the C terminus of the kinesin Kip1 (Gordon and Roof, 2001), and a Cry box in Cdc20 (Reis et al., 2006).

A bivalent substrate binding model

Substrate binding to the APC, however, is not thought to be mediated entirely by the co-activator protein. Interaction of the substrate with the APC may involve contributions from a binding site on the activator as well as on the APC core. Consistent with this, substrate interacts with the APC in the absence of activator, albeit with low affinity (Eytan et al., 2006; Yamano et al., 2004). The vertebrate kinase Nek2A can bind APC in the absence of activator, but isn't ubiquitinated unless activator is also added (Hayes et al., 2006). Substrate has also been shown to have higher affinity for an APC-activator complex than for the APC core alone (Eytan et al., 2006; Passmore and Barford, 2005). This led to the model that APC-activator binding may somehow enhance substrate-binding affinity, or that substrates interact with sites both on the activator and the APC core (Eytan et al., 2006; Passmore and Barford, 2005; Yu, 2007).

Studies done on the processivity factor, Doc1, have suggested that substrate binding is bivalent. Despite wild type levels of activator binding, APC lacking Doc1 exhibits negligible ubiquitination activity because of an inability to bind substrate (Passmore et al., 2003). This

loss of ubiquitination activity is caused by an increased rate of substrate dissociation from the active site, resulting in a decrease in reaction processivity (Carroll and Morgan, 2002; Carroll et al., 2005). Analysis of mutants defective in activator binding have also argued that the binding of substrate reduces the rate of activator dissociation (Matyskiela and Morgan, 2009). Structural analysis of the APC supports the notion that Cdh1 and Doc1 may form a bipartite substrate receptor on the APC (Buschhorn et al., 2011). A cryo-EM map of the APC^{Cdh1} bound to D box peptide argues that Cdh1 and Apc10 together create a co-receptor for the D box, and in fact, Apc10 directly contributes to the recognition of the D box by the APC^{Cdh1} complex (Da Fonseca et al., 2011). Furthermore, the C terminal tail of the human Doc1/Apc10 binds Cdc27, which contributes to activator binding (Wendt et al., 2001). Collectively, these data support a bivalent substrate-binding mechanism, whereby the substrate promotes activator binding by providing a bridge between a binding site on the activator, and a Doc1-dependent site on the APC core. The existence of multiple APC recognition motifs within a substrate also supports the idea that substrates may employ multiple interactions with sites on both the co-activator and the APC core.

Pseudosubstrate inhibitors of the APC

Several pseudosubstrate inhibitors of the APC have been identified, including the metazoan protein Emi1, the budding yeast protein Acm1, and the spindle checkpoint protein Mad3. These pseudosubstrates use substrate-like degron motifs that are recognized by the APC to competitively inhibit substrate binding. Emi1 is important for inhibiting the APC^{Cdh1} at the G1-S transition, and binds the D box receptor site on the APC^{Cdh1} (Miller et al., 2006).

Acm1 forms a ternary complex with Cdh1 and Bmh1, a 14-3-3 homolog, and inhibits APC^{Cdh1} activity. This complex has been shown to inhibit ubiquitination activity in vitro by blocking the interaction of Cdh1 with the substrate Clb2 (Dial et al., 2007; Martinez et al., 2006). Acm1 allows for an additional level of regulation of the APC^{Cdh1}, in addition to Cdk1-dependent phosphorylation of Cdh1, in order to restrict APC^{Cdh1} activity to the appropriate phase of the cell cycle. Degradation of Acm1 is partly dependent on the APC^{Cdc20} which recognizes a degron sequence within Acm1, but complete degradation of Acm1 at the end of mitosis requires an additional APC-independent, proteasome-dependent mechanism (Enquist-Newman et al., 2008; Melesse et al., 2014). The checkpoint protein Mad3 is discussed in section 1.6.

1.5 APC Phosphorylation and Activity

The APC is phosphorylated in mitosis

Since its discovery, it has been recognized that many subunits of the APC are mitotically phosphorylated (King et al., 1995; Peters et al., 1996). This extensive phosphorylation appears to be universal, despite the fact that individual sites are not necessarily well conserved, as it has been observed in fission and budding yeast, *Xenopus* and clam egg extracts, as well as in mouse and human cell lines (King et al., 1995; Kotani et al., 1998; Kraft et al., 2003; Peters et al., 1996; Rudner and Murray, 2000; Yamada et al., 1997; Yoon et al., 2006). Phosphorylation site mapping of the human APC has identified many sites, the majority of which were detected exclusively in mitosis (Kraft et al., 2003; Steen et al., 2008). In vitro phosphorylation studies demonstrated that Cdk1 could generate

the majority of these phosphorylation sites, and Cdk1 has been shown to phosphorylate APC subunits in vivo in budding yeast (Rudner and Murray, 2000).

Given that this phosphorylation corresponds to a stage of the cell cycle when the APC is active, the phosphorylation status is assumed to be important for APC activity. Early studies showed phosphorylated APC immunopurified from mitotic *Xenopus* egg extracts has greater ubiquitination activity than APC from interphase extracts (Peters et al., 1996). The inactive interphase form of the APC can also be activated by the addition of mitotic kinase in vitro (Lahav-Baratz et al., 1995; Sudakin et al., 1995), consistent with the finding that mitotic kinases are required for triggering mitotic cyclin degradation at the end of mitosis (Félix et al., 1990). Conversely, phosphatase treatment of the APC reduces its ubiquitin ligase activity, and the complex can be reactivated by addition of mitotic kinase (Lahav-Baratz et al., 1995; Peters et al., 1996), suggesting that APC activity is regulated, at least in part, by reversible phosphorylation.

PKA (protein kinase A) and Plk1 (Polo-like kinase), two serine/threonine kinases, have also been implicated in APC phosphorylation, although with opposite effects. Hyperphosphorylation of the Cut9 subunit (the *S. pombe* Cdc16) is reduced in a *pka1*Δ background, arguing PKA may be partly responsible for Cdc16 phosphorylation, at least in fission yeast (Yamada et al., 1997). PKA has also been shown to phosphorylate Cdc27, and the N terminus of Apc1, but this phosphorylation exerts an inhibitory effect on APC activity in vitro (Kotani et al., 1998). Consistent with an inhibitory role, PKA inactivating mutations suppress various *apc* mutants in both fission and budding yeasts (Anghileri et al., 1999; Irniger et al., 2000; Yamada et al., 1997; Yamashita et al., 1999; 1996). While direct

phosphorylation of APC subunits by PKA has not been shown in budding yeast, multiple PKA phosphorylation consensus sites exist (Kennelly and Krebs, 1991). Dephosphorylation of these residues may be important for APC activation at anaphase since PKA activity falls dramatically at metaphase (Kotani et al., 1998; Yamashita et al., 1996). Furthermore, PKA activation inhibits mitosis, and cells arrest with high levels of Pds1 (Anghileri et al., 1999), arguing PKA-dependent phosphorylation of the APC is likely not important for its activity in anaphase.

Many members of the highly conserved family of Polo-like kinases have been implicated in mitotic control, including Polo-like kinase-dependent phosphorylation of the APC. Cdc16, Cdc27 and the N terminus of Apc1 can be phosphorylated by the mammalian Polo-like kinase, Plk1, in vitro. This phosphorylation, however, was dependent on the presence of active Cdk (Kotani et al., 1998). In this case, Plk1-dependent phosphorylation of the APC alone had no effect on its ubiquitination activity (Kotani et al., 1998). Phosphorylation of mammalian Apc1, Apc5, Cdc27, Cdc16 and Cdc23 was detected in vitro by both Cdk1 and Plk1 (Kraft et al., 2003). Another group argued that in vitro phosphorylation of the APC purified from mitotic HeLa cells with both Cdk1 and Plk1 increased ubiquitination activity up to 75% of control, whereas treatment with either kinase alone reached only 40% activity or less (Golan et al., 2002).

Cdc5, the Polo-like kinase of *S. cerevisiae*, is important for the late stages of the cell cycle: mitotic entry and sister chromatid segregation is normal in *cdc5* mutants, but progression beyond anaphase is blocked (Charles et al., 1998; Shirayama et al., 1998). Cdc5 has been shown to phosphorylate the subunits Cdc16, Cdc27 and Apc9 (Rudner and Murray,

2000), and its activity is required for cyclin degradation, for completion of anaphase B, and for cytokinesis (Kitada et al., 1993). The degradation of Pds1, however, does not depend on Cdc5 function (Shirayama et al., 1998). Moreover, overexpression of Cdc5 causes an APC-dependent decrease in Clb2 levels, but has no significant effect on Pds1 levels, or sister chromatid separation (Charles et al., 1998). These data argue Cdc5 is not critical for the initial activation of the APC^{Cdc20} at the metaphase to anaphase transition in yeast, but rather plays a role in mitotic exit. Studies in *Xenopus laevis* extracts support this model: a catalytically inactive Polo-like kinase blocks mitotic exit, with stable levels of cyclin B2 and high histone H1 activity (Descombes and Nigg, 1998).

Phosphorylation of the co-activator Cdc20 has also been reported. Cdk1/cyclin B-dependent phosphorylation of Cdc20 prevents the ability of Cdc20 to activate the APC in both HeLa cells and *X. laevis* extracts (Yudkovsky et al., 2000). Dephosphorylation of Cdc20 is therefore considered important for APC^{Cdc20} activation, and this dephosphorylation is thought to be at least partly due to PP2A (Labit et al., 2012). Phosphorylation of Cdc20 has also been implicated in SAC function (described in section 1.6). Finally, PKA can phosphorylate Cdc20: activation of the DNA damage checkpoint triggers PKA-dependent phosphorylation of Cdc20, and this phosphorylation is important for halting cell cycle progression (Searle et al., 2004).

Of the sites mapped on the human APC by Kraft et al. (2003), Plk1 could only generate a small number, arguing that Cdk1 is the primary kinase involved in stimulatory phosphorylation of the APC. The mutation of two Cdk1 phosphorylation sites in the *D. melanogaster* Cdc27 gene indicated these sites are required for normal APC function (Huang

et al., 2007). A single study in budding yeast showed that mutation of Cdk1-dependent phosphorylation sites in three subunits of the budding yeast APC slowed mitotic progression, but didn't abolish it (Rudner and Murray, 2000). Mutation of twelve minimal Cdk1 consensus sites on the TPR subunits Cdc16, Cdc23 and Cdc27 in budding yeast (the *apc-12A* mutant) reduces APC phosphorylation, and its activity in vivo (Rudner and Murray, 2000). Loss of phosphorylation on these TPR subunits was also shown to reduce the association of the APC with its mitotic co-activator, Cdc20, and reduces the degradation of APC substrates (Rudner and Murray, 2000). The *apc-12A* mutant is still viable, however, with only a small delay in cell cycle progression.

In addition to Cdc16, Cdc23 and Cdc27, phosphorylation of Apc1, Apc2, Apc4, Apc5, and a vertebrate specific subunit, Apc7, have also been generated by Cdk1. A mass spectrometry study analyzing APC phosphorylation in budding yeast also identified a phosphorylation site in the small non-essential TPR subunit, Cdc26 (Blethrow et al., 2007), and the fission yeast homolog of Cdc26, Hcn1, is phosphorylated in vitro and in vivo by Cdk1 (Yoon et al., 2006). Mutation of this phosphorylated residue in Hcn1 (S48A) produces a modest defect in cell separation, with cells spending only a slightly longer time in anaphase (Yoon et al., 2006). Sequence alignment of the Cdc26 gene indicates that this serine residue is not conserved in budding yeast. It has, however, been replaced with an evolutionarily conserved aspartic acid (D53), which may mimic a constitutively phosphorylated state (Wang et al., 2009).

Aside from these reports, however, phosphorylation studies of the APC have been limited because of the lack of mutational analysis to correlate specific phosphorylation

events with changes in APC activity. It still remains unclear whether Cdk1 phosphorylation of the APC is required to trigger anaphase onset. The mitotic cyclins in budding yeast, Clb1 and Clb2, are required for the metaphase to anaphase transition (Rahal and Amon, 2008), supporting the model that Cdk1 phosphorylates additional subunits of the APC, and that this phosphorylation may be essential for APC^{Cdc20} activation.

APC phosphorylation and activator binding

Several lines of evidence suggest that Cdc20 binding and subsequent activation of the APC is influenced by the phosphorylation status of the APC. Cdc20 preferentially binds and activates phosphorylated APC (Kraft et al., 2003; Kramer et al., 2000; 1998a; Rudner and Murray, 2000; Shteinberg et al., 1999). In clam oocytes, treatment of mitotic APC with phosphatase prevents most of the stimulation of APC activity by Cdc20 (Shteinberg et al., 1999). As described earlier, the TPR repeats in Cdc27 and Cdc23 have been shown to form the binding site for Cdc20 and Cdh1 (Matyskiela and Morgan, 2009), and an APC containing *cdc16-6A* has been argued to have reduced affinity for Cdc20 (Rudner and Murray, 2000). While these studies suggest that Cdk1 phosphorylation of the APC promotes its activation by increasing Cdc20 association, the exact mechanism is not well understood.

1.6 The Spindle Assembly Checkpoint

Checkpoints are critical in ensuring that cell cycle progression is halted in the case of incompletion of a preceding stage, or in the case of damage (Murray, 1992). The DNA damage checkpoint, for example, detects damage or incomplete replication of DNA, and

halts cell cycle progression. This checkpoint ultimately inhibits anaphase onset in *S. cerevisiae* by activating a pathway that leads to the stabilization of Pds1 (Rhind and Russell, 1998; Sanchez et al., 1999). Arresting the cell cycle allows the cell to repair any damage, ensuring that following the completion of cell division both daughter cells will contain an accurate set of genetic information.

The spindle assembly checkpoint is another surveillance mechanism that blocks the metaphase-anaphase transition until all chromosomes have made proper bipolar attachments to the mitotic spindle (reviewed in (Jia et al., 2013)). Following duplication in S phase, sister chromatids are held together by the cohesin complex. In mitosis, a large protein scaffolding structure called the kinetochore assembles at the centromere of each sister chromatid in mitosis. The spindle microtubules emanating from opposite poles of the mitotic spindle will attach to the sister kinetochores, resulting in the alignment of the sister chromatids along the metaphase plate. This capture of kinetochores by the spindle microtubules generates tension across the sister chromatids, and is known as bi-orientation. Anaphase onset will only occur once all sister chromatids have been properly bi-oriented. The SAC senses kinetochores that are not under tension or not properly attached to spindle microtubules, and prevents anaphase onset by inhibiting the APC^{Cdc20} (Li and Nicklas, 1995; Rieder et al., 1995; 1994). Even a single unattached kinetochore is sufficient to activate the checkpoint (Rieder et al., 1994).

The existence of the SAC was first shown in budding yeast: the MAD (mitotic-arrest deficient) genes (Mad1, Mad2 and Mad3) and the BUB (budding uninhibited by benzimidazole) genes (Bub1 and Bub3) were identified in screens for mutants that no longer arrested in mitosis when treated with drugs that interfered with spindle assembly (Hoyt et al.,

1991; Li and Murray, 1991) and demonstrated that a checkpoint pathway existed. The proteins Mad1, Mad2, Mad3, Bub1 and Bub3 are essential for SAC function in budding yeast, and it was later discovered that highly conserved homologs of these proteins are also required for checkpoint function in metazoans. Other SAC components, including the conserved dual-specificity kinase Mps1, were later identified by other means (Weiss and Winey, 1996). Subsequent micro-manipulation and laser ablation experiments were important in determining that unattached kinetochores generate an inhibitory signal that turns the checkpoint on, delaying anaphase until proper attachments are made (Li and Nicklas, 1995; Rieder et al., 1995).

Studies of the vertebrate homologs of the checkpoint proteins suggested these proteins were localized to the kinetochores during a checkpoint arrest. The *X. laevis* Mad2 homolog, XMAD2, as well as the human homolog, hsMAD2, was found to localize to the kinetochores during prometaphase, but was lost from kinetochores in metaphase (Chen et al., 1996; Li and Benezra, 1996), suggesting the loss of Mad2 from the kinetochore might be related to microtubule attachment in metaphase. XMAD1, the *X. laevis* homolog of Mad1, is required for the recruitment of XMAD2 to the kinetochore (Chen et al., 1998). Live cell analysis confirmed the kinetochore localization of Mad2: fluorescent Mad2 associated with unattached kinetochores early in mitosis, but was depleted from kinetochores as they attached to the spindle (Howell et al., 2000). The mitotic localization of the murine homolog of Bub1 to kinetochores is also essential for checkpoint function in response to spindle damage (Taylor and McKeon, 1997). These experiments suggested a model whereby

unattached kinetochores serve as a catalytic site for the assembly of the SAC signaling cascade.

The current model of the SAC suggests it functions as follows. Although the recruitment of Mad1 to the kinetochore is considered the defining event in checkpoint activation, SAC signaling also depends on the kinetochore localization of the checkpoint proteins Mps1, Bub1, Bub3 and Mad2, as well as the Mad3 homolog BubR1 in metazoans (Jia et al., 2013). Phosphorylation of Spc105 by the checkpoint kinase, Mps1, recruits Bub1 which is constitutively bound to Bub3 throughout the cell cycle (Kiyomitsu et al., 2007; London et al., 2012; Primorac et al., 2013; Shepperd et al., 2012; Yamagishi et al., 2012). Once localized to the kinetochore, Mps1-dependent phosphorylation of Bub1 recruits Mad1 (London and Biggins, 2014). In addition to Mad1, Bub1 also signals the recruitment of other downstream SAC components, including Mad2 and Mad3. Mad2 exists in two conformations: when unbound, it exists in an open conformation (O-Mad2), but when bound to Mad1 or Cdc20, it undergoes a conformational change to the closed conformation (C-Mad2). Mad1 and Mad2 form a complex that acts as a scaffold to activate soluble Mad2 from the open to closed conformation (Luo et al., 2002; Sironi et al., 2002). Closed Mad2 binds Cdc20 through Mad2-interacting domains in both the N and C termini (Mondal et al., 2006; Zhang and Lees, 2001). Mad2 and Cdc20 are incorporated into the mitotic checkpoint complex (MCC), the most downstream effector of the SAC, which is assembled from two sub-complexes: Mad2-Cdc20, and Mad3-Bub3 (Chao et al., 2012; Sudakin et al., 2001). While formation of the Mad2-Cdc20 complex is triggered by the presence of unattached kinetochores, the Mad3-Bub3 complex does not appear to be cell cycle regulated (Chen,

2002; Hardwick et al., 2000). The MCC binds directly to the APC, blocking its Cdc20-dependent activity, and therefore anaphase onset, until errors are resolved (Fig. 1.4).

How does the MCC inhibit APC^{Cdc20} activity?

Two distinct mechanisms have been proposed to explain how the MCC inhibits APC^{Cdc20} activity. In the first, Mad3 acts as a pseudosubstrate to block substrate recruitment to the APC by Cdc20. Unlike canonical APC substrates, the presence of two KEN boxes and one D box in the Mad3 sequence does not target Mad3 for APC-dependent ubiquitination. Instead, Mad3 competes for Cdc20 binding with other APC substrates, and these motifs mediate its interaction with Cdc20 (Burton and Solomon, 2007). The crystal structure of the fission yeast MCC suggests that Mad2 helps optimally position one of the KEN boxes of Mad3 to bind Cdc20 (Chao et al., 2012). EM analysis of an APC^{MCC} complex also suggests that MCC binding inhibits APC activity at least in part by limiting substrate access (Herzog et al., 2009). This mechanism of APC inhibition may be conserved: the two KEN boxes found within BubR1 are also essential for spindle checkpoint function (Lara-Gonzalez et al., 2011).

In an alternative, although not mutually exclusive, mechanism, binding of the checkpoint proteins alters the binding of Cdc20 to the APC, hindering its ability to activate the APC. In support of this, EM analysis of an APC^{MCC} complex suggests that the checkpoint proteins occupy a site on the APC that partially overlaps with the Cdc20 binding site (Herzog et al., 2009). MCC-dependent displacement of Cdc20 is also evidenced by the crystal structure of the fission yeast APC^{MCC}: checkpoint proteins displace Cdc20 and disrupt the

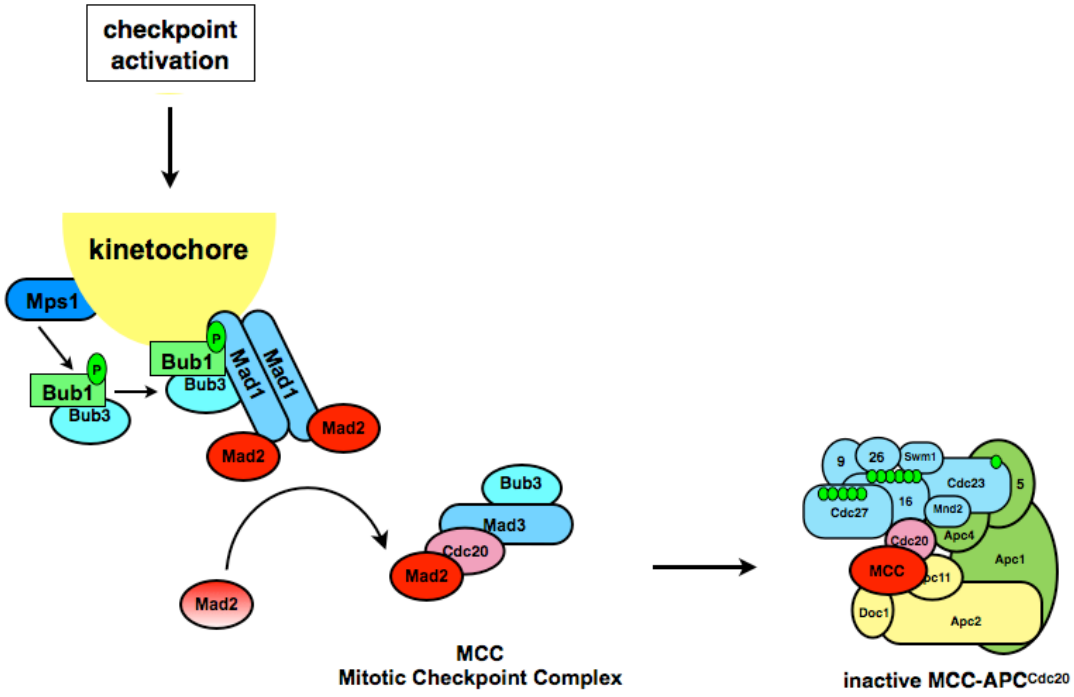
checkpoint activation
kinetochore
Mps1
Bub1
Bub3
P
Mad1
Mad2
Mad3
Cdc20
MCC
Mitotic Checkpoint Complex
9
26
Swm1
Cdc23
5
Cdc27
16
Mnd2
Apc4
Cdc20
Apc1
MCC
Apc11
Doc1
Apc2
inactive MCC-APCCdc20

Figure 1.4 The spindle assembly checkpoint and the APC^{Cdc20}

The spindle assembly checkpoint inhibits the APC^{Cdc20}. The spindle assembly checkpoint detects spindle damage and unattached kinetochores, and arrests the cell cycle to prevent progression into anaphase. Depicted here is a simplified model of the checkpoint. Upon checkpoint activation, the upstream kinase, Mps1, is recruited to the kinetochore, and phosphorylates Bub1 in order to recruit Mad1. Bub1 is constitutively bound to Bub3 throughout the cell cycle. The Bub1-Mad1 interaction at the kinetochore facilitates a conformational change in Mad2, which allows it form the mitotic checkpoint complex (MCC) with three other proteins: Mad3, Bub3 and Cdc20. The MCC binds the APC and inhibits APC-dependent ubiquitination of mitotic substrates, preventing anaphase progression until all errors are resolved. Not depicted here: phosphorylation of Spc105 by Mps1 helps recruit Bub1 to the kinetochore. Figure adapted from {Zich:2010jo}.

formation of a bipartite D box receptor with the APC subunit Doc1/Apc10 (Chao et al., 2012). Moreover, Cdc20 binding to the APC requires only Apc8 (Cdc23) when the checkpoint is activated, but requires both Apc3 (Cdc27) and Apc8 (Cdc23) when the checkpoint has been satisfied (Izawa and Pines, 2011). Mad2-Cdc20 and Mad3-Cdc20 complexes alone can prevent Cdc20-dependent activation of the APC, although to a lesser degree than the complete MCC (Tang et al., 2001a). Both mechanisms described here are likely at play in APC inhibition when the spindle assembly checkpoint is activated.

Cdc20 autoubiquitination and recovery from the spindle assembly checkpoint

How is APC inhibition by the MCC released once the checkpoint has been satisfied? During a checkpoint arrest, Cdc20 is targeted for degradation through APC-dependent ubiquitination (Nilsson et al., 2008; Pan and Chen, 2004). While it is clear that Cdc20 is autoubiquitinated during a checkpoint arrest, the exact role for this is still not clear. APC-dependent ubiquitination of Cdc20 has been argued to be important for maintaining the checkpoint (Nilsson et al., 2008). Ubiquitinated Cdc20 is associated with the APC during a checkpoint arrest, suggesting this ubiquitination does not interfere with MCC association with the APC (Mansfeld et al., 2011). Modest overexpression of Cdc20 overrides the checkpoint, further arguing that the regulation of Cdc20 levels is critical for SAC function (Pan and Chen, 2004). In disagreement with this model, however, another group showed that Cdc20 autoubiquitination contributes to MCC disassembly, and thus inactivation of the checkpoint (Uzunova et al., 2012). Despite this controversy, it is apparent that the APC subunit Mnd2/Apc15 is involved: RNAi-mediated depletion of Apc15 impairs the release of

the MCC from the APC (Mansfeld et al., 2011; Uzunova et al., 2012). In support of this role, Apc15 is positioned near the MCC binding site on the APC (Herzog et al., 2009). Mnd2 is not required for APC^{Cdc20}-dependent ubiquitination of Pds1 and the mitotic cyclins (Foster and Morgan, 2012; Mansfeld et al., 2011; Uzunova et al., 2012), however whether or not Mnd2/Apc15 is required for Cdc20 ubiquitination is still unclear. Despite the ubiquitination and subsequent degradation of Cdc20 during a checkpoint arrest, steady-state levels of Cdc20 do not vary dramatically because of continued protein synthesis (Liang et al., 2011). This constant turnover is argued to be important for a robust checkpoint: this dynamic assembly and disassembly of the MCC ensures the cell is continually responsive to the status of kinetochore attachment.

Cdk1 activity and the spindle assembly checkpoint

A number of studies have suggested that inactivation of Cdk1 is required for release from SAC arrest. The upstream checkpoint kinase, Mps1, is a target of Cdk1: Mps1 phosphorylation is essential for the recruitment of Mad1 and Mad2 to the kinetochore (Morin et al., 2012). Studies in budding yeast have also argued that active Cdk1 is required for a SAC-dependent checkpoint arrest: Cdk1 mutants are unable to arrest in response to nocodazole, a microtubule depolymerizing drug that activates the SAC (Kitazono et al., 2003; Li and Cai, 1997). It appears, then, that Cdk1 is playing two very different roles: active Cdk1 is argued to regulate anaphase onset through phosphorylation and activation of the APC^{Cdc20}, and yet Cdk1 activity is also important for indirect inhibition of the APC^{Cdc20} by contributing to the SAC-dependent arrest. Mutating Cdk1 phosphorylation sites in the APC

subunits Cdc16, Cdc27 and Cdc23 causes increased sensitivity to a spindle assembly checkpoint arrest, although this phenotype was not investigated further (Rudner and Murray, 2000).

Mitogen-activated protein kinase (MAPK)-dependent phosphorylation of Cdc20 in *X. laevis* is required for inhibition of the APC^{Cdc20} upon SAC activation (Chung and Chen, 2003). Furthermore, inhibition of Cdk activity during a checkpoint arrest results in an increase in the amount Cdc20 bound to the APC, and the dissociation of Cdc20 complexed with Mad2 (D'Angiolella et al., 2003). More recently, Cdk1 phosphorylation of Cdc20 has been shown to promote its dissociation from BubR1 (Miniowitz-Shemtov et al., 2012). Blocking this phosphorylation, however, did not completely prevent the release of BubR1, and Cdc20 remains bound to Mad2, arguing there exist additional mechanism(s) that contribute to MCC disassembly and release from the checkpoint.

1.7 General Hypothesis & Specific Objectives

Anaphase onset is an irreversible transition in the cell cycle, and errors in chromosome segregation that occur at the metaphase-anaphase transition cannot be corrected. These errors can result in chromosomal damage or loss, and genetic damage has long been associated with the development of malignant tumours (Bakhoum and Compton, 2012). In fact, some of the proteins involved in the regulation of anaphase onset are mutated in a number of different cancers. Cdc20, for example, is frequently overexpressed in lung, cervical and oral cancer, among others (Kato et al., 2012; Mondal et al., 2007; Rajkumar et al., 2011). Tumorigenesis has also been associated with the mutation of genes of the spindle

assembly checkpoint (reviewed in (Zhang et al., 2014)). Understanding how the cell is able to accurately regulate the onset of anaphase will be integral to understanding what happens when errors do occur, and may ultimately help in the development of new drugs. In fact, many of the anti-mitotic chemotherapeutics currently in use act by triggering the SAC and blocking anaphase.

Why study anaphase onset in the budding yeast, *Saccharomyces cerevisiae*? Much of our understanding of cell division has come from studies in yeast, and most of these processes are highly conserved, but simpler in yeast. Metazoan eukaryotic cell cycle transitions are also driven by cyclin dependent kinase complexes, except that there are many more Cdks and cyclins than found in yeast. Moreover, homologs for all but one of the APC subunits in *S. cerevisiae* have been identified in vertebrates. While individual phosphorylation sites on the APC are not necessarily conserved, Cdk-dependent phosphorylation of the APC has also been observed in all organisms studied to date. Finally, budding yeast is a versatile model organism that is exceptionally amenable to genetic manipulation and analysis, offering us a wide range of tools to study this conserved process that are often not available in other systems.

General hypothesis

The defining event of the metaphase-anaphase transition of the cell cycle is the segregation of sister chromatids, and this irreversible event is triggered by activation of the APC^{Cdc20}. Although this activation is essential for anaphase onset, the mechanism through which this unusually large E3 ubiquitin ligase is activated is still not well understood. Cdk1-

dependent phosphorylation of the APC is a conserved phenomenon, and correlative studies argue this phosphorylation is important for ubiquitination activity in mitosis. Whether or not this phosphorylation is essential for triggering anaphase onset and the subsequent segregation of sister chromatids, however, has not been shown. As such, we hypothesize that Cdk1-dependent phosphorylation of the APC is essential for its activation in anaphase, and for normal cell cycle progression in the budding yeast, *S. cerevisiae*. This thesis also examines whether Cdk1 phosphorylation of the APC increases the affinity of the APC core for its mitotic activator, Cdc20. Finally, activation of the spindle assembly checkpoint leads to inhibition of the APC^{Cdc20} and the delay of anaphase onset until accurate chromosome segregation can be guaranteed. As such, this thesis also explores the possibility that Cdk1 phosphorylation of the APC may be important in the recovery from activation of this important cell cycle checkpoint.

Specific objectives

1. Characterize the effect of inhibiting Cdk1-dependent phosphorylation of the APC.
2. Determine whether Cdk1-dependent phosphorylation of the subunits Cdc16, Cdc23 and Cdc27 contributes to activator binding, and determine whether additional TPR subunits are involved.
3. Determine the role of Cdk1-dependent APC phosphorylation in the spindle assembly checkpoint.

Chapter 2: Materials and Methods

2.1 Strain and Plasmid Construction

Table I in Appendix A lists the strains used in this study. All strains are derivatives of the W303 strain background (W303-1a) (see Table 1 for complete genotype). All deletions and replacements were confirmed by immunoblotting, phenotype or PCR. The bacterial strains TG1 and DH5α were used for amplification of DNA, and Rosetta (Novagen) was used for protein purification.

CDC16-TAP-HIS3 strains were made by crossing TC80 (a gift of Christopher Carroll and David Morgan, UCSF, San Francisco, CA) (Carroll and Morgan, 2005) to the appropriate strains. The *cdc16-6A-TAP-URA3* and *APC1-TAP-URA3* alleles were made by amplifying a *TAP-klURA3* cassette from pBS1539 and integrating it into the *cdc16-6A-TRP1* or wild type strain. The *CDC55-TAP-klTRP1* strain was made using pBS1479 (Rigaut et al., 1999) and the appropriate oligonucleotides.

cdc15-2 and *PDS1-myc18X-leu2::HIS3* strains were made by crossing K1993 and K6445 (gifts of Kim Nasmyth, University of Oxford, Oxford, UK) to the appropriate strains and the *LEU2* converted to *HIS3* with pLH7 (Cross, 1997). The plasmids used to make *leu2::pGAL-SWE1-HA-LEU2* and *leu2::pGAL-swe1-N584A-HA-LEU2* are pSwe1-41 (a gift of Bob Booher, Onyx Pharmaceuticals, Richmond, CA) (Booher et al., 1993) and pSH14 (a gift of Stacey Harvey and Douglas Kellogg, UCSC, Santa Cruz, CA) (Harvey et al., 2005), respectively. *SPC42-eGFP-HYG^R* was created by amplifying eGFP and a marker off pKT127 (Sheff and Thorn, 2004), and switching the marker to *HYG^R* using pAG32 (Goldstein and McCusker, 1999).

HYG^R-CDC28-Y19F was created from two overlapping PCR fragments: *HYG^R* (amplified from pAG32) and the promoter (from -334 to -1) and 5' region of the *CDC28-Y19F* allele, including the mutation (amplified from pSF38 (a gift of Peter Sorger, Harvard Medical School, Boston, MA)). These two fragments were used to create a single long cassette that was integrated by homologous recombination. Positive transformations were determined by amplifying the 5' region of *CDC28* and digesting this fragment with NdeI, which was inserted near the Y19F substitution in pSF38. Additionally, positive *KAN^R-CDC28-Y19F* strains have no detectable Cdk1-Y19 phosphorylation as determined by immunoblotting using an α-Cdk1-P-Tyr antibody.

The *bar1*Δ*, his3::pCup1-GFP12-lacI12::HIS3, trp1::lacO-256X::TRP1, mih1*Δ*::LEU2, swe1*Δ*::TRP1, CDC28-HA-URA3*, *cdc16-6A-TRP1, cdc27-5A-KAN^R,* and *mad3*Δ*::LEU2* alleles have been described previously (Rudner and Murray, 2000; Rudner et al., 2000). Alanine-substituted mutants in *CDC16* and *CDC27* were made using site-directed mutagenesis.

cdc23-A-HYG^R was created by amplifying two PCR fragments: *HYG^R* (amplified from pAG32) and the 5' region of the *CDC23* allele, including the mutation (amplified from pAR240 which was originally used to create *cdc23-A-HA*, as described previously (Rudner and Murray, 2000)). Both fragments were cotransformed and integrated by homologous recombination. The *apc9-3A-HIS3* allele was created by transformation of the *HIS3* cassette amplified from pFA6a-HIS3MX6 (Longtine et al., 1998), and three sets of annealed oligonucleotides each containing a single alanine substitution, and integrated by homologous

recombination. In both cases, positive transformations were screened by restriction digest with sites inserted at the different substitutions.

MEC1, SML1 and *MIH1* were deleted using cassettes amplified from pAG25 (Goldstein and McCusker, 1999), pRS404 and directly from the *MATa* yeast deletion array (Thermo Fisher Scientific). *APC9, SWM1, CDC26* and *MND2* were deleted by amplifying the *HIS3* cassette from pFA6a-HIS3MX6 (Longtine et al., 1998). *cdc26$^{1-31}$-HIS3* and *cdc26$^{1-52}$-HIS3* were created using PCR-targeted recombination using pFA6a-GFP(S65T)-HIS3MX6 (Longtine et al., 1998) and gene-specific primers. A HindIII-XhoI fragment of the integrating plasmid pAR946 was transformed directly into yeast to delete *MAD2*.

2.2 PHYSIOLOGY

Unless noted in the figure legend, cells were grown in yeast extract peptone media with 2% dextrose (YEPD) at 25˚C or 30˚C. Cell cycle arrests were performed with 10µg/mL nocodazole (Sigma-Aldrich), 30µg/mL benomyl (Sigma-Aldrich) or 25-100ng/mL α-factor (Biosynthesis). Following arrest, cells were washed three times and resuspended in YEPD. Where noted, cells were re-arrested in α-factor (25-800ng/mL). *cdc15-2* arrest was performed by temperature shift to 35˚C for 2.5-3hr. In experiments using the *GAL-SWE1* or *GAL-MPS1* allele, cells were grown overnight in YEP + 2% raffinose and resuspended in YEP + 2% galactose to induce Swe1 or Mps1 overexpression.

To fix cells for microscopy, ~2.0x10^6 cells were harvested and fixed with 4% paraformaldehyde in PBS pH 7.5 for 15 minutes, washed in 100mM KPO_4/1.2M sorbitol pH 7.5, sonicated, and resuspended in KPO_4/sorbitol. Samples were imaged directly using a

Nikon TI microscope (Nikon) with a Nikon Plan Apo 60X 1.4 NA objective and FITC filter set (Chroma) at room temperature with a Photometrics CoolsnapHQ2 camera (Photometrics). Spindles were visualized using Spc42-eGFP fluorescence and budding morphology was visualized using brightfield illumination. A minimum of 200 cells were scored per timepoint. Sister chromatid separation was visualized using GFP-lacI and genomic lacO repeats integrated at the *TRP1* locus as previously described (Straight et al., 1996), and a minimum of 100 cells were scored per timepoint.

For serial dilution assays, cells of the indicated genotype were grown to saturation in YEPD at 25°C. 8-fold serial dilutions were spotted onto YEPD, YEP + 2% galactose, or YEP + 7.5µg/mL or 10µg/mL benomyl plates and incubated at the indicated temperature for 2 or 3 days. Plates were imaged with ImageQuant LAS4000 system (GE).

2.3 Flow Cytometry

$1.0x10^7$ cells were harvested at each timepoint and resuspended in 70% ethanol. Samples were rotated overnight at 4˚C, pelleted and treated with 0.25 mg/mL RNAse (Fisher) for 1 hour at 50˚C. After RNAse treatment, cells were treated with 0.25mg/mL proteinase K (Fisher) for 1 hour at 60˚C, stained with Sytox Green (Molecular Probes), and incubated for 30 minutes at room temperature. Samples were sonicated prior to analysis and analyzed using either an FC500 or CyAn ADP (BeckmanCoulter) flow cytometer using a 488nm laser.

2.4 SDS-PAGE AND WESTERN BLOTS

In experiments where only Western blots are shown, $3.0x10^7$ cells were harvested at the indicated timepoints and yeast extracts were prepared by bead beating (Biospec) frozen pellets in 1X SDS sample buffer and an equal volume of acid washed glass beads (Biospec) for 1 pulse of 60 sec. Samples were run on 10-15% polyacrylamide gels, except Cdc27 phosphorylation was visualized using gels containing 12.5% acrylamide/0.025% bisacrylamide (Anderson et al., 1973). Proteins were transferred to nitrocellulose using standard methods and stained with Ponceau S to ensure even loading. Membranes were blocked with antibody-specific blocking solutions (see below), and incubated overnight at 4ºC in the indicated primary antibody solutions. Membranes were washed with TBS + 0.1% Tween-20 (TBS-T), incubated with the appropriate HRP-conjugated α-mouse or α-rabbit secondary antibody solution (BioRad) at a 1:5000 dilution in TBS-T + 4% Fat Free Milk Powder for 30 minutes, washed with TBS-T and incubated in Western Lightning Plus-ECL (PerkinElmer). Signal detection was done on HyBlot CL (Denville) or XOMAT (Kodak) autoradiography film. Quantitative immunoblotting was performed using the ImageQuant LAS4010 (GE) system.

The following antibodies were used for Western blots and immunoprecipitations: 9E10 ascites (BabCO) was used at a dilution of 1:1000 in TBS-T with 0.02% NaN_3. Affinity-purified rabbit polyclonal α-Clb2 and α-Clb3 antibodies (Kellogg and Murray, 1995) were used at a dilution of 1:2500 and 1:2000 respectively in TBS-T with 2% BSA, 0.5M NaCl and 0.02%NaN_3. 12CA5 ascites (BabCO), rabbit polyclonal α-Cdk1, α-Swe1 (Harvey and Kellogg, 2003), α-Sgo1, α-Pds1, α-Clb5, α-Cdc26, α-Swm1, α-Cdc20, α-Cdh1,

α-Mad2 were used at 1:1000, α-Cdc27 (gift of Phil Hieter; (Lamb et al., 1994)), α-Apc1 at 1:2500, and α-Cdc23 at 1:2000 in TBS-T with 4% Fat Free Milk Powder, 5% glycerol, 0.02% NaN_3. P-cdc2 (Y15) (Cell Signaling) was used at a dilution of 1:1000 in TBS-T, 4% BSA, 0.02% NaN_3. Membranes were pre-blocked with TBS-T with 4% Fat Free Milk Powder, 5% glycerol before incubation with all primary antibodies with the exception of α-Clb2 and α-Clb3 blots which were blocked with TBS-T with 2% BSA, 0.5M NaCl.

α-Clb5, α-Pds1, α-Sgo1, α-Cdh1, α-Cdc23 and α-Swm1 antibodies were generated as follows. Coding sequences for the truncated proteins $Clb5_{2\text{-}137}$, $Pds1_{178\text{-}373}$, $Sgo1_{129\text{-}326}$, $Cdh1_{1\text{-}219}$, and $Cdc23_{500\text{-}626}$ and full length Swm1 were amplified using PCR and cloned into plasmid pGEX6P-1 (Promega) as BamH1/EcoR1 fragments. N-terminal GST fusion protein expression was induced using 0.25mM IPTG, cells were lysed in 1X PBS with 1mM EDTA, 1mM EGTA, 1mM PMSF, 15mM DTT, 0.5% Triton X-100 and 200ug/mL lysozyme. Lysate was batch bound to glutathione agarose and eluted with 50mM Tris pH 8.1, 0.5M NaCl and 5mM reduced glutathione. 1mg of each GST fusion protein was injected into rabbits every 4 weeks for 8 to 16 weeks (uOttawa animal facility). Rabbit serum was harvested, clarified by centrifugation and loaded on Affigel-10 (BioRad) columns coupled to purified MBP-Clb5, MBP-Pds1, MBP-Sgo1, MBP-Cdh1, MBP-Cdc23 or MBP-Swm1 respectively. Antibody was eluted with either 100mM triethylamine pH 11.5 or 100mM glycine pH 2.3. The triethylamine and glycine elutions were then dialyzed in PBS + 50% glycerol and stored at -80°C.

Coding sequence for the truncated protein $Apc1_{1500\text{-}1748}$ was amplified using PCR and cloned into pHIS-parallel2 as a BamH1/NotI fragment. α-Apc1 antibodies were purified

using an Affigel-10 (BioRad) column coupled to purified His_6-Apc1. α-Cdc20 antibody was generated as described (Camasses et al., 2003). Rabbit sera was purified as above using an Affigel-15 (BioRad) column coupled to purified His_6-$Cdc20_{470-610}$ which was expressed from a BamH1/Not1 fragment cloned into pHIS-parallel2. Plasmid His_6-$Cdk1_{2-298}$ (pAR727) (a gift of Vu Thai and Doug Kellogg, UCSC, Santa Cruz, Santa Cruz, CA) (Sreenivasan and Kellogg, 1999) was used to produce His_6-Cdk1 protein for injection into rabbits as described above. α-Cdk1 antibodies were purified using an Affigel-15 (BioRad) column coupled to purified His_6-Cdk1. Both His_6-$Cdc20_{470-610}$ and His_6-Cdk1 are insoluble so the coupling was done in the presence of 0.3% SDS.

α-Cdc26 and α-Mad2 antibodies antibodies were generated as described (Mad2 sera was a gift of Rey-Huei Chen, Institute of Molecular Biology, Academia Sinica, Taipei, Taiwan)(Chen et al., 1999; Hwang and Murray, 1997). In both cases, rabbit sera was purified using an Affigel-10 (BioRad) column coupled to GST protein to remove anti-GST antibodies and then affinity purified by using an Affigel-10 (BioRad) column coupled to Cdc26-GST or Mad2-GST fusion protein.

2.5 Preparation of IgG-coupled Dynabeads

M270 epoxy dynabeads (Invitrogen) were resuspended in dry DMF (Fisher) at a concentration of $2x10^9$ beads/mL. Using a magnet, DMF was removed and beads were washed in 0.1M sodium phosphate buffer, pH 7.4 at $1x10^9$ beads/mL. Beads were vortexed, washed again, and incubated at 25˚C for 10 min with end-over-end rotation. Beads were resuspended in 0.1M sodium phosphate buffer at $3x10^9$ beads/mL, vortexed, and an equal volume of 1mg/mL rabbit IgG (Sigma-Aldrich) was added. IgG was made fresh in 0.1M

sodium phosphate buffer. Beads were vortexed, an equal volume of 3M ammonium sulfate was added, and beads were incubated overnight at 37˚C with end-over-end rotation. The following morning, beads were washed quickly with an equal volume sodium phosphate buffer at 25˚C, followed by two washes with 10 min incubations. Beads were washed in sodium phosphate buffer with 1% Triton-X-100 for 10 min at 37˚C, with rotation, followed by a quick wash with equal volume sodium phosphate buffer at 25˚C, and two washes with 10 min incubations. To remove loosely associated IgG, beads were washed four times with 0.1M citric acid, pH 3.1 (at a volume of $1x10^8$ beads/mL). Finally, beads were washed with an equal volume sodium phosphate buffer, followed by three washes with 10 min incubations, and stored at a final concentration of $1x10^9$ beads/mL.

2.6 Purification of the APC, Cdk1/Clb2, PP2A^{Cdc55} and Bub1-Mad1 complexes

Purification of the APC was performed using a C terminal TAP tag on Cdc16 or Apc1 as described previously (Carroll and Morgan, 2002). pRS326 containing *pGAL-CLB2-TAP*, pAR546, was created by in vivo recombination in yeast by co-transforming the *CLB2* gene with overlapping homology to a BamH1/HindIII digested pRS-AB1234 (*pGAL-TAP*) plasmid (a gift of Christopher Carroll and David O. Morgan, UCSF, San Francisco, CA) and Clb2-TAP was overexpressed by growth in 2% galactose. PP2A^{Cdc55} complexes were purified from asynchronously growing *CDC55-TAP* (ADR5465) cells.

Anaphase Promoting Complex: Harvested cells were lysed in either a high salt APC lysis buffer (50mM Hepes-KOH pH 7.8, 700mM NaCl, 150mM NaF, 150mM Na-β-glycerophosphate pH 8.3, 1mM EDTA, 1mM EGTA, 5% glycerol, 0.25% NP-40, 1mM DTT,

1mM PMSF, 1mM Na_3VO_4, 1mM benzamidine, and leupeptin, bestatin, pepstatin A and chymostatin all at 1mM), or a modified, low salt buffer where indicated (identical to high salt lysis buffer, except 75mM NaCl, 50mM NaF and 50mM Na-β-glycerophosphate pH 8.3). Protein concentration was normalized according to the Bradford method (Bradford, 1976). The clarified lysate was incubated with IgG-coupled magnetic dynabeads for 1 hr at 4˚C. After binding, beads were washed three times with TAP core buffer (20mM Hepes pH 7.8, 150mM NaCl, 0.1% NP-40), and resuspended in TAP core with 20 units TEV protease (Invitrogen) for overnight cleavage at 4˚C. Cleaved APC was collected the following morning, and flash frozen in liquid nitrogen for use in ubiquitination assays.

Cdk1/Clb2 and PP2A^{Cdc55} complexes: Harvested cells were lysed in APC lysis buffer, and immunoprecipitated with IgG-coupled sepharose beads for 1-2hr at 4˚C. After binding, beads were transferred to a column, washed twice with lysis buffer, and twice with TAP core buffer. Beads were resuspended in 500µL TAP core buffer with 60µL TEV protease, and cleaved overnight at 4˚C. The following morning, cleaved Cdk1/Clb2-CBP or PP2A$^{Cdc55\text{-}CBP}$ complexes were drained from the column and resin was rinsed with an additional 500µL of calmodulin wash buffer (20mM HEPES, 150mM NaCl, 5% glycerol, 0.1% NP-40, 1mM MgOAc, 1mM imidazole, 0.1mM EDTA, 10mM BME, 0.2mM PMSF, 2mM $CaCl_2$). 5mM $CaCl_2$, 10mM BME and 1mM MgOAc was added to the cleaved Cdk1/Clb2-CBP or PP2A$^{Cdc55\text{-}CBP}$ complexes, and transferred to a new column loaded with calmodulin sepharose beads (GE), and rotated 1hr at 4˚C. Beads were washed three times with calmodulin wash buffer. Complexes were eluted off the column in 200µL fractions with elution buffer (identical to wash buffer except 10mM EGTA and no $CaCl_2$), run on a polyacrylamide gel,

and silver stained (Cdk1/Clb2: Fig. 2.1A, $PP2A^{Cdc55}$: Fig. 2.1D) or immunoblotted (Fig. 2.1B). Activity of purified Cdk1/Clb2-CBP complexes was assessed with histone H1 kinase assays (see below) (Fig. 2.1C).

Bub1-Mad1 complexes: Harvested cells were lysed in 1.5X lysis buffer (75mM Hepes pH 8.5, 15mM $Mg(OAc)_2$, 7.5% glycerol, 7.5mM EGTA, 0.75mM EDTA, 0.3% NP40, 75mM NaF, 75mM Na-β-glycerophosphate pH 8.3, 150mM NaOAc, 1mM PMSF, 1mM Na_3VO_4, 1mM benzamidine, and leupeptin, bestatin, pepstatin A and chymostatin all at 1mM). Protein concentration was normalized according to the Bradford method (Bradford, 1976). The clarified lysate was incubated with FLAG-M2 antibody (Sigma-Aldrich) coupled to protein G dynabeads (Invitrogen) for 1-2hr at 4˚C. After binding, beads were washed 1X with lysis buffer, and twice with TAP core buffer. Samples were boiled off the beads, and run on a polyacrylamide gel.

2.7 In Vivo Labelling of the APC

CDC16-TAP cells were arrested in mitosis by spindle checkpoint activation with nocodazole, and $10x10^7$ cells were harvested by centrifugation, washed twice in phosphate-free complete synthetic medium (Rothblatt and Schekman, 1989) and labelled in 2mL phosphate-free synthetic medium containing 0.5-1mCi $^{32}PO_4$ (Perkin Elmer) as described previously (Rudner and Murray, 2000). Uptake of label was monitored by scintillation counting (Perkin Elmer TriCarb 2910TR) of the cells and media, and exceeds 98%. Cells were labelled for 30-45 minutes, harvested by centrifugation, washed once in phosphate-free

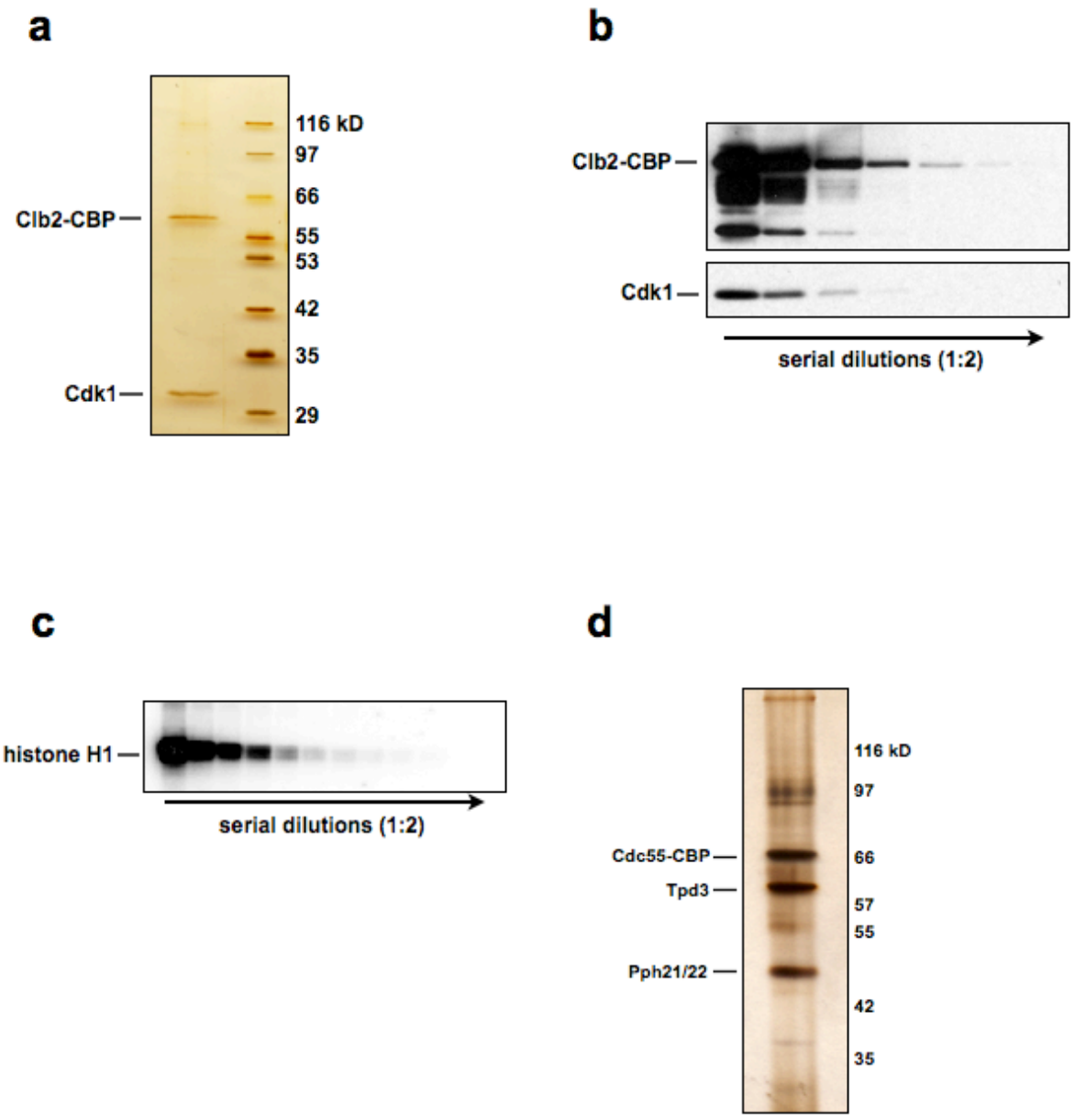
a
116 kD
97
66
55
53
42
35
29
Clb2-CBP
Cdk1
b
Clb2-CBP
Cdk1
serial dilutions (1:2)
c
histone H1
serial dilutions (1:2)
d
116 kD
97
66
57
55
42
35
Cdc55-CBP
Tpd3
Pph21/22

Figure 2.1 Purification of Cdk1/Clb2 and PP2A^{Cdc55} complexes

(A) Silver stain of purified Cdk1/Clb2-CBP complexes used for in vitro phosphorylation experiments. (B) Western blot of purified Cdk1/Clb2 complexes. Serial dilutions of Cdk1/Clb2 complexes were run on a polyacrylamide gel, and immunoblotted with the indicated antibodies. (C) Histone H1 kinase activity to confirm activity of purified Cdk1/Clb2 complexes. The substrate, histone H1, was incubated with serial dilutions of purified Cdk1/Clb2 complexes in the presence of ^{32}P-ATP at room temperature. Samples were run on a polyacrylamide gel, and exposed to phosphorimager screen. (D) Silver stain of purified PP2A^{Cdc55} complexes used for in vitro dephosphorylation experiments.

medium, and frozen in screw-cap tubes that contained a 100-fold excess of unlabelled *CDC16* cells (ADR4006).

The APC was purified as described above with the following modifications. IgG-coupled dynabeads were pre-incubated with 10-20 mg unlabelled *CDC16* lysate. The beads were washed twice in APC lysis buffer and then incubated with labelled lysate for 1-2 hr. Following this, beads were washed three times with lysis buffer, and once with 50mM Tris-HCl, pH 7.5. The beads were rotated in 50mM Tris-HCl, pH7.5, containing 0.5mg/mL RNAse A (Fisher) for 30min at 4˚C, washed twice with lysis buffer, and resuspended in sample buffer (2% SDS, 80mM Tris-Cl pH 6.8, 10% glycerol, 10mM EDTA, 0.02% bromophenol blue, 5% BME, and 1mM PMSF). Samples were run on a gradient polyacrylamide gel, exposed to phosphorimager screen, and quantified using a Typhoon Trio Phosphorimager and ImageQuant software (GE).

2.8 Kinase and Phosphatase Assays

Phosphorylation of histone H1 and the APC has been described previously (Rudner and Murray, 2000). For histone H1 kinase assays, Clb-associated complexes were purified with 1-2µL of α-Clb2, α-Clb3 or α-Clb5 antibodies and protein A magnetic beads (Invitrogen). After immunoprecipitation, beads were washed three times in kinase bead buffer (500mM NaCl, 50mM Tris-HCl pH7.4, 50mM NaF, 5mM EGTA, 5mM EDTA, 0.1% Triton X-100), and twice in kinase buffer (80mM Na-ß-glycerophosphate pH 7.4, 15mM $MgCl_2$, 20mM EGTA). Kinase reactions were performed in 15µL kinase buffer containing 1mM DTT,

25μM ATP, 2.5ug histone H1 (Upstate Biotechnology) and 1μCi of **γ-**[^{32}P]-ATP (Perkin Elmer) and were incubated for 25 min at 25˚C. Reactions were stopped by the addition of sample buffer, and heated at 65˚C for 10 min. Samples were run on a polyacrylamide gel, exposed to phosphorimager screen, and quantified using a Molecular Dynamics or a Typhoon Trio Phosphorimager and ImageQuant software (GE).

To phosphorylate the APC, the APC was purified as described above. After immunoprecipitation with IgG-coupled dynabeads, the beads were washed three times with APC lysis buffer, and once in kinase buffer. A fraction of the beads were subject to phosphorylation with Cdk1/Clb2 complexes in the presence of 1μCi of **γ-**[^{32}P]-ATP to confirm the phosphorylation reaction was successful, and the remainder was subject to a cold phosphorylation reaction. Both reactions were performed with cold ATP: 1mM for cold reactions and 0.01mM ATP for hot reactions. APC phosphorylated with labelled ATP (hot reactions) were stopped by the addition of sample buffer, run on a polyacrylamide gel, exposed to phosphorimager screen and quantified using a Molecular Dynamics or a Typhoon Trio Phosphorimager and ImageQuant software (GE). APC phosphorylated with unlabelled ATP (cold reactions) was washed, cleaved, and tested in ubiquitination or activator binding assays.

To dephosphorylate the APC, the APC was purified as described above. After immunoprecipitation with IgG-coupled dynabeads, the beads were washed three times with APC lysis buffer, and once with calmodulin buffer with 1mM DTT. PP2A^{Cdc55} reactions were performed in the calmodulin buffer, and lambda phosphatase (New England Biolabs, Inc.) reactions were performed in the buffer provided. Reactions were performed for 25 min at

room temperature and dephosphorylated APC was washed, cleaved, and tested in the activator binding assay.

2.9 Ubiquitination & in vitro Activator Binding Assays

Purification of the APC using a C terminal TAP tag on Cdc16 or Apc1 was performed as described above. ^{35}S-methionine labelled substrates Pds1-ZZ, Pds1-db/kb-ZZ and Clb5-HA-ZZ, Clb5-dbΔ-HA-ZZ, and unlabelled activators ZZ-Cdc20 and ZZ-Cdh1 (gifts of Maria Enquist, Scott Foster and David Morgan, UCSF, San Francisco, CA) were made in vitro (Promega TnT T7 Quick Coupled Transcription/Translation System), and purified with IgG-coupled magnetic beads. Proteins were cleaved from beads for 30 min at 25˚C with TEV protease. His_6-Uba1 was purified from yeast, and His_6-Ubc1, His_6-Ubc4 were purified from bacteria as described previously (Carroll and Morgan, 2005; Rodrigo-Brenni and Morgan, 2007). A typical reaction contains Uba1 (E1), Ubc1 and Ubc4 (E2), ubiquitin aldehyde (Cedarlane), 2 μM LLnL, 1mM ATP (Fisher), 150μM ubiquitin (Cedarlane), activator, substrate, and purified APC (Fig. 2.2). 0.01mg of methyl ubiquitin (Cedarlane) was used in APC^{Cdc20} assays, unless otherwise indicated. Ubiquitination reactions were incubated at room temperature for 20 minutes (Cdh1) or 40 minutes (Cdc20). Alternatively, to assess activator binding to the APC, untagged Cdh1 and Cdc20 were made in vitro as above (without subsequent purification) and incubated with APC bound to dynabeads for 25 min at room temperature, followed by three washes with modified TAP core buffer (20mM Hepes pH 7.8, 75mM NaCl, 0.1% NP-40) to remove loosely bound proteins. All reactions were stopped by the addition of sample buffer. Samples were heated 10 min at 65°C, run on a polyacrylamide

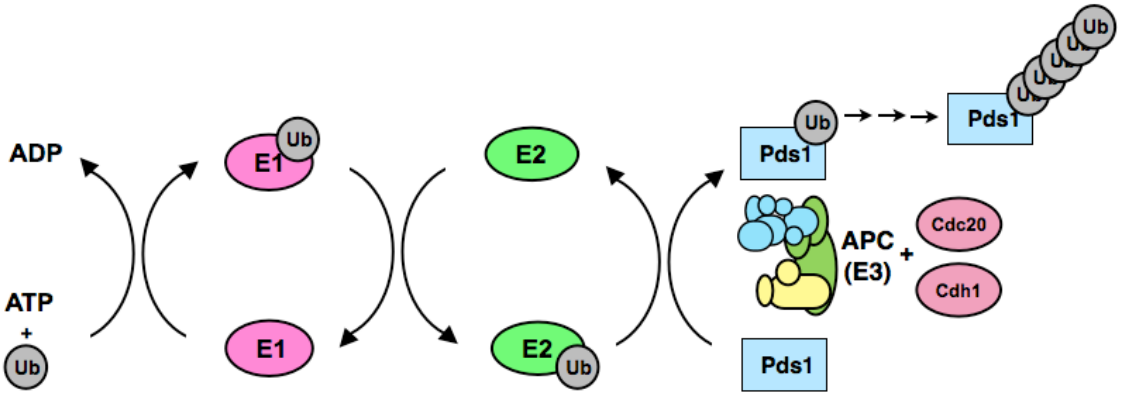
ADP
ATP
+
Ub
E1
Ub
E1
E2
E2
Ub
Pds1
Ub
Pds1
Ub
Pds1
APC
(E3)
+
Cdc20
Cdh1

Figure 2.2 Schematic of in vitro ubiquitination assay

^{35}S-methionine labeled substrate, and activators Cdc20 and Cdh1 are made in an in vitro transcription and translation reaction and purified using IgG-coupled magnetic beads. The substrate depicted here is Pds1, although other substrates may also be used. The E1 enzyme, Uba1, is purified from yeast, and two E2 enzymes, Ubc1 and Ubc4, are purified from bacteria as His6-fusion proteins. The APC is purified using a C terminal TAP tag on Cdc16, or Apc1. All the required components for ubiquitination are combined and reactions are incubated at room temperature. Cdh1 reactions are stopped by the addition of sample buffer after 25 minutes, and Cdc20 reactions after 40 minutes. Reactions are heated for 10 minutes at 65°C, and run on a polyacrylamide gel and exposed to phosphorimager screen.

gel and exposed to phosphorimager screen. Results were quantified using a Molecular Dynamics or a Typhoon Trio Phosphorimager and ImageQuant software (GE).

Chapter 3: Cdk1 phosphorylation of the APC regulates anaphase onset

3.1 Introduction

Oscillations in the activity of cyclin dependent kinases (Cdks) drive mitotic progression. Active Cdk1/cyclin complex is required to initiate the early events of mitosis, while the inactivation of Cdk1 is essential for mitotic exit and entry into the next G1. In particular, Cdk1 activity is important for anaphase onset. In support of this, Cdk1/Clb activity is required for the metaphase-anaphase transition (Félix et al., 1990; Rahal and Amon, 2008; Rudner et al., 2000). This Cdk1-dependent regulation of anaphase onset is thought to be due to phosphorylation and the activation of the APC^{Cdc20} (Félix et al., 1990; King et al., 1995; Kraft et al., 2003; Lahav-Baratz et al., 1995; Patra and Dunphy, 1998; Rudner and Murray, 2000; Shteinberg et al., 1999), but it remains unclear whether Cdk1 phosphorylation of the APC is required to trigger anaphase onset.

Although the APC^{Cdc20} is essential for triggering anaphase, it is not well understood how the APC^{Cdc20} is initially activated to trigger anaphase onset. Early studies correlated phosphorylation of the APC with an increase in ubiquitination activity (Peters et al., 1996) (Lahav-Baratz et al., 1995; Sudakin et al., 1995). These studies have been limited, however, because of the lack of mutational analysis to correlate specific phosphorylation events with changes in APC activity. A single study in budding yeast showed that mutation of Cdk1-dependent phosphorylation sites in three subunits of the budding yeast APC slowed mitotic progression, but didn't abolish it (Rudner et al., 2000). This strain, the *apc-12A* mutant (with twelve Cdk1 phosphorylation sites on APC subunits Cdc16, Cdc23 and Cdc27 mutated), is

still viable, suggesting that either Cdk1 phosphorylation of the APC is not essential, or that there are additional phosphorylation events that contribute to full activation.

Prior to mitotic entry, Cdk1 activity is inhibited by the tyrosine kinase, Swe1, by phosphorylation of a conserved tyrosine residue, Y19 (Russell and Nurse, 1987) (Fig. 1.1B). This inhibitory phosphorylation is important for regulating mitotic entry, and is reversed by the phosphatase, Mih1, once appropriate conditions are met (Harvey and Kellogg, 2003; Kellogg, 2003; Nurse, 1975; Russell et al., 1989). Using Swe1 to inhibit Cdk1 activity in mitosis, this chapter examines the role of Cdk1 phosphorylation of the APC, and how the loss of this phosphorylation affects cell cycle progression, and ubiquitination activity in vitro.

In budding yeast, Swe1 and Mih1 are also targets of a morphogenesis checkpoint that has been shown to delay mitotic onset in response to either defects in the actin cytoskeleton, small cell size, or the extent of membrane growth (Anastasia et al., 2012; Harvey and Kellogg, 2003; Lew and Reed, 1995; McMillan et al., 1998; McNulty and Lew, 2005). Inhibitory phosphorylation on Cdk1 is the target of this checkpoint (Harvey and Kellogg, 2003; Lew and Reed, 1995). The experiments presented in this chapter also complement work demonstrating that Swe1 functions to delay anaphase onset in unperturbed cells, as well as during Swe1-dependent checkpoint activation (Lianga et al., 2013).

3.2 RESULTS

Overexpression of Swe1 reduces phosphorylation of the APC and arrests cells in metaphase

In order to address the role of Cdk1-dependent phosphorylation of the APC, Swe1 was overexpressed in mitosis with the use of a galactose-inducible promoter (the *GAL-SWE1* strain) to inhibit Cdk1 activity. Since Cdk1 phosphorylates the APC (Kraft et al., 2003; Lahav-Baratz et al., 1995; Patra and Dunphy, 1998; Rudner and Murray, 2000; Shteinberg et al., 1999), and Swe1 inhibits Cdk1 activity (Russell and Nurse, 1987), we hypothesized that induction of high levels of Swe1 would result in a loss of phosphorylation of the APC. To test this, we monitored in vivo phosphorylation of purified APC after metabolic labeling of cells with inorganic ^{32}P-labelled orthophosphate. Overexpression of Swe1 in cells arrested in mitosis resulted in a loss of phosphorylation with respect to wild type of five subunits of the APC: Apc1, Cdc16, Cdc27, Cdc23 and Apc9 (Fig. 3.1A).

In order to determine the effect of this decrease in Cdk1-dependent phosphorylation of the APC on cell cycle progression, Swe1 was again overexpressed in cells arrested in mitosis with nocodazole, a microtubule depolymerizing drug that induces a mitotic arrest by activating the spindle assembly checkpoint (Hoyt et al., 1991; Li and Murray, 1991), the expression of Swe1 was induced by addition of galactose. Cells were released from the mitotic arrest by washing out the nocodazole, and any cells that released from the arrest were arrested in the following G1 by the addition of alpha factor, a mating pheromone that induces a G1 arrest in budding yeast (Duntze et al., 1970). Cell cycle progression was monitored by immunoblot analysis of the levels of several different APC substrates: the mitotic cyclins

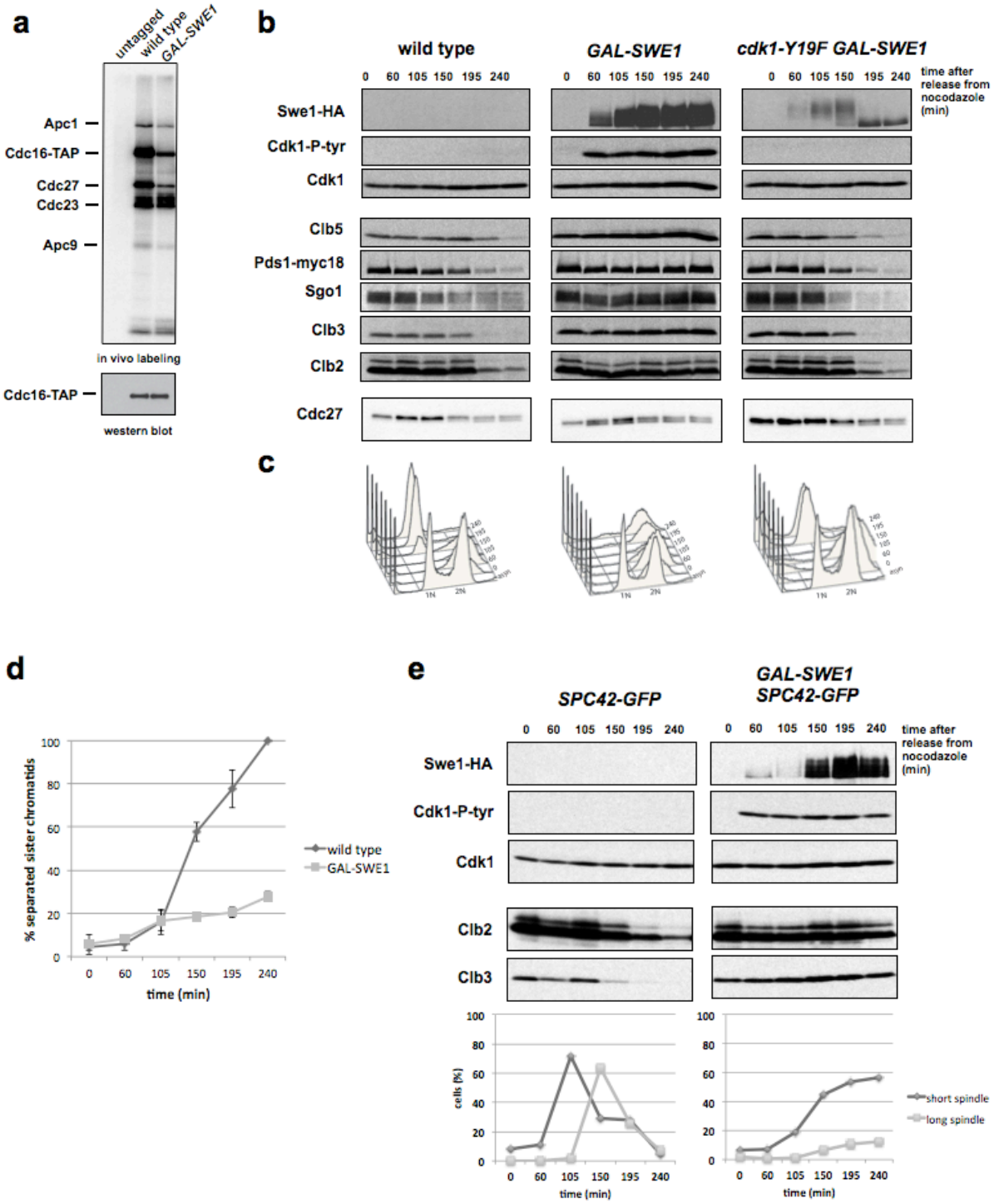
a
untagged
wild type
GAL-SWE1
Apc1
Cdc16-TAP
Cdc27
Cdc23
Apc9
in vivo labeling
Cdc16-TAP
western blot
b
wild type
GAL-SWE1
cdk1-Y19F GAL-SWE1
0 60 105 150 195 240
time after release from nocodazole (min)
Swe1-HA
Cdk1-P-tyr
Cdk1
Clb5
Pds1-myc18
Sgo1
Clb3
Clb2
Cdc27
c
1N
2N
d
% separated sister chromatids
time (min)
wild type
GAL-SWE1
e
SPC42-GFP
GAL-SWE1 SPC42-GFP
0 60 105 150 195 240
time after release from nocodazole (min)
Swe1-HA
Cdk1-P-tyr
Cdk1
Clb2
Clb3
cells (%)
time (min)
short spindle
long spindle

Figure 3.1 Overexpression of Swe1 blocks cells in metaphase

(A) Wild type (ADR22), *CDC16-TAP* (ADR3877) and *GAL-SWE1 CDC16-TAP* (ADR3858) cells were grown in YEP + 2% raffinose, arrested in mitosis with nocodazole (10µg/mL) and *GAL-SWE1* was induced with 2% galactose for 90 minutes. Cells were then washed in medium lacking phosphate, and grown for 45 minutes in the presence of [^{32}P] orthophosphate. The APC was purified, run on a polyacrylamide gel and exposed to phosphorimager screen or immunoblotted. (B and C) Overexpression of Swe1 in mitosis stabilizes APC substrates and arrests cells with a 2N DNA content. Wild type (ADR2617), *GAL-SWE1* (ADR3871) and *GAL-SWE1 cdk1-Y19F* (ADR4228) cells were grown in YEP + 2% raffinose, arrested in nocodazole (10µg/mL), and *GAL-SWE1* was induced with 2% galactose (t=0) for 1 hour. Nocodazole was washed out, and cells released into YEP + 2% galactose. α-factor (25ng/mL) was added (t=150) to arrest cells in the following G1. Samples were taken for immunoblotting (B) and flow cytometry (C) at the indicated timepoints. Cdk1 is used as a loading control. (D) Overexpression of Swe1 impairs sister chromatid separation. Wild type (ADR1393) and *GAL-SWE1* (ADR1395) strains were grown as in (B), except 1mM $CuSO_4$ was added at t=-30 to induce expression of GFP-lacI, and the separation of sister *lacO* arrays at *TRP1* (~12kb from *CENIV)* was visualized by fluorescence microscopy. (E) Overexpression of Swe1 blocks anaphase spindle elongation. *SPC42-eGFP* (ADR4169) and *GAL-SWE1 SPC42-eGFP* (ADR4171) strains were grown as in (B), and samples were taken for immunoblotting and fluorescence microscopy at the indicated timepoints. Cdk1 is used as a loading control. Short and long mitotic spindles were visualized by measuring the distance between Spc42-eGFP labelled spindle pole bodies using fluorescence microscopy. The graphs shown are representative of one of two repeats.

Clb2, Clb3 and Clb5, the anaphase inhibitor Pds1, and Shugoshin (Sgo1), a protein that protects centromeric cohesion during meiosis (Kitajima et al., 2004), and is required for sensing a lack of tension on mitotic chromosomes (Indjeian et al., 2005) (see (Lianga et al., 2013) for evidence that Sgo1 degradation depends on the APC). As expected, inhibitory phosphorylation on Cdk1 accumulates when Swe1 is induced to high levels (Fig. 3.1B, Cdk1-P-tyr blot). Fig. 3.1B shows that all of these substrates are degraded in wild type cells as the cells release into G1, but remain stable in the *GAL-SWE1* strain, consistent with a metaphase block of the cell cycle.

The stabilization of protein levels of the mitotic substrates shown in Fig. 3.1B suggests that Swe1 overexpression is preventing APC activation and proteolysis of its substrates, through inhibition of Cdk1. When the conserved tyrosine residue in Cdk1 is mutated to phenylalanine so it can no longer be phosphorylated by Swe1 (*cdk1-Y19F GAL-SWE1* - third panel, Fig. 3.1B), substrates of the APC are degraded as in wild type, arguing the cell cycle block is due to specific phosphorylation and inhibition of Cdk1 activity by Swe1. Flow cytometry indicates that both the wild type and *cdk1-Y19F GAL-SWE1* strains release from the mitotic arrest into G1, with 1N DNA content (Fig. 3.1C). Since the degradation of Pds1 and the mitotic cyclins is required for the completion of anaphase and mitotic exit, cells overexpressing Swe1 do not exit from mitosis, and remain arrested with a 2N DNA content (Fig. 3.1C).

Changes in the phosphorylation status of the APC subunit Cdc27 are also evident by the electrophoretic mobility shift seen in Fig. 3.1B. The mitotic arrest (T=0) shows a predominance of the phosphorylated or slower migrating form of Cdc27 (Rudner and

Murray, 2000). After Swe1 induction, Cdc27 immediately becomes dephosphorylated (T=60), while the dephosphorylated form is not visible in wild type cells until they have re-entered G1 (T=195). These differences argue that high levels of Swe1 result in dephosphorylation of Cdc27, confirming the decrease seen in Fig. 3.1A.

There are clear differences in the phosphorylated forms of Swe1 when the *GAL-SWE1* and the *cdk1-Y19F GAL-SWE1* strains are compared (Fig. 3.1B, Swe1 blot). The relationship between Cdk1 and Swe1 is more complex than previously described. Rather than Swe1 solely inhibiting Cdk1, Cdk1 initially phosphorylates and activates Swe1 before Swe1 can inhibit Cdk1 (Harvey et al., 2005). Preventing Cdk1 inhibition by Swe1 (using the *cdk1-Y19F* allele) has been shown to cause an increase in Swe1 phosphorylation and leads to the dramatic changes in electrophoretic mobility of Swe1 seen here. Although these differences are a limitation of these experiments, they don't alter the conclusion that Swe1-dependent inhibition of Cdk1 blocks the destruction of APC substrates and the onset of anaphase.

The metaphase-anaphase transition can also be assayed by directly monitoring sister chromatid separation. Visualization of this process was accomplished by expression of a copper-inducible (using the *CUP1* promoter) GFP-lacI fusion protein that binds an integrated array of 256 repeats of the lactose operon near the centromere (Biggins and Murray, 2001; Straight et al., 1996), using the same experimental setup as described for Fig. 3.1B. Upon induction, the GFP-lacI fusion protein binds the lacO array, and the fluorescence is visualized by microscopy. The appearance of two dots in a single cell suggests that pairs of sister chromatids have separated. Cells that fail to separate remain as a single diffraction limited dot. As expected, wild type cells separate their sister chromatids after release from

nocodazole (Fig. 3.1D, T=60), whereas the overexpression of Swe1 impairs sister chromatid separation (Fig. 3.1D).

Rapid elongation of the mitotic spindle also occurs in anaphase. In order to visualize spindles, a GFP-tagged component of the spindle pole body, *SPC42*, was used to monitor spindle length. Fig. 3.1E shows that *GAL-SWE1 SPC42-GFP* cells also stabilize APC substrates using the same experimental setup as described for Fig. 3.1B. Visualization of the mitotic spindles using fluorescence microscopy indicates that *GAL-SWE1* cells rebuild metaphase spindles following release from the nocodazole arrest at a slightly slower rate than wild type cells, but the spindles do not elongate (Fig. 3.1E, graphs). Unlike wild type, *GAL-SWE1* cells are unable to undergo the rapid spindle elongation that occurs in anaphase, further arguing these cells are arrested in metaphase.

Other work from the Rudner laboratory, in a parallel set of experiments, has shown that induction of the Swe1-dependent morphogenesis or cell size checkpoint also results in a metaphase arrest, and stabilization of the APC substrates (Lianga et al., 2013), arguing that the APC is a target of this checkpoint. These results are consistent with those presented above, and with overexpression of Swe1 and morphogenesis checkpoint activation similar levels of Y19 phosphorylation accumulate on Cdk1.

Stabilization of APC substrates is not due to activation of cell cycle checkpoints

The DNA damage checkpoint inhibits the metaphase-anaphase transition by activating a pathway that ultimately leads to the stabilization of Pds1 (Sanchez et al., 1999). In order to address the possibility that overexpression of Swe1 activates the DNA damage checkpoint

pathway, the timecourse experiment in Fig. 3.1B was repeated with wild type and *GAL-SWE1* strains in which the checkpoint kinase, *MEC1,* was deleted in order to inactivate the checkpoint (Weinert et al., 1994). Overexpression of Swe1 in the absence of Mec1 still stabilized APC substrates, arguing that the metaphase arrest seen with high levels of Swe1 is not due to activation of the DNA damage checkpoint (Fig. 3.2A, B).

The spindle assembly checkpoint also blocks the metaphase-anaphase transition until all chromosomes have made proper bipolar attachments to the mitotic spindle. Unattached kinetochores signal the production of the mitotic checkpoint complex (MCC), which includes the co-activator Cdc20, thus inhibiting APC^{Cdc20} activity, and preventing anaphase onset until errors are resolved (Chao et al., 2012; Sudakin et al., 2001). Deletion of a spindle checkpoint component, *MAD2*, inactivates the spindle checkpoint (Li and Murray, 1991), and still leads to stabilization of APC substrates upon Swe1 overexpression (Fig. 3.2C). In this experiment, Swe1 was induced as cells were released from a G1 arrest rather than a nocodazole arrest because spindle depolymerization will not induce a mitotic arrest in the absence of a functional spindle checkpoint (Hoyt et al., 1991; Li and Murray, 1991). These results argue that Swe1-dependent stabilization of APC substrates is not due to the activation of cell cycle checkpoints that act to inhibit anaphase initiation.

Stabilization of APC substrates depends on Swe1 kinase activity

One study has suggested that Swe1 may be a substrate of the APC (Thornton and Toczyski, 2003). If this is the case, overexpression of Swe1 could saturate the active site of

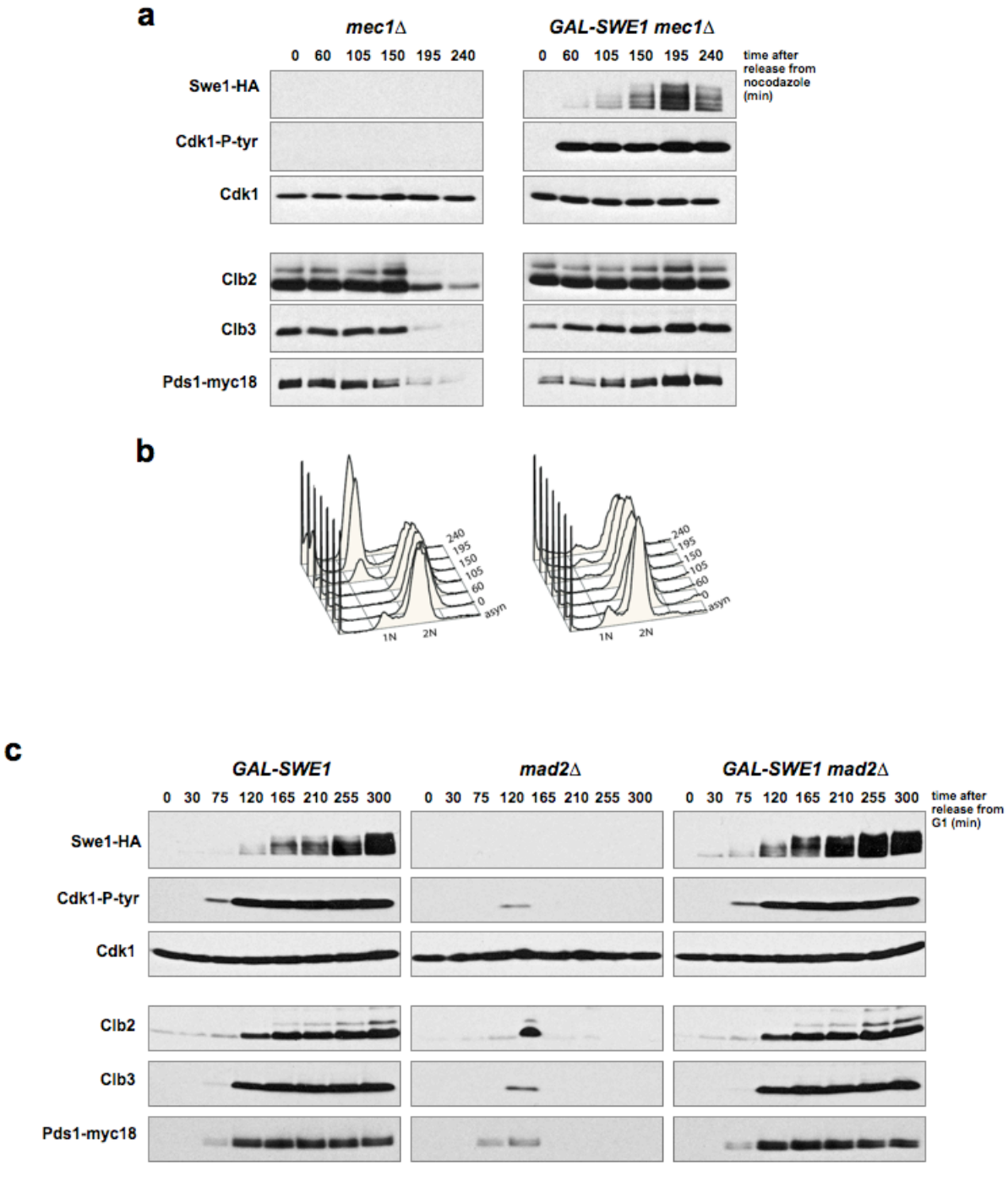
a
mec1Δ
GAL-SWE1 mec1Δ
0 60 105 150 195 240
0 60 105 150 195 240
time after release from nocodazole (min)
Swe1-HA
Cdk1-P-tyr
Cdk1
Clb2
Clb3
Pds1-myc18
b
240
195
150
105
60
0
asyn
1N
2N
c
GAL-SWE1
mad2Δ
GAL-SWE1 mad2Δ
0 30 75 120 165 210 255 300
0 30 75 120 165 210 255 300
0 30 75 120 165 210 255 300
time after release from G1 (min)
Swe1-HA
Cdk1-P-tyr
Cdk1
Clb2
Clb3
Pds1-myc18

Figure 3.2 Swe1-dependent cell cycle arrest does not depend on cell cycle checkpoints

(A and B) Metaphase arrest caused by Swe1 overexpression is not due to activation of the DNA damage checkpoint. *mec1*Δ (ADR3921) and *GAL-SWE1 mec1*Δ (ADR3919) cells were grown as described in Fig. 1B, and samples were taken for immunoblotting (A) and flow cytometry (B). (C) Metaphase arrest caused by Swe1 overexpression is not due to activation of the spindle checkpoint. *GAL-SWE1* (ADR3871)*, mad2*Δ (ADR3938) and *GAL-SWE1 mad2*Δ **(**ADR3940**)** cells were grown overnight in YEP + 2% raffinose at 30˚C, arrested in α-factor (1ug/mL) for 3 hours, α-factor was washed out and cells were released into YEP + 2% galactose. α-factor (1ug/mL) was added (t=165) to arrest cells in the following G1 and samples were taken for immunoblotting. Cdk1 is used as a loading control in both (A) and (C).

the APC, and prevent the ubiquitination and degradation of other APC substrates. Overexpression of a kinase dead Swe1, which mutates a conserved asparagine in the catalytic domain to an alanine (N584A) (Harvey et al., 2005), does not slow the degradation of APC substrates (Fig. 3.3A). Flow cytometry also confirms the strain expressing the kinase dead version of Swe1 releases from the mitotic arrest into G1 (Fig. 3.3B), arguing that the stabilization is dependent on the kinase activity of Swe1, and is therefore not due to saturation of the active site of the APC. Again, there are clear differences in the phosphorylated forms of Swe1 when the *GAL-SWE1* and the *GAL-swe1-N584A* strains are compared (Fig. 3.3A, Swe1 blot). As described earlier, preventing Cdk1 inhibition by Swe1 (using the kinase dead Swe1 in this case) increases Swe1 phosphorylation, and results in the dramatic changes in electrophoretic mobility seen here.

Swe1 inhibits Clb-associated kinase activity

Past work has shown Wee1 phosphorylation of Cdk1 causes complete inhibition of Cdk1 (Parker et al., 1992), so we were surprised that overexpression of the budding yeast homolog Swe1 did not drive cells out of mitosis, as overexpression of the Cdk1 inhibitor, Sic1, does (Amon, 1997). Swe1-dependent inhibition of Cdk1 can be seen by the increase in phosphotyrosine levels when Swe1 expression is induced (Fig. 3.1B, Cdk1-P-tyr blot). As an alternative way to look at Swe1 inhibition, the activity of immunoprecipitated Clb2-, Clb3-, and Clb5-associated Cdk1 complexes was measured using the model substrate histone H1 in a kinase assay. When Cdk1 activity is measured using histone H1, we can see that, as

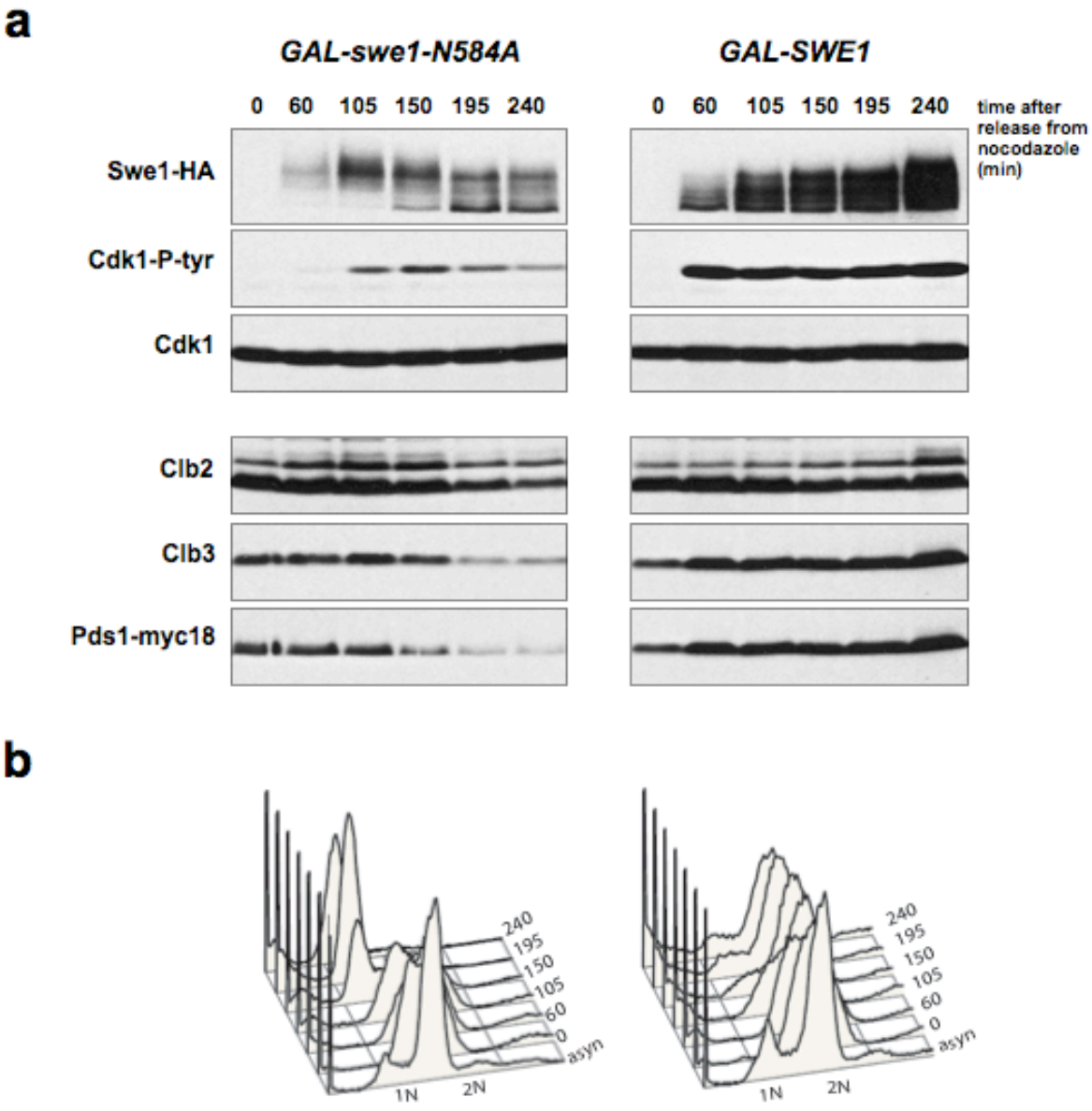
a
GAL-swe1-N584A
GAL-SWE1
0 60 105 150 195 240
0 60 105 150 195 240
time after release from nocodazole (min)
Swe1-HA
Cdk1-P-tyr
Cdk1
Clb2
Clb3
Pds1-myc18
b
240
195
150
105
60
0
asyn
1N
2N
240
195
150
105
60
0
asyn
1N
2N

Figure 3.3 Swe1-dependent cell cycle arrest depends on Swe1 kinase activity

(A and B) Overexpression of a kinase-dead Swe1 does not cause mitotic arrest. *GAL-swe1-N584A* (ADR3738) and *GAL-SWE1* (ADR3740) cells were grown as described in Fig. 1B, and samples were taken for immunoblotting (B), and flow cytometry (C). Cdk1 is used as a loading control.

expected, activity falls as tyrosine phosphorylation accumulates on Cdk1 (Fig. 3.4A, graphs). After an hour of Swe1 induction, the cyclin-associated activity of the *GAL-SWE1* strain falls to 60-80% of its starting activity, whereas wild type cyclin-associated activity falls to undetectable levels as they exit mitosis (Fig. 3.4A). When these precipitates are probed for tyrosine-phosphorylated Cdk1, all three mitotic cyclins are associated with phosphorylated Cdk1 (Fig. 3.4B), revealing that Swe1 does not preferentially target a particular Cdk1-Clb complex. Rather, Swe1 appears to be inhibiting each complex similarly. The levels of Cdk1 activity are similar following the induction of Swe1 in the wild type and *cdk1-Y19F GAL-SWE1* strains, indicating the change in activity is due to Swe1-dependent phosphorylation and inhibition of Cdk1-cyclin complexes.

We also wondered whether morphogenesis checkpoint activation, using the actin depolymerizing drug latrunculin A (latA), would cause preferential phosphorylation of a specific Cdk1/Clb complex. Nearly identical levels of inhibitory phosphorylation accumulate on Cdk1 in a latA arrest as with *GAL-SWE1*, despite the enormous difference in the levels of Swe1 (Fig. 3.4C). We therefore immunoprecipitated different Cdk1/Clb complexes during a latA-induced checkpoint arrest and found that the ratio of tyrosine-phosphorylated Cdk1 to total Cdk1 is nearly identical for each Clb complex (Fig. 3.4D). Consistent with the experiment in Fig. 3.4B, Swe1 has no obvious preference in vivo for a specific Cdk1/Clb complex during morphogenesis checkpoint arrest.

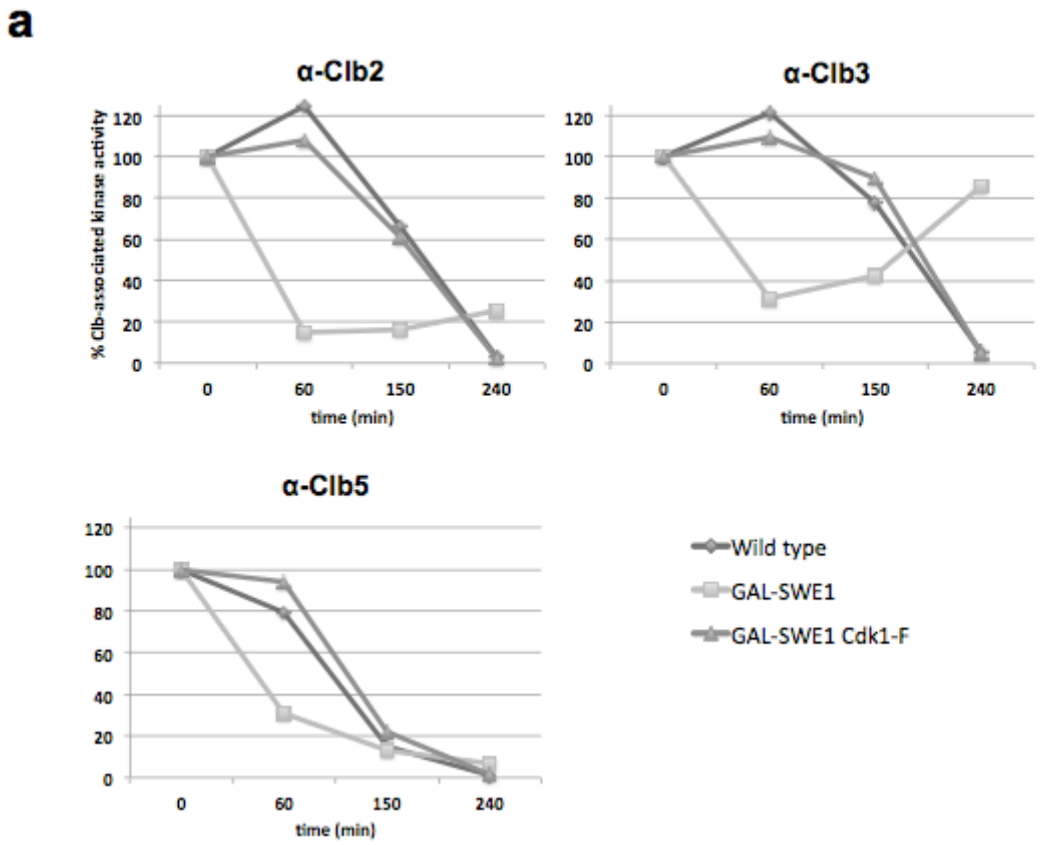
a
α-Clb2
α-Clb3
α-Clb5
% Clb-associated kinase activity
120
100
80
60
40
20
0
0
60
150
240
time (min)
Wild type
GAL-SWE1
GAL-SWE1 Cdk1-F

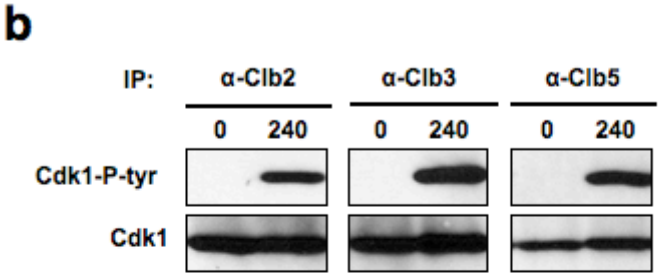
b
IP:
α-Clb2
α-Clb3
α-Clb5
0
240
Cdk1-P-tyr
Cdk1

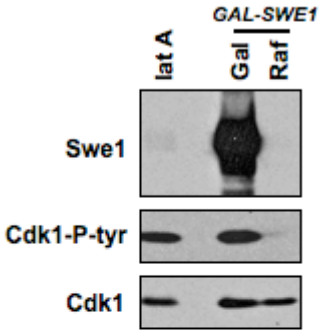
c
GAL-SWE1
lat A
Gal
Raf
Swe1
Cdk1-P-tyr
Cdk1

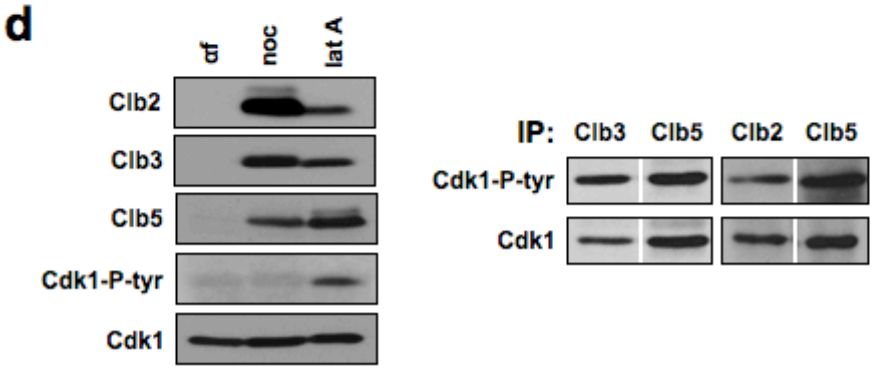
d
αf
noc
lat A
Clb2
Clb3
Clb5
Cdk1-P-tyr
Cdk1
IP:
Clb3
Clb5
Clb2
Clb5
Cdk1-P-tyr
Cdk1

Figure 3.4 Swe1 inhibits Clb-associated kinase activity

(A) Swe1 inhibits Clb-associated kinase activity. Strains were grown as in described in Fig. 1B, and Cdk1-Clb2, Clb3 or Clb5 complexes were immunoprecipitated with anti-Clb antibodies at the indicated timepoints and their histone H1 kinase activity was measured to assess the inhibition of Cdk1 activity. Samples were run on a polyacrylamide gel, exposed to phosphorimager screen, and quantified using ImageQuant software. The graphs shown are representative of one of three repeats. (B) Overexpressed Swe1 does not preferentially phosphorylate a particular Cdk1-cyclin complex. *GAL-SWE1* cells (ADR3871) were grown as described in Fig. 1B. Cdk1-Clb2, Clb3 or Clb5 complexes were immunoprecipitated at the indicated timepoints, and analyzed by immunoblotting with anti-Cdk1 and anti-Cdk1-P-tyr antibodies. (C) Swe1 overexpression and latA induce similar levels of tyrosine phosphorylation on Cdk1. Wild type (ADR4009) cells were treated with latA and *GAL-SWE1* (ADR4289) cells were grown in YEP + 2% raffinose (Raf) and induced by addition of 2% galactose (Gal). Cells were harvested and immunoblotted for Swe1, Cdk1, and Cdk1-P-tyr. (D) LatA-activated Swe1 does not preferentially phosphorylate a particular Cdk1/cyclin complex. Wild type (ADR4006) cells were arrested with 100ng/mL α-factor, 10ug/mL nocodazole, or 2.5 uM latA. Cells were harvested for immonoblotting (left), or, for the latA-arrested cells, immunoprecipitation. Cdk1/Clb2, Clb3 or Clb5 complexes were immunoprecipitated, normalized for Cdk1 levels, and blotted for Cdk1 and Cdk1-P-tyr to compare the relative stoichiometry of tyrosine-phosphorylated Cdk1. Two independent experiments are shown, one that compares Clb3 and Clb5 immunoprecipitates (left) and one that compares Clb2 and Clb5 immunoprecipitates (right).

Overexpression of Swe1 in anaphase is sufficient to turn off the APC^{Cdc20}

Overexpression of Swe1 in mitosis, through inhibition of Cdk1, causes a metaphase block in the cell cycle, which prevents activation of the APC^{Cdc20}. APC-dependent degradation of mitotic substrates, including Pds1 and the mitotic cyclins, occurs throughout anaphase, and so we wondered whether inhibition of Cdk1 during anaphase, after the initial activation of the APC^{Cdc20} has already occurred, could turn off the APC. The protein kinase Cdc15 is a component of the mitotic exit network (MEN), and inactivation of this kinase through the use of a temperature sensitive allele, *cdc15-2*, blocks cells in anaphase when grown at the restrictive temperature. Using this allele, we found that expression of Swe1 during anaphase, after the APC^{Cdc20} has been activated, is also sufficient to turn off the APC^{Cdc20}. When Swe1 expression is induced in anaphase-arrested *cdc15-2* cells, Clb2, Clb5, Pds1 and Sgo1 are restabilized, accumulating to levels as high as seen during a mitotic arrest (Fig. 3.5, noc panel).

Overexpression of Swe1 reduces APC^{Cdc20} activity in vitro

The stabilization of APC substrates seen under conditions of Swe1 overexpression argues that inhibition of Cdk1 is inhibiting activation of the APC^{Cdc20}, and preventing anaphase onset. In order to confirm that this phenotype is due to a direct effect on APC activity, we wanted to show that overexpression of Swe1 would reduce APC^{Cdc20}-dependent activity in vitro. Wild type and *GAL-SWE1* strains were arrested in mitosis with the microtubule depolymerizing drug, benomyl, and Swe1 expression was induced after the

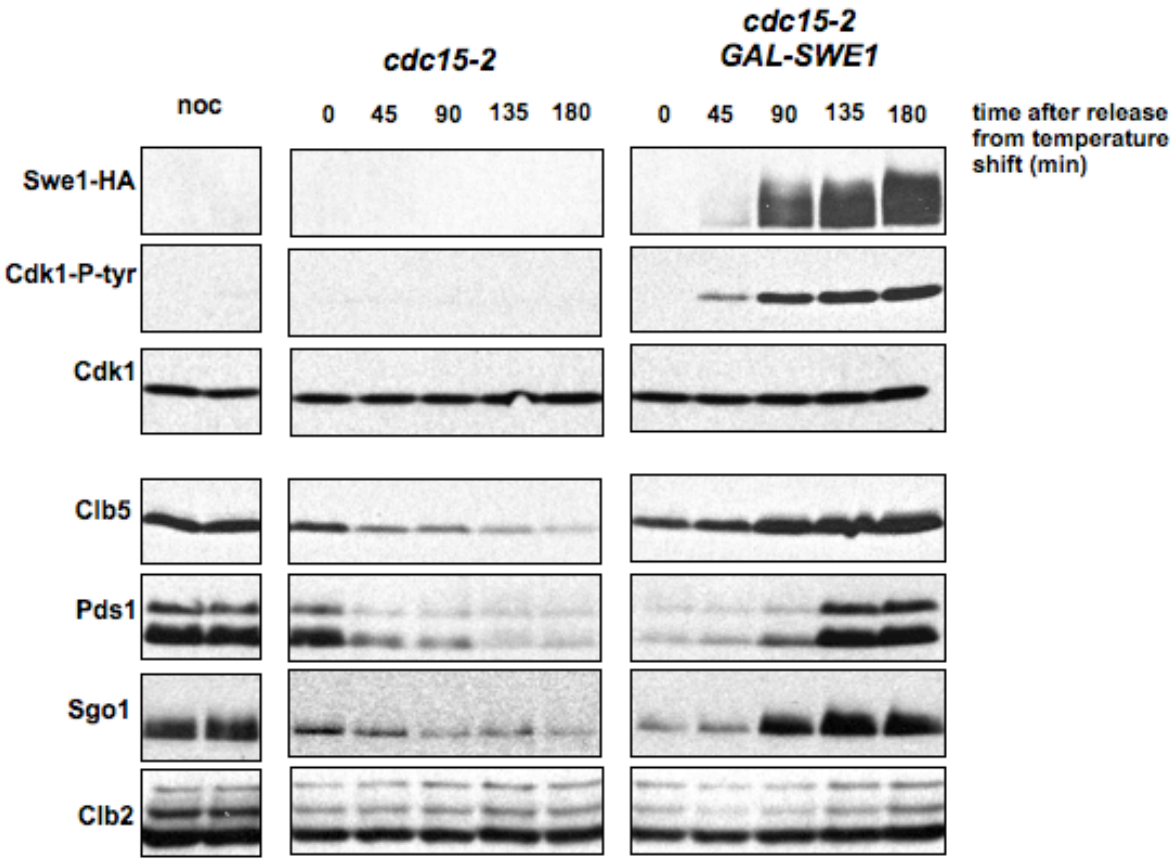
cdc15-2
cdc15-2
GAL-SWE1
noc
0 45 90 135 180
0 45 90 135 180
time after release from temperature shift (min)
Swe1-HA
Cdk1-P-tyr
Cdk1
Clb5
Pds1
Sgo1
Clb2

Figure 3.5 Overexpression of Swe1 in anaphase re-stabilizes APC^{Cdc20} substrates

Overexpression of Swe1 in anaphase restabilizes APC^{Cdc20} substrates. *cdc15-2* (ADR4252) and *cdc15-2 GAL-SWE1* (ADR4245) cells were grown in YEP + 2% raffinose and arrested in anaphase by temperature shift to 35˚C, followed by induction with 2% galactose (t=0), and samples were taken for immunoblotting. Parallel cultures were arrested in nocodazole (noc, 10µg/mL) at 25˚C to illustrate peak levels of APC substrates. Cdk1 is used as a loading control.

arrest. Following Swe1 induction, purified APC was tested in an in vitro ubiquitination assay to assess APC activity.

The in vitro ubiquitination assay consists of purified APC from yeast, purified Uba1 (ubiquitin activating enzyme) and Ubc1, Ubc4 (ubiquitin conjugating enzymes), as well as substrate and co-activators (Cdc20 or Cdh1) made in an in vitro transcription and translation reaction, and finally, ATP and ubiquitin (Fig. 2.2) (Carroll and Morgan, 2005; Passmore and Barford, 2005). The substrate, Pds1 or Clb5, is transcribed and translated in the presence of ^{35}S-methionine so ubiquitination can be monitored by migration in polyacrylamide gels. Pds1-db/kb is a mutated version of Pds1 where the two motifs recognized by the APC, the destruction box and KEN box, have been removed.

The silver stain in Fig. 3.6A shows the purification of the wild type and *GAL-SWE1* APCs. Again, note the migratory difference of Cdc27 in the two strains. In cells overexpressing Swe1, the Cdc27 subunit becomes completely dephosphorylated (Fig. 3.6A), similar to what was observed by western blotting (Fig. 3.1B). We assayed APC activity from cells overexpressing Swe1 and found that Swe1-inhibited APC shows reduced APC^{Cdc20} activity against Pds1, and Clb5 (Fig. 3.6B, D and E), consistent with the in vivo data. Pds1 ubiquitination is reduced to approximately 50% of wild type in the Swe1-inhibited APC (Fig. 3.6B, APC^{Cdc20} quantification). Each ubiquitinated species is reduced approximately twofold, with little difference between individual ubiquitinated species (Fig. 3.6C). The two strains exhibit similar Cdh1-dependent activity, however, which is consistent with previous data that the phosphorylation status of core APC subunits does not affect its Cdh1-dependent activity (Kramer et al., 2000; Rudner and Murray, 2000; Zachariae et al., 1998a). The APC^{Cdc20} is

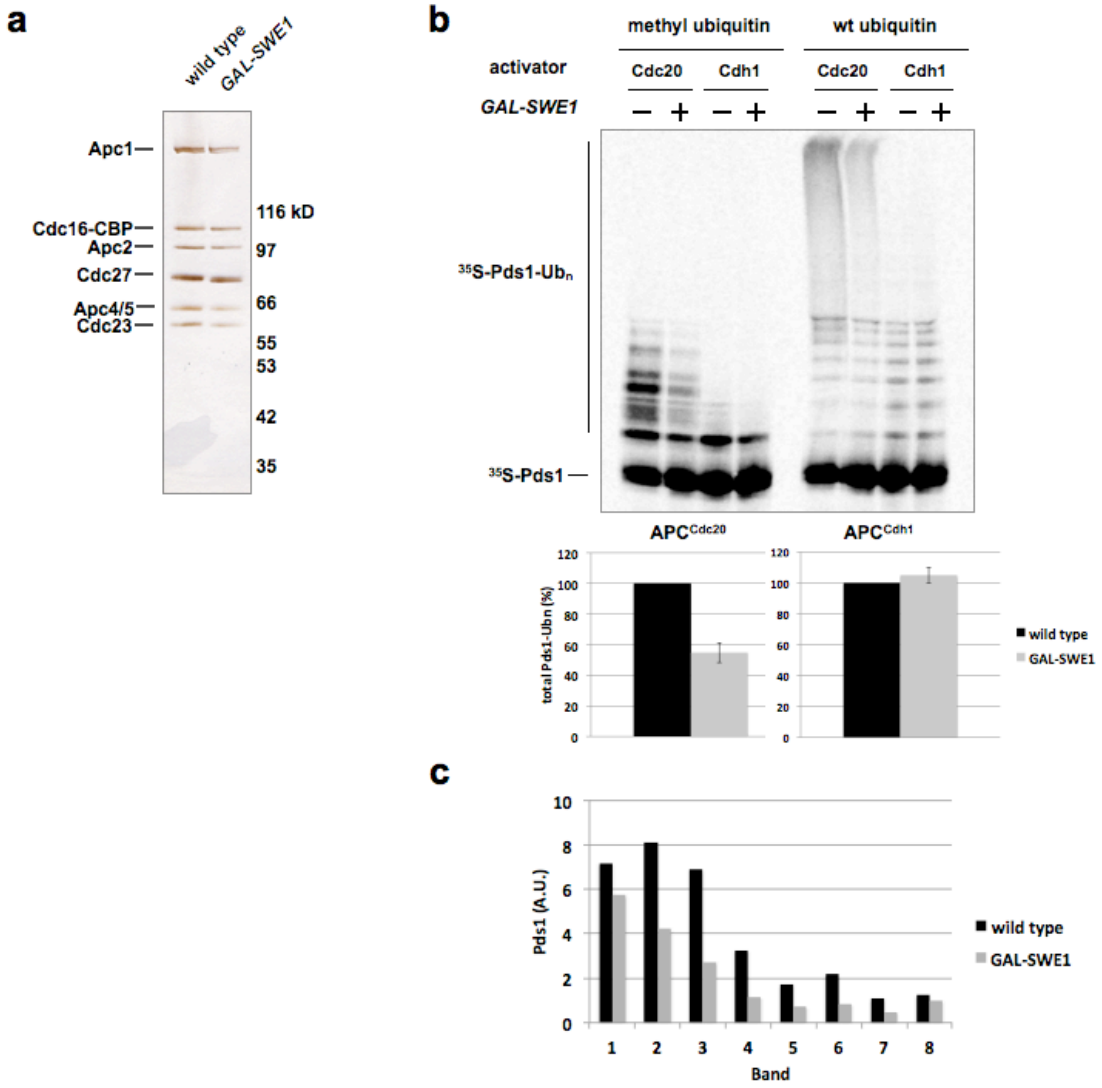
a
wild type
GAL-SWE1
Apc1
Cdc16-CBP
Apc2
Cdc27
Apc4/5
Cdc23
116 kD
97
66
55
53
42
35
b
methyl ubiquitin
wt ubiquitin
activator
Cdc20
Cdh1
Cdc20
Cdh1
GAL-SWE1
− + − + − + − +
35S-Pds1-Ubn
35S-Pds1
APCCdc20
APCCdh1
total Pds1-Ubn (%)
120
100
80
60
40
20
0
wild type
GAL-SWE1
c
Pds1 (A.U.)
10
8
6
4
2
0
1 2 3 4 5 6 7 8
Band
wild type
GAL-SWE1
d
substrate
activator
GAL-SWE1
Pds1
Pds1-db/kb
Cdc20
Cdh1
Cdc20
Cdh1
− + − + − + − +
35S-Pds1-Ubn
35S-Pds1
e
substrate
activator
GAL-SWE1
Clb5
Clb5-mut
Cdc20
Cdh1
Cdc20
Cdh1
− + − + − + − +
35S-Clb5-Ubn
35S-Clb5

Figure 3.6 Overexpression of Swe1 inhibits APC^{Cdc20} activity in vitro

(A) Silver stain of purified APC used in Fig. 6B. (B) Overexpression of Swe1 inhibits ubiquitination of Pds1 in vitro. *swe1*Δ *CDC16-TAP* (ADR3877) and *GAL-SWE1 CDC16-TAP* (ADR3858) cells were grown in YEP + 2% raffinose, arrested in mitosis with benomyl (30µg/mL), and induced with 2% galactose. The APC was purified and its activity assayed in an in vitro ubiquitination assay. Reactions were run on a polyacrylamide gel, exposed to phosphorimager screen, and quantified using ImageQuant software. The average activity (±SEM) of three independent experiments is plotted below a representative assay. APC^{Cdc20} activity was quantified from assays containing methylated ubiquitin (Ub) and APC^{Cdh1} activity was quantified from assays containing wild type ubiquitin. (C) Quantification of individual ubiquitinated species from Fig. 6B. APC assay was quantified as described, but the quantity of labelled Pds1 in each band is plotted for wild type and *GAL-SWE1* APCs using Cdc20 as an activator protein. Band 1 is free substrate, band 2 the mono-ubiquitinated species, etc. (D and E) Overexpression of Swe1 inhibits Cdc20-dependent ubiquitination of Pds1 (D), and Clb5 (E) in vitro. APC was isolated and assayed as in Fig. 6B, but (D) shows destruction box (db) and KEN box (kb) dependence. Methylated ubiquitin was used in this experiment. In (E) the Clb5-mut contains a P55Q substitution, as well as deletion of residues 56-64. The experiment shown is representative of one of two repeats.

more processive than the APC^{Cdh1} (Carroll and Morgan, 2002), and as such, differences in APC^{Cdc20} ubiquitination are more readily apparent when the formation of polyubiquitin chains is prevented with the use of methyl ubiquitin (Fig. 3.6B compares wild type and methyl ubiquitin, in which the lysine residues in ubiquitin have been methylated to prevent the formation of polyubiquitin chains).

To test if the decrease in APC^{Cdc20} activity is due to loss of Cdk1-dependent phosphorylation of the APC, we tested if the activity of APC purified under *GAL-SWE1* conditions could be restored back to wild type levels by in vitro phosphorylation with purified Cdk1/Clb2 complexes. The silver stain in Fig. 3.7A shows the purified APCs after treatment with Cdk1/Clb2. After phosphorylation with Cdk1/Clb2 complexes, both wild type and Swe1-inhibited APCs are phosphorylated primarily on Cdc16 and Cdc27 (Fig. 3.7B). In the absence of Cdk1/Clb2 phosphorylation, wild type APC exhibits greater ubiquitination activity towards Pds1 than *GAL-SWE1* APC (Fig. 3.7C, no ATP lanes). Phosphorylation, however, increases the ability of *GAL-SWE1* APC^{Cdc20} to ubiquitinate Pds1, suggesting the initial loss of ubiquitination activity shown in Fig. 3.6 was due to a loss of Cdk1 phosphorylation of the APC (Fig. 3.7C). We also note that the wild type APC has more activity than the *GAL-SWE1* APC, which may suggest either that some sites weren't phosphorylated, or that some dephosphorylation occurred during purification of the APC.

Cdk1/Clb2 treatment only partially restores activity of APC-A mutants

The Swe1 overexpression experiments provide strong evidence that Cdk1-dependent phosphorylation of the APC is important for triggering anaphase onset. Mutation of Cdk1

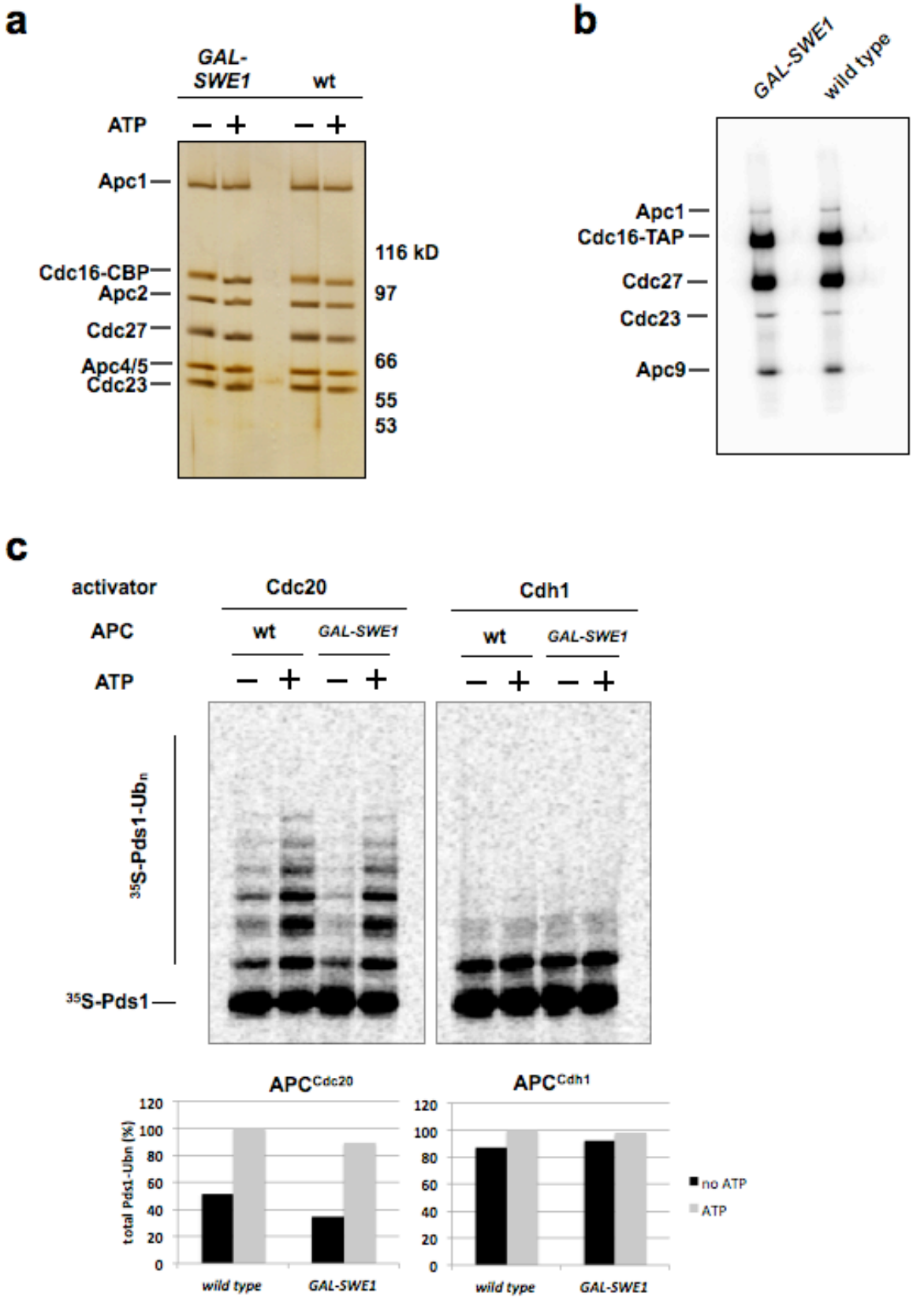
a
GAL-SWE1
wt
ATP
– + – +
Apc1
Cdc16-CBP
Apc2
Cdc27
Apc4/5
Cdc23
116 kD
97
66
55
53
b
GAL-SWE1
wild type
Apc1
Cdc16-TAP
Cdc27
Cdc23
Apc9
c
activator
Cdc20
Cdh1
APC
wt
GAL-SWE1
wt
GAL-SWE1
ATP
– + – + – + – +
35S-Pds1-Ubn
35S-Pds1
APCCdc20
APCCdh1
total Pds1-Ubn (%)
120
100
80
60
40
20
0
wild type
GAL-SWE1
no ATP
ATP

Figure 3.7 Cdk1/Clb2 kinase treatment re-activates Swe1-inhibits APC

(A) Silver stain of purified APC used in Fig. 7C. (B) In vitro phosphorylation of the APC. A fraction of the APCs purified in Fig. 7C were incubated with **γ-**[^{32}P]ATP and purified Cdk1/Clb2-CBP, washed and run on a polyacrylamide gel, and exposed to phosphorimager screen to confirm efficient phosphorylation. The pattern of phosphorylation is identical to what has been published previously(Rudner and Murray, 2000). (C) Cdk1-Clb2 kinase treatment re-activates Swe1-inhibited APC. APC was purified from *swe1*Δ *CDC16-TAP* (ADR3877) and *GAL-SWE1 CDC16-TAP* (ADR3858) cells as described in Fig. 6B. The APC was incubated with purified Cdk1/Clb2 complexes +/- ATP before cleavage from IgG-coupled magnetic beads. The activity of the purified APC was then measured as in Fig. 6B. Quantification of a representative assay is shown below. The experiment shown is representative of one of two repeats.

phosphorylation sites in Cdc16, Cdc23 and Cdc27 have previously been described, and were shown to delay cell cycle progression, but not block it (Rudner and Murray, 2000) (Fig. 3.8A). If these Cdk1 phosphorylation sites are important for APC activity, we would expect that mutation of these sites would result in a decrease of APC activity in vitro. *cdc16-6A*, and *cdc16-6A cdc27-5A* APC do not show any obvious difference in APC^{Cdc20} activity in vitro (Fig. 3.8A). These sites, however, are required for full in vitro activation of the APC (Fig. 3.8E). When phosphorylated with purified Cdk1/Clb2 complexes, these phosphorylation site mutant APCs showed an increase in ubiquitination activity, although they did not reach wild type levels (Fig. 3.8D). The silver stain shown in Fig. 3.8B shows the purified APCs tested in the ubiquitination assay, and in vitro phosphorylation of these APCs using radiolabelled ^{32}P-ATP shows the decrease in phosphorylation of Cdc16 and Cdc27 compared to wild type (Fig. 3.8C). Mutating Cdk1 phosphorylation sites on Cdc16 (*cdc16-6A)* partially blocks reactivation, whereas mutating sites in both Cdc16 and Cdc27 (*cdc16-6A cdc27-5A)* further prevents this reactivation (Fig. 3.8D).

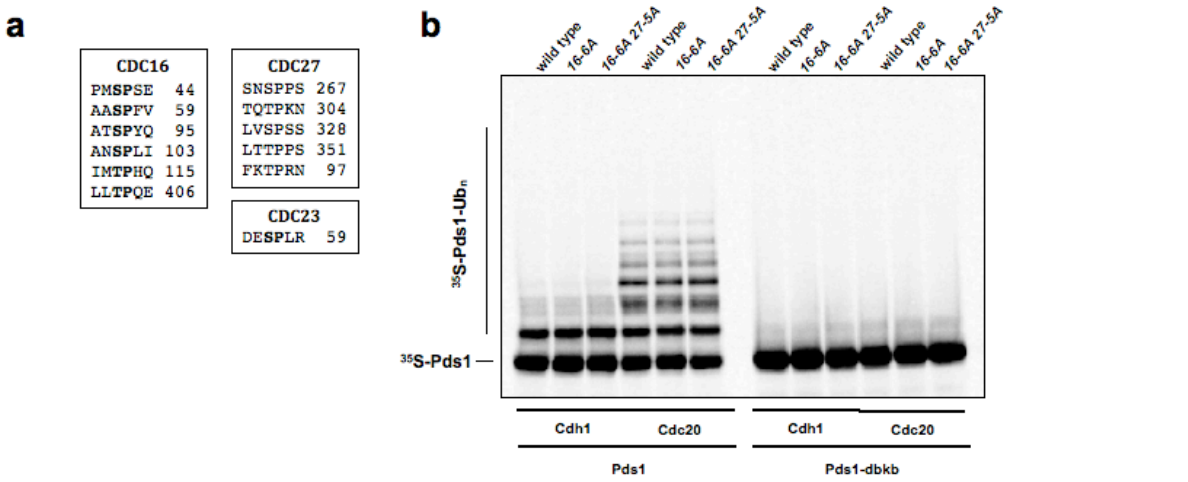
a
CDC16
PMSPSE 44
AASPFV 59
ATSPYQ 95
ANSPLI 103
IMTPHQ 115
LLTPQE 406
CDC27
SNSPPS 267
TQTPKN 304
LVSPSS 328
LTTPPS 351
FKTPRN 97
CDC23
DESPLR 59
b
wild type
16-6A
16-6A 27-5A
35S-Pds1-Ubn
35S-Pds1
Cdh1
Cdc20
Pds1
Pds1-dbkb
c
APC
16-6A 27-5A
16-6A
wt
ATP
Apc1
Cdc16-CBP
Apc2
Cdc27
Apc4/5
Cdc23
d
cdc16-6A cdc27-5A
cdc16-6A
wild type
Apc1
Cdc16-TAP
Cdc27
Cdc23
Apc9
e
activator
Cdc20
Cdh1
APC
16-6A 27-5A
16-6A
wt
ATP
35S-Pds1-Ubn
35S-Pds1
APCCdc20
APCCdh1
total Pds1-Ubn (%)
120
100
80
60
40
20
0
16-6A 27-5A
16-6A
wild type
no ATP
ATP

Figure 3.8 Cdk1/Clb2 kinase treatment only partially restores activity of *apc-a* mutants

(A) All serine-proline (SP) and threonine-proline (TP) sites on Cdc16, Cdc23 and Cdc27 were mutated to alanine-proline (AP). (B) *apc-a* mutations do not cause a defect in ubiquitination activity in vitro. APC was purified from *CDC16-TAP* (ADR3089), *cdc16-6A-TAP* (ADR3822), and *cdc16-6A-TAP cdc27-5A* (ADR3891), and tested in the ubiquitination assay. Reactions were run on a polyacrylamide gel, and exposed to phosphorimager screen. (B) Silver stain of purified APC used in Fig. 8D. Note that mutations in Cdk1 consensus sites in Cdc16 and Cdc27 prevent phosphorylation-dependent mobility shifts. (C) A fraction of the APCs purified in Fig. 8D were incubated with **γ-**[^{32}P]ATP and purified Cdk1/Clb2-CBP, washed and run on a polyacrylamide gel, and exposed to phosphorimager screen to confirm efficient phosphorylation. (C) *CDC16-TAP* (ADR3089), *cdc16-6A-TAP* (ADR3822), and *cdc16-6A-TAP cdc27-5A* (ADR3891) cells were arrested in mitosis with benomyl (30µg/mL). Purified APC was phosphorylated by purified Cdk1/Clb2 complexes as in Fig. 7C and its activity measured. Quantification of a representative assay is shown on the right. The experiment shown is representative of one of two repeats.

3.3 DISCUSSION

Anaphase onset is an irreversible process, and must be monitored closely to ensure the genomic integrity of daughter cells. Activation of the APC^{Cdc20} initiates anaphase, but the exact trigger for this activation is not well understood. This chapter sought to determine whether Cdk1 phosphorylation of the APC is essential for activation of the APC^{Cdc20} at the metaphase-anaphase transition. We found, through the use of Swe1 as a Cdk1 inhibitor, that Swe1 overexpression provides us with a unique opportunity to assess the role of Cdk1 in mitosis because it lowers Cdk1 activity enough to inhibit this transition, but not enough to turn on the APC^{Cdh1} and drive cells into G1, as is seen with overexpression of the Cdk1 inhibitor Sic1 (Amon, 1997; Bishop et al., 2000).

The results presented here suggest that inhibition of Cdk1-dependent phosphorylation of the APC in mitosis inhibits APC^{Cdc20} activation, and prevents the onset of anaphase. This is evident by the stabilization of APC substrates, the impairment in sister chromatid separation and anaphase spindle elongation, and the mitotic arrest seen in cells expressing high levels of Swe1 (Fig. 3.1). The stability of APC substrates after overexpression of Swe1 depends on the presence of tyrosine 19 in Cdk1, arguing against the possibility that there are additional targets of Swe1 that could impact activation of the APC. The ability of Swe1 to inhibit mitotic substrate degradation in an anaphase arrest also argues that Cdk1 phosphorylation of the APC is important for activity throughout anaphase, and not simply for an initial activation step at the metaphase-anaphase transition (Fig. 3.5). This is consistent with the APC^{Cdc20} remaining active in anaphase to degrade Clb2, allowing for sufficient downregulation of Cdk1/cyclin activity to allow release of the phosphatase Cdc14, and

activation of the APC^{Cdh1} (Shou et al., 1999; Visintin et al., 1999; Yeong et al., 2000).

Cdk1 phosphorylation regulates APC^{Cdc20} activity

The metaphase block of cells overexpressing Swe1 is consistent with a previous report that mutagenesis of Cdk1 phosphorylation sites on the APC subunits Cdc16, Cdc23 and Cdc27 slowed mitotic progression (Rudner and Murray, 2000), but also suggests that there are additional Cdk1-dependent sites on the APC that were not mutated in that study. We have shown here that overexpression of Swe1 reduces phosphorylation of the APC subunits Apc1, Cdc16, Cdc27, Cdc23 and Apc9 (Fig. 3.1A). It seems likely that phosphorylation of Apc1 might contribute to the metaphase block seen in Fig. 3.1B, although a number of studies have identified Cdk1 phosphorylation sites on additional subunits (Blethrow et al., 2007; Kraft et al., 2003; Torres and Borchers, 2007; Yoon et al., 2006) (unpublished data). The mutagenesis of additional phosphorylation sites on other APC subunits may be necessary to see a phenotype similar to that caused by Swe1-dependent inhibition of Cdk1. The phosphorylation of Apc9 is discussed in Chapter 4.

Cdk1 phosphorylation of the APC directly affects ubiquitination activity, as APC purified under conditions of Swe1 overexpression exhibits reduced activity in vitro (Fig. 3.6). Phosphorylation does not appear to affect enzyme processivity, however, as individual ubiquitinated species are reduced equally (Fig. 3.6C). On the other hand, APC purified with alanine mutations in Cdc16 and Cdc27 still exhibits a moderate level of activity (Fig. 3.8A).

The difference in activity between the *apc-a* and Swe1-inhibited APC also argues that Cdk1-dependent phosphorylation of other subunits is important for full APC activity.

We have shown that in budding yeast, as in other eukaryotes (Kraft et al., 2003; Kramer et al., 2000; Lahav-Baratz et al., 1995; Shteinberg et al., 1999), Cdk1/Clb2 can activate the APC^{Cdc20} in vitro. APC lacking the Cdk1 consensus sites in Cdc16 and Cdc27 was not rescued back to wild type ubiquitination activity when treated with Cdk1/Clb2, arguing that full activation of the APC^{Cdc20} requires these phosphorylation sites. This is the first demonstration that defects caused by APC phosphorylation site mutants in vivo correlate with changes in APC activity in vitro (Rudner and Murray, 2000). It has been suggested that Cdc20 association with the APC depends on Cdk1 phosphorylation of the APC (Kramer et al., 1998a; Shteinberg et al., 1999) (Kraft et al., 2003; Kramer et al., 2000; Rudner and Murray, 2000), but the challenges of mutational analysis of the APC have left this model unproven (see Chapter 4).

The APC is a target of the morphogenesis checkpoint

Swe1-dependent inhibition of Cdk1 reduces APC activity in vivo and in vitro, and this inhibition is accompanied by dephosphorylation of the APC, suggesting the APC is a target of the Swe1-dependent morphogenesis checkpoint. Previous work from the Rudner laboratory analyzed the checkpoint defect of *cdc55*Δ cells, which is characterized by bypass of the morphogenesis checkpoint despite relatively slow degradation of APC substrates (Chiroli et al., 2007; Minshull et al., 1996; Wang and Burke, 1997). Deletion of *CDC55* was shown to increase APC phosphorylation in vivo and purified $PP2A^{Cdc55}$ dephosphorylates the

APC in vitro suggesting a model that in *cdc55*Δ cells checkpoint inhibition of the APC is countered by increased phosphorylation and activation of the APC (Lianga et al., 2013). Consistent with this model, mutation of 12 APC phosphorylation sites in *cdc55*Δ cells suppresses premature APC activation during both morphogenesis and spindle checkpoint activation. These results are consistent with prior studies that have suggested that PP2A may dephosphorylate and inhibit the APC^{Cdc20} in yeast, insect, and human cells (Burgess et al., 2010; Deak et al., 2003; Mui et al., 2010; Voets and Wolthuis, 2010).

Stepwise activation of Cdk1 triggers anaphase

This work also suggests that tyrosine dephosphorylation of Cdk1 may be an important step for triggering anaphase onset, through activation of the APC^{Cdc20}. Numerous studies have suggested that inhibitory phosphorylation regulates Cdk1 activation in a stepwise manner in both vertebrates and yeast (Deibler and Kirschner, 2010; Harvey et al., 2011; Pomerening et al., 2005; 2003; Stern and Nurse, 1996). These studies have primarily focused on how Cdk1 dephosphorylation by Cdc25 allows cells to transition from G2 to mitosis. Other work has suggested a second step in Cdk1 activation during mitosis that regulates anaphase onset (Lindqvist et al., 2007; Rahal and Amon, 2008; Rudner et al., 2000). Mutation of the two mitotic cyclins in budding yeast, *CLB1* and *CLB2*, arrests cells in metaphase, showing that a low level of Cdk1 activity can drive spindle assembly, but additional activity is needed to trigger anaphase (Rahal and Amon, 2008). Our work suggests that dephosphorylation of Cdk1 may cause the increase in Cdk1 activity that triggers anaphase onset, in part by activation of the APC. In support of this, *swe1*Δ mutants shorten

and *mih1*Δ mutants lengthen the time spent in metaphase in unperturbed cell cycles (Lianga et al., 2013).

After overexpression of Swe1, residual Cdk1/cyclin activity remains in cells (Fig. 3.4A). Because tyrosine dephosphorylation of Cdk1 has been shown to completely inhibit Cdk1 activity (Parker et al., 1992), we believe only a fraction of Cdk1 is targeted by Swe1, and this pool of Cdk1 is equally phosphorylated when the morphogenesis checkpoint is activated, despite far lower levels of Swe1 (Fig. 3.4C). How cells restrict Swe1 activity even when it is overexpressed is unknown, but may reflect limited import of Swe1 into the nucleus where its function is needed to activate the morphogenesis checkpoint (Keaton et al., 2008).

Cdk1 regulates anaphase onset

While we have not rigorously proven, using mutational analysis, that Cdk1 phosphorylation is essential for activation of the APC^{Cdc20} at the metaphase-anaphase transition, the Swe1 overexpression studies argue that inhibiting this phosphorylation does block cell cycle progression. Furthermore, it is apparent that Cdk1 phosphorylation is important for APC activity in vitro. The model that Cdk1 activity is necessary for APC^{Cdc20} activation is also consistent with recent data indicating Cdk1/Clb activity is required for the metaphase to anaphase transition (Rahal and Amon, 2008). Identification and mutagenesis of additional Cdk1 sites will be important to indicate whether this function of Cdk1 is essential for triggering anaphase onset, and whether this phosphorylation contributes to activator binding.

Chapter 4: TPR subunit phosphorylation and co-activator binding

4.1 Introduction

Activation of the APC during mitosis requires the association of one of two homologous sub-stoichiometric co-activators, Cdh1 or Cdc20, which allows for the recruitment of substrates to the APC (Fang et al., 1998; Schwab et al., 1997; Visintin et al., 1997). Association of Cdc20 to the APC is important at the metaphase-anaphase transition, when Cdk1 activity levels are high, while Cdh1 associates with the APC during mitotic exit and in the following G1. In fact, phosphorylation of Cdh1 by Cdk1 prevents the association of Cdh1 with the APC, limiting the APC^{Cdh1} to periods of low Cdk1 activity (Jaspersen et al., 1999; Zachariae et al., 1998a).

Conserved motifs within these related proteins have been identified that contribute both to binding to the APC core, and to substrates. The N-terminal C box and the C-terminal IR tail are important for co-activator binding to the APC core (Passmore et al., 2003; Schwab et al., 2001; Vodermaier et al., 2003), while the C terminal WD-40 domain repeats are important for recruiting substrates to the APC (Burton and Solomon, 2001; Hilioti et al., 2001; Kraft et al., 2005; Schwab et al., 2001). The TPR subcomplex of the APC is thought to contribute to co-activator binding (Kraft et al., 2005; Matyskiela and Morgan, 2009; Rudner and Murray, 2000; Thornton et al., 2006; Vodermaier et al., 2003). In particular, Cdc27 has been implicated in the APC-co-activator interaction: peptides with an IR motif can bind Cdc27 (Vodermaier et al., 2003), and co-activator can be cross-linked to Cdc27 (Kraft et al., 2005). Although APC lacking Cdc27 shows reduced affinity for co-activator (Thornton et al., 2006), binding is not completely abolished as would be expected if Cdc27 were the only

subunit involved in co-activator binding. The C terminal IR motif of Cdh1 and Cdc20 also interacts with Apc7, a vertebrate TPR subunit of the APC with no homolog in *S. cerevisiae* (Vodermaier et al., 2003).

Although Cdc27 is essential for viability in budding yeast, this requirement can be bypassed with overexpression of the Cdk1 inhibitor, Sic1. Increased levels of Sic1 are necessary for the downregulation of Cdk1 activity in the *cdc27*Δ background, which would normally be regulated by the APC^{Cdh1} after the initial degradation of Pds1 is completed by the APC^{Cdc20} (Thornton and Toczyski, 2003). The fact that the loss of Cdc27 can be rescued by overexpression of Sic1 argues that Cdc27 is not required for the degradation of Pds1, an essential APC^{Cdc20} function. While Cdc27 is important for Cdh1 binding, this bypass suggests that the binding of Cdc20 to the APC may employ additional sites of contact that have yet to be identified. In support of this, mutational analysis of Cdc16, Cdc27, and Cdc23 has identified sites in the TPR repeats of both Cdc27 and Cdc23 that contribute to co-activator binding (Matyskiela and Morgan, 2009).

Structural analysis of the human Cdc26 has shown that Cdc26 interacts directly with Cdc16 to form a TPR repeat, although whether or not this interaction contributes to co-activator binding was not evaluated in this study (Wang et al., 2009). Consistent with a role for Cdk1 phosphorylation in promoting anaphase, mutation of a single Cdk1 phosphorylation site (S48A) in the fission yeast homolog of Cdc26, Hcn1, produced a defect in cell separation, with cells spending a slightly longer time in anaphase (Yoon et al., 2006). In addition to Cdc26, the relative contribution of the remaining non-essential subunits of the

TPR subcomplex of the APC (Apc9, Swm1, and Mnd2) to co-activator binding has not been rigorously evaluated.

Phosphorylation of the APC has also been shown to contribute to Cdc20 binding. It is thought that Cdc20 preferentially binds and activates phosphorylated APC (Kraft et al., 2003; Kramer et al., 2000; 1998a; Rudner and Murray, 2000; Shteinberg et al., 1999). However, apart from a single study that showed the *cdc16-6A* mutant has reduced affinity for Cdc20 in vivo (Rudner and Murray, 2000), no study has rigorously tested this model with mutational analysis. The results presented in Chapter 3 argue that inhibition of Cdk1 phosphorylation of the APC by Swe1 overexpression prevents activation of the APC^{Cdc20}, and the subsequent progression into anaphase. A likely explanation for this metaphase block and decreased APC activity in vitro is that Cdk1 phosphorylation of the APC contributes to mitotic activation by increasing the affinity of Cdc20 for the APC core.

This chapter seeks to establish whether Cdk1-dependent phosphorylation of the TPR subunits of the APC contributes to association of Cdc20. Given that the human Cdc26 forms a TPR repeat with Cdc16 (Wang et al., 2009), we also examine whether Cdc26 might cooperate with Cdk1 phosphorylation of the TPR subunits and help define an essential role for Cdk1 in activating the APC. Furthermore, we characterize the deletion of the remaining non-essential TPR subunits, Apc9, Swm1 and Mnd2, in the *apc-12A* mutant background.

4.2 RESULTS

Phosphorylation of the APC does not influence co-activator binding

In order to address whether Cdk1 phosphorylation of the APC contributes to binding of the mitotic co-activator, Cdc20, we established a co-activator binding assay that allows assessment of the relative binding of Cdh1 and Cdc20 to purified APC in vitro. Briefly, ^{35}S-labelled co-activator (Cdh1 or Cdc20), which is prepared by transcription and translation in vitro, is added to immunopurified APC bound to magnetic beads. Following a short incubation, the beads are washed to remove any unbound co-activator. We've previously shown that overexpression of Swe1 reduces Cdk1-dependent phosphorylation of the APC, and induces a metaphase block (Fig. 3.1A, B), so we first tested whether APCs purified +/- *GAL-SWE1* overexpression showed any difference in co-activator binding in vitro. For all of these binding assays, the APC is purified from asynchronous cultures under high salt conditions to ensure that Cdc20 or the MCC is not pulled down with the APC, and that the amount of Cdh1 bound to the APC is negligible (Fig. 4.2A, and data not shown). Fig. 4.1A shows no difference in the binding of Cdc20 or Cdh1 relative to wild type. While we hypothesized we would see a difference in Cdc20 binding with a decrease in Cdk1-dependent phosphorylation of the APC (the *GAL-SWE1* condition), we didn't expect any change in Cdh1 binding since the APC^{Cdh1} is active at a cell cycle stage when Cdk1 is inactive. We also found no obvious difference among the *apc-A* mutants in this binding assay, arguing Cdc20 binds equally well to the phosphorylation site mutants compared to wild type (Fig. 4.1B).

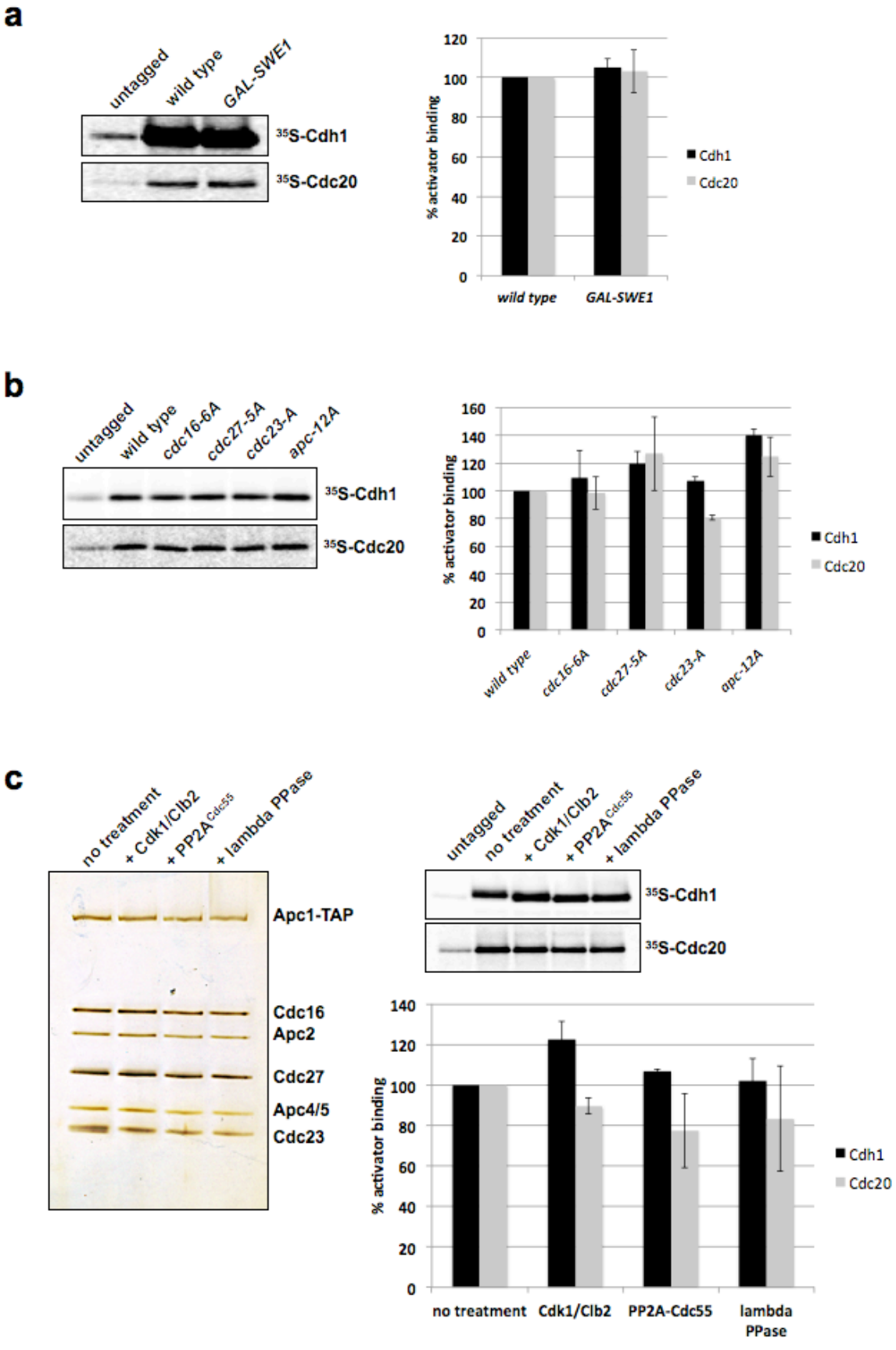
a
untagged
wild type
GAL-SWE1
35S-Cdh1
35S-Cdc20
% activator binding
120
100
80
60
40
20
0
wild type
GAL-SWE1
Cdh1
Cdc20
b
untagged
wild type
cdc16-6A
cdc27-5A
cdc23-A
apc-12A
35S-Cdh1
35S-Cdc20
% activator binding
160
140
120
100
80
60
40
20
0
wild type
cdc16-6A
cdc27-5A
cdc23-A
apc-12A
Cdh1
Cdc20
c
no treatment
+ Cdk1/Clb2
+ PP2A Cdc55
+ lambda PPase
Apc1-TAP
Cdc16
Apc2
Cdc27
Apc4/5
Cdc23
untagged
no treatment
+ Cdk1/Clb2
+ PP2A Cdc55
+ lambda PPase
35S-Cdh1
35S-Cdc20
% activator binding
140
120
100
80
60
40
20
0
no treatment
Cdk1/Clb2
PP2A-Cdc55
lambda PPase
Cdh1
Cdc20

Figure 4.1 Cdk1 phosphorylation of the APC does not influence co-activator binding in vitro

(A) Untagged (ADR4006), *CDC16-TAP* (ADR3877), and *GAL-SWE1 CDC16-TAP* ADR3858) cells were grown in YEP + 2% raffinose, arrested in mitosis with benomyl (30µg/mL), and induced with 2% galactose. The APC was purified and incubated with ^{35}S-labelled Cdh1 or Cdc20, and washed to remove any loosely bound proteins. Reactions were run on a polyacrylamide gel, exposed to phosphorimager screen, and quantified using ImageQuant software. The average binding (+/- SEM) relative to wild type levels of two independent experiments is shown. (B) APC was purified from untagged (ADR4006), wild type (ADR6174), *cdc16-6A* (ADR6581), *cdc27-5A* (ADR6577), *cdc23-A* (ADR6537), and *apc-12A* (ADR6589) cells, and treated as in (A). All strains except untagged are *APC1-TAP.* The average binding (+/- SEM) relative to wild type levels of three independent experiments is shown. (C) In vitro phosphorylation or dephosphorylation of wild type APC does not influence co-activator binding. APC was purified from *APC1-TAP* (ADR6174) cells, and incubated with purified Cdk1/Clb2, PP2A^{Cdc55}, or lambda phosphatase before cleavage from IgG-coupled magnetic beads. Cleaved APC was then treated as in (A). A silver stain of the purified APC is shown on the left, and the average binding (+/- SEM) of two independent experiments is shown. The slight shift in Cdh1 seen in the no treatment lane in the in vitro binding experiment is an anomaly resulting from electrophoresis: Cdh1 is unmodified in these conditions, and would not undergo a shift in electrophoretic mobility.

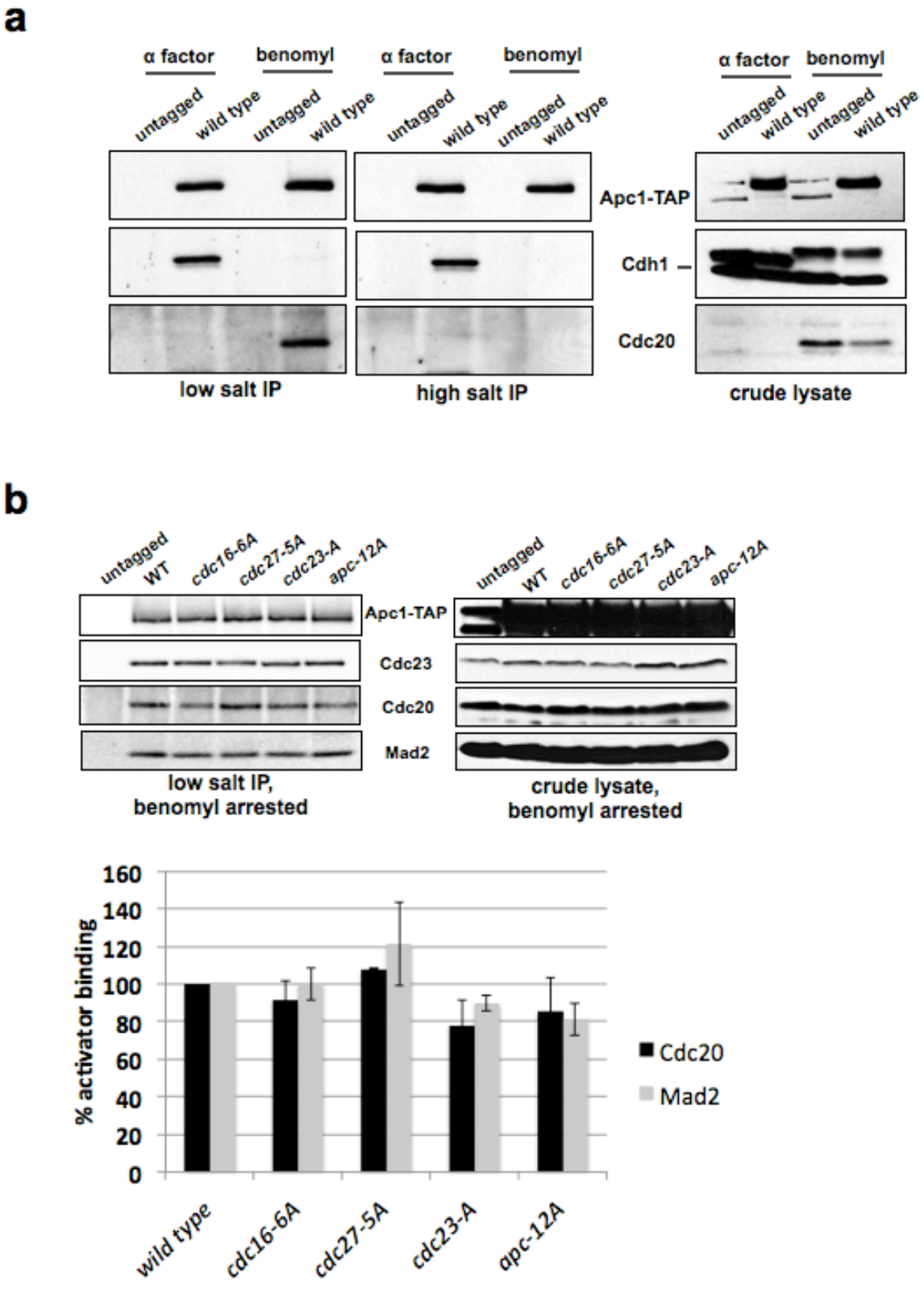
a
α factor
benomyl
α factor
benomyl
α factor
benomyl
untagged
wild type
untagged
wild type
untagged
wild type
untagged
wild type
untagged
wild type
untagged
wild type
Apc1-TAP
Cdh1
Cdc20
low salt IP
high salt IP
crude lysate
b
untagged
WT
cdc16-6A
cdc27-5A
cdc23-A
apc-12A
Apc1-TAP
Cdc23
Cdc20
Mad2
low salt IP,
benomyl arrested
crude lysate,
benomyl arrested
% activator binding
160
140
120
100
80
60
40
20
0
wild type
cdc16-6A
cdc27-5A
cdc23-A
apc-12A
Cdc20
Mad2

Figure 4.2 Loss of Cdk1-dependent phosphorylation of the TPR subunits does not change Cdc20 binding in vivo

(A) Cdc20 binding to the APC can be detected in mitotically arrested cells under low salt conditions. Untagged (ADR4006) and *APC1-TAP* (ADR6174) cells were arrested in G1 with α factor (1µg/mL), or in mitosis with benomyl (30µg/mL). The APC was purified in high, or low salt conditions (see Materials & Methods), and run on a polyacrylamide gel and immunoblotted with the indicated antibodies. (B) Untagged (ADR4006), wild type (ADR6174), *cdc16-6A* (ADR6581), *cdc27-5A* (ADR6577), *cdc23-A* (ADR6537), and *apc-12A* (ADR6589) cells were arrested in mitosis with benomyl (30µg/mL). All strains except untagged are *APC1-TAP.* The APC was purified, and run on a polyacrylamide gel. Immunopurified samples were quantified using ImageQuant software. The average amount of bound Cdc20 and Mad2 (+/- SEM) relative to wild type levels of three independent experiments is shown below.

We previously showed that in vitro phosphorylation of the APC with purified Cdk1/Clb2 complexes increases APC^{Cdc20} activity (Fig. 3.7C) (Lianga et al., 2013). This increase in activity, however, is not caused by an increase in the ability of Cdc20 to bind the APC. In vitro phosphorylation of wild type APC with Cdk1/Clb2 complexes did not increase Cdc20 binding in vitro (Fig. 4.1C). $PP2A^{Cdc55}$ has been shown to dephosphorylate the APC (Lianga et al., 2013), and lambda phosphatase is a non-specific phosphatase with activity towards phosphorylated serine, threonine and tyrosine residues. Dephosphorylation of the APC with either of these phosphatases did not produce any dramatic differences in Cdc20 binding, as would be predicted if phosphorylation contributes to the association of Cdc20 with the APC (Fig. 4.1C).

Cdc20 binding to the APC can also be detected in vivo in mitotically arrested cells, by purifying the APC under low salt conditions. Cdh1 binds the APC with higher affinity than Cdc20, and can be detected in G1 arrested cells when purified in both high and low salt conditions (Fig. 4.2A). In agreement with the in vitro data shown in Fig. 4.1, Cdc20 binding to the APC does not change significantly in the phosphorylation site mutants in vivo (Fig. 4.2B). In this experiment, cells were arrested in mitosis with benomyl, a microtubule depolymerizing agent which activates the spindle assembly checkpoint, triggering formation of the MCC. In addition to being able to detect Cdc20 bound to the APC, another component of the MCC, Mad2, was also bound to the APC (Fig. 4.2B). Mad2 and the spindle assembly checkpoint will be discussed further in Chapter 5. In summary, our data argues that Cdk1 phosphorylation of the TPR subunits Cdc16, Cdc23 and Cdc27 does not increase the affinity of Cdc20 for the APC in vivo and in vitro.

TPR subunit phosphorylation and the non-essential subunits Apc9 and Swm1

While the Cdk1 phosphorylation sites on Cdc16, Cdc23 and Cdc27 are important for APC^{Cdc20} activity in vitro, the *GAL-SWE1* overexpression studies also argue the existence of additional Cdk1 phosphorylation sites on the APC. The *apc-A* mutants described in Chapter 3 contain mutations in the three essential components of the TPR sub-complex of the APC: Cdc16, Cdc23, and Cdc27. We've previously mapped Cdk1 phosphorylation sites, both in vitro and in vivo, on nine of the thirteen APC subunits (unpublished data), and other groups have also identified sites on additional TPR subunits (Blethrow et al., 2007; Kraft et al., 2003; Steen et al., 2008; Torres and Borchers, 2007; Yoon et al., 2006). There are four additional subunits considered part of this arm of the APC in budding yeast: the non-essential subunits Apc9, Swm1, Mnd2 and Cdc26 (see Fig. 1.3). We therefore wondered if we could identify a function for one or more of these subunits in Cdc20 binding, in combination with Cdk1 phosphorylation of the TPR subunits Cdc16, Cdc23 and Cdc27.

The *apc-A* mutants alone do not exhibit temperature sensitivity (Rudner and Murray, 2000), however, we wondered if the loss of any of the non-essential TPR subunits in the *apc-A* backgrounds might uncover a genetic interaction. Consistent with previous reports, deletion of Apc9 caused loss of Cdc27 from the complex (Fig. 4.3B and C) (Passmore et al., 2003; Zachariae et al., 1998a), but did not interact genetically with the *apc-A* mutants when assessed by temperature sensitivity (Fig. 4.3A). *apc9*Δ cells are viable up to 37˚C, and loss of the 12 Cdk1 sites in Cdc16, Cdc23 and Cdc27 did not lower the maximum permissive temperature of the *apc9*Δ mutant. The loss of Cdc27 reduced ubiquitination of Pds1 in vitro (Fig. 4.3D), but the APC in these conditions retains enough Cdh1 activity to maintain

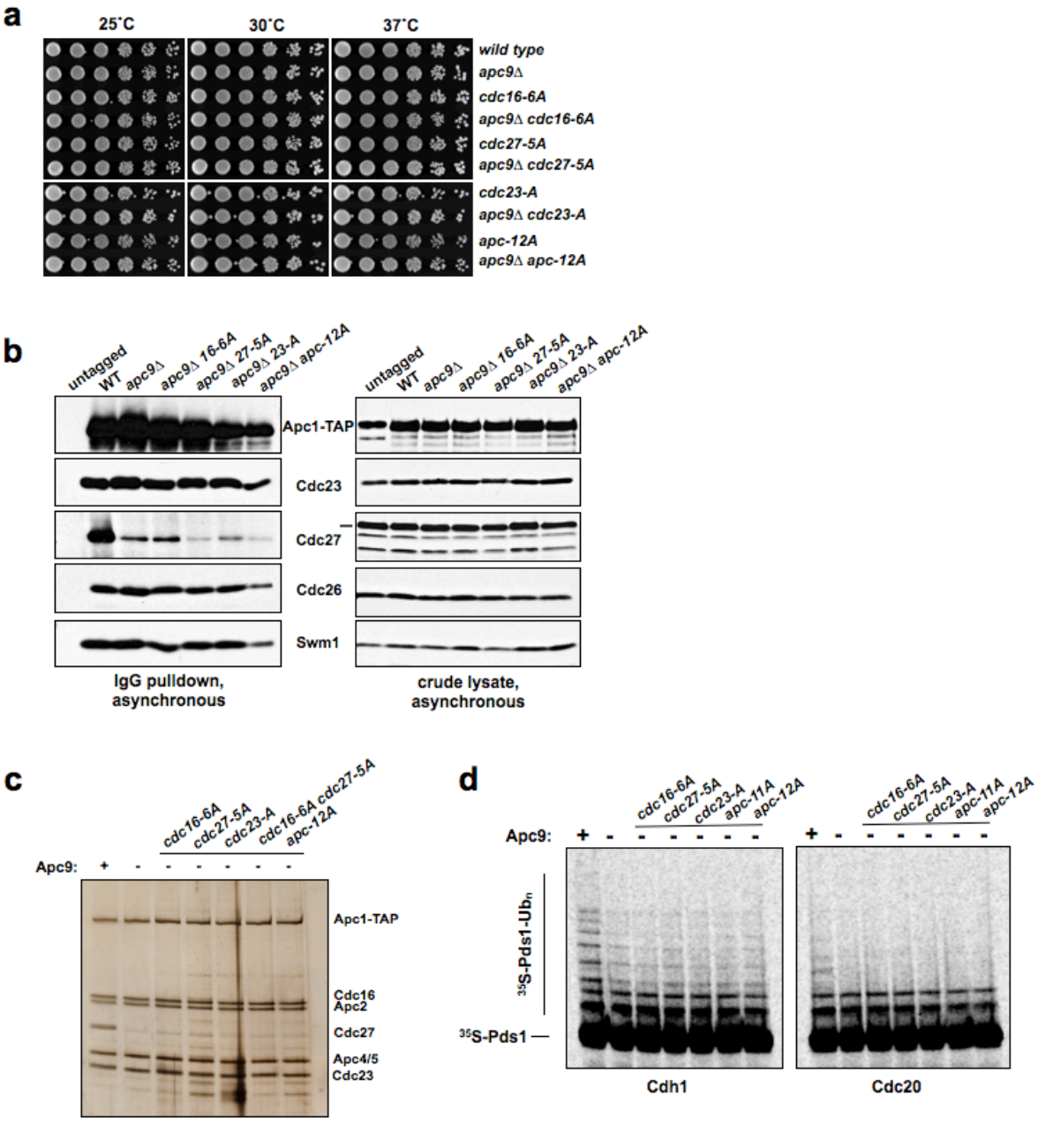
a
25˚C
30˚C
37˚C
wild type
apc9Δ
cdc16-6A
apc9Δ cdc16-6A
cdc27-5A
apc9Δ cdc27-5A
cdc23-A
apc9Δ cdc23-A
apc-12A
apc9Δ apc-12A
b
untagged WT
apc9Δ
apc9Δ 16-6A
apc9Δ 27-5A
apc9Δ 23-A
apc9Δ apc-12A
Apc1-TAP
Cdc23
Cdc27
Cdc26
Swm1
IgG pulldown, asynchronous
crude lysate, asynchronous
c
cdc16-6A
cdc27-5A
cdc23-A
cdc16-6A cdc27-5A
apc-12A
Apc9:
Apc1-TAP
Cdc16
Apc2
Cdc27
Apc4/5
Cdc23
d
cdc16-6A
cdc27-5A
cdc23-A
apc-11A
apc-12A
Apc9:
35S-Pds1-Ubn
35S-Pds1
Cdh1
Cdc20

Figure 4.3 *apc9*Δ does not interact genetically with the *apc-A* mutants, but exhibits a loss of Cdc27

(A) *apc9*Δ does not interact genetically with the *apc-A* mutations. Wild type (ADR4006), *apc9*Δ (ADR2067), *cdc16-6A* (ADR5237), *apc9*Δ *cdc16-6A* (ADR5722), *cdc27–5A* (ADR2031), *apc9*Δ *cdc27-5A* (ADR5724), *cdc23-A* (ADR6463), *apc9*Δ *cdc23-A* (ADR6895), *apc-12A* (ADR6623), and *apc9*Δ *apc-12A* (ADR6825) cells were grown to saturation in YEPD at 25˚C. Eight-fold serial dilutions were spotted onto YEPD plates and grown for two days at the indicated temperatures. (B and C) Deletion of Apc9 causes a loss of Cdc27 from the complex. Untagged (ADR4006), wild type (ADR6174), *apc9*Δ (ADR6890), *apc9*Δ *cdc16-6A* (ADR6821), *apc9*Δ *cdc27-5A* (ADR6898), *apc9*Δ *cdc23-A* (ADR6895), *apc9*Δ *apc-12A* (ADR6825) cells were grown overnight in YEPD at 25˚C to log phase. All strains except untagged are *APC1-TAP.* The APC was purified, run on a polyacrylamide gel, and immunoblotted with the indicated antibodies (B) or silver stained (C). (D) Loss of Cdc27 from *apc9*Δ cells results in decreased APC ubiquitination activity in vitro. APC used in this experiment was purified as described in (B), and the activity assayed in an in vitro ubiquitination assay. Reactions were run on a polyacrylamide gel and exposed to phosphorimager screen.

viability, even at elevated temperatures (Fig. 4.3A). This is consistent with reports that the APC purified from a *cdc27*Δ background still retains detectable Cdh1 activity (Thornton et al., 2006).

More specifically, we also investigated Cdk1 phosphorylation of Apc9. In vivo metabolic labeling and in vitro phosphorylation of the APC with purified Cdk1/Clb2 complexes argues Apc9 is phosphorylated by Cdk1 (Fig. 3.1A, 3.7B, and 3.8D) (Lianga et al., 2013). Three minimal Cdk1 consensus sites are found within the Apc9 sequence (Fig. 4.4A), and these serine and threonine residues were mutated to alanine to create the *apc9-3A* mutant. In contrast to *apc9*Δ, Cdc27 remains associated with the complex in the *apc9-3A* mutant (Fig. 4.4B), but mutation of these residues did not show any obvious decrease in phosphorylation in vitro (Fig. 4.4C), and was not pursued any further.

Swm1 is important for complex integrity, and has been shown in budding yeast to be required for efficient binding of Cdc16, Cdc27, and Apc9 (Schwickart et al., 2004). *swm1*Δ mutants display a synthetic interaction with the *apc-A* mutants at elevated temperatures (Fig. 4.5A). This interaction is most dramatic with the loss of phosphorylation sites on Cdc16, and consistent with a synthetically lethal interaction, the *swm1*Δ *apc-12A* mutant was never isolated (data not shown). Analysis of APC purified from a *swm1*Δ background indicates that the loss of Swm1 disrupts complex integrity when purified under high salt conditions, despite the fact that the *swm1*Δ mutant alone is not temperature sensitive (Fig. 4.5B). We note that different sub-complexes of the APC can be pulled down depending on the subunit used to pull down the APC: Cdc27 and Cdc26 are lost when Apc1-TAP is used, whereas Apc1 and Cdc23 are lost when Cdc16-TAP is used (Fig. 4.5B). Other reports have confirmed

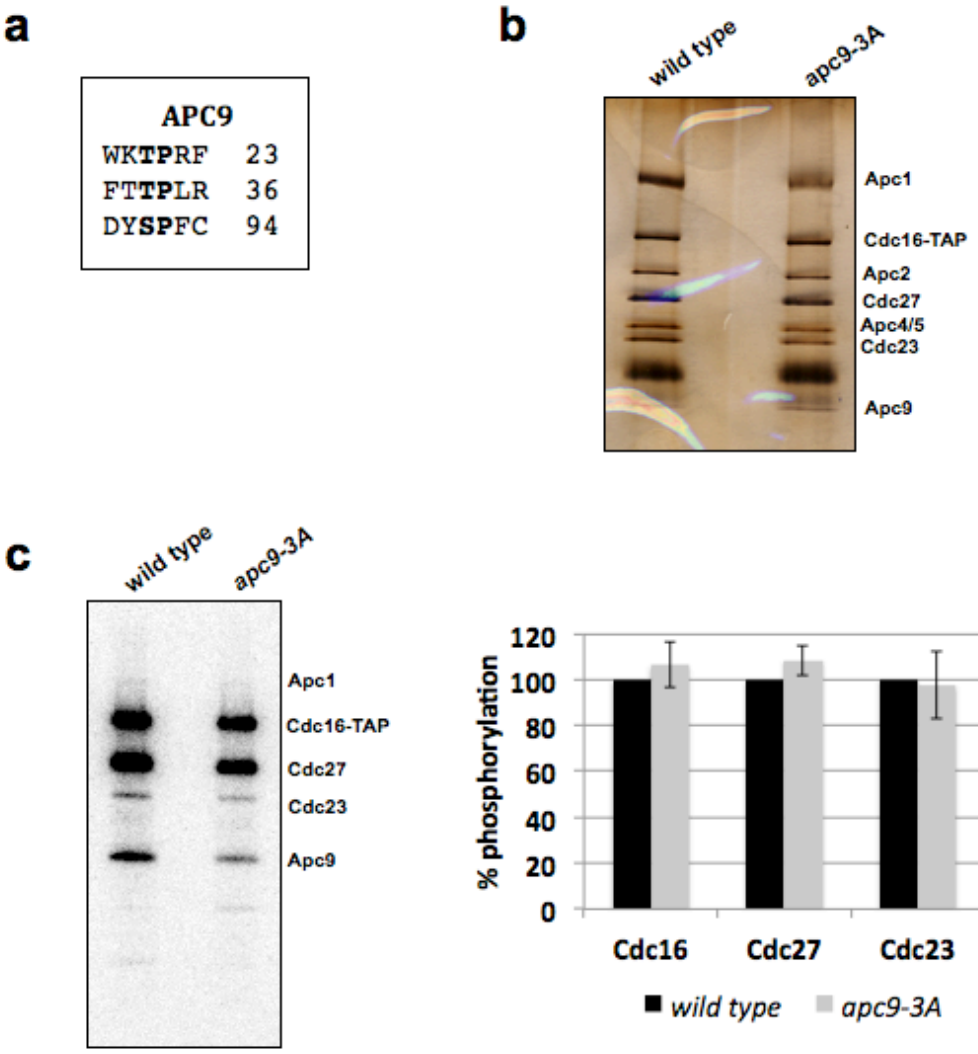
a
APC9
WKTPRF 23
FTTPLR 36
DYSPFC 94
b
wild type
apc9-3A
Apc1
Cdc16-TAP
Apc2
Cdc27
Apc4/5
Cdc23
Apc9
c
wild type
apc9-3A
Apc1
Cdc16-TAP
Cdc27
Cdc23
Apc9
% phosphorylation
120
100
80
60
40
20
0
Cdc16
Cdc27
Cdc23
Apc9
wild type
apc9-3A

Figure 4.4 Mutation of Cdk1 phosphorylation sites does not reduce phosphorylation of Apc9 in vitro

(A) All serine/proline (SP) and threonine/proline (TP) sites on Apc9 were mutated to alanine/proline (AP). (B) *CDC16-TAP* (ADR3089) and *apc9-3A CDC16-TAP* (ADR6969) cells were grown overnight in YEPD at 25˚C to log phase. The APC was purified, run on a polyacrylamide gel, and silver stained. (C) In vitro phosphorylation of wild type and *apc9-3A* APC. A fraction of the APCs purified in (B) were incubated with **γ-**[^{32}P]ATP and purified Cdk1/Clb2 complexes. Phosphorylated samples were run on a polyacrylamide gel, exposed to phosphorimager screen, and quantified using ImageQuant software. The average phosphorylation of the subunits Cdc16, Cdc27, Cdc23 and Apc9 (+/- SEM) relative to wild type levels of three independent experiments is shown.

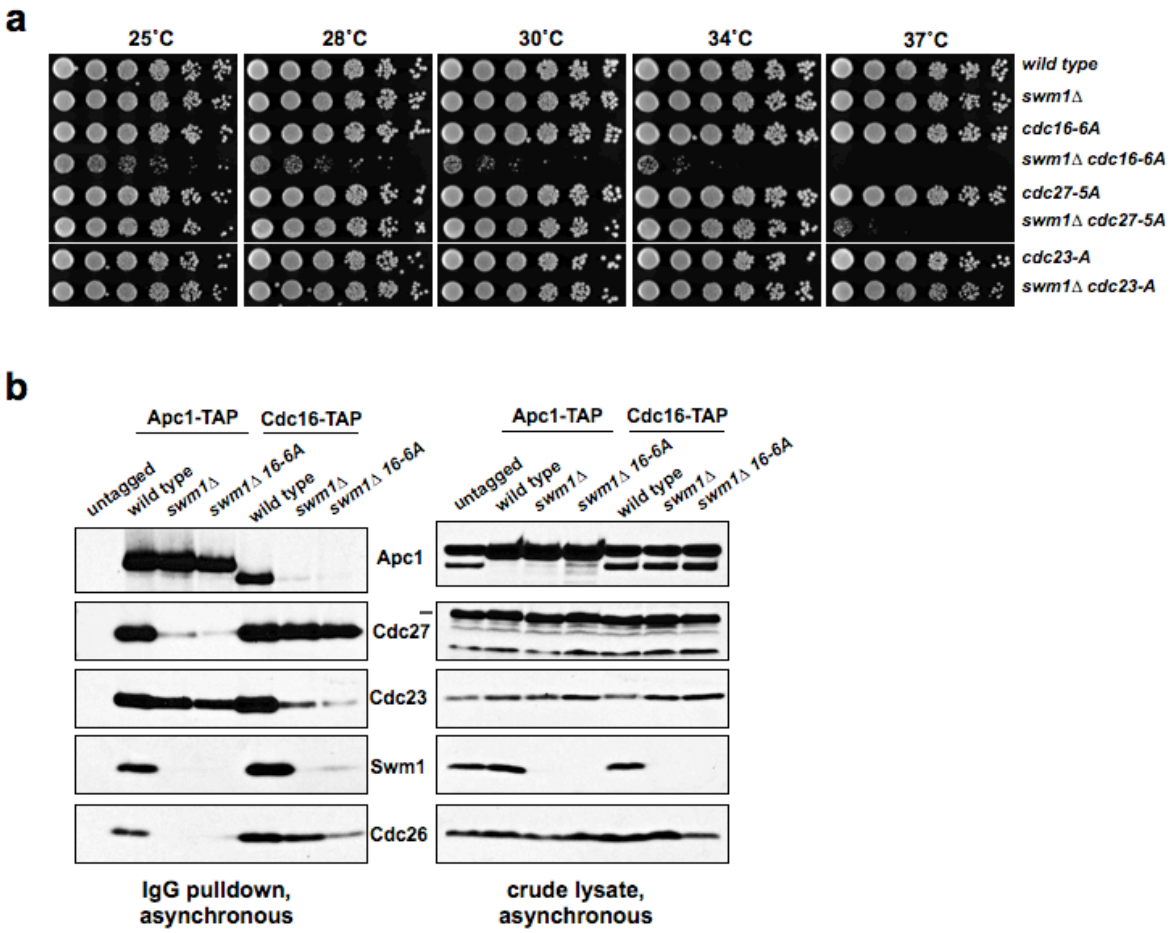
a
25˚C
28˚C
30˚C
34˚C
37˚C
wild type
swm1Δ
cdc16-6A
swm1Δ cdc16-6A
cdc27-5A
swm1Δ cdc27-5A
cdc23-A
swm1Δ cdc23-A
b
Apc1-TAP
Cdc16-TAP
untagged
wild type
swm1Δ
swm1Δ 16-6A
Apc1
Cdc27
Cdc23
Swm1
Cdc26
IgG pulldown, asynchronous
crude lysate, asynchronous

Figure 4.5 *swm1*Δ interacts with the *apc-A* mutants, but causes a loss of complex integrity

(A) *swm1*Δ interacts genetically with *apc-A* mutations. Wild type (ADR4006), *swm1*Δ (ADR5710), *cdc16-6A* (ADR5237), *swm1*Δ *cdc16-6A* (ADR5712), *cdc27–5A* (ADR2031), *swm1*Δ *cdc27-5A* (ADR5978), *cdc23-A* (ADR6463), and *swm1*Δ *cdc23-A* (ADR6678) cells were grown to saturation in YEPD at 25˚C. Eight-fold serial dilutions were spotted onto YEPD plates and grown for two days at the indicated temperatures. (B) Deletion of Swm1 disrupts complex integrity. Untagged (ADR4006), *APC1-TAP* (ADR6174), *swm1*Δ *APC1-TAP* (ADR5964), *swm1*Δ *cdc16-6A APC1-TAP* (ADR6175), *CDC16-TAP* (ADR3089), *swm1*Δ *CDC16-TAP* (ADR6073), and *swm1*Δ *cdc16-6A-TAP* (ADR5759) cells were grown overnight in YEPD at 25˚C to log phase. The APC was purified, run on a polyacrylamide gel, and immunoblotted with the indicated antibodies.

the loss of Cdc27 and Cdc26 in *APC2-TAP* or *APC4-TAP* purifications, and yielded only trace amounts of Cdc16 and Apc9 (Schwickart et al., 2004).

TPR subunit phosphorylation and the non-essential subunits Mnd2 and Cdc26

The non-essential TPR subunit Mnd2 was originally identified because of its involvement in the meiotic recombination process (Rabitsch et al., 2001), and in fact, mitotic phosphorylation of Mnd2 is important for normal meiotic progression (Torres and Borchers, 2007). More recently, Mnd2 has been shown to be important for removal of the MCC from the APC during recovery from a spindle assembly checkpoint arrest (Foster and Morgan, 2012; Mansfeld et al., 2011; Uzunova et al., 2012). Cdc20 is a component of the MCC, and so we wondered whether Mnd2 might be involved in co-activator binding to the APC. Deletion of Mnd2 in combination with the *apc-A* mutations did not exhibit temperature sensitivity (Fig. 4.6A). Consistent with previous reports, loss of Mnd2 does not affect complex integrity (Fig. 4.6B) (Hall et al., 2003; Oelschlaegel et al., 2005; Passmore et al., 2003). Furthermore, there are no significant differences in Cdh1 or Cdc20 binding in vitro (Fig. 4.6C), arguing that, at least in the absence of spindle assembly checkpoint activation, Mnd2 is not essential for Cdc20 binding to the APC.

While it behaves as a cell division cycle (cdc) mutant (Hartwell et al., 1973), Cdc26 is generally considered a non-essential subunit of the budding yeast APC. Only at elevated temperatures does Cdc26 become essential for cell viability, and arrests in metaphase as large-budded cells with an undivided nucleus (Zachariae et al., 1996) (see also Fig. 4.7A). Since the human Cdc26 has been shown to interact with Cdc16 and form a TPR repeat

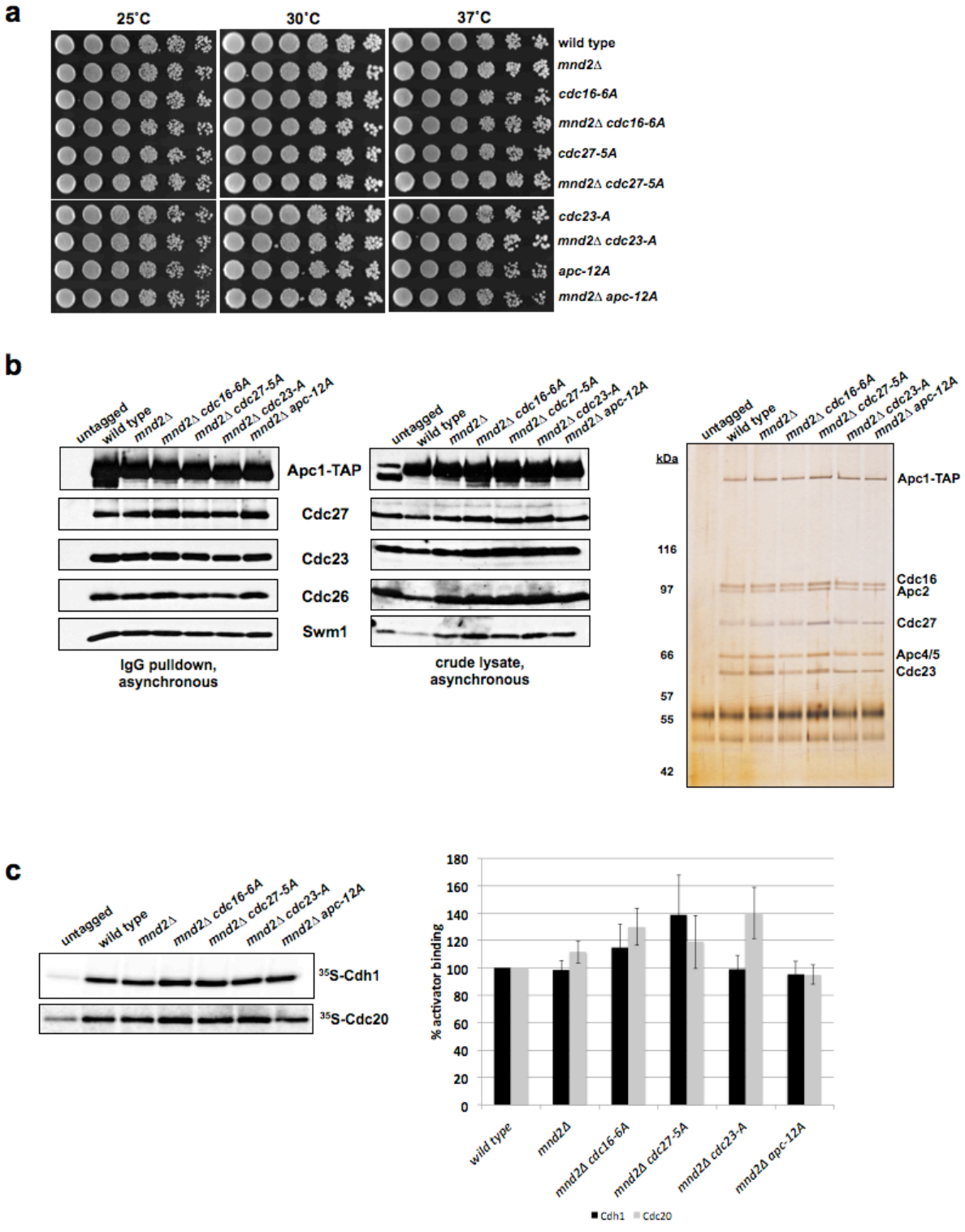
a
25°C
30°C
37°C
wild type
mnd2Δ
cdc16-6A
mnd2Δ cdc16-6A
cdc27-5A
mnd2Δ cdc27-5A
cdc23-A
mnd2Δ cdc23-A
apc-12A
mnd2Δ apc-12A
b
untagged
wild type
mnd2Δ
mnd2Δ cdc16-6A
mnd2Δ cdc27-5A
mnd2Δ cdc23-A
mnd2Δ apc-12A
Apc1-TAP
Cdc27
Cdc23
Cdc26
Swm1
IgG pulldown, asynchronous
crude lysate, asynchronous
kDa
116
97
66
57
55
42
Apc1-TAP
Cdc16
Apc2
Cdc27
Apc4/5
Cdc23
c
35S-Cdh1
35S-Cdc20
% activator binding
180
160
140
120
100
80
60
40
20
0
wild type
mnd2Δ
mnd2Δ cdc16-6A
mnd2Δ cdc27-5A
mnd2Δ cdc23-A
mnd2Δ apc-12A
Cdh1
Cdc20

Figure 4.6 Loss of Mnd2 does not affect complex integrity or co-activator binding

(A) *mnd2*Δ does not interact genetically with the *apc-A* mutations. Wild type (ADR4006), *mnd2*Δ (ADR7451), *cdc16-6A* (ADR5237), *mnd2*Δ *cdc16-6A* (ADR5574), *cdc27–5A* (ADR2031), *mnd2*Δ *cdc27-5A* (ADR5681), *cdc23-A* (ADR6463), *mnd2*Δ *cdc23-A* (ADR7643), *apc-12A* (ADR6623), and *mnd2*Δ *apc-12A* (ADR7646) cells were grown to saturation in YEPD at 25˚C. Eight-fold serial dilutions were spotted onto YEPD plates and grown for two days at the indicated temperatures. (B) Deletion of Mnd2 does not affect complex integrity. Untagged (ADR4006), wild type (ADR6174), *mnd2*Δ (ADR7624), *mnd2*Δ *cdc16-6A* (ADR7653), *mnd2*Δ *cdc27-5A* (ADR7656), *mnd2*Δ *cdc23-A* (ADR7658), *mnd2*Δ *apc-12A* (ADR7650) cells were grown overnight in YEPD at 25˚C to log phase. All strains except untagged are *APC1-TAP.* The APC was purified, run on a polyacrylamide gel, and immunoblotted with the indicated antibodies (left) or silver stained (right). (C) A fraction of the APCs purified in (B) were incubated with ^{35}S-labelled Cdh1 or Cdc20, and washed to remove any loosely bound proteins. Reactions were run on a polyacrylamide gel, exposed to phosphorimager screen, and quantified using ImageQuant software. The average binding (+/- SEM) relative to wild type levels of three independent experiments is shown.

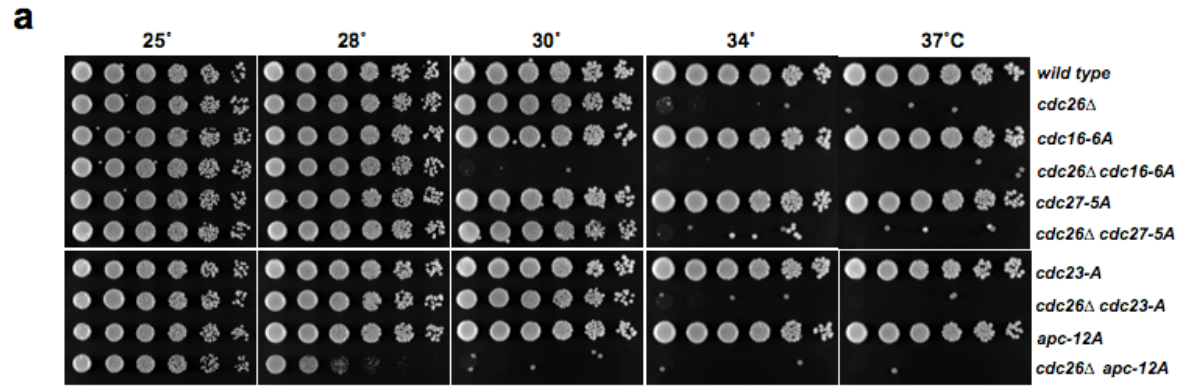
a
25˚
28˚
30˚
34˚
37˚C
wild type
cdc26Δ
cdc16-6A
cdc26Δ cdc16-6A
cdc27-5A
cdc26Δ cdc27-5A
cdc23-A
cdc26Δ cdc23-A
apc-12A
cdc26Δ apc-12A

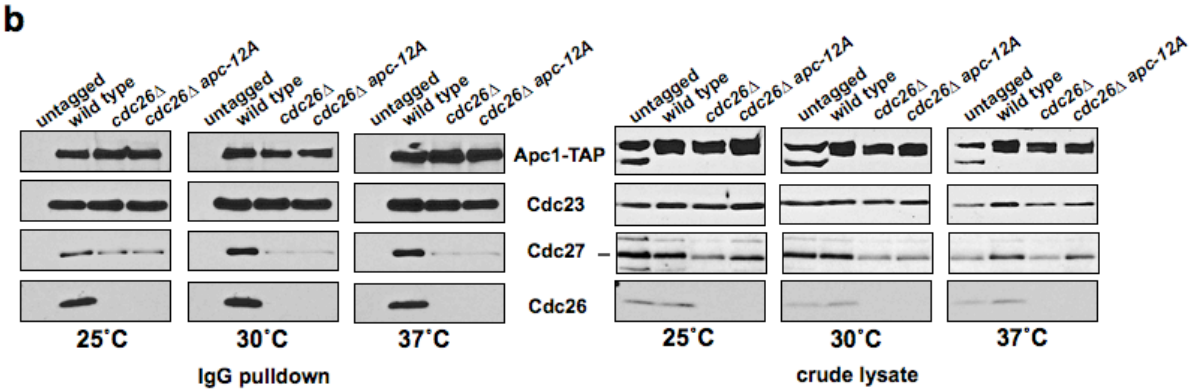
b
untagged
wild type
cdc26Δ
cdc26Δ apc-12A
Apc1-TAP
Cdc23
Cdc27
Cdc26
25˚C
30˚C
37˚C
IgG pulldown
crude lysate

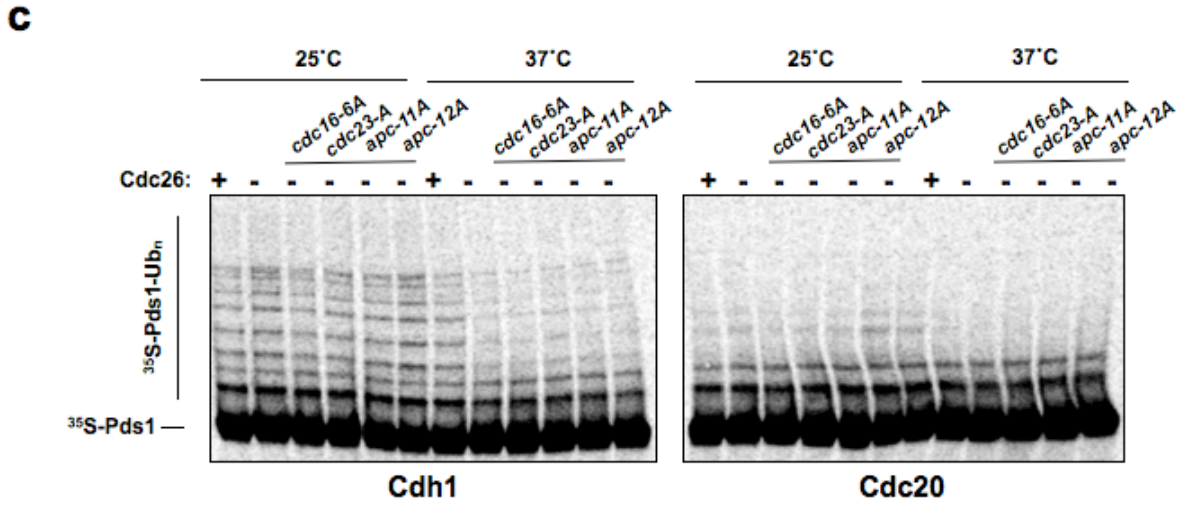
c
25˚C
37˚C
cdc16-6A
cdc23-A
apc-11A
apc-12A
Cdc26:
35S-Pds1-Ubn
35S-Pds1
Cdh1
Cdc20

Figure 4.7 *cdc26*Δ interacts genetically with the *apc-A* mutants, but exhibits a loss of complex integrity at elevated temperatures

(A) *cdc26*Δ lowers the maximum permissive temperature of the *apc-A* mutations. Wild type (ADR4006), *cdc26*Δ (ADR6967), *cdc16-6A* (ADR5237), *cdc26*Δ *cdc16-6A* (ADR5864), *cdc27–5A* (ADR2031), *cdc26*Δ *cdc27-5A* (ADR5867), *cdc23-A* (ADR6463), *cdc26*Δ *cdc23-A* (ADR6601), *apc-12A* (ADR6623), and *cdc26*Δ *apc-12A* (ADR6555) cells were grown to saturation in YEPD at 25˚C. Eight-fold serial dilutions were spotted onto YEPD plates and grown for two days at the indicated temperatures. (B) Untagged (ADR4006), wild type (ADR6174), *cdc26*Δ (ADR5970), and *cdc26*Δ *apc-12A* (ADR6533) cells were grown overnight in YEPD at 25˚C to log phase, and shifted to the indicated temperature for 1hr before harvesting. All strains except untagged are *APC1-TAP.* The APC was purified, run on a polyacrylamide gel, and immunoblotted with the indicated antibodies. (C) Loss of Cdc26 at 37˚C leads to reduced ubiquitination activity in vitro. APC was purified from wild type (ADR6174), *cdc26*Δ (ADR5970), *cdc26*Δ *cdc16-6A* (ADR6172), *cdc26*Δ *cdc23-A* (ADR6535), *cdc26*Δ *apc-11A* (ADR6170), and *cdc26*Δ *apc-12A* (ADR6533) cells, and the activity assayed in an in vitro ubiquitination assay. *apc-11A* refers to the loss of 11 phosphorylation sites: 6 in Cdc16, and 5 in Cdc27. All strains are *APC1-TAP.* Ubiquitination reactions were run on a polyacrylamide gel and exposed to a phosphorimager screen.

(Wang et al., 2009), and the TPR subunits of the APC are involved in co-activator binding, we wondered if Cdc26 might cooperate with Cdk1 phosphorylation of the TPR subunits and contribute to Cdc20 binding and subsequent activation of the APC. When we combined a deletion of *CDC26* with the *apc-12A* mutant, we found that the loss of Cdk1 phosphorylation sites on the TPR subunits Cdc16, Cdc23 and Cdc27 lowered the maximum permissive temperature of the *cdc26*Δ mutant (Fig. 4.7A). This genetic interaction is primarily due to loss of phosphorylation on Cdc16 (compare *cdc26*Δ *cdc16-6A* with other phosphorylation site mutants), although *cdc26*Δ *apc-12A* shows reduced growth even at 28˚C.

Several reports have suggested that the loss of Cdc26 leads to a decrease in the amounts of purified Cdc16, Cdc27 and Apc9 (Schwickart et al., 2004; Thornton et al., 2006; Zachariae et al., 1998b), while another report argues the APC subunit stoichiometry and ubiquitination activity in a *cdc26*Δ mutant appears normal (Passmore et al., 2003). When we purified the APC using a TAP-tagged Apc1 subunit from wild type, *cdc26*Δ and *cdc26*Δ *apc-12A* mutants grown at 25˚C, 30˚C and the restrictive temperature of 37˚C, we discovered a minor loss of Cdc27 at 25˚C, with further losses at 30˚C and 37˚C in both the *cdc26*Δ and *cdc26*Δ *apc-12A* backgrounds (Fig. 4.7B). This effect appears to be primarily due to the loss of Cdc26: the addition of the *apc-12A* mutations to the *cdc26*Δ mutant did not greatly increase the loss of Cdc27. Levels of Cdc16 also appear to be reduced, when assessed by silver stain (data not shown).

Given the conflicting reports with respect to the integrity and activity of the APC purified from a *cdc26*Δ background, we also directly assayed the ubiquitination activity of the APC purified from *cdc26*Δ cells. We wondered if the decrease in the maximum

permissive temperature seen in the *cdc26*Δ *apc-12A* mutant corresponded with a decrease in APC ubiquitination in vitro. We have previously shown that the *apc-12A* mutant only displays a modest defect in ubiquitination activity in vitro, but that the twelve Cdk1 sites appear to be required for full activation of the APC in vitro (Lianga et al., 2013) (see also Fig. 3.8). Here we show that when grown at 25˚C, the APC purified from a *cdc26*Δ background exhibits wild type levels of Cdh1 and Cdc20-dependent activity (Fig. 4.7C). When grown at 37˚C, however, we see a drop in both Cdh1 and Cdc20-dependent activity. Similar to the loss of Apc9, this drop in ubiquitination activity is not exacerbated by the addition of the *apc-A* mutations, arguing the effect is likely primarily due to the loss of the Cdc27 subunit (Fig. 4.7C).

The human Cdc26 interacts directly with Cdc16, and completes a TPR repeat (Wang et al., 2009). This same group also showed that expression of the N terminal fragment of Cdc26 that interacts with Cdc16 is sufficient to rescue the temperature sensitive growth of a *cdc26*Δ mutant (Wang et al., 2009). We created an identical truncation to that described by Wang et al., $Cdc26^{1-31}$, as well as a larger truncation that includes the first 52 N terminal residues of the Cdc26 protein, $Cdc26^{1-52}$. In contrast to published results, we found that expression of the $Cdc26^{1-31}$ truncation did not restore viability at 37˚C, and essentially behaved as a *cdc26*Δ mutant (Fig. 4.8A). This truncation was created by replacing the endogenous copy of Cdc26, resulting in endogenous levels of protein expression, while Wang et al. expressed the truncation on a high copy number plasmid. The resulting

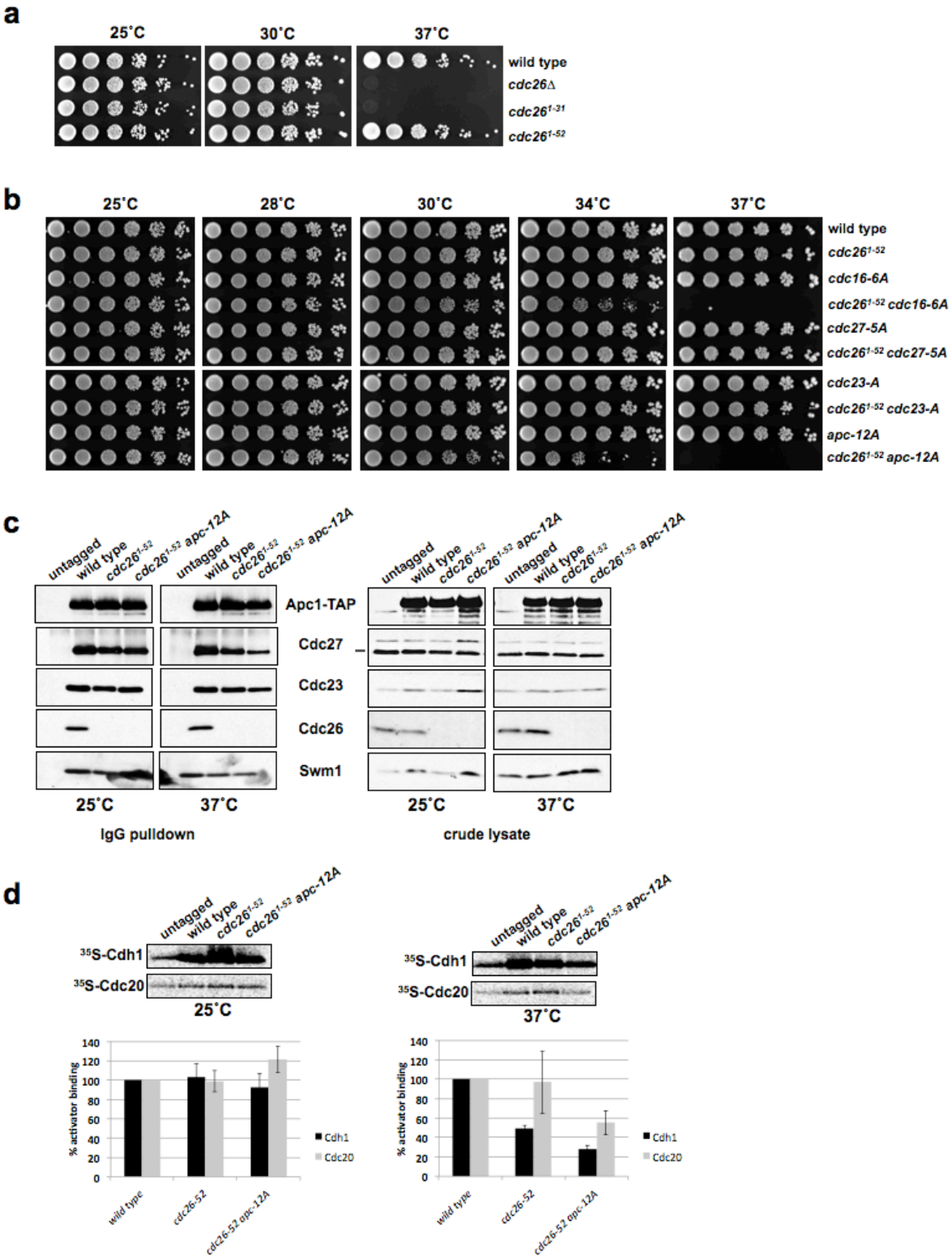
a
25˚C
30˚C
37˚C
wild type
cdc26Δ
cdc26^1-31
cdc26^1-52
b
25˚C
28˚C
30˚C
34˚C
37˚C
wild type
cdc26^1-52
cdc16-6A
cdc26^1-52 cdc16-6A
cdc27-5A
cdc26^1-52 cdc27-5A
cdc23-A
cdc26^1-52 cdc23-A
apc-12A
cdc26^1-52 apc-12A
c
untagged
wild type
cdc26^1-52
cdc26^1-52 apc-12A
Apc1-TAP
Cdc27
Cdc23
Cdc26
Swm1
25˚C
37˚C
IgG pulldown
crude lysate
d
35S-Cdh1
35S-Cdc20
25˚C
37˚C
% activator binding
Cdh1
Cdc20
wild type
cdc26-52
cdc26-52 apc-12A

Figure 4.8 Cdc26$^{1-52}$ is not temperature sensitive, but maintains genetic interaction with the *apc-A* mutants

(A) *cdc26$^{1-52}$* is no longer temperature sensitive. Wild type (ADR4006), *cdc26*Δ (ADR5230), *cdc26$^{1-31}$* (ADR6337), and *cdc26$^{1-52}$* (ADR6354) cells were grown to saturation in YEPD at 25˚C. Eight-fold serial dilutions were spotted onto YEPD plates and grown for two days at the indicated temperatures. (B) *cdc26$^{1-52}$* exhibits a genetic interaction with the *apc-A* mutations. Wild type (ADR4006), *cdc26$^{1-52}$* (ADR6396), *cdc16-6A* (ADR5237), *cdc26$^{1-52}$ cdc16-6A* (ADR6316), *cdc27–5A* (ADR2031), *cdc26$^{1-52}$ cdc27-5A* (ADR6326), *cdc23-A* (ADR6463), *cdc26$^{1-52}$ cdc23-A* (ADR6549), *apc-12A* (ADR6623), and *cdc26$^{1-52}$ apc-12A* (ADR6545) cells were grown as in (A). (C) Untagged (ADR4006), wild type (ADR6174), *cdc26$^{1-52}$* (ADR6488), and *cdc26$^{1-52}$ apc-12A* (ADR7053) cells were grown overnight in YEPD at 25˚C to log phase, and shifted to the indicated temperature for 1hr before harvesting. All strains except untagged are *APC1-TAP.* The APC was purified, run on a polyacrylamide gel, and immunoblotted with the indicated antibodies. (D) A fraction of the APCs purified in (C) were incubated with ^{35}S-labelled Cdh1 or Cdc20, and washed to remove any loosely bound proteins. Reactions were run on a polyacrylamide gel, exposed to phosphorimager screen, and quantified using ImageQuant software. The average binding (+/- SEM) relative to wild type levels of three independent experiments is shown.

overexpression of Cdc26$^{1-31}$ likely explains this discrepancy. We did find, however, that expression of the larger truncation, Cdc26$^{1-52}$, rescued the temperature sensitivity of a *cdc26*Δ strain (Fig. 4.8A), but still lowered the maximum permissive temperature of the *apc-A* mutants (Fig. 4.8B). These genetic experiments suggest the isolation of two independent functions of Cdc26: the Cdc26$^{1-52}$ truncation alone is no longer temperature sensitive, but the C terminal portion of Cdc26 is important for cell viability at elevated temperatures in the *apc-A* backgrounds.

When we purified the Cdc26$^{1-52}$ APCs as described previously for the *cdc26*Δ mutants, we discovered that APC purified from cells expressing the Cdc26$^{1-52}$ truncation, grown at the restrictive temperature of 37˚C, remains largely intact, apart from a minor loss of Cdc27 in the *cdc26$^{1-52}$ apc-12A* background (Fig. 4.8C). The slight loss of Cdc27 in the *cdc26$^{1-52}$ apc-12A* background suggests that mutation of the five Cdk1 phosphorylation sites in Cdc27 may have some weak loss of function. Note that the Cdc26$^{1-52}$ truncated protein is not recognized by our Cdc26 antibody because the antibody was raised against the C terminal portion of Cdc26. These APCs exhibit wild type levels of Cdh1 and Cdc20 binding in vitro when grown at 25˚C. The loss of Cdc27 seen when grown at 37˚C, however, resulted in a decrease in the binding of both co-activators in vitro relative to wild type (Fig. 4.8D). Binding of Cdh1 and Cdc20 to the APC purified from the *cdc26$^{1-52}$ apc-12A* background was reduced even further, compared with the *cdc26$^{1-52}$* background alone. This decrease was more dramatic with Cdh1, which suggests that Cdc27 may play a more important role in the binding of Cdh1, than of Cdc20.

Since truncation of Cdc26 interacts with the *apc-A* mutations, but doesn't cause any major defects at 25˚C, we wondered how these mutants might behave with the loss of an additional non-essential TPR subunit. Loss of both Cdc26 and Mnd2 greatly reduces the maximum permissive temperature compared to the *mnd2*Δ and *cdc26*Δ mutants alone (Fig. 4.9A), consistent with a previous report (Page et al., 2005). The *mnd2*Δ *cdc26*$^{1\text{-}52}$ mutant, however, is viable up to 37˚C (Fig. 4.9B). The loss of the 12 Cdk1 phosphorylation sites in the *mnd2*Δ *cdc26*$^{1\text{-}52}$ background further reduces the viability of this mutant at all temperatures tested, compared to the *mnd2*Δ *apc-12A* and *cdc26*$^{1\text{-}52}$ *apc-12A* mutants (Fig. 4.9B). This genetic interaction is primarily due to the loss of phosphorylation sites on Cdc16 (compare *cdc16-6A* with *cdc27-5A* and *cdc23-A* mutants).

Again we first assessed whether this temperature sensitivity was due to disruption of complex integrity. The *mnd2*Δ *cdc26*$^{1\text{-}52}$ *apc-12A* mutant APC shows a slight loss of the subunits Cdc27, Cdc23 and Swm1 when grown at 25˚C (Fig. 4.9C). The loss of Cdc27 in the *mnd2*Δ *cdc26*$^{1\text{-}52}$ *apc-12A* background is slightly more dramatic than that seen in the *cdc26*$^{1\text{-}52}$ *apc-12A* background. As shown in Figures 4.6 and 4.8, the *mnd2*Δ *apc-12A* and *cdc26*$^{1\text{-}52}$ *apc-12A* mutant APCs exhibit wild type levels of co-activator binding in vitro when grown at 25˚C (Fig. 4.9D). The *mnd2*Δ *cdc26*$^{1\text{-}52}$, and *mnd2*Δ *cdc26*$^{1\text{-}52}$ *apc-12A* mutant APCs, however, show only about 60-80% binding of both Cdh1 and Cdc20 relative to wild type (Fig. 4.9D). Despite the greater loss of Cdc27 in the *mnd2*Δ *cdc26*$^{1\text{-}52}$ *apc-12A* background, the loss of Cdk1 phosphorylation sites in the *mnd2*Δ *cdc26*$^{1\text{-}52}$ background does not further reduce co-activator binding in vitro.

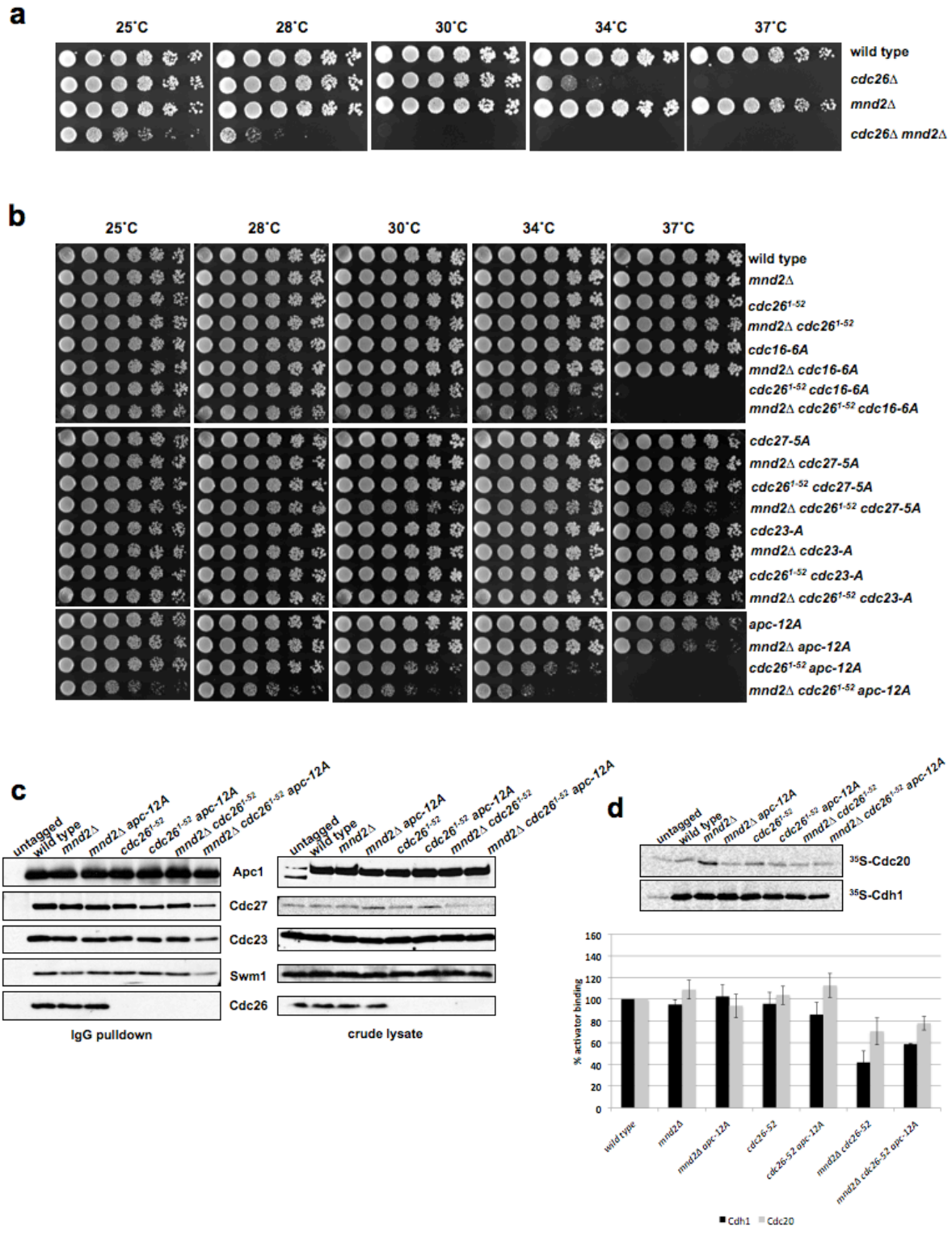
a
25˚C
28˚C
30˚C
34˚C
37˚C
wild type
cdc26Δ
mnd2Δ
cdc26Δ mnd2Δ
b
25˚C
28˚C
30˚C
34˚C
37˚C
wild type
mnd2Δ
cdc26^1-52
mnd2Δ cdc26^1-52
cdc16-6A
mnd2Δ cdc16-6A
cdc26^1-52 cdc16-6A
mnd2Δ cdc26^1-52 cdc16-6A
cdc27-5A
mnd2Δ cdc27-5A
cdc26^1-52 cdc27-5A
mnd2Δ cdc26^1-52 cdc27-5A
cdc23-A
mnd2Δ cdc23-A
cdc26^1-52 cdc23-A
mnd2Δ cdc26^1-52 cdc23-A
apc-12A
mnd2Δ apc-12A
cdc26^1-52 apc-12A
mnd2Δ cdc26^1-52 apc-12A
c
untagged
wild type
mnd2Δ
mnd2Δ apc-12A
cdc26^1-52
cdc26^1-52 apc-12A
mnd2Δ cdc26^1-52
mnd2Δ cdc26^1-52 apc-12A
Apc1
Cdc27
Cdc23
Swm1
Cdc26
IgG pulldown
crude lysate
d
35S-Cdc20
35S-Cdh1
% activator binding
wild type
mnd2Δ
mnd2Δ apc-12A
cdc26-52
cdc26-52 apc-12A
mnd2Δ cdc26-52
mnd2Δ cdc26-52 apc-12A
Cdh1
Cdc20

Figure 4.9 Mutation of Mnd2 and Cdc26 reduces co-activator binding in vitro

(A) Loss of Cdc26 and Mnd2 reduces growth at 25˚C. Wild type (ADR4006), *cdc26*Δ (ADR6967), *mnd2*Δ (ADR5542), and *cdc26*Δ *mnd2*Δ (ADR7328) cells were grown to saturation in YEPD at 25˚C. Eight-fold serial dilutions were spotted onto YEPD plates and grown for two days at the indicated temperatures. (B) Loss of Mnd2 reduces the maximum permissive temperature of the *cdc26$^{1-52}$ apc-A* mutants. Wild type (ADR4006), *mnd2*Δ (ADR7451), *cdc26$^{1-52}$* (ADR6393), *mnd2*Δ *cdc26$^{1-52}$* (ADR7568), *cdc16-6A* (ADR5237), *mnd2*Δ *cdc16-6A* (ADR5574), *cdc26$^{1-52}$ cdc16-6A* (ADR6316), *mnd2*Δ *cdc26$^{1-52}$ cdc16-6A* (ADR7617), *cdc27-5A* (ADR2031), *mnd2*Δ *cdc27-5A* (ADR5681), *cdc26$^{1-52}$ cdc27-5A* (ADR6326), *mnd2*Δ *cdc26$^{1-52}$ cdc27-5A* (ADR7619), *cdc23-A* (ADR6463), *mnd2*Δ *cdc23-A* (ADR7643), *cdc26$^{1-52}$ cdc23-A* (ADR6549), *mnd2*Δ *cdc26$^{1-52}$ cdc23-A* (ADR7621), *apc-12A* (ADR6623), *mnd2*Δ *apc-12A* (ADR7646), *cdc26$^{1-52}$ apc-12A* (ADR6545), *mnd2*Δ *cdc26$^{1-52}$ apc-12A* (ADR7623) cells were grown as in (A). (C) Untagged (ADR4006), wild type (ADR6174), *mnd2*Δ (ADR7624), *mnd2*Δ *apc-12A* (ADR7650), *cdc26$^{1-52}$* (ADR6488), *cdc26$^{1-52}$ apc-12A* (ADR7053), *mnd2*Δ *cdc26$^{1-52}$* (ADR7628) and *mnd2*Δ *cdc26$^{1-52}$ apc-12A* (ADR7642) cells were grown overnight in YEPD at 25˚C to log phase. All strains except untagged are *APC1-TAP.* The APC was purified, run on a polyacrylamide gel, and immunoblotted with the indicated antibodies. (D) A fraction of the APCs purified in (C) were incubated with ^{35}S-labelled Cdh1 or Cdc20, and washed to remove any loosely bound proteins. Reactions were run on a polyacrylamide gel, exposed to phosphorimager screen, and quantified using ImageQuant software. The average binding (+/- SEM) relative to wild type levels of two independent experiments is shown.

4.3 DISCUSSION

Phosphorylation of the essential TPR subunits does not influence Cdc20 binding

Cdk1 phosphorylation of the APC is argued to contribute to activation of the APC at the metaphase-anaphase transition by increasing association of the mitotic co-activator, Cdc20 (Kraft et al., 2003; Kramer et al., 2000; 1998a; Rudner and Murray, 2000; Shteinberg et al., 1999). While this model is generally accepted in the literature, it has not yet been rigorously tested using mutational analysis. The data presented here contradict this model: we show that Cdc20 binds at wild type levels, both in vitro and in vivo, in the absence of Cdk1 phosphorylation of the TPR subunits Cdc16, Cdc23 and Cdc27. This directly contradicts the one study that used mutational analysis to find that the *cdc16-6A* APC has reduced affinity for Cdc20 (Rudner and Murray, 2000), although this difference is likely attributable to recent improvements in the ability to detect co-activator binding both in vitro and in vivo. The original study assessed the binding of a tagged Cdc20, using the *Cdc20-myc12* allele, in an anaphase arrest in vivo. Recent work has led us to question the functionality of tagged Cdc20. The binding of Cdc20 in Fig. 4.2A bypasses this issue, as the antibody used was raised directly against the Cdc20 protein, avoiding the use of a tag altogether. The development of an in vitro co-activator binding assay has also aided these studies.

Our data argues that the affinity of Cdc20 for the APC is unchanged regardless of the phosphorylation state of Cdc16, Cdc23 and Cdc27. This suggests two possibilities: that global Cdk1 phosphorylation does not impact Cdc20 binding, or that there are additional phosphorylation sites that are important. We've previously shown that inhibition of Cdk1

activity, by overexpression of Swe1, arrests cells in metaphase with stable levels of APC substrates, and exhibits reduced APC activity in vitro (Lianga et al., 2013) (see also Chapter 3). The difference in ubiquitination activity between the *apc-12A* and the Swe1-inhibited APC phenotypes strongly suggests that further Cdk1-dependent phosphorylation is important for full APC activity (Fig. 3.6). In vitro phosphorylation of the APC with Cdk1/Clb2 complexes, which phosphorylates Apc1, Apc9, Apc4, and Mnd2 (Fig. 3.7B, 3.8D and unpublished data), in addition to Cdc16, Cdc23 and Cdc27, however, does not greatly affect the ability of Cdc20 to bind in vitro (Fig. 4.1C). In addition, Cdc20 binds equally well to the *GAL-SWE1* APC as to wild type APC (Fig. 4.1A), suggesting that any additional Cdk1 phosphorylation sites that may be important for activity are not affecting the ability of Cdc20 to bind the APC.

The *cdc55*Δ mutant is characterized by its ability to bypass the morphogenesis checkpoint (Chiroli et al., 2007), and exhibits slow degradation of APC substrates upon checkpoint activation with latA (Lianga et al., 2013). $PP2A^{Cdc55}$ dephosphorylates the APC in vitro, and the *cdc55*Δ mutant exhibits increased APC phosphorylation in vitro (Lianga et al., 2013). Loss of the twelve Cdk1 phosphorylation sites in the *cdc55*Δ mutant, however, suppresses premature activation of the APC during both morphogenesis and spindle checkpoint activation (Lianga et al., 2013), suggesting that, in *cdc55*Δ cells, checkpoint inhibition of the APC is countered by increased phosphorylation and activation of the APC. This further suggests that these twelve Cdk1 phosphorylation sites on the APC are important for its activity in anaphase.

It has been suggested that co-activator must be bound to substrate before binding to the APC can occur (Burton et al., 2005). While our in vitro binding assay does not address the relative contribution of substrate to co-activator binding, it does, however, show that in the absence of substrate, we are still able to quantify the relative binding of both Cdh1 and Cdc20 to the APC. The concept that substrate is not required for APC-co-activator binding is also consistent with previous work (Matyskiela and Morgan, 2009; Passmore and Barford, 2005; Thornton et al., 2006). When we assessed Cdc20 binding from a metaphase arrest in vivo (and therefore in the presence of substrate), we found that Cdc20 binding was unchanged in the phosphorylation sites mutants (Fig. 4.2B).

The metaphase arrest used to assess the binding of Cdc20 in vivo is induced by activation of the SAC. The positioning of bound Cdc20 differs whether it is complexed with the checkpoint proteins as the MCC, or if Cdc20 is binding as a co-activator of the APC (Chao et al., 2012; Herzog et al., 2009; Izawa and Pines, 2011). Presently, we cannot distinguish whether the Cdc20 bound in this experiment is the interaction of Cdc20 as a component of the MCC, or Cdc20 bound as a co-activator, or both. Given that the SAC is activated in these conditions, we believe at least a fraction of the Cdc20 bound is complexed with the MCC. Assessing a metaphase arrest not induced by the SAC will allow us to determine the relative differences of Cdc20 and the other checkpoint proteins bound to the APC, and compare this with checkpoint arrested cells. MCC binding and the spindle assembly checkpoint are discussed in greater detail in Chapter 5.

The non-essential TPR subunits Apc9 and Swm1

We explored the possibility that the less studied non-essential TPR subunits might be involved in co-activator binding, in cooperation with Cdk1 phosphorylation of Cdc16, Cdc23 and Cdc27. Consistent with previous reports, we found that Apc9 is not essential for viability at elevated temperatures, but that loss of Apc9 causes a loss of the outermost TPR subunit, Cdc27, from the complex (Hall et al., 2003; Page et al., 2005; Passmore et al., 2003; Zachariae et al., 1998b). This loss results in decreased ubiquitination activity in vitro, consistent with the inability of Cdh1 to bind *apc9*Δ APC (Passmore et al., 2003). In vivo metabolic labeling, and in vitro phosphorylation of the APC with Cdk1/Clb2 indicates Apc9 is phosphorylated (Fig. 3.1A, 3.7B, and 3.8D), and three Cdk1 consensus sites are found within the Apc9 sequence. The *apc9*Δ *apc-12A* viability at 37˚C, however, suggests that these sites don't make an important contribution to APC activity.

Previous groups have argued that *swm1*Δ cells exhibit poor growth at temperatures above 30˚C (Hall et al., 2003; Page et al., 2005; Passmore et al., 2003; Schwickart et al., 2004), while we found that loss of Swm1 did not cause any temperature sensitivity (Fig. 4.5A). This difference is likely a result of the use of different strain backgrounds. Cdc16 no longer associates efficiently with other subunits in APC purified from *swm1*Δ cells (Schwickart et al., 2004), so the loss of the phosphorylation sites in Cdc16 may have been sufficient to further disrupt interactions among the TPR subunits and result in the genetic interaction seen in the *swm1*Δ *cdc16-6A* background (Fig. 4.5). Structural analysis of reconstituted APC confirms that Apc13, the vertebrate Swm1, mediates the interaction of Cdc16 and Cdc23 (Schreiber et al., 2011), which is also consistent with biochemical evidence supporting direct Swm1-Cdc23 interactions (Hall et al., 2003). Swm1 is required

for normal ubiquitination activity, but the disruption of the complex causes defects in both Cdh1 and Cdc20-dependent activity (Schwickart et al., 2004), arguing the role of Swm1 within the complex is not specific to APC^{Cdc20} activity and Cdk1 phosphorylation of the TPR subunits.

The non-essential TPR subunits Mnd2 and Cdc26

Little is known about the function of Cdc26, although it appears to play some role in maintaining complex integrity. Consistent with the data presented here, several reports have shown that the loss of Cdc26 causes a decrease in the amounts of purified Cdc16, Cdc27 and Apc9 (Schwickart et al., 2004; Zachariae et al., 1998b). Another report has argued that APC subunit stoichiometry in the *cdc26*Δ background appears normal, although this group only assessed the *cdc26*Δ APC at 25˚C (Passmore et al., 2003). By creating the $Cdc26^{1-52}$ truncation we have isolated two functions of Cdc26: the $Cdc26^{1-52}$ truncation alone is no longer temperature sensitive, but the C terminal portion of Cdc26 is important for cell viability at elevated temperatures in the *apc-A* mutants. In other words, the $Cdc26^{1-52}$ truncation keeps the APC nearly intact at elevated temperature, unlike *cdc26*Δ, but has still lost the C terminal portion of Cdc26 that interacts with the *apc-A* mutations. It is possible that a different truncation of Cdc26, with a larger portion of the N terminus, could maintain normal APC architecture. While the role of Cdk1 phosphorylation of the TPR subunits of the APC is currently unclear, it seems likely that the C terminus of Cdc26 participates in the same pathway (Chapter 5).

The Cdc26 homolog in fission yeast, Hcn1, is phosphorylated by Cdk1, and mutation of this residue (S48A) causes cells to spend a slightly longer time in anaphase (Yoon et al., 2006). This serine residue is not conserved in budding yeast, but it has, however, been replaced by an evolutionarily conserved aspartic acid, which may mimic a constitutively phosphorylated state (Wang et al., 2009). The Cdc26$^{1-52}$ truncation, which removes this conserved aspartic acid (D53), rescues the temperature sensitivity of a *cdc26*Δ mutant, but retains the genetic interaction with the *apc-A* mutations. While we have yet to test a point mutation of this residue (D53A), these experiments suggest that the C terminal portion of Cdc26, which includes this aspartic acid residue, may be important for cell viability in the *apc-A* backgrounds, and may work in cooperation with Cdk1 phosphorylation of the essential TPR subunits.

The C terminal IR motif of Cdh1 binds to Cdc27, as loss of this motif doesn't further reduce the ubiquitination activity of APC purified from a *cdc27*Δ background (Thornton et al., 2006). Mutation of the N terminal C box, however, leads to the inability of Cdh1 to stimulate the ubiquitination activity of the *cdc27*Δ APC, arguing the C box binds elsewhere on the APC, independent of the Cdc27-IR motif interaction (Kraft et al., 2005; Thornton et al., 2006). Loss of Cdc27 from the *cdc26$^{1-52}$* and *cdc26$^{1-52}$ apc-12A* complexes when grown at elevated temperature resulted in a decrease in the ability to bind Cdh1, consistent with its established role in co-activator binding (Kraft et al., 2005; Matyskiela and Morgan, 2009; Thornton and Toczyski, 2003; Thornton et al., 2006; Vodermaier et al., 2003). This decrease in Cdh1 binding is likely due to a disruption of the Cdc27-IR motif interaction, although we

can't rule out the possibility that the interaction of the C box of Cdh1 with the APC is also affected.

The decrease in co-activator binding seen with the *cdc26*$^{1-52}$ and *cdc26*$^{1-52}$ *apc-12A* complexes was much less prominent with Cdc20, however, further supporting the notion that the interaction of Cdc20 with the APC is less dependent on Cdc27 than Cdh1, and additional sites of contact on the APC may exist. In support of the notion that the mechanisms of APC-Cdh1 and APC-Cdc20 binding are different, the IR motif of Cdc20 is not essential for viability, although it is definitively important for Cdh1 function in vitro and in vivo (Kraft et al., 2005; Thornton et al., 2006).

The lowered maximum permissive temperature of the *cdc26*Δ *mnd2*Δ strain suggests that Cdc26 and Mnd2 may perform a similar function. Furthermore, the loss of Cdk1 phosphorylation sites on Cdc16, Cdc23 and Cdc27 interacts with *mnd2*Δ *cdc26*$^{1-52}$, and lowers the viability of these mutant backgrounds at elevated temperatures (Fig 4.9). The loss of Mnd2 combined with the Cdc26$^{1-52}$ truncation reduces the binding of both Cdh1 and Cdc20 to approximately 60-80% of wild type levels. The addition of the *apc-12A* mutations, however, doesn't further decrease binding, despite a greater loss of Cdc27 in this background. While this does suggest that Mnd2, in combination with Cdc26, may contribute to co-activator binding in vitro, it also suggests that the decrease in the maximum permissive temperature of the *mnd2*Δ *cdc26*$^{1-52}$ *apc-12A* mutant background may be due to a defect independent of co-activator binding.

Searching for a role for Cdk1 phosphorylation of the APC

Cdc20 is argued to bind preferentially to phosphorylated APC. Our results here, however, argue that Cdk1 phosphorylation of the TPR subunits does not increase the affinity of Cdc20 for the APC. While we have not exhausted all possibilities, or mutated all Cdk1 phosphorylation sites, our results question the current view that phosphorylation of the APC contributes to Cdc20 binding. It is clear that Cdk1 phosphorylation of the APC^{Cdc20} is important for its catalytic activity: Swe1-inhibited APC has reduced activity in vitro, and in vitro phosphorylation of the APC with Cdk1/Clb2 complexes boosts ubiquitination activity. While this strongly suggests that additional phosphorylation sites are involved, we have also explored the possibility that Cdk1 phosphorylation may be important for recovery from activation of the spindle assembly checkpoint (Chapter 5).

Chapter 5: Cdk1 phosphorylation and the spindle assembly checkpoint

5.1 Introduction

The spindle assembly checkpoint (SAC) is a surveillance mechanism that blocks the metaphase-anaphase transition until all chromosomes have made proper bipolar attachments to the mitotic spindle. The most downstream effector of this checkpoint is the MCC, which consists of the proteins Mad2, BubR1/Mad3, Bub3 and Cdc20. The MCC inhibits the APC^{Cdc20} and prevents cell cycle progression until errors can be resolved. MCC-dependent inhibition of the APC is two-fold: (1) Mad3 acts as a pseudo-substrate to the APC, competing with other substrates for Cdc20 binding (Burton and Solomon, 2007), and (2) the binding of the MCC displaces Cdc20, disrupting the interactions required for the activating function of Cdc20 (Chao et al., 2012; Herzog et al., 2009).

While a lot remains to be understood about how cells recover from activation of the SAC, experiments in both yeast and human cells have argued that Mnd2/Apc15 plays an important role in the disassembly of the MCC from the APC during checkpoint recovery (Foster and Morgan, 2012; Mansfeld et al., 2011; Uzunova et al., 2012). While it is clear that Cdc20 is autoubiquitinated during a checkpoint arrest, the exact role for this autoubiquitination is still not clear. APC-dependent ubiquitination of Cdc20 has been argued to be important for maintaining the checkpoint (Nilsson et al., 2008). Ubiquitinated Cdc20 is associated with the APC during a checkpoint arrest, arguing this ubiquitination does not interfere with MCC association with the APC (Mansfeld et al., 2011). Modest overexpression of Cdc20 overrides the checkpoint, further arguing that regulation of Cdc20 levels is critical for SAC function (Pan and Chen, 2004). In disagreement with this model, however, another

group showed that Cdc20 autoubiquitination contributes to MCC disassembly, and thus inactivation of the checkpoint (Uzunova et al., 2012). Despite this controversy, it is apparent that the APC subunit Mnd2/Apc15 is involved: Mnd2/Apc15 mediates the turnover of MCC on the APC, although whether or not Mnd2/Apc15 is required for Cdc20 ubiquitination is still unclear (Foster and Morgan, 2012; Mansfeld et al., 2011; Uzunova et al., 2012).

Since Cdk1 phosphorylation of the TPR subunits does not affect Cdc20 binding (Chapter 4), we wondered if it may instead play a role in recovery from activation of the SAC. Previous work has shown that mutation of the twelve Cdk1 sites in Cdc16, Cdc23 and Cdc27 causes an increased sensitivity to hyperactivation of the SAC (Rudner and Murray, 2000; Vernieri et al., 2013). Loss of both Cdc26 and Mnd2 results in much greater temperature sensitivity than either of the single mutants alone (Fig. 4.9A), suggesting these two subunits may function in a similar pathway. This chapter explores the possibility that these twelve phosphorylation sites function with the non-essential subunits Mnd2 and Cdc26 to regulate silencing of the spindle assembly checkpoint. This would define a novel function for Cdk1 phosphorylation of the APC, and would alter the current model that Cdk1 phosphorylation solely regulates the catalytic activity of the APC.

5.2 RESULTS

Release from checkpoint activation is delayed in the apc-12A mutant

Mps1 is an upstream kinase in the SAC signaling cascade, and its kinase activity is required for the spindle checkpoint (Weiss and Winey, 1996). Overexpression of Mps1, using the galactose promoter (*GAL-MPS1*), allows for activation of the SAC without disruption of the mitotic spindle (Hardwick et al., 1996). Previous work has shown that the *apc-12A* mutant exhibits an increase in sensitivity to the SAC induced by Mps1 overexpression (Rudner and Murray, 2000). This sensitivity, however, is not accompanied by an increase in the binding of the MCC to the APC: purification of benomyl-arrested *apc-A* mutants indicates no change in the amount of Cdc20 or Mad2 bound to the APC (Fig. 4.2B). In order to further explore the SAC sensitivity exhibited by the *apc-12A* mutant, we analyzed recovery from an Mps1-induced checkpoint arrest. In this experiment, cells are released from a synchronous G1 arrest into media containing galactose to induce the expression of Mps1. Following induction, dextrose is added to shut off transcription, and cells are monitored for a delay in the release from checkpoint activation. We found that the *apc-12A* mutant is delayed in recovery from this checkpoint activation, as assessed by the levels of Pds1 and Clb2 (Fig. 5.1). The degradation of these substrates is delayed by 30 minutes compared to wild type in the *apc-12A* mutant background, suggesting that phosphorylation of the TPR subunits may be important for efficient release of the MCC once the checkpoint has been satisfied. The *cdc26*$^{1\text{-}52}$ *apc-12A* mutant, which displays increased sensitivity to SAC activation (discussed below), does not delay the degradation of Pds1 and Clb2 any further, suggesting this phenotype is primarily due to loss of phosphorylation of the TPR subunits.

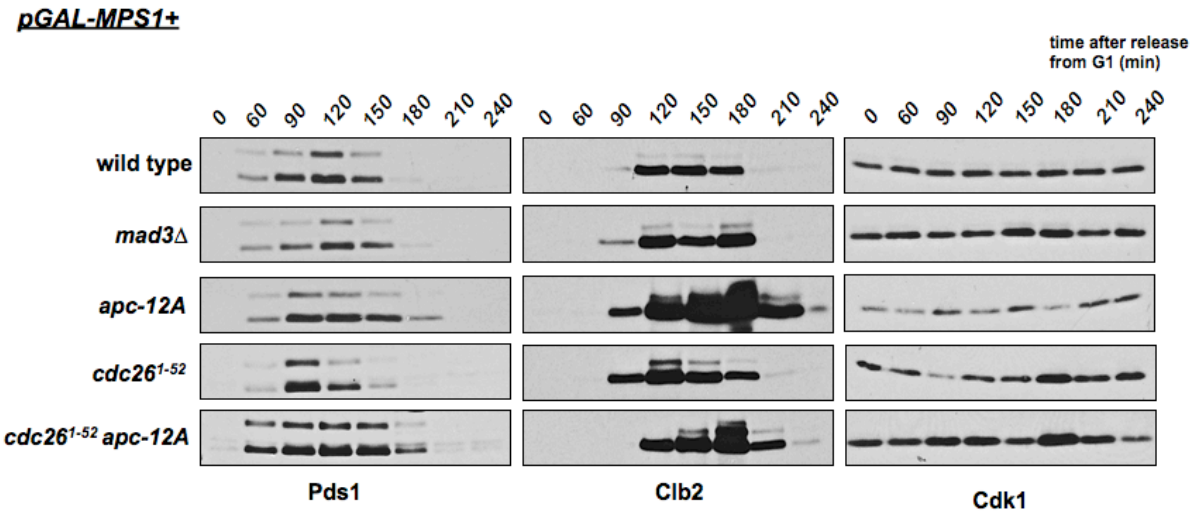
pGAL-MPS1+
time after release from G1 (min)
0 60 90 120 150 180 210 240
wild type
mad3Δ
apc-12A
cdc26^1-52
cdc26^1-52 apc-12A
Pds1
Clb2
Cdk1

Figure 5.1 The *apc-12A* mutant is delayed in recovery from the spindle assembly checkpoint

GAL-MPS1 (ADR7345), *mad3*Δ *GAL-MPS1* (ADR7347), *apc-12A GAL-MPS1* (ADR7444), *cdc26*$^{1-52}$ *GAL-MPS1* (ADR7351), and *cdc26*$^{1-52}$ *apc-12A GAL-MPS1* (ADR7362) cells were grown overnight in YEP + 2% raffinose, arrested in α factor (1ug/mL) for 3 hours, α-factor was washed out and cells were released into YEP + 2% galactose. After 1 hour of galactose induction, cells were released into YEPD media to repress Mps1 transcription, and α-factor (1ug/mL) was added (t=120) to arrest cells in the following G1 and samples were taken for immunoblotting. Time refer to the time after release from the G1 arrest (min). Cdk1 is used as a loading control.

Mnd2 and the spindle assembly checkpoint

*mnd2*Δ has previously been shown to have in vitro defects in releasing the MCC from the APC (Foster and Morgan, 2012), and depletion of the vertebrate Apc15 causes the MCC to remain locked onto the APC (Mansfeld et al., 2011). Both studies have argued a role for Apc15 in MCC disassembly and release from the checkpoint. Given this evidence, we were surprised to find that *mnd2*Δ mutants did not show an increased sensitivity to activation of the SAC by growth on the microtubule-depolymerizing agent benomyl (Fig. 5.2A), or by overexpression of Mps1 (Fig. 5.3A). Loss of TPR phosphorylation, however, sensitized the *mnd2Δ* background to SAC activation and showed an increase in sensitivity to both Mps1 overexpression and growth on benomyl, compared to wild type (Fig. 5.2A, 5.3A and B).

We wondered whether the increased sensitivity to growth on benomyl seen in the *mnd2Δ apc-12A* mutant might be accompanied by an increase in MCC binding to the APC. Unexpectedly, we found a dramatic reduction in the binding of Cdc20 to the APC in the *mnd2Δ* background when purified from a checkpoint arrest: *mnd2Δ* cells exhibit approximately 30% bound Cdc20 compared to wild type, while the loss of Cdk1 phosphorylation sites in the *mnd2Δ* background reduces this to approximately 20% (Fig. 5.2B, *mnd2Δ apc-12A* mutant). The levels of Mad2 bound to the APC are even further reduced compared to Cdc20: *mnd2Δ* mutants exhibit only about 20% of bound Mad2 compared to wild type. We also note a moderate increase in steady state levels of Cdc20 in the *mnd2Δ* background (Fig. 5.2B, crude lysate), which is consistent with previous reports that the loss of Mnd2 increases Cdc20 levels because of its role in promoting SAC-dependent Cdc20 autoubiquitination (Foster and Morgan, 2012; Uzunova et al., 2012).

a

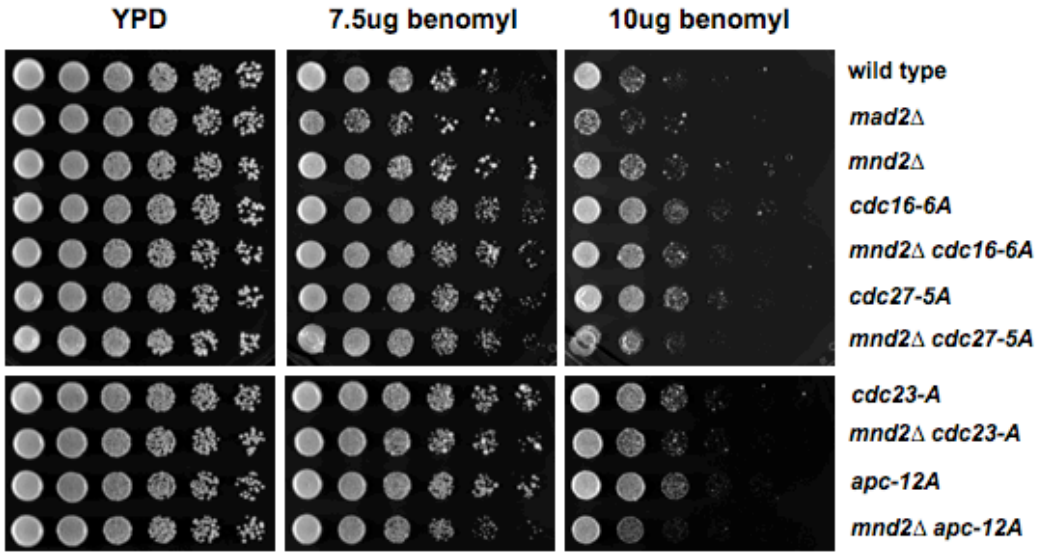
YPD
7.5ug benomyl
10ug benomyl
wild type
mad2Δ
mnd2Δ
cdc16-6A
mnd2Δ cdc16-6A
cdc27-5A
mnd2Δ cdc27-5A
cdc23-A
mnd2Δ cdc23-A
apc-12A
mnd2Δ apc-12A

b

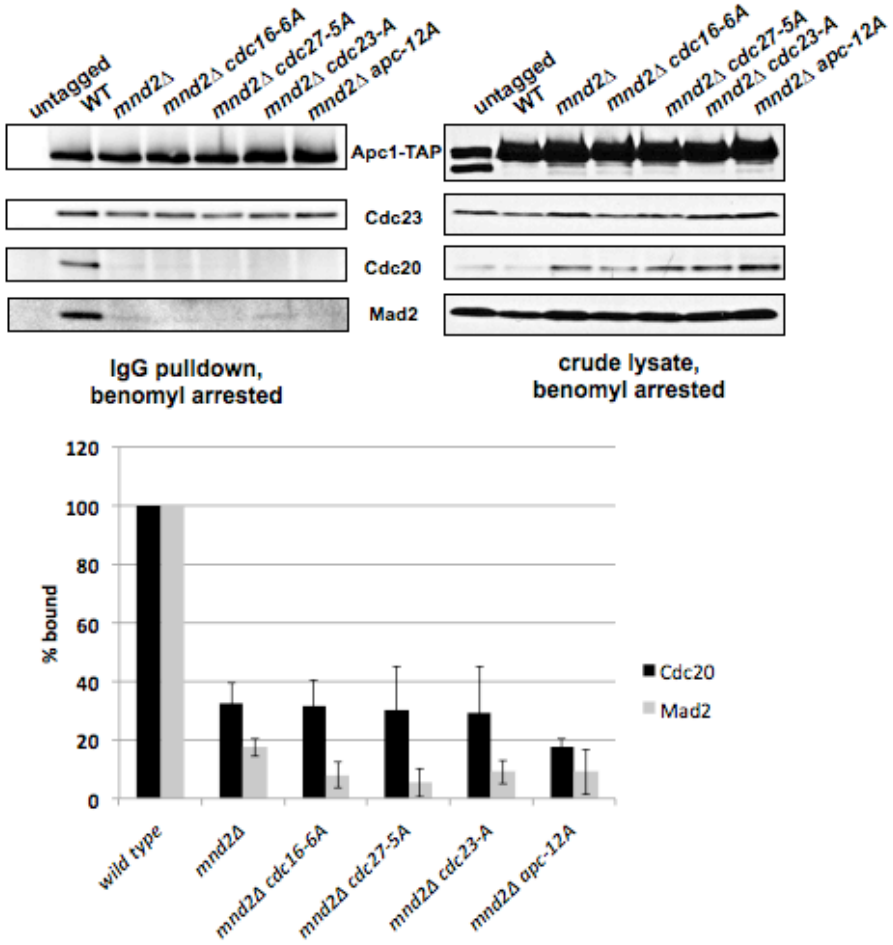
untagged WT
mnd2Δ
mnd2Δ cdc16-6A
mnd2Δ cdc27-5A
mnd2Δ cdc23-A
mnd2Δ apc-12A
Apc1-TAP
Cdc23
Cdc20
Mad2
IgG pulldown, benomyl arrested
crude lysate, benomyl arrested
% bound
120
100
80
60
40
20
0
Cdc20
Mad2
wild type
mnd2Δ
mnd2Δ cdc16-6A
mnd2Δ cdc27-5A
mnd2Δ cdc23-A
mnd2Δ apc-12A

Figure 5.2 The *mnd2*Δ *apc-12A* mutant is sensitive to SAC activation

(A) Wild type (ADR4006), *mad2*Δ (ADR55), *mnd2*Δ (ADR7451), *cdc16-6A* (ADR5237), *mnd2*Δ *cdc16-6A* (ADR5574), *cdc27-5A* (ADR2031), *mnd2*Δ *cdc27-5A* (ADR5681), *cdc23-A* (ADR6463), *mnd2*Δ *cdc23-A* (ADR7643), *apc-12A* (ADR6623) and *mnd2*Δ *apc-12A* (ADR7646) cells were grown to saturation in YEPD at 25˚C. Eight-fold serial dilutions were spotted onto YEPD and benomyl plates (7.5ug or 10ug/mL) and grown for two days at 25˚C. (B) *mnd2*Δ checkpoint arrested cells have less Cdc20 bound than wild type. Untagged (ADR4006), wild type (ADR6174), *mnd2*Δ (ADR7624), *mnd2*Δ *cdc16-6A* (ADR7653), *mnd2*Δ *cdc27-5A* (ADR7656), *mnd2*Δ *cdc23-A* (ADR7658), and *mnd2*Δ *apc-12A* (ADR7650) cells were arrested in mitosis with benomyl (30µg/mL). All strains except untagged are *APC1-TAP.* The APC was purified, and run on a polyacrylamide gel. Immunopurified samples were quantified using ImageQuant software. The average amount of bound Cdc20 and Mad2 (+/- SEM) relative to wild type levels of three independent experiments is shown below.

a

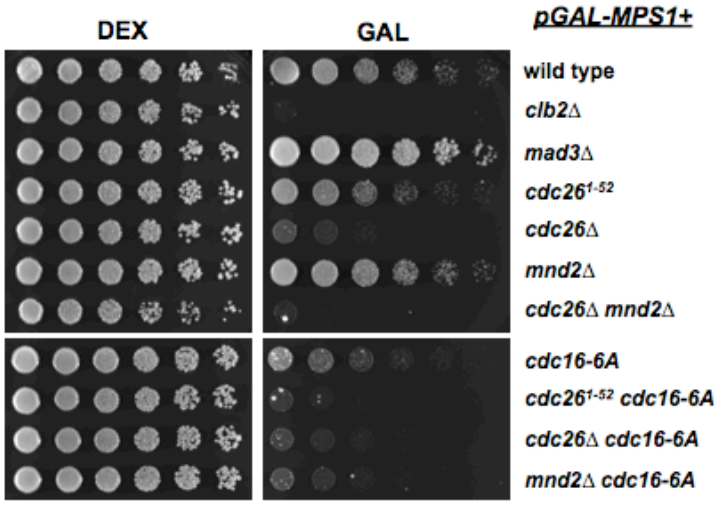
DEX
GAL
pGAL-MPS1+
wild type
clb2Δ
mad3Δ
cdc26¹⁻⁵²
cdc26Δ
mnd2Δ
cdc26Δ mnd2Δ
cdc16-6A
cdc26¹⁻⁵² cdc16-6A
cdc26Δ cdc16-6A
mnd2Δ cdc16-6A

b

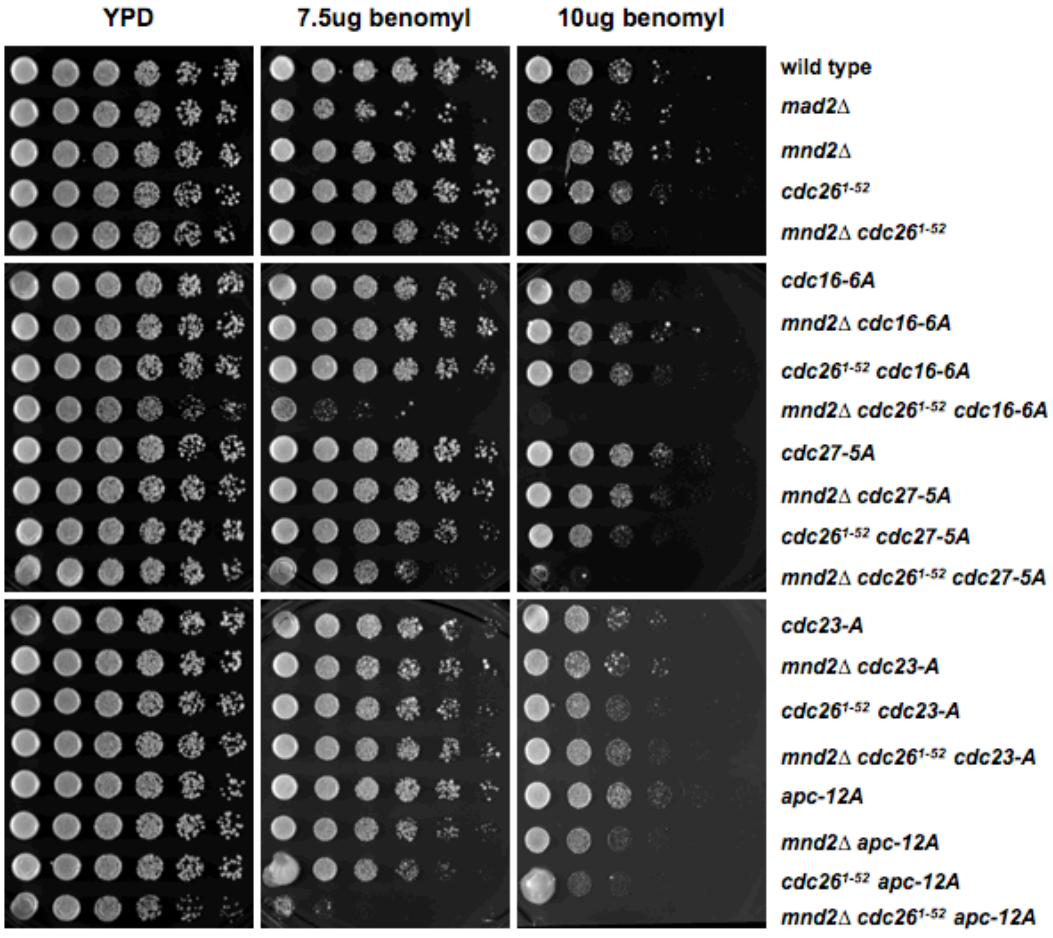
YPD
7.5ug benomyl
10ug benomyl
wild type
mad2Δ
mnd2Δ
cdc26¹⁻⁵²
mnd2Δ cdc26¹⁻⁵²
cdc16-6A
mnd2Δ cdc16-6A
cdc26¹⁻⁵² cdc16-6A
mnd2Δ cdc26¹⁻⁵² cdc16-6A
cdc27-5A
mnd2Δ cdc27-5A
cdc26¹⁻⁵² cdc27-5A
mnd2Δ cdc26¹⁻⁵² cdc27-5A
cdc23-A
mnd2Δ cdc23-A
cdc26¹⁻⁵² cdc23-A
mnd2Δ cdc26¹⁻⁵² cdc23-A
apc-12A
mnd2Δ apc-12A
cdc26¹⁻⁵² apc-12A
mnd2Δ cdc26¹⁻⁵² apc-12A

Figure 5.3 *mnd2*Δ *cdc26*$^{1-52}$ *apc-A* mutants are sensitive to checkpoint activation

(A) Wild type (ADR4006), *clb2*Δ (ADR1606), *mad3*Δ (ADR1249), *cdc26*$^{1-52}$ (ADR7350), *cdc26*Δ (ADR7392), *mnd2*Δ (ADR7330), *cdc26*Δ *mnd2*Δ (ADR7334), *cdc16-6A* (ADR1975), *cdc26*$^{1-52}$ *cdc16-6A* (ADR7353), *cdc26*Δ *cdc16-6A* (ADR7395) and *mnd2*Δ *cdc16-6A* (ADR7405) cells were grown to saturation in YEPD at 25˚C. All strains are *GAL-MPS1*. Eight-fold serial dilutions were spotted onto YEPD and YEP + 2% galactose plates and grown for two (YEPD) or three (galactose) days at 25˚C. (B) Wild type (ADR4006), *mad2*Δ (ADR55), *mnd2*Δ (ADR7451), *cdc26*$^{1-52}$ (ADR6396), *mnd2*Δ *cdc26*$^{1-52}$ (ADR7568), *cdc16-6A* (ADR5237), *mnd2*Δ *cdc16-6A* (ADR5574), *cdc26*$^{1-52}$ *cdc16-6A* (ADR6316), *mnd2*Δ *cdc26*$^{1-52}$ *cdc16-6A* (ADR7617), *cdc27-5A* (ADR2031), *mnd2*Δ *cdc27-5A* (ADR5681), *cdc26*$^{1-52}$ *cdc27-5A* (ADR6326), *mnd2*Δ *cdc26*$^{1-52}$ *cdc27-5A* (ADR7619), *cdc23-A* (ADR6463), *mnd2*Δ *cdc23-A* (ADR7643), *cdc26*$^{1-52}$ *cdc23-A* (ADR6549), *mnd2*Δ *cdc26*$^{1-52}$ *cdc23-A* (ADR7621), *apc-12A* (ADR6623), *mnd2*Δ *apc-12A* (ADR7646), *cdc26*$^{1-52}$ *apc-12A* (ADR6545), and *mnd2*Δ *cdc26*$^{1-52}$ *apc-12A* (ADR7623) cells were grown to saturation in YEPD at 25˚C. Eight-fold serial dilutions were spotted onto YEPD and benomyl plates (7.5ug or 10ug/mL) and grown for two (YEPD) or three (benomyl) days at 25˚C.

A similar role for Cdc26, Mnd2 and TPR phosphorylation in the SAC?

We previously showed that *cdc26Δ mnd2Δ* cells display poor growth at 25˚C and are inviable at 30˚C, even in the absence of checkpoint activation (Fig. 4.9A). When subject to Mps1 overexpression, we found that *cdc26*Δ *apc-12A* and *cdc26$^{1-52}$ apc-12A* mutants also showed an increased sensitivity to checkpoint activation compared to wild type (Fig. 5.3B). This made us consider the possibility that Mnd2 may work in cooperation with Cdc26 and Cdk1 phosphorylation of the TPR subunits. In support of this, *cdc26Δ mnd2Δ* cells are inviable when exposed to Mps1-induced checkpoint activation (Fig. 5.3A). In addition, the *mnd2*Δ *cdc26$^{1-52}$* mutant in the *apc-12A* background also exhibits a heightened sensitivity to spindle checkpoint activation (Fig. 5.3B, compare *mnd2*Δ, *cdc26$^{1-52}$* and *mnd2*Δ *cdc26$^{1-52}$ apc-12A*). Overall, these genetic interactions argue that Cdc26 and phosphorylation of the TPR subunits Cdc16, Cdc23 and Cdc27 may function in a pathway parallel to Mnd2 to regulate the recovery from SAC activation.

*mnd2*Δ *cdc26*Δ *mutants are delayed in recovery from SAC activation*

In support of a combinatorial role of Cdc26 and Mnd2 in SAC function, *mnd2*Δ *cdc26*Δ mutants are impaired in their recovery from *GAL-MPS1* induced checkpoint activation. Using identical experimental conditions as those described for Fig. 5.1, *mnd2*Δ *cdc26*Δ cells never release from checkpoint activation during the course of the experiment: Pds1 and Clb2 levels remain high until the final timepoint (T=240) (Fig. 5.4), arguing the APC has not been released from MCC-dependent inhibition and can't initiate ubiquitination of its APC^{Cdc20} substrates to allow for continued cell cycle progression.

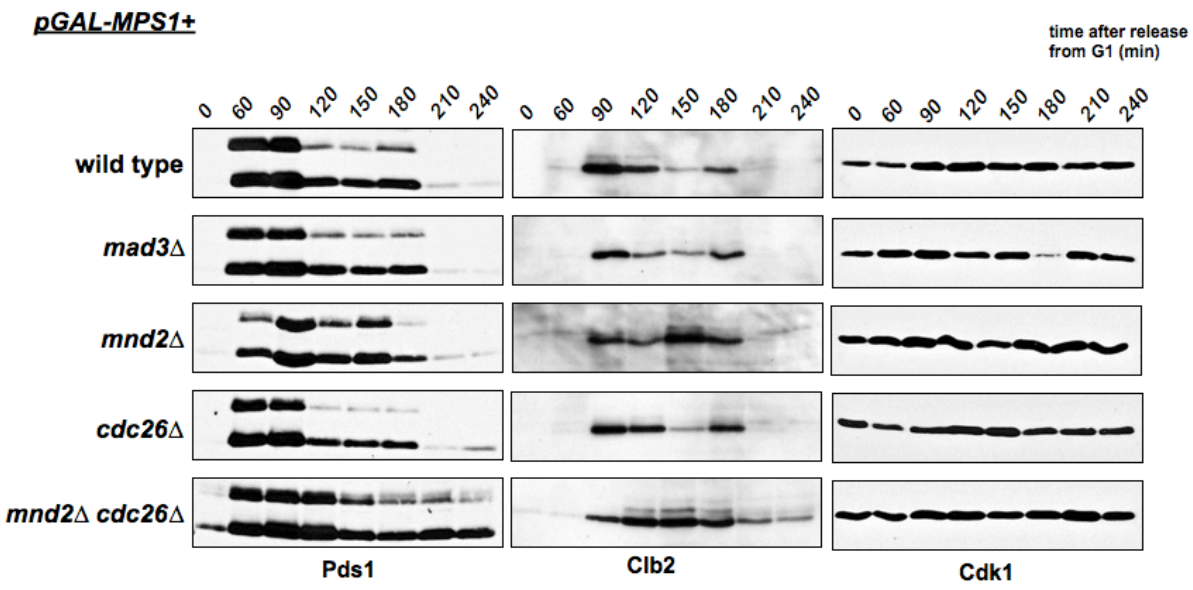
pGAL-MPS1+
time after release from G1 (min)
0 60 90 120 150 180 210 240
wild type
mad3Δ
mnd2Δ
cdc26Δ
mnd2Δ cdc26Δ
Pds1
Clb2
Cdk1

Figure 5.4 The *mnd2*Δ *cdc26*Δ mutant is delayed in recovery from the spindle assembly checkpoint

GAL-MPS1 (ADR7345), *mad3*Δ *GAL-MPS1* (ADR7347), *mnd2*Δ *GAL-MPS1* (ADR7726), *cdc26*Δ *GAL-MPS1* (ADR7905), and *mnd2*Δ *cdc26*Δ *GAL-MPS1* (ADR7901) cells were grown overnight in YEP + 2% raffinose, arrested in α factor (1ug/mL) for 3 hours, α-factor was washed out and cells were released into YEP + 2% galactose. After 1 hour of galactose induction, cells were released into YEPD media to repress Mps1 transcription, and α-factor (1ug/mL) was added (t=120) to arrest cells in the following G1 and samples were taken for immunoblotting. Time refer to the time after release from the G1 arrest (min). Cdk1 is used as a loading control.

Deletion of MAD2 suppresses temperature sensitivity of the APC mutants

The 1-52 truncation of Cdc26 interacts genetically with the loss of TPR phosphorylation of the APC, and results in a temperature sensitive phenotype in the *cdc26$^{1-52}$ apc-12A* background (Fig. 4.8B). While there is no obvious genetic interaction with the loss of Mnd2 in the *apc-12A* background, the *mnd2*Δ *cdc26$^{1-52}$ apc-12A* cells exhibit reduced growth compared to *cdc26$^{1-52}$ apc-12A* cells at all temperatures up to 30˚C (Fig. 4.9B, compare *mnd2*Δ, *mnd2*Δ *cdc26$^{1-52}$*, and *mnd2*Δ *cdc26$^{1-52}$ apc-12A*). The data presented in Fig. 5.3 argues that the reduced viability seen at elevated temperatures may at least be partly due to an inability to recover from SAC activation. If this is indeed the case, we expect that deletion of SAC genes should suppress this phenotype. In fact, deletion of the *MAD2* gene partly suppresses the temperature sensitivity of the *cdc26*Δ *apc-12A*, *cdc26$^{1-52}$ apc-12A*, *mnd2*Δ *apc-12A*, *mnd2*Δ *cdc26$^{1-52}$ apc-12A* and *cdc26*Δ *mnd2*Δ mutants (Fig. 5.5). Suppression of the *mnd2*Δ *cdc26$^{1-52}$ apc-12A* mutant is arguably the most dramatic (Fig. 5.5D). Deletion of *MAD2* also partially suppresses the temperature sensitivity of the *cdc26*Δ mutant (Fig. 5.5A, compare *cdc26*Δ and *cdc26*Δ *mad2*Δ*,* 34˚C panel). Furthermore, deletion of each of the *MAD1, MAD2* and *MAD3* genes partially suppresses the temperature sensitivity of the APC mutants, *cdc16-1* and *cdc23-1*, with *mad3*Δ exhibiting the most dramatic rescue (data not shown).

An assay to look at spindle assembly checkpoint recovery

The recruitment of Mad1 to the kinetochore is considered the defining event in

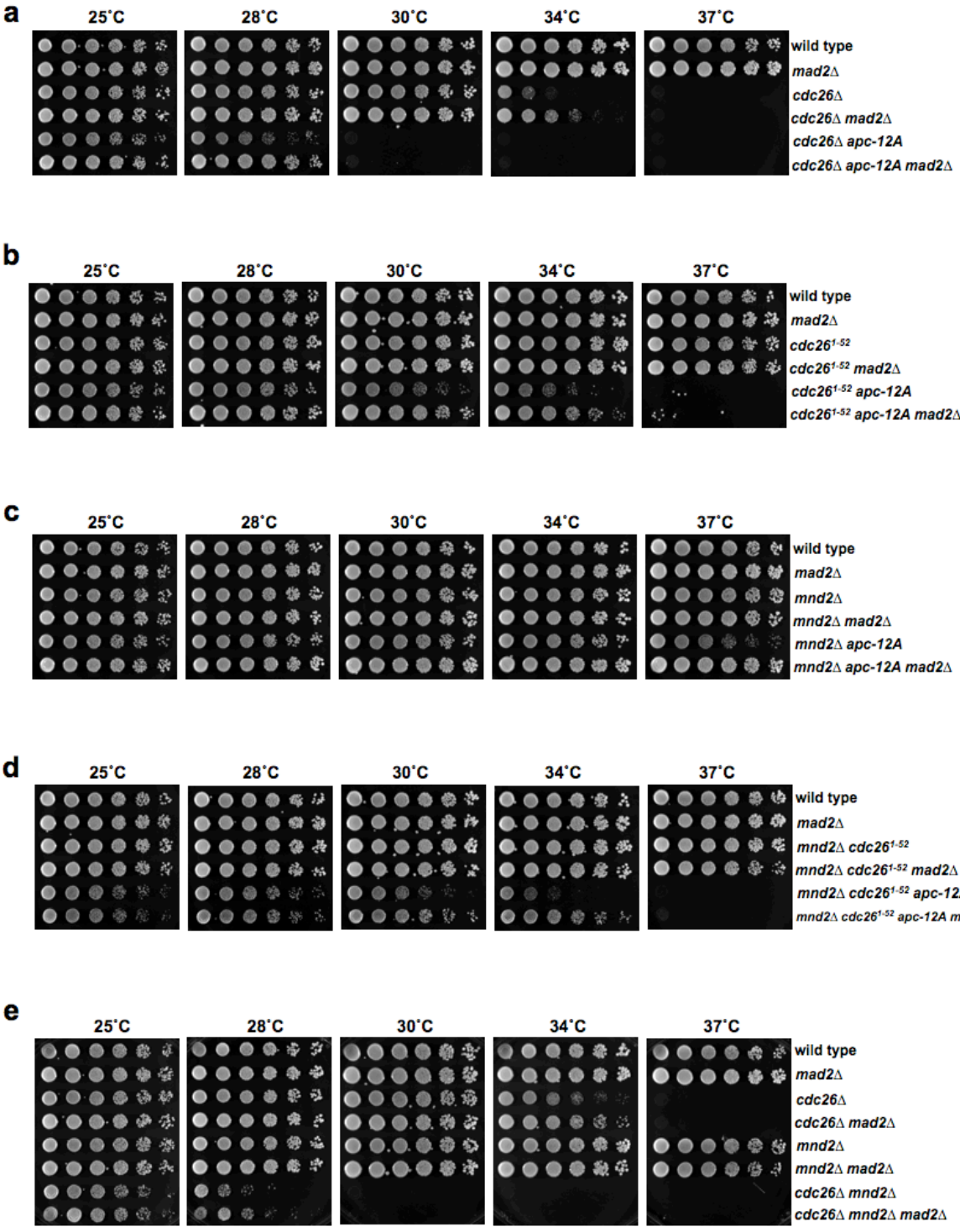
a
25˚C
28˚C
30˚C
34˚C
37˚C
wild type
mad2Δ
cdc26Δ
cdc26Δ mad2Δ
cdc26Δ apc-12A
cdc26Δ apc-12A mad2Δ
b
25˚C
28˚C
30˚C
34˚C
37˚C
wild type
mad2Δ
cdc26¹-⁵²
cdc26¹-⁵² mad2Δ
cdc26¹-⁵² apc-12A
cdc26¹-⁵² apc-12A mad2Δ
c
25˚C
28˚C
30˚C
34˚C
37˚C
wild type
mad2Δ
mnd2Δ
mnd2Δ mad2Δ
mnd2Δ apc-12A
mnd2Δ apc-12A mad2Δ
d
25˚C
28˚C
30˚C
34˚C
37˚C
wild type
mad2Δ
mnd2Δ cdc26¹-⁵²
mnd2Δ cdc26¹-⁵² mad2Δ
mnd2Δ cdc26¹-⁵² apc-12A
mnd2Δ cdc26¹-⁵² apc-12A mad2Δ
e
25˚C
28˚C
30˚C
34˚C
37˚C
wild type
mad2Δ
cdc26Δ
cdc26Δ mad2Δ
mnd2Δ
mnd2Δ mad2Δ
cdc26Δ mnd2Δ
cdc26Δ mnd2Δ mad2Δ

Figure 5.5 Deletion of Mad2, a component of the spindle assembly checkpoint, suppresses the temperature sensitivity of *APC* mutants

(A) Wild type (ADR4006), *mad2*Δ (ADR55), *cdc26*Δ (ADR6967), *cdc26*Δ *mad2*Δ (ADR7335), *cdc26*Δ *apc-12A* (ADR6555), and *cdc26*Δ *apc-12A mad2*Δ (ADR7531) cells were grown to saturation in YEPD at 25˚C. Eight-fold serial dilutions were spotted onto YEPD plates and grown for two days at the indicated temperatures. (B) Wild type (ADR4006), *mad2*Δ (ADR55), $cdc26^{1\text{-}52}$ (ADR6396), $cdc26^{1\text{-}52}$ *mad2*Δ (ADR7528), $cdc26^{1\text{-}52}$ *apc-12A* (ADR6546) and $cdc26^{1\text{-}52}$ *apc-12A mad2*Δ (ADR7530) cells were grown as in (A). (C) Wild type (ADR4006), *mad2*Δ (ADR55), *mnd2*Δ (ADR5542), *mnd2*Δ *mad2*Δ (ADR7526), *mnd2*Δ *apc-12A* (ADR7646), and *mnd2*Δ *apc-12A mad2*Δ (ADR8271) cells were grown as in (A). (D) Wild type (ADR4006), *mad2*Δ (ADR55), *mnd2*Δ $cdc26^{1\text{-}52}$ (ADR7568), *mnd2*Δ $cdc26^{1\text{-}52}$ *mad2*Δ (ADR7613), *mnd2*Δ $cdc26^{1\text{-}52}$ *apc-12A* (ADR7623), and *mnd2*Δ $cdc26^{1\text{-}52}$ *apc-12A mad2*Δ (ADR8270) were grown as in (A). (E) Wild type (ADR4006), *mad2*Δ (ADR55), *cdc26*Δ (ADR6967), *cdc26*Δ *mad2*Δ (ADR7335), *mnd2*Δ (ADR5542), *mnd2*Δ *mad2*Δ (ADR7526), *cdc26*Δ *mnd2*Δ (ADR7627) and *cdc26*Δ *mnd2*Δ *mad2*Δ (ADR8269) cells were grown as in (A).

spindle assembly checkpoint activation. Once localized to the kinetochore, Mps1-dependent phosphorylation of Bub1 recruits Mad1 (London and Biggins, 2014). Given the significance of this Bub1-Mad1 interaction, we developed an assay that would allow us to look carefully at recovery from checkpoint activation. The interaction of Bub1 with Mad1 is indicative of checkpoint activation, and this interaction is abolished once the signal has been turned off. This will allow us to be certain any changes are not due to persistent signaling of the checkpoint. Using the *GAL-MPS1* allele, we activated the checkpoint by growth in galactose, and assessed whether Bub1-FLAG interacts with Mad1 by co-immunoprecipitation. After an hour of Mps1 induction, immunopurification of Bub1-FLAG pulled down Mad1, indicating the checkpoint has been activated (Fig. 5.6, T=60). When Mps1 transcription is shut off by switching to dextrose media, the Bub1-FLAG-Mad1 interaction is lost within the first 45 minutes (T=105), arguing checkpoint signalling has been turned off. Using this assay, we can assess whether the APC mutants described in this thesis are defective in recovery from spindle assembly checkpoint activation.

pGAL-MPS1:

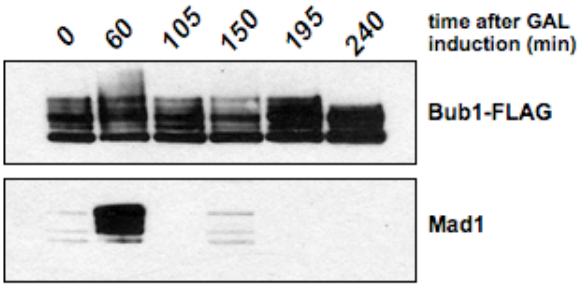
0
60
105
150
195
240
time after GAL induction (min)
Bub1-FLAG
Mad1

Figure 5.6 An assay to detect decay of the spindle assembly checkpoint

APC1-TAP BUB1-FLAG GAL-MPS1 (ADR8323) cells were grown overnight in YEP + 2% raffinose (T=0), and induced by addition of 2% galactose. After an hour of induction, cells were harvested and released into fresh YEPD to repress Mps1 transcription and samples were harvested for α-FLAG immunoprecipitation of Bub1 at the indicated timepoints. Time refers to the time after galactose induction (min).

5.3 DISCUSSION

Although a number of questions still remain, the data presented here suggests that Cdk1 phosphorylation of the TPR subunits of the APC, in combination with the non-essential subunits Cdc26 and Mnd2, is important for recovery from spindle assembly checkpoint activation. The *apc-12A* mutant exhibits only moderate sensitivity to SAC activation, but this phenotype is exacerbated by the loss of Mnd2 and/or truncation of Cdc26. The *mnd2*Δ *cdc26*Δ mutant also displays an inability to release from a checkpoint induced arrest, suggesting these two APC subunits function in a similar pathway.

MCC binding in a checkpoint arrest

The loss of Cdk1 phosphorylation sites does not alter the ability of Cdc20 to bind the APC in vitro (Fig. 4.1), although Cdc20 is argued to bind differently when complexed with the checkpoint proteins than that of Cdc20 as co-activator of the APC. In the APC^{MCC}, Cdc20 is shifted away from the Doc1/Apc10 subunit, and Cdc23 is particularly important in Cdc20 binding in checkpoint activated cells (Herzog et al., 2009; Izawa and Pines, 2011). We found that *apc-12A* cells are delayed in their recovery from SAC activation, and we expect that this mutant is defective in its ability to release MCC-dependent inhibition of the APC^{Cdc20} to allow for continued cell cycle progression (Fig. 5.1). Despite this delay, we found no apparent difference in the amount of Mad2 or Cdc20 bound to checkpoint activated cells in vivo in the phosphorylation site mutants (Fig. 4.2B), although this may be partly explained by the use of different methods of checkpoint activation: Mps1 overexpression compared with benomyl treatment. Benomyl is a microtubule depolymerizing agent that activates the

checkpoint by interfering with formation of the mitotic spindle, while overexpression of Mps1 allows for activation of the SAC without disruption of the spindle. Studies of the conserved protein kinase Ipl1, a member of the Aurora kinase family, have suggested there exist differences in SAC function depending on the nature of the activation. Ipl1 is required for SAC function in response to Mps1 overexpression, but is not required for an arrest resulting from spindle depolymerization (Biggins and Murray, 2001), arguing the mechanism of checkpoint activation may differ when tension is lost compared with the use of agents that disassemble microtubules.

Future work will assess the relative binding of the MCC components following a *GAL-MPS1* induced spindle checkpoint arrest. Furthermore, the experiment in Fig. 4.2B focused on the relative ability of the MCC components Mad2 and Cdc20 to bind the APC during a static checkpoint arrest. Assessing the relative levels of these checkpoint proteins bound to the APC following release from an arrest, as was done in Fig. 5.1, will allow us to determine whether Cdk1 phosphorylation of the APC is important for disassembly of the MCC, and subsequent activation of the APC^{Cdc20} to allow for the onset of anaphase.

We have not yet been able to assess if the remaining MCC components, Mad3 and Bub3, also bind the APC at similar levels as Mad2 and Cdc20. Some reports have argued that the MCC components exist in near equal stoichiometry (Chao et al., 2012; Sudakin et al., 2001), while another report argues that Cdc20 does not accumulate in a stoichiometric complex with Mad2, but primarily with Mad3 and Bub3 (Nilsson et al., 2008). Nilsson et al. (2008) proposed that the checkpoint is maintained by the BubR1-Bub3 complex presenting Cdc20 as a substrate to the APC, and that the primary role of Mad2 is to generate the BubR1-

Bub3-Cdc20 complex. In support of this, Mad3 (alone or in combination with Bub3) can inhibit APC^{Cdc20}-dependent ubiquitination of Pds1 in vitro (Foster and Morgan, 2012; Tang et al., 2001b). Moreover, Mad2 has been shown to be a poor inhibitor of APC activity in vitro, and in *S. pombe*, Mad3/BubR1 function is essential for Mad2 to block cells in mitosis (Millband and Hardwick, 2002). Experiments in *S. cerevisiae* also demonstrated that the addition of purified Mad2 to the APC inhibits binding of Cdc20 in vitro, while the addition of the Mad3-Bub3 complex reverses this, and stimulates Cdc20 binding (Foster and Morgan, 2012). Given this, it remains possible that the binding and release of Mad3 and Bub3 from the APC may be a more relevant indicator of SAC activation, and subsequent recovery.

Mnd2 and its role in MCC turnover

Although the exact mechanism is still unclear, it has been well established that Mnd2/Apc15 is important in the turnover of MCCs on the APC (Foster and Morgan, 2012; Mansfeld et al., 2011; Uzunova et al., 2012). Given this checkpoint function, we were surprised to discover that *mnd2*Δ mutants do not show any sensitivity to SAC activation, either by overexpression of the checkpoint kinase Mps1, or by growth on benomyl (Fig. 5.2A and 5.3). This is, however, consistent with the slight phenotype seen in vivo: Pds1 degradation and chromosome segregation were only delayed by approximately 10 minutes in an *mnd2*Δ mutant released from a spindle checkpoint arrest (Foster and Morgan, 2012).

We showed previously that the loss of Mnd2, whether in conjunction with the *apc-A* mutations or not, did not greatly affect the ability of either Cdh1 or Cdc20 to bind the APC in vitro (Fig. 4.6C). Consistent with a shift in the binding of Cdc20 when part of the MCC, we

found that when the APC was purified from a checkpoint arrest in the *mnd2*Δ background the levels of both Cdc20 and Mad2 bound to the APC were reduced. Loss of the twelve phosphorylation sites in the *mnd2*Δ background further reduced the levels of Cdc20 and Mad2, although only to a small extent (Fig. 5.2B). Why we see reduced levels of these MCC components bound to the APC in the *mnd2*Δ background is not clear. It is inconsistent with reports that have showed that depletion of Apc15 causes the MCC to remain 'locked' onto the APC, and delays the release of checkpoint proteins (Mansfeld et al., 2011; Uzunova et al., 2012).

Lower levels of Cdc20 could be explained by APC-dependent ubiquitination and proteasomal degradation, as Cdc20 ubiquitination has been suggested to be important for the release of the MCC (Uzunova et al., 2012). Loss of Mnd2 in *S. cerevisiae* did not prevent the ability of the Mad3-Bub3 complex to stimulate Cdc20 binding in vitro, but did prevent Cdc20 autoubiquitination, arguing that Mnd2 is required to shift the binding of Cdc20 for optimal checkpoint-induced autoubiquitination (Foster and Morgan, 2012). The binding site of the MCC supports an interaction with Mnd2: Mad2 interacts with Cdc23 and Apc5, while Mad3 contacts Apc1, and Mnd2 has been shown to interact with Apc1, Apc5 and Cdc23 (Chao et al., 2012; Hall et al., 2003; Herzog et al., 2009; Passmore et al., 2003; Schreiber et al., 2011). The lower levels of APC-bound Cdc20 (Fig. 5.2B) could be the result of autoubiquitinated Cdc20 bound to the APC, which would not have been included in the quantification of unmodified Cdc20. If Cdc20 bound to the APC is ubiquitinated, it could suggest there is actually more Cdc20 bound to the APC, rather than less. Whether or not Mnd2/Apc15 is required for Cdc20 ubiquitination is still unclear (Foster and Morgan, 2012;

Mansfeld et al., 2011; Uzunova et al., 2012), so determining whether the APC-bound Cdc20 is ubiquitinated in our experimental conditions will be important in assessing the role of Mnd2 in this process. The use of the *CDC20-5K* mutant, which lacks all major ubiquitination sites but is still able to function as an APC co-activator (Foster and Morgan, 2012), will be integral in determining the role of Cdc20 ubiquitination in this process. Any additional factors that contribute to this process in vivo would have been unaccounted for in our in vitro experiments. As described earlier, assessing the relative binding of Mad3 and Bub3 in the *mnd2*Δ mutants, as well as the release of these MCC components once the checkpoint has been satisfied will also be important.

*mad2*Δ *suppression of temperature sensitivity*

Suppression of the temperature sensitivity of the *cdc26*Δ *apc-12A*, *cdc26*$^{1-52}$ *apc-12A*, *mnd2*Δ *apc-12A*, *mnd2*Δ *cdc26*$^{1-52}$ *apc-12A*, *cdc26*Δ *mnd2*Δ and *cdc26*Δ mutants by the deletion of the *MAD2* gene also supports a role for the subunits Mnd2 and Cdc26, as well as Cdk1 phosphorylation of the TPR subunits, in the SAC (Fig. 5.5). In fact, suppression of the *mnd2*Δ *cdc26*$^{1-52}$ *apc-12A* mutant is arguably the most dramatic (Fig. 5.5D). We don't see complete suppression, however, as might be expected if the sole reason for the temperature sensitivity was a defective checkpoint. Minor disruption of complex integrity is evident in the *mnd2*Δ *cdc26*$^{1-52}$ *apc-12A* mutant: a slight loss of the outermost essential TPR subunit Cdc27 is evident. The loss of this subunit alone is not likely the cause of the temperature sensitivity, as the *apc9*Δ mutant exhibits a more dramatic loss of Cdc27, and is viable up to

37˚C (Fig. 4.3). We also see minor losses of Cdc23 and Swm1, which, in combination with the slight loss of Cdc27, could be sufficient to result in a temperature sensitive phenotype.

The amount of Mad2 bound to Mad3/BubR1-Bub3-Cdc20 has been argued to reflect the number of unattached kinetochores: Mad2 is easily detected when several kinetochores are unattached, but a decrease in Mad2 bound to Mad3/BubR1-Cdc20 is evident when only a few kinetochores are unattached (Lara-Gonzalez et al., 2012; Westhorpe et al., 2011). The amount of Mad2 bound to the APC has thus been argued to differ depending on the mechanism of checkpoint activation. Given this, we may find that suppression of the temperature sensitivity of the APC mutants in Fig. 5.5 is more pronounced with deletion of *MAD3* compared with *MAD2*.

The suppression of the temperature sensitivity of the APC mutants seen Fig. 5.5, however, argues that the checkpoint is activated in these conditions. In mammalian cells, the SAC is activated in every cell cycle, and this checkpoint is important for the normal timing of anaphase. This is not believed to be the case in yeast, however: mutation of checkpoint genes has little effect on the timing of anaphase, unless the cell is presented with spindle damage. The suppression seen with the deletion of *MAD2* suggests then that either this checkpoint is activated by growth at elevated temperatures, or that the checkpoint is active in every cell cycle. An activated checkpoint at higher temperatures is plausible: the spindle would be more stable, and could cause slower attachment of kinetochores, but preliminary evidence from the Rudner laboratory argues this is not the case (data not shown). This then raises the possibility that the checkpoint is activated in every cell cycle in budding yeast.

Bub1-Mad1 interaction: an assay to look at spindle assembly checkpoint recovery

We've developed an interaction assay based on the Bub1-Mad1 interaction at the kinetochore that will allow us to look at recovery from SAC activation, while ensuring that checkpoint signaling has decayed (Fig. 5.6). This assay is particularly compelling because, while a number of studies have looked at spindle checkpoint recovery, many have not assessed whether the observed phenotypes are a result of persistent checkpoint signaling. The catalytic subunit of PP1 in budding yeast, Glc7, contributes to checkpoint silencing by reversing key phosphorylation events (Pinsky et al., 2009). In particular, Glc7 dephosphorylates Spc105, which allows for the release of Bub1 from the kinetochore (London et al., 2012). These PP1 phenotypes, however, may be caused by persistent signaling through the checkpoint: neither of these reports tested whether the checkpoint signal had decayed. Persistent checkpoint signaling could result in stronger phenotypes: Glc7 is required for exit from a nocodazole arrest, but the effect is much less dramatic than the exit from a *GAL-MPS1* induced arrest (Pinsky et al., 2009). With excess Mps1 present, the *glc7-10* mutant may overpower any other silencing mechanism.

In summary, our data suggests a role for these subunits in SAC function, although the mechanism remains to be determined. These results also imply that Cdk1 phosphorylation of the TPR subunits may regulate more than the catalytic activity of the APC at the metaphase-anaphase transition. Future work will help elucidate the roles of Cdc26 and Mnd2, and whether they work in conjunction with phosphorylation of the TPR subunits to regulate the affinity of the MCC for the APC, and ultimately recovery from spindle checkpoint activation.

Chapter 6: General Discussion

6.1 SUMMARY

Anaphase onset, characterized by the segregation of sister chromatids, is an irreversible transition in the cell cycle, and as such, must be tightly regulated in order to ensure the genomic integrity of daughter cells. Although activation of the APC^{Cdc20} has long been understood to trigger anaphase onset, a number of questions remain to be answered. Cdk1 activity is important for driving cell cycle transitions, and anaphase onset is no exception. Correlative studies have argued that Cdk1 phosphorylation of the APC in mitosis is important for its ubiquitination activity, and this phosphorylation contributes to the binding of the mitotic co-activator, Cdc20 (Félix et al., 1990; King et al., 1995; Kraft et al., 2003; Lahav-Baratz et al., 1995; Patra and Dunphy, 1998; Rudner and Murray, 2000; Shteinberg et al., 1999). One important question that has yet to be answered is whether Cdk1-dependent phosphorylation of the APC^{Cdc20} is essential for its activation, and the subsequent transition into anaphase.

The first objective of this thesis was to characterize the effect of inhibiting Cdk1 phosphorylation of the APC in an effort to determine whether this phosphorylation is essential for triggering anaphase onset. Using overexpression of Swe1 as a means of inhibiting Cdk1, we were able to show that reducing Cdk1 activity in mitosis decreases phosphorylation of the APC and arrests cells in metaphase. This metaphase arrest was apparent by the stabilization of APC substrates, and the impairment of sister chromatid segregation and anaphase spindle elongation. The ability of Swe1 to inhibit mitotic substrate degradation in an anaphase arrest also argued that Cdk1-dependent phosphorylation of the

APC is important for its activity throughout anaphase. While we were not able to rigorously prove using mutational analysis that Cdk1 phosphorylation of the APC is essential for APC^{Cdc20} activation at the metaphase-anaphase transition, our data strongly argues that this phosphorylation is important for APC^{Cdc20} activity, and that it regulates anaphase onset. We show that in budding yeast, as in other eukaryotes, Cdk1/Clb2 can activate the APC^{Cdc20} in vitro (Kraft et al., 2003; Kramer et al., 2000; Lahav-Baratz et al., 1995; Shteinberg et al., 1999), and that this activity depends on the presence of Cdk1 phosphorylation sites in Cdc16 and Cdc27. These in vitro studies suggest that, although Cdk1 phosphorylation of additional subunits likely contributes to maximal activity, these Cdk1 sites are important for ubiquitination activity of the APC^{Cdc20}. Overall, these findings support a model in which high Cdk1 activity regulates anaphase onset through phosphorylation of the APC^{Cdc20}.

The second objective of this thesis was to determine whether Cdk1-dependent phosphorylation of the TPR subunits Cdc16, Cdc23 and Cdc27 contributes to co-activator binding. We found that this phosphorylation did not make a significant contribution to the binding of Cdc20 to the APC in vitro or in vivo, contrary to what is generally accepted in the literature (Kraft et al., 2003; Kramer et al., 2000; 1998a; Rudner and Murray, 2000; Shteinberg et al., 1999). Furthermore, we also analyzed the possibility that additional TPR subunits might be involved in this process. We found that truncation of the non-essential subunit Cdc26, the *cdc26*$^{1-52}$ mutant, exhibits a genetic interaction with the *apc-12A* mutant. Despite this, we were not able to define a role for *cdc26*$^{1-52}$, or the loss of Mnd2, in cooperation with the *apc-12A* mutant in co-activator binding in vitro.

The data presented in Chapter 4 argued that Cdk1 phosphorylation of the APC does not contribute to activation of the APC^{Cdc20} by increasing the association of Cdc20, so the final objective of this thesis was to investigate another possible role of Cdk1-dependent phosphorylation of the APC: regulation of the spindle assembly checkpoint. We found that the *apc-12A* mutant exhibits only moderate sensitivity to SAC activation, but this is exacerbated by the loss of Mnd2 and/or truncation of Cdc26. This suggested that these two APC subunits, in cooperation with Cdk1 phosphorylation of the TPR subunits, function in a similar pathway. The temperature sensitivity exhibited by many of the APC mutants described in Chapter 4 is also partially suppressed by deletion of the checkpoint gene, *MAD2.* While we still do not fully understand the mechanism, we believe we have defined a novel role for Cdk1 phosphorylation of the APC: our results suggest that Cdk1 phosphorylation does not only regulate catalytic activity of the APC, but also SAC function.

6.2 CDK1 PHOSPHORYLATION OF THE APC REGULATES ANAPHASE ONSET

By overexpressing the tyrosine kinase Swe1 to inhibit Cdk1 activity in mitosis, we were able to lower Cdk1 activity enough to inhibit the transition from metaphase to anaphase. We were able to show this both in vitro and in vivo: overexpression of Swe1 in mitosis induces a metaphase block of the cell cycle, and APC purified under *GAL-SWE1* conditions exhibits reduced ubiquitination activity in vitro. We found that maximal activation of the APC^{Cdc20} in vitro requires the Cdk1 phosphorylation sites in Cdc16 and Cdc27, which is the first demonstration that defects caused by APC phosphorylation site mutants in vivo correlate with changes in APC activity in vitro (Rudner and Murray, 2000). Finally, our data

also suggests that $PP2A^{Cdc55}$-dependent dephosphorylation of the APC will result in decreased ubiquitination activity in vitro.

It still remains unclear, however, whether APC phosphorylation is an essential function of Cdk1, as it has not been shown that mutating APC subunits to prevent APC phosphorylation blocks anaphase. Although past work has suggested that the TPR subunits are the primary phosphorylated subunits of the APC (Rudner and Murray, 2000; Steen et al., 2008; Yoon et al., 2006), we have shown that both Apc1 and Apc9 are phosphorylated by Cdk1 both in vitro and in vivo, and there may also exist additional unidentified Cdk1 sites on the APC. We did find, however, that mutation of the Cdk1 sites in Apc9 does not decrease phosphorylation in vitro, suggesting that this subunit, which is not conserved in other eukaryotes, does not play an important role in Cdk1-dependent regulation of anaphase onset. A single study in *D. melanogaster* has shown that mutating two sites in cdc27 cannot rescue a lethal P-element insertion into the endogenous cdc27 (Huang et al., 2007), suggesting that phosphorylation of the APC may be essential in multicellular organisms.

Our findings also suggest that tyrosine dephosphorylation of Cdk1 by Mih1 (Cdc25 in vertebrates) may cause the increase in Cdk1 activity that triggers anaphase onset, at least in part through activation of the APC^{Cdc20} (Fig. 6.1A). In fission yeast and vertebrates high levels of tyrosine-phosphorylated Cdk1 arrests cells in G2, and mitotic entry requires a large change in Cdk1 activity. Budding yeast may use different Cdk1 activity thresholds, rendering mitotic onset relatively impervious to Swe1-dependent Cdk1 inhibition, and instead use this inhibition to control anaphase onset.

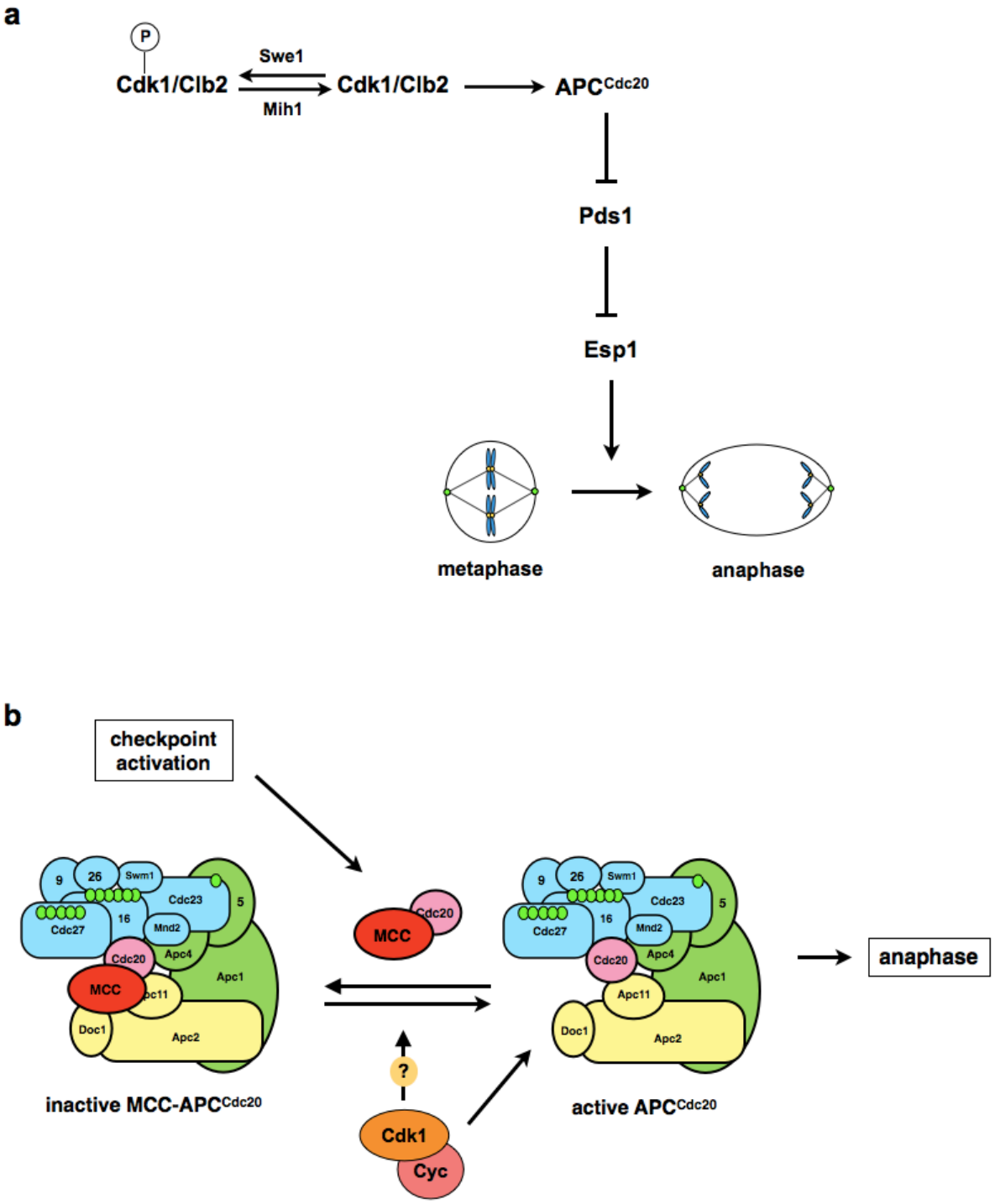
a
P
Swe1
Cdk1/Clb2
Mih1
Cdk1/Clb2
APCCdc20
Pds1
Esp1
metaphase
anaphase
b
checkpoint activation
9
26
Swm1
Cdc23
5
Cdc27
16
Mnd2
Cdc20
Apc4
MCC
Apc1
Apc11
Doc1
Apc2
inactive MCC-APCCdc20
MCC
Cdc20
?
Cdk1
Cyc
active APCCdc20
anaphase

Figure 6.1 Regulation of the metaphase-anaphase transition

(A) Cdk1 activates anaphase onset. Dephosphorylation of tyrosine 19 on Cdk1 by Mih1 allows normal anaphase onset by activating Cdk1, whereas Swe1 phosphorylation slows anaphase onset by phosphorylation and inhibiting Cdk1. Active Cdk1 phosphorylates the APC, and this phosphorylation contributes to APC^{Cdc20} activity, triggering anaphase. (B) Activation of the spindle assembly checkpoint triggers the formation of the MCC, which includes the APC co-activator Cdc20. The MCC binds the APC, inhibiting its ubiquitination activity, preventing progression into anaphase. The data presented in this thesis suggests that Cdk1/Clb activity is important for both the ubiquitination activity of the APC^{Cdc20}, and the recovery from SAC activation.

Finally, the data presented in Chapter 3 suggest the possibility that Wee1 and Cdc25 in other organisms may also influence anaphase onset. One study in unperturbed human cells correlated mitotic progression with Cdk1 tyrosine phosphorylation and showed that spindle assembly begins before an appreciable change in Cdk1 tyrosine phosphorylation (Lindqvist et al., 2007). In addition, Cdk1 dephosphorylation is completed just before maximal APC3 (the human Cdc27 homologue) phosphorylation and cyclin B proteolysis. This work suggests that as in yeast (Rahal and Amon, 2008; Rudner et al., 2000), vertebrates have a Cdk1 activity threshold that is required to initiate anaphase, and the complete dephosphorylation of Cdk1 during mitosis may assist in achieving this threshold.

6.3 TPR SUBUNIT PHOSPHORYLATION AND CO-ACTIVATOR BINDING

Protein phosphorylation is a widely studied post-translational modification important for many cellular functions. The phosphorylation pattern of the APC is particularly complex, and it is still not fully understood why the APC contains so many phosphorylation sites. Cdk consensus motifs are frequently found clustered in Cdk substrates (Moses et al., 2007), and the phosphorylation sites in the TPR subunits are no exception. Since clusters of phosphorylation sites are thought to affect the surface charge distribution, it is conceivable that these modifications could induce structural changes, and alter subunit interactions. This would have provided a reasonable explanation as to why phosphorylation of the APC was believed to contribute to Cdc20 binding, and subsequent activation of the APC^{Cdc20}. By using mutations that prevent Cdk1-mediated phosphorylation of Cdc16, Cdc23 and Cdc27, however, we demonstrated that phosphorylation of these TPR subunits did not influence

Cdc20 binding to the APC in vitro or in vivo. While the experiments presented in Chapter 3 argued the existence of additional phosphorylation sites on the APC that may be important for activity, we found that Cdc20 binds equally well to the Swe1-inhibited APC, which has lost phosphorylation on subunits in addition to Cdc16, Cdc23 and Cdc27. We favour the possibility that phosphorylation of the APC instead contributes to SAC function.

6.4 Cdk1 PHOSPHORYLATION AND THE SPINDLE ASSEMBLY CHECKPOINT

Activation of the SAC inhibits the APC^{Cdc20}, and prevents progression into anaphase in response to unattached kinetochores. Inhibition of the APC^{Cdc20} is accomplished by the generation of the MCC, which binds to the APC and blocks its ability to ubiquitinate mitotic substrates. Overall, our data argues that Cdk1/Clb activity regulates the catalytic activity of the APC^{Cdc20}, and additionally, may also regulate its recovery from the SAC (Fig. 6.1B). Consistent with this, checkpoint adaptation in yeast requires Cdk1-mediated APC phosphorylation (Vernieri et al., 2013). When the checkpoint is constantly induced, cells can adapt and transition into anaphase after several hours of checkpoint arrest, although this transition is dependent on Cdk1/Clb activity (Brito and Rieder, 2006; Rossio et al., 2010; Rudner et al., 2000).

Additional work remains in order to fully understand the role Cdk1/Clb activity plays in regulating the checkpoint. It is clear that Mnd2/Apc15 is important for SAC function, and in particular is argued to be important for autoubiquitination of Cdc20 when bound as part of the MCC (Foster and Morgan, 2012; Mansfeld et al., 2011; Uzunova et al., 2012). The loss of Mnd2 in the *apc-12A* background increases the sensitivity of this mutant to checkpoint

activation, so perhaps Cdk1 phosphorylation of the APC is important for Cdc20 ubiquitination. In vitro experiments with purified checkpoint proteins have argued that Mnd2 is required to shift the position of Cdc20 to allow for checkpoint induced autoubiquitination (Foster and Morgan, 2012). Phosphorylation of the APC could participate in the shift of the MCC and Cdc20 to a position that reduces substrate interactions, while favouring autoubiquitination. The regulation of Cdc20 turnover, through autoubiquitination, is thought to be important for the constant turnover of MCCs on the APC, which allows for rapid activation of the APC^{Cdc20} once the checkpoint has been satisfied.

Our data suggests a role for Cdk1 phosphorylation of the TPR subunits and the subunits Cdc26 and Mnd2 in SAC function, although how exactly the APC regulates SAC function remains to be determined. Furthermore, Cdk1 phosphorylation of the TPR subunits is argued to regulate more than the catalytic activity of the APC at the metaphase-anaphase transition. Future work will help elucidate the roles of the non-essential subunits Cdc26 and Mnd2, and whether they work in conjunction with phosphorylation of the TPR subunits to regulate the affinity of the MCC for the APC, and ultimately recovery from spindle checkpoint activation.

Appendix A

TABLE 1: STRAINS USED IN THIS STUDY

STRAIN	Mating Type	Genotype
ADR22	*MAT*α	wild type W303-1a[1]
ADR55	*MAT**a***	*mad2Δ::URA3*
ADR1249	*MAT*α	*ura3::pGAL-MPS1-myc-URA3 mad3Δ::LEU2*
ADR1393	*MAT**a***	*trp1::lacO-256X::TRP1 his3::pCup1-GFP12-lacI12::HIS3 bar1Δ*
ADR1395	*MAT**a***	*trp1::lacO-256X::TRP1 his3::pCup1-GFP12-lacI12::HIS3 mih1Δ::LEU2 leu2::pGAL-SWE1-HA-LEU2 CDC28-HA-URA3 bar1Δ*
ADR1606	*MAT**a***	*ura3::pGAL-MPS1-myc-URA3 clb2Δ::LEU2*
ADR1975	*MAT**a***	*ura3::pGAL-MPS1-myc-URA3 cdc16-6A-TRP1*
ADR2031	*MAT**a***	*bar1Δ cdc27-5A-KAN^R*
ADR2067	*MAT*α	*apc9Δ::HIS5*
ADR2617	*MAT**a***	*PDS1-myc18X-leu2::HIS3 bar1Δ*
ADR3089	*MAT**a***	*CDC16-TAP-HIS3 bar1Δ*
ADR3738	*MAT**a***	*PDS1-myc18X-leu2::HIS3 mih1Δ::KAN^R leu2::pGAL-swe1-N584A-HA-LEU2 bar1Δ*
ADR3740	*MAT**a***	*PDS1-myc18X-leu2::HIS3 mih1Δ::KAN^R leu2::pGAL-SWE1-HA-LEU2 bar1Δ*
ADR3822	*MAT*α	*cdc16-6A-TAP-KlURA3*
ADR3858	*MAT**a***	*CDC16-TAP-HIS3 mih1Δ::KAN^R leu2::pGAL-SWE1-HA-LEU2 bar1Δ*
ADR3871	*MAT**a***	*PDS1-myc18X-leu2::HIS3 mih1Δ::KAN^R leu2::pGAL-SWE1-HA-LEU2 bar1Δ*
ADR3877	*MAT*α	*CDC16-TAP-HIS3 swe1Δ::TRP1 mih1Δ::LEU2*
ADR3891	*MAT**a***	*cdc16-6A-TAP-KlURA3 cdc27-5A-KAN^R*
ADR3919	*MAT**a***	*PDS1-myc18X-leu2::HIS3 mih1Δ::KAN^R mec1Δ::TRP1 sml1Δ::NAT^R leu2::pGAL-SWE1-HA-LEU2 bar1Δ*
ADR3921	*MAT**a***	*PDS1-myc18X-leu2::HIS3 mec1Δ::TRP1 sml1Δ::NAT^R bar1Δ*
ADR3938	*MAT**a***	*PDS1-myc18X-leu2::HIS3 mad2Δ::URA3*
ADR3940	*MAT**a***	*PDS1-myc18X-leu2::HIS3 mad2Δ::URA3 mih1Δ:KAN^R leu2::pGAL-SWE1-HA-LEU2*
ADR4006	*MAT**a***	*bar1Δ*
ADR4009	*MAT**a***	*SPC42-eGFP-KAN^R bar1Δ*
ADR4169	*MAT**a***	*PDS1-myc18X-leu2::HIS3 SPC42-GFP-HYG^R bar1Δ*

STRAIN	Mating Type	Genotype
ADR4171	*MAT**a***	*PDS1-myc18X-leu2::HIS3 SPC42-GFP-HYG^{R} mih1Δ::KAN^{R} leu2::pGAL-SWE1-HA-LEU2 bar1Δ*
ADR4228	*MAT**a***	*PDS1-myc18X-leu2::HIS3 mih1Δ::KAN^{R} HYG^{R} -cdc28-Y19F leu2::pGAL-SWE1-HA-LEU2 bar1Δ*
ADR4245	*MAT**a***	*PDS1-myc18X-leu2::HIS3 mih1Δ::KAN^{R} cdc15-2 leu2::pGAL-SWE1-HA-LEU2*
ADR4252	*MAT**a***	*PDS1-myc18X-leu2::HIS3 cdc15-2*
ADR4289	*MAT**a***	*mih1Δ::KAN^{R} leu2::pGAL-SWE1-HA-LEU2 CIN8-eGFP-HYG^{R} bar1Δ*
ADR5230	*MAT**a***	*cdc26Δ::HIS3*
ADR5237	*MAT*α	*cdc16-6A-TRP1*
ADR5465	*MAT**a***	*CDC55-TAP-klTRP1 bar1Δ*
ADR5542	*MAT**a***	*bar1Δ mnd2Δ::HIS3*
ADR5574	*MAT*α	*mnd2Δ::HIS3 cdc16-6A-TRP1*
ADR5681	*MAT**a***	*mnd2Δ::HIS3 cdc27-5A-KAN^{R}*
ADR5722	*MAT**a***	*apc9Δ::HIS3 cdc16-6A-TRP1*
ADR5710	*MAT**a***	*swm1Δ::HIS3*
ADR5712	*MAT*α	*swm1Δ::HIS3 cdc16-6A-TRP1*
ADR5724	*MAT**a***	*apc9Δ::HIS3 cdc27-5A-KAN^{R}*
ADR5759	*MAT**a***	*swm1Δ::HIS3 cdc16-6A-TAP-URA3*
ADR5864	*MAT*α	*cdc26Δ::HIS3 cdc16-6A-TRP1*
ADR5867	*MAT**a***	*cdc26Δ::HIS3 cdc27-5A-KAN^{R}*
ADR5964	*MAT**a***	*swm1Δ APC1-TAP-URA3*
ADR5970	*MAT**a***	*cdc26Δ::HIS3 APC1-TAP-URA3*
ADR5978	*MAT**a***	*swm1Δ::HIS3 cdc27-5A-KAN^{R}*
ADR6073	*MAT*α	*swm1Δ::HIS3 CDC16-TAP-HIS3*
ADR6170	*MAT*α	*cdc26Δ::HIS3 cdc16-6A-TRP1 cdc27-5A-KAN^{R} APC1-TAP-URA3*
ADR6172	*MAT**a***	*cdc26Δ::HIS3 cdc16-6A-TRP1 APC1-TAP-URA3*
ADR6174	*MAT**a***	*bar1Δ APC1-TAP-URA3*
ADR6175	*MAT**a***	*swm1Δ::HIS3 cdc16-6A-TRP1 APC1-TAP-URA3*
ADR6316	*MAT**a***	*bar1Δ cdc26$^{1-52}$-HIS3 cdc16-6A-TRP1*
ADR6326	*MAT*α	*cdc26$^{1-52}$-HIS3 cdc27-5A-KAN^{R}*
ADR6337	*MAT**a***	*cdc26$^{1-31}$-HIS3*
ADR6354	*MAT*α	*cdc26$^{1-52}$-HIS3*

STRAIN	Mating Type	Genotype
ADR6396	*MAT**a***	*bar1Δ cdc26$^{1-52}$-HIS3*
ADR6463	*MAT**a***	*bar1Δ cdc23-A-HYG^{R}*
ADR6488	*MAT*α	*cdc26$^{1-52}$-HIS3 APC1-TAP-URA3*
ADR6533	*MAT**a***	*cdc26Δ::HIS3 cdc16-6A-TRP1 cdc27-5A-KAN^{R} cdc23-A-HYG^{R} APC1-TAP-URA3*
ADR6535	*MAT**a***	*cdc26Δ::HIS3 cdc23-A-HYG^{R} APC1-TAP-URA3*
ADR6537	*MAT**a***	*APC1-TAP-URA3 cdc23-A-HYG^{R}*
ADR6545	*MAT**a***	*cdc26$^{1-52}$-HIS3 cdc16-6A-TRP1 cdc27-5A-KAN^{R} cdc23-A-HYG^{R}*
ADR6546	*MAT**a***	*bar1Δ cdc26$^{1-52}$-HIS3 cdc16-6A-TRP1 cdc27-5A-KAN^{R} cdc23-A-HYG^{R}*
ADR6549	*MAT*α	*cdc26$^{1-52}$-HIS3 cdc23-A-HYG^{R}*
ADR6555	*MAT**a***	*bar1Δ cdc26Δ::HIS3 cdc16-6A-TRP1 cdc27-5A-KAN^{R} cdc23-A-HYG^{R}*
ADR6577	*MAT**a***	*APC1-TAP-URA cdc27-5A-KAN^{R}*
ADR6581	*MAT**a***	*APC1-TAP-URA cdc16-6A-TRP1*
ADR6589	*MAT**a***	*bar1Δ APC1-TAP-URA3 cdc16-6A-TRP1 cdc27-5A-KAN^{R} cdc23-A-HYG^{R}*
ADR6601	*MAT**a***	*cdc26Δ::HIS3 cdc23-A-HYG^{R}*
ADR6623	*MAT*α	*cdc16-6A-TRP1 cdc27-5A-KAN^{R} cdc23-A-HYG^{R}*
ADR6678	*MAT**a***	*swm1Δ::HIS3 cdc23-A-HYG^{R}*
ADR6821	*MAT*α	*apc9Δ::HIS3 cdc16-6A-TRP1 APC1-TAP-URA3*
ADR6825	*MAT**a***	*apc9Δ::HIS3 cdc16-6A-TRP1 cdc27-5A-KAN^{R} cdc23-A-HYG^{R} APC1-TAP-URA3*
ADR6890	*MAT*α	*apc9Δ::HIS3 APC1-TAP-URA3*
ADR6895	*MAT*α	*apc9Δ::HIS3 APC1-TAP-URA3 cdc23-A-HYG^{R}*
ADR6898	*MAT**a***	*apc9Δ::HIS3 cdc27-5A-KAN^{R} APC1-TAP-URA3*
ADR6967	*MAT**a***	*bar1Δ cdc26Δ::NAT^{R}*
ADR6969	*MAT**a***	*bar1Δ CDC16-TAP-HIS3 apc9-3A-HYG^{R}*
ADR7053	*MAT**a***	*cdc26$^{1-52}$-HIS3 cdc16-6A-TRP1 cdc27-5A-KAN^{R} cdc23-A-HYG^{R} APC1-TAP-URA3*
ADR7328	*MAT**a***	*mnd2Δ::HIS3 cdc26Δ::LEU2*
ADR7330	*MAT*α	*ura3::pGAL-MPS1-myc-URA3 mnd2Δ::HIS3*
ADR7334	*MAT*α	*ura3::pGAL-MPS1-myc-URA3 mnd2Δ::HIS3 cdc26Δ::LEU2*
ADR7335	*MAT*α	*cdc26Δ::HIS3 mad2Δ::URA3*
ADR7345	*MAT**a***	*ura3::pGAL-MPS1-myc-URA3 bar1Δ*
ADR7347	*MAT**a***	*ura3::pGAL-MPS1-myc-URA3 mad3Δ::LEU2 bar1Δ*
ADR7350	*MAT**a***	*ura3::pGAL-MPS1-myc-URA3 cdc26$^{1-52}$-HIS3*

STRAIN	Mating Type	Genotype
ADR7351	*MAT**a***	*ura3::pGAL-MPS1-myc-URA3 cdc26$^{1-52}$-HIS3*
ADR7353	*MAT**a***	*ura3::pGAL-MPS1-myc-URA3 cdc26$^{1-52}$-HIS3 cdc16-6A-TPR1*
ADR7362	*MAT**a***	*ura3::pGAL-MPS1-myc-URA3 cdc26$^{1-52}$-HIS3 cdc16-6A-TPR1 cdc27-5A-KAN^{R} cdc23-A-HYG^{R}*
ADR7392	*MAT**a***	*ura3::pGAL-MPS1-myc-URA3 cdc26Δ::HIS3*
ADR7395	*MAT**a***	*ura3::pGAL-MPS1-myc-URA3 cdc26Δ::HIS3 cdc16-6A-TRP1*
ADR7405	*MAT*α	*ura3::pGAL-MPS1-myc-URA3 mnd2Δ::HIS3 cdc16-6A-TRP1*
ADR7444	*MAT**a***	*ura3::pGAL-MPS1-myc-URA3 cdc16-6A-TRP1 cdc27-5A-KAN^{R} cdc23-A-HYG^{R} bar1Δ*
ADR7451	*MAT*α	*mnd2Δ::NAT^{R}*
ADR7526	*MAT**a***	*bar1Δ mnd2Δ::HIS3 mad2Δ::URA3*
ADR7527	*MAT**a***	*bar1Δ mnd2Δ::HIS3 mad2Δ::URA3*
ADR7528	*MAT**a***	*bar1Δ cdc26$^{1-52}$-HIS3 mad2Δ::URA3*
ADR7530	*MAT**a***	*bar1Δ cdc26$^{1-52}$-HIS3 cdc16-6A-TRP1 cdc27-5A-KAN^{R} cdc23-A-HYG^{R} mad2Δ::URA3*
ADR7531	*MAT**a***	*bar1Δ cdc26Δ::HIS3 cdc16-6A-TRP1 cdc27-5A-KAN^{R} cdc23-A-HYG^{R} mad2Δ::URA3*
ADR7568	*MAT*α	*mnd2Δ::NAT^{R} cdc26$^{1-52}$-HIS3*
ADR7613	*MAT*α	*mnd2Δ::NAT^{R} cdc26$^{1-52}$-HIS3 mad2Δ::URA3*
ADR7617	*MAT*α	*mnd2Δ::NAT^{R} cdc26$^{1-52}$-HIS3 cdc16-6A-TRP1*
ADR7619	*MAT*α	*mnd2Δ::NAT^{R} cdc26$^{1-52}$-HIS3 cdc27-5A-KAN^{R}*
ADR7621	*MAT*α	*mnd2Δ::NAT^{R} cdc26$^{1-52}$-HIS3 cdc23-A-HYG^{R}*
ADR7623	*MAT*α	*mnd2Δ::NAT^{R} cdc26$^{1-52}$-HIS3 cdc16-6A-TRP1 cdc27-5A-KAN^{R} cdc23-A-HYG^{R}*
ADR7624	*MAT**a***	*mnd2Δ::NAT^{R} APC1-TAP-URA3*
ADR7628	*MAT**a***	*mnd2Δ::NAT^{R} cdc26$^{1-52}$-HIS3 APC1-TAP-URA3*
ADR7642	*MAT**a***	*mnd2Δ::NAT^{R} cdc26$^{1-52}$-HIS3 cdc16-6A-TRP1 cdc27-5A-KAN^{R} cdc23-A-HYG^{R} APC1-TAP-URA3*
ADR7643	*MAT**a***	*mnd2Δ::NAT^{R} cdc23-A-HYG^{R}*
ADR7646	*MAT*α	*mnd2Δ::NAT^{R} cdc16-6A-TRP1 cdc27-5A-KAN^{R} cdc23-A-HYG^{R}*
ADR7650	*MAT*α	*mnd2Δ::NAT^{R} cdc16-6A-TRP1 cdc27-5A-KAN^{R} cdc23-A-HYG^{R} APC1-TAP-URA3*
ADR7653	*MAT**a***	*mnd2Δ::NAT^{R} cdc16-6A-TRP1 APC1-TAP-URA3*
ADR7656	*MAT*α	*mnd2Δ::NAT^{R} cdc27-5A-KAN^{R} APC1-TAP-URA3*
ADR7658	*MAT*α	*mnd2Δ::NAT^{R} cdc23-A-HYG^{R} APC1-TAP-URA3*

STRAIN	Mating Type	Genotype
ADR7726	*MAT**a***	*ura3::pGAL-MPS1-myc-URA3 mnd2Δ::HIS3 bar1Δ*
ADR7901	*MAT**a***	*ura3::pGAL-MPS1-myc-URA3 mnd2Δ::HIS3 cdc26Δ::LEU2 bar1Δ*
ADR7905	*MAT**a***	*ura3::pGAL-MPS1-myc-URA3 cdc26Δ::LEU2 bar1Δ*
ADR8269	*MAT*α	*mnd2Δ::HIS3 cdc26Δ::LEU2 mad2Δ::URA3*
ADR8270	*MAT*α	*mnd2Δ::NAT^{R} cdc26$^{1-52}$-HIS3 cdc16-6A-TRP1 cdc27-5A-KAN^{R} cdc23-A-HYG^{R} mad2Δ::URA3*
ADR8271	*MAT**a***	*mnd2Δ::NAT^{R} cdc16-6A-TRP1 cdc27-5A-KAN^{R} cdc23-A-HYG^{R} mad2Δ::URA3*
ADR8323	*MAT**a***	*APC1-TAP-ADE2 BUB1-FLAG-NAT^{R} ura3::pGAL-MPS1-myc-URA3 bar1Δ*

References

Amon, A. (1997). Regulation of B-type cyclin proteolysis by Cdc28-associated kinases in budding yeast. Embo J *16*, 2693–2702.

Anastasia, S.D., Nguyen, D.L., Thai, V., Meloy, M., MacDonough, T., and Kellogg, D.R. (2012). A link between mitotic entry and membrane growth suggests a novel model for cell size control. J Cell Biol *197*, 89–104.

Anderson, C.W., Baum, P.R., and Gesteland, R.F. (1973). Processing of adenovirus 2-induced proteins. J. Virol. *12*, 241–252.

Anghileri, P., Branduardi, P., Sternieri, F., Monti, P., Visintin, R., Bevilacqua, A., Alberghina, L., Martegani, E., and Baroni, M.D. (1999). Chromosome separation and exit from mitosis in budding yeast: dependence on growth revealed by cAMP-mediated inhibition. Exp. Cell Res. *250*, 510–523.

Bakhoum, S.F., and Compton, D.A. (2012). Chromosomal instability and cancer: a complex relationship with therapeutic potential. J. Clin. Invest. *122*, 1138–1143.

Biggins, S., and Murray, A.W. (2001). The budding yeast protein kinase Ipl1/Aurora allows the absence of tension to activate the spindle checkpoint. Genes Dev *15*, 3118–3129.

Bishop, A., Buzko, O., Heyeck-Dumas, S., Jung, I., Kraybill, B., Liu, Y., Shah, K., Ulrich, S., Witucki, L., Yang, F., et al. (2000). Unnatural ligands for engineered proteins: new tools for chemical genetics. Annual Review of Biophysics and Biomolecular Structure *29*, 577–606.

Blethrow, J.D., Tang, C., Deng, C., and Krutchinsky, A.N. (2007). Modular Mass Spectrometric Tool for Analysis of Composition and Phosphorylation of Protein Complexes. PLoS ONE *2*, e358.

Booher, R.N., Deshaies, R.J., and Kirschner, M.W. (1993). Properties of Saccharomyces cerevisiae wee1 and its differential regulation of p34CDC28 in response to G1 and G2 cyclins. Embo J *12*, 3417–3426.

Borden, K.L., and Freemont, P.S. (1996). The RING finger domain: a recent example of a sequence-structure family. Curr Opin Struct Biol *6*, 395–401.

Bouchoux, C., and Uhlmann, F. (2011). A Quantitative Model for Ordered Cdk Substrate Dephosphorylation during Mitotic Exit. Cell *147*, 803–814.

Bradford, M.M. (1976). A rapid and sensitive method for the quantitation of microgram quantities of protein utilizing the principle of protein-dye binding. Anal. Biochem. *72*, 248–254.

Brito, D.A., and Rieder, C.L. (2006). Mitotic checkpoint slippage in humans occurs via cyclin B destruction in the presence of an active checkpoint. Curr Biol *16*, 1194–1200.

Burgess, A., Vigneron, S., Brioudes, E., Labbé, J.-C., Lorca, T., and Castro, A. (2010). Loss of human Greatwall results in G2 arrest and multiple mitotic defects due to deregulation of the cyclin B-Cdc2/PP2A balance. Proceedings of the National Academy of Sciences *107*, 12564–12569.

Burton, J.L., and Solomon, M.J. (2001). D box and KEN box motifs in budding yeast Hsl1p are required for APC-mediated degradation and direct binding to Cdc20p and Cdh1p. Genes Dev *15*, 2381–2395.

Burton, J.L., and Solomon, M.J. (2007). Mad3p, a pseudosubstrate inhibitor of APCCdc20 in the spindle assembly checkpoint. Genes Dev *21*, 655–667.

Burton, J.L., Tsakraklides, V., and Solomon, M.J. (2005). Assembly of an APC-Cdh1-substrate complex is stimulated by engagement of a destruction box. Mol Cell *18*, 533–542.

Buschhorn, B.A., Petzold, G., Galova, M., Dube, P., Kraft, C., Herzog, F., Stark, H., and Peters, J.-M. (2011). Substrate binding on the APC/C occurs between the coactivator Cdh1 and the processivity factor Doc1. Nat Struct Mol Biol *18*, 6–13.

Camasses, A., Bogdanova, A., Shevchenko, A., and Zachariae, W. (2003). The CCT chaperonin promotes activation of the anaphase-promoting complex through the generation of functional Cdc20. Mol Cell *12*, 87–100.

Cardozo, T., and Pagano, M. (2004). The SCF ubiquitin ligase: insights into a molecular machine. Nat Rev Mol Cell Biol *5*, 739–751.

Carroll, C.W., and Morgan, D.O. (2002). The Doc1 subunit is a processivity factor for the anaphase-promoting complex. Nat Cell Biol *4*, 880–887.

Carroll, C.W., and Morgan, D.O. (2005). Enzymology of the anaphase-promoting complex. Meth Enzymol *398*, 219–230.

Carroll, C.W., Enquist-Newman, M., and Morgan, D.O. (2005). The APC subunit Doc1 promotes recognition of the substrate destruction box. Curr Biol *15*, 11–18.

Castilho, P.V., Williams, B.C., Mochida, S., Zhao, Y., and Goldberg, M.L. (2009). The M phase kinase Greatwall (Gwl) promotes inactivation of PP2A/B55delta, a phosphatase directed against CDK phosphosites. Mol Biol Cell *20*, 4777–4789.

Castro, A., Vigneron, S., Bernis, C., Labbé, J.-C., Prigent, C., and Lorca, T. (2002). The D-Box-activating domain (DAD) is a new proteolysis signal that stimulates the silent D-Box sequence of Aurora-A. EMBO Rep *3*, 1209–1214.

Chao, W.C.H., Kulkarni, K., Zhang, Z., Kong, E.H., and Barford, D. (2012). Structure of the mitotic checkpoint complex. Nature *484*, 208–213.

Charles, J.F., Jaspersen, S.L., Tinker-Kulberg, R.L., Hwang, L., Szidon, A., and Morgan, D.O. (1998). The Polo-related kinase Cdc5 activates and is destroyed by the mitotic cyclin destruction machinery in S. cerevisiae. Curr Biol *8*, 497–507.

Chau, V., Tobias, J.W., Bachmair, A., Marriott, D., Ecker, D.J., Gonda, D.K., and Varshavsky, A. (1989). A multiubiquitin chain is confined to specific lysine in a targeted short-lived protein. Science *243*, 1576–1583.

Chen, F., Archambault, V., Kar, A., Lio, P., D'Avino, P.P., Sinka, R., Lilley, K., Laue, E.D., Deak, P., Capalbo, L., et al. (2007). Multiple protein phosphatases are required for mitosis in Drosophila. Curr Biol *17*, 293–303.

Chen, R.H., Brady, D.M., Smith, D., Murray, A.W., and Hardwick, K.G. (1999). The spindle checkpoint of budding yeast depends on a tight complex between the Mad1 and Mad2 proteins. Mol Biol Cell *10*, 2607–2618.

Chen, R.H., Shevchenko, A., Mann, M., and Murray, A.W. (1998). Spindle checkpoint protein Xmad1 recruits Xmad2 to unattached kinetochores. J Cell Biol *143*, 283–295.

Chen, R.H., Waters, J.C., Salmon, E.D., and Murray, A.W. (1996). Association of spindle assembly checkpoint component XMAD2 with unattached kinetochores. Science *274*, 242–246.

Chen, R.-H. (2002). BubR1 is essential for kinetochore localization of other spindle checkpoint proteins and its phosphorylation requires Mad1. J Cell Biol *158*, 487–496.

Chiroli, E., Rossio, V., Lucchini, G., and Piatti, S. (2007). The budding yeast PP2ACdc55 protein phosphatase prevents the onset of anaphase in response to morphogenetic defects. J Cell Biol *177*, 599–611.

Chung, E., and Chen, R.-H. (2003). Phosphorylation of Cdc20 is required for its inhibition by the spindle checkpoint. Nat Cell Biol *5*, 748–753.

Ciosk, R., Zachariae, W., Michaelis, C., Shevchenko, A., Mann, M., and Nasmyth, K. (1998). An ESP1/PDS1 complex regulates loss of sister chromatid cohesion at the metaphase to anaphase transition in yeast. Cell *93*, 1067–1076.

Cohen-Fix, O., Peters, J.M., Kirschner, M.W., and Koshland, D. (1996). Anaphase initiation in Saccharomyces cerevisiae is controlled by the APC-dependent degradation of the anaphase inhibitor Pds1p. Genes Dev *10*, 3081–3093.

Cross, F.R. (1997). “Marker swap” plasmids: convenient tools for budding yeast molecular genetics. Yeast *13*, 647–653.

D'Andrea, L.D., and Regan, L. (2003). TPR proteins: the versatile helix. Trends Biochem. Sci. *28*, 655–662.

D'Angiolella, V., Mari, C., Nocera, D., Rametti, L., and Grieco, D. (2003). The spindle checkpoint requires cyclin-dependent kinase activity. Genes Dev *17*, 2520–2525.

Da Fonseca, P.C.A., Kong, E.H., Zhang, Z., Schreiber, A., Williams, M.A., Morris, E.P., and Barford, D. (2011). Structures of APC/C(Cdh1) with substrates identify Cdh1 and Apc10 as the D-box co-receptor. Nature *470*, 274–278.

Dawson, I.A., Roth, S., Akam, M., and Artavanis-Tsakonas, S. (1993). Mutations of the fizzy locus cause metaphase arrest in Drosophila melanogaster embryos. Development *117*, 359–376.

Deak, P., Donaldson, M., and Glover, D.M. (2003). Mutations in mákos, a Drosophila gene encoding the Cdc27 subunit of the anaphase promoting complex, enhance centrosomal defects in polo and are suppressed by mutations in twins/aar, which encodes a regulatory subunit of PP2A. J Cell Sci *116*, 4147–4158.

Deibler, R.W., and Kirschner, M.W. (2010). Quantitative reconstitution of mitotic CDK1 activation in somatic cell extracts. Mol Cell *37*, 753–767.

Descombes, P., and Nigg, E.A. (1998). The polo-like kinase Plx1 is required for M phase exit and destruction of mitotic regulators in Xenopus egg extracts. Embo J *17*, 1328–1335.

Deshaies, R.J., and Joazeiro, C.A.P. (2009). RING domain E3 ubiquitin ligases. Annu. Rev. Biochem. *78*, 399–434.

Dial, J.M., Petrotchenko, E.V., and Borchers, C.H. (2007). Inhibition of APCCdh1 activity by Cdh1/Acm1/Bmh1 ternary complex formation. J Biol Chem *282*, 5237–5248.

Dube, P., Herzog, F., Gieffers, C., Sander, B., Riedel, D., Müller, S.A., Engel, A., Peters, J.-M., and Stark, H. (2005). Localization of the coactivator Cdh1 and the cullin subunit Apc2 in a cryo-electron microscopy model of vertebrate APC/C. Mol Cell *20*, 867–879.

Dunphy, W.G., and Kumagai, A. (1991). The cdc25 protein contains an intrinsic phosphatase activity. Cell *67*, 189–196.

Duntze, W., MacKay, V., and Manney, T.R. (1970). Saccharomyces cerevisiae: a diffusible sex factor. Science *168*, 1472–1473.

Enquist-Newman, M., Sullivan, M., and Morgan, D.O. (2008). Modulation of the mitotic regulatory network by APC-dependent destruction of the Cdh1 inhibitor Acm1. Mol Cell *30*, 437–446.

Evans, T., Rosenthal, E.T., Youngblom, J., Distel, D., and Hunt, T. (1983). Cyclin: a protein specified by maternal mRNA in sea urchin eggs that is destroyed at each cleavage division. Cell *33*, 389–396.

Eytan, E., Moshe, Y., Braunstein, I., and Hershko, A. (2006). Roles of the anaphase-promoting complex/cyclosome and of its activator Cdc20 in functional substrate binding. Proc Natl Acad Sci USA *103*, 2081–2086.

Fang, G., Yu, H., and Kirschner, M.W. (1998). Direct binding of CDC20 protein family members activates the anaphase-promoting complex in mitosis and G1. Mol Cell *2*, 163–171.

Félix, M.A., Labbé, J.C., Dorée, M., Hunt, T., and Karsenti, E. (1990). Triggering of cyclin degradation in interphase extracts of amphibian eggs by cdc2 kinase. Nature *346*, 379–382.

Foster, S.A., and Morgan, D.O. (2012). The APC/C Subunit Mnd2/Apc15 Promotes Cdc20 Autoubiquitination and Spindle Assembly Checkpoint Inactivation. Mol Cell.

Funabiki, H., Yamano, H., Kumada, K., Nagao, K., Hunt, T., and Yanagida, M. (1996). Cut2 proteolysis required for sister-chromatid seperation in fission yeast. Nature *381*, 438–441.

Gautier, J., Solomon, M.J., Booher, R.N., Bazan, J.F., and Kirschner, M.W. (1991). cdc25 is a specific tyrosine phosphatase that directly activates p34cdc2. Cell *67*, 197–211.

Gerhart, J., Wu, M., and Kirschner, M. (1984). Cell cycle dynamics of an M-phase-specific cytoplasmic factor in Xenopus laevis oocytes and eggs. J Cell Biol *98*, 1247–1255.

Ghiara, J.B., Richardson, H.E., Sugimoto, K., Henze, M., Lew, D.J., Wittenberg, C., and Reed, S.I. (1991). A cyclin B homolog in S. cerevisiae: chronic activation of the Cdc28 protein kinase by cyclin prevents exit from mitosis. Cell *65*, 163–174.

Glotzer, M., Murray, A.W., and Kirschner, M.W. (1991). Cyclin is degraded by the ubiquitin pathway. Nature *349*, 132–138.

Gmachl, M., Gieffers, C., Podtelejnikov, A.V., Mann, M., and Peters, J.M. (2000). The RING-H2 finger protein APC11 and the E2 enzyme UBC4 are sufficient to ubiquitinate substrates of the anaphase-promoting complex. Proc Natl Acad Sci USA *97*, 8973–8978.

Golan, A., Yudkovsky, Y., and Hershko, A. (2002). The cyclin-ubiquitin ligase activity of cyclosome/APC is jointly activated by protein kinases Cdk1-cyclin B and Plk. J Biol Chem *277*, 15552–15557.

Goldstein, A.L., and McCusker, J.H. (1999). Three new dominant drug resistance cassettes for gene disruption in Saccharomyces cerevisiae. Yeast *15*, 1541–1553.

Gordon, D.M., and Roof, D.M. (2001). Degradation of the kinesin Kip1p at anaphase onset is mediated by the anaphase-promoting complex and Cdc20p. Proc Natl Acad Sci USA *98*, 12515–12520.

Gould, K.L., Moreno, S., Tonks, N.K., and Nurse, P. (1990). Complementation of the mitotic activator, p80cdc25, by a human protein-tyrosine phosphatase. Science *250*, 1573–1576.

Gould, K.L., and Nurse, P. (1989). Tyrosine phosphorylation of the fission yeast cdc2+ protein kinase regulates entry into mitosis. Nature *342*, 39–45.

Hall, M.C., Torres, M.P., Schroeder, G.K., and Borchers, C.H. (2003). Mnd2 and Swm1 are core subunits of the Saccharomyces cerevisiae anaphase-promoting complex. J Biol Chem *278*, 16698–16705.

Hardwick, K.G., Johnston, R.C., Smith, D.L., and Murray, A.W. (2000). MAD3 encodes a novel component of the spindle checkpoint which interacts with Bub3p, Cdc20p, and Mad2p. J Cell Biol *148*, 871–882.

Hardwick, K.G., Weiss, E., Luca, F.C., Winey, M., and Murray, A.W. (1996). Activation of the budding yeast spindle assembly checkpoint without mitotic spindle disruption. Science *273*, 953–956.

Hartwell, L.H., Culotti, J., and Reid, B. (1970). Genetic control of the cell-division cycle in yeast. I. Detection of mutants. Proc Natl Acad Sci USA *66*, 352–359.

Hartwell, L.H., Culotti, J., Pringle, J.R., and Reid, B.J. (1974). Genetic control of the cell division cycle in yeast. Science *183*, 46–51.

Hartwell, L.H., Mortimer, R.K., Culotti, J., and Culotti, M. (1973). Genetic Control of the Cell Division Cycle in Yeast: V. Genetic Analysis of cdc Mutants. Genetics *74*, 267–286.

Harvey, S.L., and Kellogg, D.R. (2003). Conservation of mechanisms controlling entry into mitosis: budding yeast wee1 delays entry into mitosis and is required for cell size control. Curr Biol *13*, 264–275.

Harvey, S.L., Charlet, A., Haas, W., Gygi, S.P., and Kellogg, D.R. (2005). Cdk1-dependent regulation of the mitotic inhibitor Wee1. Cell *122*, 407–420.

Harvey, S.L., Enciso, G., Dephoure, N., Gygi, S.P., Gunawardena, J., and Kellogg, D.R. (2011). A phosphatase threshold sets the level of Cdk1 activity in early mitosis in budding yeast. Mol Biol Cell *22*, 3595–3608.

Hayes, M.J., Kimata, Y., Wattam, S.L., Lindon, C., Mao, G., Yamano, H., and Fry, A.M. (2006). Early mitotic degradation of Nek2A depends on Cdc20-independent interaction with the APC/C. Nat Cell Biol *8*, 607–614.

Healy, A.M., Zolnierowicz, S., Stapleton, A.E., Goebl, M., DePaoli-Roach, A.A., and Pringle, J.R. (1991). CDC55, a Saccharomyces cerevisiae gene involved in cellular morphogenesis: identification, characterization, and homology to the B subunit of mammalian type 2A protein phosphatase. Mol Cell Biol *11*, 5767–5780.

Hershko, A., and Ciechanover, A. (1998). The ubiquitin system. Annu. Rev. Biochem. *67*, 425–479.

Herzog, F., Primorac, I., Dube, P., Lenart, P., Sander, B., Mechtler, K., Stark, H., and Peters, J.-M. (2009). Structure of the anaphase-promoting complex/cyclosome interacting with a mitotic checkpoint complex. Science *323*, 1477–1481.

Hildebrandt, E.R., and Hoyt, M.A. (2001). Cell cycle-dependent degradation of the Saccharomyces cerevisiae spindle motor Cin8p requires APC(Cdh1) and a bipartite destruction sequence. Mol Biol Cell *12*, 3402–3416.

Hilioti, Z., Chung, Y.S., Mochizuki, Y., Hardy, C.F., and Cohen-Fix, O. (2001). The anaphase inhibitor Pds1 binds to the APC/C-associated protein Cdc20 in a destruction box-dependent manner. Curr Biol *11*, 1347–1352.

Hirano, T., Kinoshita, N., Morikawa, K., and Yanagida, M. (1990). Snap helix with knob and hole: essential repeats in S. pombe nuclear protein nuc2+. Cell *60*, 319–328.

Holloway, S.L., Glotzer, M., King, R.W., and Murray, A.W. (1993). Anaphase is initiated by proteolysis rather than by the inactivation of maturation-promoting factor. Cell *73*, 1393–1402.

Holt, L.J., Krutchinsky, A.N., and Morgan, D.O. (2008). Positive feedback sharpens the anaphase switch. Nature *454*, 353–357.

Howell, B.J., Hoffman, D.B., Fang, G., Murray, A.W., and Salmon, E.D. (2000). Visualization of Mad2 dynamics at kinetochores, along spindle fibers, and at spindle poles in living cells. J Cell Biol *150*, 1233–1250.

Hoyt, M.A., Totis, L., and Roberts, B.T. (1991). S. cerevisiae genes required for cell cycle arrest in response to loss of microtubule function. Cell *66*, 507–517.

Huang, J.-Y., Morley, G., Li, D., and Whitaker, M. (2007). Cdk1 phosphorylation sites on Cdc27 are required for correct chromosomal localisation and APC/C function in syncytial Drosophila embryos. J Cell Sci *120*, 1990–1997.

Hwang, L.H., and Murray, A.W. (1997). A novel yeast screen for mitotic arrest mutants identifies DOC1, a new gene involved in cyclin proteolysis. Mol Biol Cell *8*, 1877–1887.

Indjeian, V.B., Stern, B.M., and Murray, A.W. (2005). The centromeric protein Sgo1 is required to sense lack of tension on mitotic chromosomes. Science *307*, 130–133.

Irniger, S., Bäumer, M., and Braus, G.H. (2000). Glucose and ras activity influence the ubiquitin ligases APC/C and SCF in Saccharomyces cerevisiae. Genetics *154*, 1509–1521.

Irniger, S., Piatti, S., Michaelis, C., and Nasmyth, K. (1995). Genes involved in sister chromatid separation are needed for B-type cyclin proteolysis in budding yeast. Cell *81*, 269–278.

Izawa, D., and Pines, J. (2011). How APC/C-Cdc20 changes its substrate specificity in mitosis. Nat Cell Biol *13*, 223–233.

Jaspersen, S.L., Charles, J.F., and Morgan, D.O. (1999). Inhibitory phosphorylation of the APC regulator Hct1 is controlled by the kinase Cdc28 and the phosphatase Cdc14. Curr Biol *9*, 227–236.

Jia, L., Kim, S., and Yu, H. (2013). Tracking spindle checkpoint signals from kinetochores to APC/C. Trends Biochem. Sci. *38*, 302–311.

Jin, L., Williamson, A., Banerjee, S., Philipp, I., and Rape, M. (2008). Mechanism of ubiquitin-chain formation by the human anaphase-promoting complex. Cell *133*, 653–665.

Kato, T., Daigo, Y., Aragaki, M., Ishikawa, K., Sato, M., and Kaji, M. (2012). Overexpression of CDC20 predicts poor prognosis in primary non-small cell lung cancer patients. J Surg Oncol *106*, 423–430.

Keaton, M.A., Szkotnicki, L., Marquitz, A.R., Harrison, J., Zyla, T.R., and Lew, D.J. (2008). Nucleocytoplasmic trafficking of G2/M regulators in yeast. Mol Biol Cell *19*, 4006–4018.

Kellogg, D.R., and Murray, A.W. (1995). NAP1 acts with Clb1 to perform mitotic functions and to suppress polar bud growth in budding yeast. J Cell Biol *130*, 675–685.

Kellogg, D.R. (2003). Wee1-dependent mechanisms required for coordination of cell growth and cell division. J Cell Sci *116*, 4883–4890.

Kennelly, P.J., and Krebs, E.G. (1991). Consensus sequences as substrate specificity determinants for protein kinases and protein phosphatases. J Biol Chem *266*, 15555–15558.

King, R.W., Peters, J.M., Tugendreich, S., Rolfe, M., Hieter, P., and Kirschner, M.W. (1995). A 20S complex containing CDC27 and CDC16 catalyzes the mitosis-specific conjugation of ubiquitin to cyclin B. Cell *81*, 279–288.

Kitada, K., Johnson, A.L., Johnston, L.H., and Sugino, A. (1993). A multicopy suppressor gene of the Saccharomyces cerevisiae G1 cell cycle mutant gene dbf4 encodes a protein kinase and is identified as CDC5. Mol Cell Biol *13*, 4445–4457.

Kitajima, T.S., Kawashima, S.A., and Watanabe, Y. (2004). The conserved kinetochore protein shugoshin protects centromeric cohesion during meiosis. Nature *427*, 510–517.

Kitazono, A.A., Garza, D.A., and Kron, S.J. (2003). Mutations in the yeast cyclin-dependent kinase Cdc28 reveal a role in the spindle assembly checkpoint. Mol. Genet. Genomics *269*, 672–684.

Kiyomitsu, T., Obuse, C., and Yanagida, M. (2007). Human Blinkin/AF15q14 is required for chromosome alignment and the mitotic checkpoint through direct interaction with Bub1 and BubR1. Dev Cell *13*, 663–676.

Kotani, S., Tugendreich, S., Fujii, M., Jorgensen, P.M., Watanabe, N., Hoog, C., Hieter, P., and Todokoro, K. (1998). PKA and MPF-activated polo-like kinase regulate anaphase-promoting complex activity and mitosis progression. Mol Cell *1*, 371–380.

Kraft, C., Herzog, F., Gieffers, C., Mechtler, K., Hagting, A., Pines, J., and Peters, J.-M. (2003). Mitotic regulation of the human anaphase-promoting complex by phosphorylation. Embo J *22*, 6598–6609.

Kraft, C., Vodermaier, H.C., Maurer-Stroh, S., Eisenhaber, F., and Peters, J.-M. (2005). The WD40 propeller domain of Cdh1 functions as a destruction box receptor for APC/C substrates. Mol Cell *18*, 543–553.

Kramer, E.R., Scheuringer, N., Podtelejnikov, A.V., Mann, M., and Peters, J.M. (2000). Mitotic regulation of the APC activator proteins CDC20 and CDH1. Mol Biol Cell *11*, 1555–1569.

Kramer, E.R., Gieffers, C., Hölzl, G., Hengstschläger, M., and Peters, J.-M. (1998a). Activation of the human anaphase-promoting complex by proteins of the CDC20/Fizzy family. Current Biology *8*, 1207–S4.

Kramer, K.M., Fesquet, D., Johnson, A.L., and Johnston, L.H. (1998b). Budding yeast RSI1/APC2, a novel gene necessary for initiation of anaphase, encodes an APC subunit. Embo J *17*, 498–506.

Kumagai, A., and Dunphy, W.G. (1992). Regulation of the cdc25 protein during the cell cycle in Xenopus extracts. Cell *70*, 139–151.

Kurasawa, Y., and Todokoro, K. (1999). Identification of human APC10/Doc1 as a subunit of anaphase promoting complex. Oncogene *18*, 5131–5137.

Labit, H., Fujimitsu, K., Bayin, N.S., Takaki, T., Gannon, J., and Yamano, H. (2012). Dephosphorylation of Cdc20 is required for its C-box-dependent activation of the APC/C. Embo J.

Lahav-Baratz, S., Sudakin, V., Ruderman, J.V., and Hershko, A. (1995). Reversible phosphorylation controls the activity of cyclosome-associated cyclin-ubiquitin ligase. Proc Natl Acad Sci USA *92*, 9303–9307.

Lamb, J.R., Michaud, W.A., Sikorski, R.S., and Hieter, P.A. (1994). Cdc16p, Cdc23p and Cdc27p form a complex essential for mitosis. Embo J *13*, 4321–4328.

Lara-Gonzalez, P., Scott, M.I.F., Diez, M., Sen, O., and Taylor, S.S. (2011). BubR1 blocks substrate recruitment to the APC/C in a KEN-box-dependent manner. J Cell Sci *124*, 4332–4345.

Lara-Gonzalez, P., Westhorpe, F.G., and Taylor, S.S. (2012). The spindle assembly checkpoint. Curr Biol *22*, R966–R980.

Lee, M.G., and Nurse, P. (1987). Complementation used to clone a human homologue of the fission yeast cell cycle control gene cdc2. Nature *327*, 31–35.

Leverson, J.D., Joazeiro, C.A., Page, A.M., Huang, H.K., Hieter, P., and Hunter, T. (2000). The APC11 RING-H2 finger mediates E2-dependent ubiquitination. Mol Biol Cell *11*, 2315–2325.

Lew, D.J., and Reed, S.I. (1995). A cell cycle checkpoint monitors cell morphogenesis in budding yeast. J Cell Biol *129*, 739–749.

Li, R., and Murray, A.W. (1991). Feedback control of mitosis in budding yeast. Cell *66*, 519–531.

Li, X., and Cai, M. (1997). Inactivation of the cyclin-dependent kinase Cdc28 abrogates cell cycle arrest induced by DNA damage and disassembly of mitotic spindles in Saccharomyces cerevisiae. Mol Cell Biol *17*, 2723–2734.

Li, X., and Nicklas, R.B. (1995). Mitotic forces control a cell-cycle checkpoint. Nature *373*, 630–632.

Li, Y., and Benezra, R. (1996). Identification of a human mitotic checkpoint gene: hsMAD2. Science *274*, 246–248.

Liang, H., Lim, H.H., Venkitaraman, A., and Surana, U. (2011). Cdk1 promotes kinetochore bi-orientation and regulates Cdc20 expression during recovery from spindle checkpoint arrest. Embo J.

Lianga, N., Williams, E.C., Kennedy, E.K., Doré, C., Pilon, S., Girard, S.L., Deneault, J.-S., and Rudner, A.D. (2013). A Wee1 checkpoint inhibits anaphase onset. J Cell Biol *201*, 843–862.

Lin, F.C., and Arndt, K.T. (1995). The role of Saccharomyces cerevisiae type 2A phosphatase in the actin cytoskeleton and in entry into mitosis. Embo J *14*, 2745–2759.

Lindqvist, A., van Zon, W., Karlsson Rosenthal, C., and Wolthuis, R.M.F. (2007). Cyclin B1-Cdk1 activation continues after centrosome separation to control mitotic progression. PLoS Biol *5*, e123.

Littlepage, L.E., and Ruderman, J.V. (2002). Identification of a new APC/C recognition domain, the A box, which is required for the Cdh1-dependent destruction of the kinase Aurora-A during mitotic exit. Genes Dev *16*, 2274–2285.

London, N., and Biggins, S. (2014). Mad1 kinetochore recruitment by Mps1-mediated phosphorylation of Bub1 signals the spindle checkpoint. Genes Dev *28*, 140–152.

London, N., Ceto, S., Ranish, J.A., and Biggins, S. (2012). Phosphoregulation of Spc105 by Mps1 and PP1 regulates Bub1 localization to kinetochores. Curr Biol *22*, 900–906.

Longtine, M.S., McKenzie, A., Demarini, D.J., Shah, N.G., Wach, A., Brachat, A., Philippsen, P., and Pringle, J.R. (1998). Additional modules for versatile and economical PCR-based gene deletion and modification in Saccharomyces cerevisiae. Yeast *14*, 953–961.

Luo, X., Tang, Z., Rizo, J., and Yu, H. (2002). The Mad2 spindle checkpoint protein undergoes similar major conformational changes upon binding to either Mad1 or Cdc20. Mol Cell *9*, 59–71.

Lupas, A., Baumeister, W., and Hofmann, K. (1997). A repetitive sequence in subunits of the 26S proteasome and 20S cyclosome (anaphase-promoting complex). Trends Biochem. Sci. *22*, 195–196.

Mansfeld, J., Collin, P., Collins, M.O., Choudhary, J.S., and Pines, J. (2011). APC15 drives the turnover of MCC-CDC20 to make the spindle assembly checkpoint responsive to kinetochore attachment. Nat Cell Biol.

Martinez, J.S., Jeong, D.-E., Choi, E., Billings, B.M., and Hall, M.C. (2006). Acm1 is a negative regulator of the CDH1-dependent anaphase-promoting complex/cyclosome in budding yeast. Mol Cell Biol *26*, 9162–9176.

Masui, Y., and Markert, C.L. (1971). Cytoplasmic control of nuclear behavior during meiotic maturation of frog oocytes. J Exp Zool *177*, 129–145.

Matyskiela, M.E., and Morgan, D.O. (2009). Analysis of Activator-Binding Sites on the APC/C Supports a Cooperative Substrate-Binding Mechanism. Mol Cell *34*, 68–80.

McGrath, J.P., Jentsch, S., and Varshavsky, A. (1991). UBA 1: an essential yeast gene encoding ubiquitin-activating enzyme. Embo J *10*, 227–236.

McMillan, J.N., Sia, R.A., and Lew, D.J. (1998). A morphogenesis checkpoint monitors the actin cytoskeleton in yeast. J Cell Biol *142*, 1487–1499.

McNulty, J.J., and Lew, D.J. (2005). Swe1p responds to cytoskeletal perturbation, not bud size, in S. cerevisiae. Curr Biol *15*, 2190–2198.

Melesse, M., Choi, E., Hall, H., Walsh, M.J., Geer, M.A., and Hall, M.C. (2014). Timely Activation of Budding Yeast APCCdh1 Involves Degradation of Its Inhibitor, Acm1, by an Unconventional Proteolytic Mechanism. PLoS ONE *9*, e103517.

Metzger, M.B., Hristova, V.A., and Weissman, A.M. (2012). HECT and RING finger families of E3 ubiquitin ligases at a glance. J Cell Sci *125*, 531–537.

Millband, D.N., and Hardwick, K.G. (2002). Fission yeast Mad3p is required for Mad2p to inhibit the anaphase-promoting complex and localizes to kinetochores in a Bub1p-, Bub3p-, and Mph1p-dependent manner. Mol Cell Biol *22*, 2728–2742.

Miller, J.J., Summers, M.K., Hansen, D.V., Nachury, M.V., Lehman, N.L., Loktev, A., and Jackson, P.K. (2006). Emi1 stably binds and inhibits the anaphase-promoting complex/cyclosome as a pseudosubstrate inhibitor. Genes Dev *20*, 2410–2420.

Miniowitz-Shemtov, S., Eytan, E., Ganoth, D., Sitry-Shevah, D., Dumin, E., and Hershko, A. (2012). Role of phosphorylation of Cdc20 in p31(comet)-stimulated disassembly of the mitotic checkpoint complex. Proceedings of the National Academy of Sciences *109*, 8056–8060.

Minshull, J., Straight, A., Rudner, A.D., Dernburg, A.F., Belmont, A., and Murray, A.W. (1996). Protein phosphatase 2A regulates MPF activity and sister chromatid cohesion in budding yeast. Curr Biol *6*, 1609–1620.

Mochida, S., and Hunt, T. (2012). Protein phosphatases and their regulation in the control of mitosis. EMBO Rep *13*, 197–203.

Mochida, S., Ikeo, S., Gannon, J., and Hunt, T. (2009). Regulated activity of PP2A-B55 delta is crucial for controlling entry into and exit from mitosis in Xenopus egg extracts. Embo J *28*, 2777–2785.

Mondal, G., Baral, R.N., and Roychoudhury, S. (2006). A new Mad2-interacting domain of Cdc20 is critical for the function of Mad2-Cdc20 complex in the spindle assembly checkpoint. Biochem J *396*, 243–253.

Mondal, G., Sengupta, S., Panda, C.K., Gollin, S.M., Saunders, W.S., and Roychoudhury, S. (2007). Overexpression of Cdc20 leads to impairment of the spindle assembly checkpoint and aneuploidization in oral cancer. Carcinogenesis *28*, 81–92.

Morin, V., Prieto, S., Melines, S., Hem, S., Rossignol, M., Lorca, T., Espeut, J., Morin, N., and Abrieu, A. (2012). CDK-dependent potentiation of MPS1 kinase activity is essential to the mitotic checkpoint. Curr Biol *22*, 289–295.

Moses, A.M., Hériché, J.-K., and Durbin, R. (2007). Clustering of phosphorylation site recognition motifs can be exploited to predict the targets of cyclin-dependent kinase. Genome Biol *8*, R23.

Mui, M.Z., Roopchand, D.E., Gentry, M.S., Hallberg, R.L., Vogel, J., and Branton, P.E. (2010). Adenovirus protein E4orf4 induces premature APCCdc20 activation in Saccharomyces cerevisiae by a protein phosphatase 2A-dependent mechanism. J. Virol. *84*, 4798–4809.

Murray, A.W. (1992). Creative blocks: cell-cycle checkpoints and feedback controls. Nature *359*, 599–604.

Murray, A.W., and Kirschner, M.W. (1989). Cyclin synthesis drives the early embryonic cell cycle. Nature *339*, 275–280.

Murray, A.W., Solomon, M.J., and Kirschner, M.W. (1989). The role of cyclin synthesis and degradation in the control of maturation promoting factor activity. Nature *339*, 280–286.

Nilsson, J., Yekezare, M., Minshull, J., and Pines, J. (2008). The APC/C maintains the spindle assembly checkpoint by targeting Cdc20 for destruction. Nat Cell Biol *10*, 1411–1420.

Nurse, P. (1975). Genetic control of cell size at cell division in yeast. Nature *256*, 547–551.

Nurse, P. (1990). Universal control mechanism regulating onset of M-phase. Nature *344*, 503–508.

Nurse, P., and Thuriaux, P. (1980). Regulatory genes controlling mitosis in the fission yeast Schizosaccharomyces pombe. Genetics *96*, 627–637.

Oelschlaegel, T., Schwickart, M., Matos, J., Bogdanova, A., Camasses, A., Havlis, J., Shevchenko, A., and Zachariae, W. (2005). The yeast APC/C subunit Mnd2 prevents

premature sister chromatid separation triggered by the meiosis-specific APC/C-Ama1. Cell *120*, 773–788.

Ohi, M.D., Feoktistova, A., Ren, L., Yip, C., Cheng, Y., Chen, J.-S., Yoon, H.-J., Wall, J.S., Huang, Z., Penczek, P.A., et al. (2007). Structural organization of the anaphase-promoting complex bound to the mitotic activator Slp1. Mol Cell *28*, 871–885.

Ohta, T., Michel, J.J., Schottelius, A.J., and Xiong, Y. (1999). ROC1, a homolog of APC11, represents a family of cullin partners with an associated ubiquitin ligase activity. Mol Cell *3*, 535–541.

Page, A.M., Aneliunas, V., Lamb, J.R., and Hieter, P. (2005). In vivo characterization of the nonessential budding yeast anaphase-promoting complex/cyclosome components Swm1p, Mnd2p and Apc9p. Genetics *170*, 1045–1062.

Pan, J., and Chen, R.-H. (2004). Spindle checkpoint regulates Cdc20p stability in Saccharomyces cerevisiae. Genes Dev *18*, 1439–1451.

Parker, L.L., Atherton-Fessler, S., and Piwnica-Worms, H. (1992). p107wee1 is a dual-specificity kinase that phosphorylates p34cdc2 on tyrosine 15. Proc Natl Acad Sci USA *89*, 2917–2921.

Passmore, L.A., and Barford, D. (2005). Coactivator functions in a stoichiometric complex with anaphase-promoting complex/cyclosome to mediate substrate recognition. EMBO Rep *6*, 873–878.

Passmore, L.A., Booth, C.R., Vénien-Bryan, C., Ludtke, S.J., Fioretto, C., Johnson, L.N., Chiu, W., and Barford, D. (2005). Structural analysis of the anaphase-promoting complex reveals multiple active sites and insights into polyubiquitylation. Mol Cell *20*, 855–866.

Passmore, L.A., McCormack, E.A., Au, S.W.N., Paul, A., Willison, K.R., Harper, J.W., and Barford, D. (2003). Doc1 mediates the activity of the anaphase-promoting complex by contributing to substrate recognition. Embo J *22*, 786–796.

Patra, D., and Dunphy, W.G. (1998). Xe-p9, a Xenopus Suc1/Cks protein, is essential for the Cdc2-dependent phosphorylation of the anaphase- promoting complex at mitosis. Genes Dev *12*, 2549–2559.

Patton, E.E., Willems, A.R., and Tyers, M. (1998). Combinatorial control in ubiquitin-dependent proteolysis: don't Skp the F-box hypothesis. Trends Genet *14*, 236–243.

Peters, J.M., King, R.W., Höög, C., and Kirschner, M.W. (1996). Identification of BIME as a subunit of the anaphase-promoting complex. Science *274*, 1199–1201.

Pfleger, C.M., and Kirschner, M.W. (2000). The KEN box: an APC recognition signal distinct from the D box targeted by Cdh1. Genes Dev *14*, 655–665.

Pinsky, B.A., Nelson, C.R., and Biggins, S. (2009). Protein phosphatase 1 regulates exit from the spindle checkpoint in budding yeast. Curr Biol *19*, 1182–1187.

Pomerening, J.R., Kim, S.Y., and Ferrell, J.E. (2005). Systems-level dissection of the cell-cycle oscillator: bypassing positive feedback produces damped oscillations. Cell *122*, 565–578.

Pomerening, J.R., Sontag, E.D., and Ferrell, J.E. (2003). Building a cell cycle oscillator: hysteresis and bistability in the activation of Cdc2. Nat Cell Biol *5*, 346–351.

Primorac, I., Weir, J.R., Chiroli, E., Gross, F., Hoffmann, I., van Gerwen, S., Ciliberto, A., and Musacchio, A. (2013). Bub3 reads phosphorylated MELT repeats to promote spindle assembly checkpoint signaling. Elife *2*, e01030.

Prinz, S., Hwang, E.S., Visintin, R., and Amon, A. (1998). The regulation of Cdc20 proteolysis reveals a role for APC components Cdc23 and Cdc27 during S phase and early mitosis. Curr Biol *8*, 750–760.

Rabitsch, K.P., Tóth, A., Gálová, M., Schleiffer, A., Schaffner, G., Aigner, E., Rupp, C., Penkner, A.M., Moreno-Borchart, A.C., Primig, M., et al. (2001). A screen for genes required for meiosis and spore formation based on whole-genome expression. Curr Biol *11*, 1001–1009.

Rahal, R., and Amon, A. (2008). Mitotic CDKs control the metaphase-anaphase transition and trigger spindle elongation. Genes Dev *22*, 1534–1548.

Rajkumar, T., Sabitha, K., Vijayalakshmi, N., Shirley, S., Bose, M.V., Gopal, G., and Selvaluxmy, G. (2011). Identification and validation of genes involved in cervical tumourigenesis. BMC Cancer *11*, 80.

Rao, P.N., and Johnson, R.T. (1970). Mammalian cell fusion: studies on the regulation of DNA synthesis and mitosis. Nature *225*, 159–164.

Rape, M., Reddy, S.K., and Kirschner, M.W. (2006). The processivity of multiubiquitination by the APC determines the order of substrate degradation. Cell *124*, 89–103.

Reis, A., Levasseur, M., Chang, H.-Y., Elliott, D.J., and Jones, K.T. (2006). The CRY box: a second APCcdh1-dependent degron in mammalian cdc20. EMBO Rep *7*, 1040–1045.

Rhind, N., and Russell, P. (1998). Mitotic DNA damage and replication checkpoints in yeast. Curr Opin Cell Biol *10*, 749–758.

Rieder, C.L., Cole, R.W., Khodjakov, A., and Sluder, G. (1995). The checkpoint delaying anaphase in response to chromosome monoorientation is mediated by an inhibitory signal produced by unattached kinetochores. J Cell Biol *130*, 941–948.

Rieder, C.L., Schultz, A., Cole, R., and Sluder, G. (1994). Anaphase onset in vertebrate somatic cells is controlled by a checkpoint that monitors sister kinetochore attachment to the spindle. J Cell Biol *127*, 1301–1310.

Rigaut, G., Shevchenko, A., Rutz, B., Wilm, M., Mann, M., and Séraphin, B. (1999). A generic protein purification method for protein complex characterization and proteome exploration. Nat Biotechnol *17*, 1030–1032.

Rodrigo-Brenni, M.C., and Morgan, D.O. (2007). Sequential E2s drive polyubiquitin chain assembly on APC targets. Cell *130*, 127–139.

Rossio, V., Galati, E., and Piatti, S. (2010). Adapt or die: how eukaryotic cells respond to prolonged activation of the spindle assembly checkpoint. Biochem Soc Trans *38*, 1645–1649.

Rothblatt, J., and Schekman, R. (1989). A hitchhiker's guide to analysis of the secretory pathway in yeast. Methods Cell Biol. *32*, 3–36.

Rudner, A.D., and Murray, A.W. (2000). Phosphorylation by Cdc28 activates the Cdc20-dependent activity of the anaphase-promoting complex. J Cell Biol *149*, 1377–1390.

Rudner, A.D., Hardwick, K.G., and Murray, A.W. (2000). Cdc28 activates exit from mitosis in budding yeast. J Cell Biol *149*, 1361–1376.

Russell, P., and Nurse, P. (1986). cdc25+ functions as an inducer in the mitotic control of fission yeast. Cell *45*, 145–153.

Russell, P., and Nurse, P. (1987). Negative regulation of mitosis by wee1+, a gene encoding a protein kinase homolog. Cell *49*, 559–567.

Russell, P., Moreno, S., and Reed, S.I. (1989). Conservation of mitotic controls in fission and budding yeasts. Cell *57*, 295–303.

Sanchez, Y., Bachant, J., Wang, H., Hu, F., Liu, D., Tetzlaff, M., and Elledge, S.J. (1999). Control of the DNA damage checkpoint by chk1 and rad53 protein kinases through distinct mechanisms. Science *286*, 1166–1171.

Schreiber, A., Stengel, F., Zhang, Z., Enchev, R.I., Kong, E.H., Morris, E.P., Robinson, C.V., Da Fonseca, P.C.A., and Barford, D. (2011). Structural basis for the subunit assembly of the anaphase-promoting complex. Nature *470*, 227–232.

Schwab, M., Lutum, A.S., and Seufert, W. (1997). Yeast Hct1 is a regulator of Clb2 cyclin proteolysis. Cell *90*, 683–693.

Schwab, M., Neutzner, M., Möcker, D., and Seufert, W. (2001). Yeast Hct1 recognizes the mitotic cyclin Clb2 and other substrates of the ubiquitin ligase APC. Embo J *20*, 5165–5175.

Schwickart, M., Havlis, J., Habermann, B., Bogdanova, A., Camasses, A., Oelschlaegel, T., Shevchenko, A., and Zachariae, W. (2004). Swm1/Apc13 is an evolutionarily conserved subunit of the anaphase-promoting complex stabilizing the association of Cdc16 and Cdc27. Mol Cell Biol *24*, 3562–3576.

Searle, J.S., Schollaert, K.L., Wilkins, B.J., and Sanchez, Y. (2004). The DNA damage checkpoint and PKA pathways converge on APC substrates and Cdc20 to regulate mitotic progression. Nat Cell Biol *6*, 138–145.

Sethi, N., Monteagudo, M.C., Koshland, D., Hogan, E., and Burke, D.J. (1991). The CDC20 gene product of Saccharomyces cerevisiae, a beta-transducin homolog, is required for a subset of microtubule-dependent cellular processes. Mol Cell Biol *11*, 5592–5602.

Sheff, M.A., and Thorn, K.S. (2004). Optimized cassettes for fluorescent protein tagging in Saccharomyces cerevisiae. Yeast *21*, 661–670.

Shepperd, L.A., Meadows, J.C., Sochaj, A.M., Lancaster, T.C., Zou, J., Buttrick, G.J., Rappsilber, J., Hardwick, K.G., and Millar, J.B.A. (2012). Phosphodependent recruitment of Bub1 and Bub3 to Spc7/KNL1 by Mph1 kinase maintains the spindle checkpoint. Curr Biol *22*, 891–899.

Shirayama, M., Tóth, A., Gálová, M., and Nasmyth, K. (1999). APC(Cdc20) promotes exit from mitosis by destroying the anaphase inhibitor Pds1 and cyclin Clb5. Nature *402*, 203–207.

Shirayama, M., Zachariae, W., Ciosk, R., and Nasmyth, K. (1998). The Polo-like kinase Cdc5p and the WD-repeat protein Cdc20p/fizzy are regulators and substrates of the anaphase promoting complex in Saccharomyces cerevisiae. Embo J *17*, 1336–1349.

Shou, W., Seol, J.H., Shevchenko, A., Baskerville, C., Moazed, D., Chen, Z.W., Jang, J., Shevchenko, A., Charbonneau, H., and Deshaies, R.J. (1999). Exit from mitosis is triggered by Tem1-dependent release of the protein phosphatase Cdc14 from nucleolar RENT complex. Cell *97*, 233–244.

Shteinberg, M., Protopopov, Y., Listovsky, T., Brandeis, M., and Hershko, A. (1999). Phosphorylation of the cyclosome is required for its stimulation by Fizzy/cdc20. Biochem Biophys Res Commun *260*, 193–198.

Shu, Y., Yang, H., Hallberg, E., and Hallberg, R. (1997). Molecular genetic analysis of Rts1p, a B' regulatory subunit of Saccharomyces cerevisiae protein phosphatase 2A. Mol Cell Biol *17*, 3242–3253.

Sigrist, S., Jacobs, H., Stratmann, R., and Lehner, C.F. (1995). Exit from mitosis is regulated by Drosophila fizzy and the sequential destruction of cyclins A, B and B3. Embo J *14*, 4827–4838.

Sikorski, R.S., Boguski, M.S., Goebl, M., and Hieter, P. (1990). A repeating amino acid motif in CDC23 defines a family of proteins and a new relationship among genes required for mitosis and RNA synthesis. Cell *60*, 307–317.

Sironi, L., Mapelli, M., Knapp, S., de Antoni, A., Jeang, K.-T., and Musacchio, A. (2002). Crystal structure of the tetrameric Mad1-Mad2 core complex: implications of a "safety belt" binding mechanism for the spindle checkpoint. Embo J *21*, 2496–2506.

Sreenivasan, A., and Kellogg, D. (1999). The elm1 kinase functions in a mitotic signaling network in budding yeast. Mol Cell Biol *19*, 7983–7994.

Stark, M.J. (1996). Yeast protein serine/threonine phosphatases: multiple roles and diverse regulation. Yeast *12*, 1647–1675.

Steen, J.A.J., Steen, H., Georgi, A., Parker, K., Springer, M., Kirchner, M., Hamprecht, F., and Kirschner, M.W. (2008). Different phosphorylation states of the anaphase promoting complex in response to antimitotic drugs: a quantitative proteomic analysis. Proc Natl Acad Sci USA *105*, 6069–6074.

Stegmeier, F., and Amon, A. (2004). Closing mitosis: the functions of the Cdc14 phosphatase and its regulation. Annu Rev Genet *38*, 203–232.

Stern, B., and Nurse, P. (1996). A quantitative model for the cdc2 control of S phase and mitosis in fission yeast. Trends Genet *12*, 345–350.

Straight, A.F., Belmont, A.S., Robinett, C.C., and Murray, A.W. (1996). GFP tagging of budding yeast chromosomes reveals that protein-protein interactions can mediate sister chromatid cohesion. Curr Biol *6*, 1599–1608.

Sudakin, V., Chan, G.K., and Yen, T.J. (2001). Checkpoint inhibition of the APC/C in HeLa cells is mediated by a complex of BUBR1, BUB3, CDC20, and MAD2. J Cell Biol *154*, 925–936.

Sudakin, V., Ganoth, D., Dahan, A., Heller, H., Hershko, J., Luca, F.C., Ruderman, J.V., and Hershko, A. (1995). The cyclosome, a large complex containing cyclin-selective ubiquitin ligase activity, targets cyclins for destruction at the end of mitosis. Mol Biol Cell *6*, 185–197.

Surana, U., Amon, A., Dowzer, C., McGrew, J., Byers, B., and Nasmyth, K. (1993). Destruction of the CDC28/CLB mitotic kinase is not required for the metaphase to anaphase transition in budding yeast. Embo J *12*, 1969–1978.

Tang, Z., Bharadwaj, R., Li, B., and Yu, H. (2001a). Mad2-Independent inhibition of APCCdc20 by the mitotic checkpoint protein BubR1. Dev Cell *1*, 227–237.

Tang, Z., Li, B., Bharadwaj, R., Zhu, H., Ozkan, E., Hakala, K., Deisenhofer, J., and Yu, H. (2001b). APC2 Cullin protein and APC11 RING protein comprise the minimal ubiquitin ligase module of the anaphase-promoting complex. Mol Biol Cell *12*, 3839–3851.

Taylor, S.S., and McKeon, F. (1997). Kinetochore localization of murine Bub1 is required for normal mitotic timing and checkpoint response to spindle damage. Cell *89*, 727–735.

Thornton, B.R., and Toczyski, D.P. (2003). Securin and B-cyclin/CDK are the only essential targets of the APC. Nat Cell Biol *5*, 1090–1094.

Thornton, B.R., and Toczyski, D.P. (2006). Precise destruction: an emerging picture of the APC. Genes Dev *20*, 3069–3078.

Thornton, B.R., Ng, T.M., Matyskiela, M.E., Carroll, C.W., Morgan, D.O., and Toczyski, D.P. (2006). An architectural map of the anaphase-promoting complex. Genes Dev *20*, 449–460.

Thrower, J.S., Hoffman, L., Rechsteiner, M., and Pickart, C.M. (2000). Recognition of the polyubiquitin proteolytic signal. Embo J *19*, 94–102.

Torres, M.P., and Borchers, C.H. (2007). Mitotic phosphorylation of the anaphase-promoting complex inhibitory subunit Mnd2 is necessary for efficient progression through meiosis i. J Biol Chem *282*, 17351–17362.

Tugendreich, S., Tomkiel, J., Earnshaw, W., and Hieter, P. (1995). CDC27Hs colocalizes with CDC16Hs to the centrosome and mitotic spindle and is essential for the metaphase to anaphase transition. Cell *81*, 261–268.

Ufano, S., San-Segundo, P., del Rey, F., and Vázquez de Aldana, C.R. (1999). SWM1, a developmentally regulated gene, is required for spore wall assembly in Saccharomyces cerevisiae. Mol Cell Biol *19*, 2118–2129.

Uhlmann, F., Lottspeich, F., and Nasmyth, K. (1999). Sister-chromatid separation at anaphase onset is promoted by cleavage of the cohesin subunit Scc1. Nature *400*, 37–42.

Uhlmann, F., Wernic, D., Poupart, M.A., Koonin, E.V., and Nasmyth, K. (2000). Cleavage of cohesin by the CD clan protease separin triggers anaphase in yeast. Cell *103*, 375–386.

Uhlmann, F., Bouchoux, C., and López-Avilés, S. (2011). A quantitative model for cyclin-dependent kinase control of the cell cycle: revisited. Philos. Trans. R. Soc. Lond., B, Biol. Sci. *366*, 3572–3583.

Uzunova, K., Dye, B.T., Schutz, H., Ladurner, R., Petzold, G., Toyoda, Y., Jarvis, M.A., Brown, N.G., Poser, I., Novatchkova, M., et al. (2012). APC15 mediates CDC20 autoubiquitylation by APC/C(MCC) and disassembly of the mitotic checkpoint complex. Nat Struct Mol Biol *19*, 1116–1123.

Vernieri, C., Chiroli, E., Francia, V., Gross, F., and Ciliberto, A. (2013). Adaptation to the spindle checkpoint is regulated by the interplay between Cdc28/Clbs and PP2ACdc55. J Cell Biol *202*, 765–778.

Visintin, R., Craig, K., Hwang, E.S., Prinz, S., Tyers, M., and Amon, A. (1998). The phosphatase Cdc14 triggers mitotic exit by reversal of Cdk-dependent phosphorylation. Mol Cell *2*, 709–718.

Visintin, R., Hwang, E.S., and Amon, A. (1999). Cfi1 prevents premature exit from mitosis by anchoring Cdc14 phosphatase in the nucleolus. Nature *398*, 818–823.

Visintin, R., Prinz, S., and Amon, A. (1997). CDC20 and CDH1: a family of substrate-specific activators of APC-dependent proteolysis. Science *278*, 460–463.

Vodermaier, H.C., Gieffers, C., Maurer-Stroh, S., Eisenhaber, F., and Peters, J.-M. (2003). TPR subunits of the anaphase-promoting complex mediate binding to the activator protein CDH1. Curr Biol *13*, 1459–1468.

Voets, E., and Wolthuis, R.M.F. (2010). MASTL is the human orthologue of Greatwall kinase that facilitates mitotic entry, anaphase and cytokinesis. Cell Cycle *9*, 3591–3601.

Wang, J., Dye, B.T., Rajashankar, K.R., Kurinov, I., and Schulman, B.A. (2009). Insights into anaphase promoting complex TPR subdomain assembly from a CDC26-APC6 structure. Nat Struct Mol Biol *16*, 987–989.

Wang, Y., and Burke, D.J. (1997). Cdc55p, the B-type regulatory subunit of protein phosphatase 2A, has multiple functions in mitosis and is required for the kinetochore/spindle checkpoint in Saccharomyces cerevisiae. Mol Cell Biol *17*, 620–626.

Wasserman, W.J., and Smith, L.D. (1978). The cyclic behavior of a cytoplasmic factor controlling nuclear membrane breakdown. J Cell Biol *78*, R15–R22.

Weinert, T.A., Kiser, G.L., and Hartwell, L.H. (1994). Mitotic checkpoint genes in budding yeast and the dependence of mitosis on DNA replication and repair. Genes Dev *8*, 652–665.

Weinstein, J. (1997). Cell cycle-regulated expression, phosphorylation, and degradation of p55Cdc. A mammalian homolog of CDC20/Fizzy/slp1. J Biol Chem *272*, 28501–28511.

Weiss, E., and Winey, M. (1996). The Saccharomyces cerevisiae spindle pole body duplication gene MPS1 is part of a mitotic checkpoint. J Cell Biol *132*, 111–123.

Wendt, K.S., Vodermaier, H.C., Jacob, U., Gieffers, C., Gmachl, M., Peters, J.M., Huber, R., and Sondermann, P. (2001). Crystal structure of the APC10/DOC1 subunit of the human anaphase-promoting complex. Nat. Struct. Biol. *8*, 784–788.

Westhorpe, F.G., Tighe, A., Lara-Gonzalez, P., and Taylor, S.S. (2011). p31comet-mediated extraction of Mad2 from the MCC promotes efficient mitotic exit. J Cell Sci *124*, 3905–3916.

Wicky, S., Tjandra, H., Schieltz, D., Yates, J., and Kellogg, D.R. (2011). The Zds proteins control entry into mitosis and target protein phosphatase 2A to the Cdc25 phosphatase. Mol Biol Cell *22*, 20–32.

Willems, A.R., Lanker, S., Patton, E.E., Craig, K.L., Nason, T.F., Mathias, N., Kobayashi, R., Wittenberg, C., and Tyers, M. (1996). Cdc53 targets phosphorylated G1 cyclins for degradation by the ubiquitin proteolytic pathway. Cell *86*, 453–463.

Williamson, A., Wickliffe, K.E., Mellone, B.G., Song, L., Karpen, G.H., and Rape, M. (2009). Identification of a physiological E2 module for the human anaphase-promoting complex. Proceedings of the National Academy of Sciences *106*, 18213–18218.

Wurzenberger, C., and Gerlich, D.W. (2011). Phosphatases: providing safe passage through mitotic exit. Nat Rev Mol Cell Biol *12*, 469–482.

Yamada, H., Kumada, K., and Yanagida, M. (1997). Distinct subunit functions and cell cycle regulated phosphorylation of 20S APC/cyclosome required for anaphase in fission yeast. J Cell Sci *110 (Pt 15)*, 1793–1804.

Yamagishi, Y., Yang, C.-H., Tanno, Y., and Watanabe, Y. (2012). MPS1/Mph1 phosphorylates the kinetochore protein KNL1/Spc7 to recruit SAC components. Nat Cell Biol *14*, 746–752.

Yamamoto, A., Guacci, V., and Koshland, D. (1996). Pds1p is required for faithful execution of anaphase in the yeast, Saccharomyces cerevisiae. J Cell Biol *133*, 85–97.

Yamano, H., Gannon, J., Mahbubani, H., and Hunt, T. (2004). Cell cycle-regulated recognition of the destruction box of cyclin B by the APC/C in Xenopus egg extracts. Mol Cell *13*, 137–147.

Yamashita, Y.M., Nakaseko, Y., Kumada, K., Nakagawa, T., and Yanagida, M. (1999). Fission yeast APC/cyclosome subunits, Cut20/Apc4 and Cut23/Apc8, in regulating metaphase-anaphase progression and cellular stress responses. Genes Cells *4*, 445–463.

Yamashita, Y.M., Nakaseko, Y., Samejima, I., Kumada, K., Yamada, H., Michaelson, D., and Yanagida, M. (1996). 20S cyclosome complex formation and proteolytic activity inhibited by the cAMP/PKA pathway. Nature *384*, 276–279.

Yeong, F.M., Lim, H.H., Padmashree, C.G., and Surana, U. (2000). Exit from mitosis in budding yeast: biphasic inactivation of the Cdc28-Clb2 mitotic kinase and the role of Cdc20. Mol Cell *5*, 501–511.

Yoon, H.-J., Feoktistova, A., Chen, J.-S., Jennings, J.L., Link, A.J., and Gould, K.L. (2006). Role of Hcn1 and its phosphorylation in fission yeast anaphase-promoting complex/cyclosome function. J Biol Chem *281*, 32284–32293.

Yu, H., Peters, J.M., King, R.W., Page, A.M., Hieter, P., and Kirschner, M.W. (1998). Identification of a cullin homology region in a subunit of the anaphase-promoting complex. Science *279*, 1219–1222.

Yu, H. (2007). Cdc20: a WD40 activator for a cell cycle degradation machine. Mol Cell *27*, 3–16.

Yudkovsky, Y., Shteinberg, M., Listovsky, T., Brandeis, M., and Hershko, A. (2000). Phosphorylation of Cdc20/fizzy negatively regulates the mammalian cyclosome/APC in the mitotic checkpoint. Biochem Biophys Res Commun *271*, 299–304.

Zachariae, W., and Nasmyth, K. (1996). TPR proteins required for anaphase progression mediate ubiquitination of mitotic B-type cyclins in yeast. Mol Biol Cell *7*, 791–801.

Zachariae, W., Schwab, M., Nasmyth, K., and Seufert, W. (1998a). Control of cyclin ubiquitination by CDK-regulated binding of Hct1 to the anaphase promoting complex. Science *282*, 1721–1724.

Zachariae, W., Shevchenko, A., Andrews, P.D., Ciosk, R., Gálová, M., Stark, M.J., Mann, M., and Nasmyth, K. (1998b). Mass spectrometric analysis of the anaphase-promoting complex from yeast: identification of a subunit related to cullins. Science *279*, 1216–1219.

Zachariae, W., Shin, T.H., Gálová, M., Obermaier, B., and Nasmyth, K. (1996). Identification of subunits of the anaphase-promoting complex of Saccharomyces cerevisiae. Science *274*, 1201–1204.

Zhang, J., Wan, L., Dai, X., Sun, Y., and Wei, W. (2014). Functional characterization of Anaphase Promoting Complex/Cyclosome (APC/C) E3 ubiquitin ligases in tumorigenesis. Biochim Biophys Acta *1845*, 277–293.

Zhang, Y., and Lees, E. (2001). Identification of an overlapping binding domain on Cdc20 for Mad2 and anaphase-promoting complex: model for spindle checkpoint regulation. Mol Cell Biol *21*, 5190–5199.

Zur, A., and Brandeis, M. (2002). Timing of APC/C substrate degradation is determined by fzy/fzr specificity of destruction boxes. Embo J *21*, 4500–4510.

Elizabeth C. Williams

EDUCATION & RESEARCH EXPERIENCE

Ph.D., Biochemistry

2007-2014 Ottawa Institute of Systems Biology & Department of Biochemistry, University of Ottawa.
Thesis: Cdk1-dependent phosphorylation of the APC^{Cdc20} regulates its activation at anaphase onset in *S. cerevisiae*

Bachelor of Science, Anatomy and Cell Biology

2003-2007 McGill University, Montreal, Quebec. 2003-2007.
CGPA: 3.53 / 4.00

High School Diploma (French Immersion Program)

1998-2003 South Carleton High School, Richmond, Ontario. 1998-2003.

HONOURS & AWARDS

2009-2012 Canada Graduate Scholarship (CGS) Doctoral Award from Canadian Institutes of Health Research (CIHR). $30,000 annual stipend + $5,000 research allowance for 3 years.

2008-2009 Canada Graduate Scholarship (CGS) Master's Award from CIHR. $11,667.

2007-2008 Ontario Graduate Scholarship. $10,000.

2007-2013 National Excellence Scholarship Research Award, University of Ottawa. $33,000 to cover tuition fees.

2007 Summer Rotation Scholarship, University of Ottawa. $4,500.

2005-2006 Dean's Honour List, McGill University.

2003 Silver Medallion (90% average or greater), South Carleton High School

2003 Lieutenant Governor's Community Volunteer Award, South Carleton High School

TEACHING EXPERIENCE

Graduate Teaching Assistant (University of Ottawa)

2014 Lab demonstrator for third year undergraduate biochemistry lab (BCH3346)

- Guided students through weekly lab sessions
- Marked formal lab reports, and evaluated in lab performance

2013 Marker for undergraduate molecular biology lab (BCH3346)

- Marked formal lab reports

2011-2013 Teaching assistant for fourth year undergraduate cell regulation and control class (BCH4125)

- Proctored and marked midterms and final exams
- Available to answer students questions throughout the course

2010-2011 Lab demonstrator for third year undergraduate molecular biology lab (BCH3356)

- Guided students through weekly lab sessions and marked assignments
- Evaluated in lab performance, as well as short presentations

Supervision of Honours Thesis (University of Ottawa)

2012-2013 Supervised completion of undergraduate student's honours project
Thesis: Cdc26 cooperates with Cdk1 phosphorylation to activate the APC^{Cdc20}

PUBLICATIONS

Peer Review Publications

2014 Szeto, S., **Williams, E.C.**, Rudner, A.D., Lee, J. 2013. Mitotic phosphorylation of filamin A by cyclin B1/cdk1 regulates cell shape, motility and clustering behaviour. *Accepted to Experimental Cell Research*.

2014 Delgoshaie, N., Tang, X., Kanshin, E.D., **Williams, E.C.**, Rudner, A.D., Thibault, P., Tyers, M., and Verreault, A. (2014). Regulation of the histone deacetylase Hst3 by cyclin-dependent kinases and the ubiquitin ligase SCFCdc4. Journal of Biological Chemistry *289,* 13186-13196.

2013 Lianga, N.*, **Williams, E.C.***, Kennedy, E.K., Doré, C., Pilon, S., Girard, S.L., Deneault, J.-S., Rudner, A.D. 2013. A Wee1 checkpoint inhibits anaphase onset. *The Journal of Cell Biology, 201*(6), 843-862. doi:10.1083/jcb.201212038. *These authors contributed equally.

Manuscripts in preparation

2014 **Williams, E.C.**, Ferguson, E., Rudner, A.D. The APC subunits Cdc26 and Mnd2 cooperate with Cdk1 phosphorylation to regulate the spindle assembly checkpoint, *in preparation.*

Conference Presentations

2012 **Williams, E.C.**, Ferguson, E.F., and Rudner, A.D. Cdc26 cooperates with Cdk1 phosphorylation to activate the APC^{Cdc20}.

- Poster: American Society for Cell Biology: Annual Meeting. San Francisco, California.

2011 **Williams, E.C.**, Kennedy, E.K., and Rudner, A.D. Is Cdk1 phosphorylation of the APC essential?

- Poster: American Society for Cell Biology: Annual Meeting. Denver, Colorado.

2010 **Williams, E.C.**, Lianga, N., Kennedy, E.K., and Rudner, A.D. Budding yeast Wee1 inhibits the metaphase to anaphase transition.

- Talk: Cold Spring Harbor Meeting: The Cell Cycle. Cold Spring Harbor, New York.

2009 **Williams, E.C.**, Kennedy, E.K., and Rudner, A.D. Is Cdk1 phosphorylation of the APC essential?

- Poster: OISB Symposium: Progress in Systems Biology. Ottawa.
- Poster: FASEB Summer Research Conference: Mitosis: Spindle Assembly and Function. Lucca, Tuscany, Italy.

2008 **Williams, E.C.**, Lianga, N., Girard, S. and Rudner, A.D. Is Cdk1 phosphorylation of the APC essential?

- Poster: FASEB Summer Research Conference: Yeast Chromosome Structure, Replication and Segregation. Carefree, Arizona.

2008 **Williams, E.C.**, Girard, S. and Rudner, A.D. Is Cdk1 phosphorylation of the APC essential?

- Poster: Department of Biochemistry, Microbiology & Immunology Poster Day, University of Ottawa.
- First place prize ($125).